



National Library  
of Canada

Acquisitions and  
Bibliographic Services Branch

395 Wellington Street  
Ottawa, Ontario  
K1A 0N4

Bibliothèque nationale  
du Canada

Direction des acquisitions et  
des services bibliographiques

395, rue Wellington  
Ottawa (Ontario)  
K1A 0N4

*Votre bibliothèque*

*Votre bibliothèque*

## NOTICE

The quality of this microform is heavily dependent upon the quality of the original thesis submitted for microfilming. Every effort has been made to ensure the highest quality of reproduction possible.

If pages are missing, contact the university which granted the degree.

Some pages may have indistinct print especially if the original pages were typed with a poor typewriter ribbon or if the university sent us an inferior photocopy.

Reproduction in full or in part of this microform is governed by the Canadian Copyright Act, R.S.C. 1970, c. C-30, and subsequent amendments.

## AVIS

La qualité de cette microforme dépend grandement de la qualité de la thèse soumise au microfilmage. Nous avons tout fait pour assurer une qualité supérieure de reproduction.

S'il manque des pages, veuillez communiquer avec l'université qui a conféré le grade.

La qualité d'impression de certaines pages peut laisser à désirer, surtout si les pages originales ont été dactylographiées à l'aide d'un ruban usé ou si l'université nous a fait parvenir une photocopie de qualité inférieure.

La reproduction, même partielle, de cette microforme est soumise à la Loi canadienne sur le droit d'auteur, SRC 1970, c. C-30, et ses amendements subséquents.

**Assessment of the Effect of Mean and Fluctuating Wind-Induced Pressures  
on Air Infiltration and Ventilation in Buildings: A System Theoretic Approach**

**Jiwu Rao**

**A Thesis**

**in**

**The Centre**

**for**

**Building Studies**

**Presented in Partial Fulfilment of the Requirements  
for the Degree of Doctor of Philosophy at  
Concordia University  
Montreal, Quebec, Canada**

**FEBRUARY 1993**

**©Jiwu Rao, 1993**



National Library  
of Canada

Bibliothèque nationale  
du Canada

Acquisitions and  
Bibliographic Services Branch

Direction des acquisitions et  
des services bibliographiques

395 Wellington Street  
Ottawa, Ontario  
K1A 0N4

395, rue Wellington  
Ottawa (Ontario)  
K1A 0N4

*Votre bibliothèque* - *Vostra biblioteca*

*Votre bibliothèque* - *Vostra biblioteca*

The author has granted an irrevocable non-exclusive licence allowing the National Library of Canada to reproduce, loan, distribute or sell copies of his/her thesis by any means and in any form or format, making this thesis available to interested persons.

L'auteur a accordé une licence irrévocable et non exclusive permettant à la Bibliothèque nationale du Canada de reproduire, prêter, distribuer ou vendre des copies de sa thèse de quelque manière et sous quelque forme que ce soit pour mettre des exemplaires de cette thèse à la disposition des personnes intéressées.

The author retains ownership of the copyright in his/her thesis. Neither the thesis nor substantial extracts from it may be printed or otherwise reproduced without his/her permission.

L'auteur conserve la propriété du droit d'auteur qui protège sa thèse. Ni la thèse ni des extraits substantiels de celle-ci ne doivent être imprimés ou autrement reproduits sans son autorisation.

ISBN 0-315-84682-8

Canada

Name Tina Rice

Dissertation Abstracts International is arranged by broad, general subject categories. Please select the one subject which most nearly describes the content of your dissertation. Enter the corresponding four-digit code in the spaces provided.

Phil Linguistics

SUBJECT TERM

1543

U·M·I

SUBJECT CODE

## Subject Categories

### THE HUMANITIES AND SOCIAL SCIENCES

#### COMMUNICATIONS AND THE ARTS

Architecture ..... 0729  
Art History ..... 0377  
Cinema ..... 0900  
Dance ..... 0378  
Fine Arts ..... 0357  
Information Science ..... 0723  
Journalism ..... 0391  
Library Science ..... 0399  
Mass Communications ..... 0708  
Music ..... 0413  
Speech Communication ..... 0459  
Theater ..... 0465

#### EDUCATION

General ..... 0515  
Administration ..... 0514  
Adult and Continuing ..... 0516  
Agricultural ..... 0517  
Art ..... 0273  
Bilingual and Multicultural ..... 0282  
Business ..... 0688  
Community College ..... 0275  
Curriculum and Instruction ..... 0727  
Early Childhood ..... 0518  
Elementary ..... 0524  
Finance ..... 0277  
Guidance and Counseling ..... 0519  
Health ..... 0680  
Higher ..... 0745  
History of ..... 0520  
Home Economics ..... 0278  
Industrial ..... 0521  
Language and Literature ..... 0279  
Mathematics ..... 0280  
Music ..... 0522  
Philosophy of ..... 0998  
Physical ..... 0523

Psychology ..... 0525  
Reading ..... 0535  
Religious ..... 0527  
Sciences ..... 0714  
Secondary ..... 0533  
Social Sciences ..... 0534  
Sociology of ..... 0340  
Special ..... 0529  
Teacher Training ..... 0530  
Technology ..... 0710  
Tests and Measurements ..... 0288  
Vocational ..... 0747

#### LANGUAGE, LITERATURE AND LINGUISTICS

Language ..... 0679  
  General ..... 0289  
  Ancient ..... 0290  
  Linguistics ..... 0291  
  Modern ..... 0401  
Literature ..... 0294  
  General ..... 0295  
  Classical ..... 0297  
  Comparative ..... 0298  
  Medieval ..... 0316  
  Modern ..... 0317  
  African ..... 0318  
  American ..... 0319  
  Asian ..... 0320  
  Canadian (English) ..... 0352  
  Canadian (French) ..... 0355  
  English ..... 0593  
  Germanic ..... 0311  
  Latin American ..... 0312  
  Middle Eastern ..... 0315  
  Romance ..... 0313  
  Slavic and East European ..... 0314

#### PHILOSOPHY, RELIGION AND THEOLOGY

Philosophy ..... 0422  
Religion ..... 0318  
  General ..... 0321  
  Biblical Studies ..... 0319  
  Clergy ..... 0320  
  History of ..... 0322  
  Philosophy of ..... 0469  
Theology ..... 0323

#### SOCIAL SCIENCES

American Studies ..... 0323  
Anthropology ..... 0324  
  Archaeology ..... 0326  
  Cultural ..... 0327  
  Physical ..... 0310  
Business Administration ..... 0272  
  General ..... 0770  
  Accounting ..... 0454  
  Banking ..... 0338  
  Management ..... 0385  
Canadian Studies ..... 0501  
Economics ..... 0503  
  General ..... 0505  
  Agricultural ..... 0508  
  Commerce-Business ..... 0509  
  Finance ..... 0510  
  History ..... 0511  
  Labor ..... 0358  
  Theory ..... 0366  
Folklore ..... 0351  
Geography ..... 0578  
Gerontology ..... 0578  
History ..... 0578  
  General ..... 0578

Ancient ..... 0579  
Medieval ..... 0581  
Modern ..... 0582  
Black ..... 0328  
African ..... 0331  
Asia, Australia and Oceania ..... 0332  
Canadian ..... 0334  
European ..... 0335  
Latin American ..... 0336  
Middle Eastern ..... 0333  
United States ..... 0337  
History of Science ..... 0585  
Law ..... 0398  
Political Science ..... 0615  
  General ..... 0616  
  International Law and ..... 0617  
  Relations ..... 0814  
  Public Administration ..... 0452  
Recreation ..... 0626  
Social Work ..... 0627  
Sociology ..... 0938  
  General ..... 0631  
  Criminology and Penology ..... 0628  
  Demography ..... 0629  
  Ethnic and Racial Studies ..... 0630  
  Individual and Family ..... 0700  
  Studies ..... 0344  
  Industrial and Labor ..... 0709  
  Relations ..... 0999  
  Public and Social Welfare ..... 0453  
  Social Structure and ..... 0453  
  Development ..... 0453  
  Theory and Methods ..... 0453  
Transportation ..... 0453  
Urban and Regional Planning ..... 0453  
Women's Studies ..... 0453

### THE SCIENCES AND ENGINEERING

#### BIOLOGICAL SCIENCES

Agriculture ..... 0473  
  General ..... 0285  
  Agronomy ..... 0475  
  Animal Culture and ..... 0476  
  Nutrition ..... 0359  
  Animal Pathology ..... 0478  
  Food Science and ..... 0479  
  Technology ..... 0480  
  Forestry and Wildlife ..... 0817  
  Plant Culture ..... 0777  
  Plant Pathology ..... 0746  
  Plant Physiology ..... 0306  
  Range Management ..... 0287  
  Wood Technology ..... 0308  
Biology ..... 0309  
  General ..... 0379  
  Anatomy ..... 0329  
  Biostatistics ..... 0353  
  Botany ..... 0359  
  Cell ..... 0410  
  Ecology ..... 0307  
  Entomology ..... 0317  
  Genetics ..... 0416  
  Limnology ..... 0433  
  Microbiology ..... 0821  
  Molecular ..... 0778  
  Neuroscience ..... 0472  
  Oceanography ..... 0786  
  Physiology ..... 0760  
  Radiation ..... 0425  
  Veterinary Science ..... 0996  
  Zoology ..... 0760  
Biophysics ..... 0786  
  General ..... 0760  
  Medical ..... 0760

#### EARTH SCIENCES

Biogeochemistry ..... 0425  
Geochemistry ..... 0996

Geology ..... 0370  
  General ..... 0372  
  Geophysics ..... 0373  
  Hydrology ..... 0388  
  Mineralogy ..... 0411  
  Paleobotany ..... 0345  
  Paleoecology ..... 0426  
  Paleontology ..... 0418  
  Paleozoology ..... 0985  
  Palynology ..... 0427  
  Physical Geography ..... 0368  
  Physical Oceanography ..... 0415

#### HEALTH AND ENVIRONMENTAL SCIENCES

Environmental Sciences ..... 0768  
Health Sciences ..... 0566  
  General ..... 0300  
  Audiology ..... 0992  
  Chemotherapy ..... 0567  
  Dentistry ..... 0350  
  Education ..... 0769  
  Hospital Management ..... 0758  
  Human Development ..... 0982  
  Immunology ..... 0564  
  Medicine and Surgery ..... 0347  
  Mental Health ..... 0569  
  Nursing ..... 0570  
  Nutrition ..... 0380  
  Obstetrics and Gynecology ..... 0354  
  Occupational Health and ..... 0381  
  Therapy ..... 0571  
  Ophthalmology ..... 0419  
  Pathology ..... 0572  
  Pharmacology ..... 0382  
  Pharmacy ..... 0573  
  Physical Therapy ..... 0574  
  Public Health ..... 0575  
  Radiology ..... 0575  
  Recreation ..... 0575

Speech Pathology ..... 0460  
Toxicology ..... 0383  
Home Economics ..... 0386

#### PHYSICAL SCIENCES

Pure Sciences ..... 0485  
Chemistry ..... 0749  
  General ..... 0486  
  Agricultural ..... 0487  
  Analytical ..... 0488  
  Biochemistry ..... 0738  
  Inorganic ..... 0490  
  Nuclear ..... 0491  
  Organic ..... 0494  
  Pharmaceutical ..... 0495  
  Physical ..... 0754  
  Polymer ..... 0405  
Mathematics ..... 0605  
Physics ..... 0986  
  General ..... 0606  
  Acoustics ..... 0608  
  Astronomy and ..... 0748  
  Astrophysics ..... 0607  
  Atmospheric Science ..... 0798  
  Atomic ..... 0759  
  Electronics and Electricity ..... 0609  
  Elementary Particles and ..... 0610  
  High Energy ..... 0752  
  Fluid and Plasma ..... 0756  
  Molecular ..... 0611  
  Nuclear ..... 0463  
  Optics ..... 0346  
  Radiation ..... 0984  
  Solid State ..... 0984  
Statistics ..... 0984

#### Applied Sciences

Applied Mechanics ..... 0346  
Computer Science ..... 0984

Engineering ..... 0537  
  General ..... 0538  
  Aerospace ..... 0539  
  Agricultural ..... 0540  
  Automotive ..... 0541  
  Biomedical ..... 0542  
  Chemical ..... 0543  
  Civil ..... 0544  
  Electronics and Electrical ..... 0348  
  Heat and Thermodynamics ..... 0545  
  Hydraulic ..... 0546  
  Industrial ..... 0547  
  Marine ..... 0794  
  Materials Science ..... 0548  
  Mechanical ..... 0743  
  Metallurgy ..... 0551  
  Mining ..... 0552  
  Nuclear ..... 0549  
  Packaging ..... 0765  
  Petroleum ..... 0554  
  Sanitary and Municipal ..... 0790  
  System Science ..... 0428  
Geotechnical ..... 0796  
Operations Research ..... 0795  
Plastics Technology ..... 0994  
Textile Technology ..... 0994

#### PSYCHOLOGY

General ..... 0621  
Behavioral ..... 0384  
Clinical ..... 0622  
Developmental ..... 0620  
Experimental ..... 0623  
Industrial ..... 0624  
Personality ..... 0625  
Physiological ..... 0989  
Psychobiology ..... 0349  
Psychometrics ..... 0632  
Social ..... 0451



CONCORDIA UNIVERSITY  
SCHOOL OF GRADUATE STUDIES

This is to certify that the thesis prepared

By: **JIWU RAO**

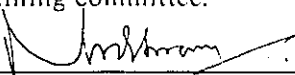
Entitled: **Assessment of the Effect of Mean and Fluctuating Wind-Induced Pressures on Air Infiltration and Ventilation in Buildings: A System Theoretic Approach**

and submitted in partial fulfillment of the requirements for the degree of

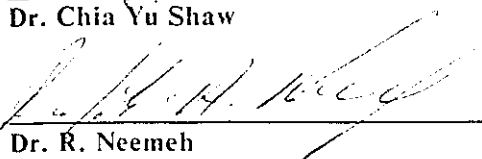
**DOCTOR OF PHILOSOPHY (Building Studies)**


complies with the regulations of the University and meets the accepted standards with respect to originality and quality.

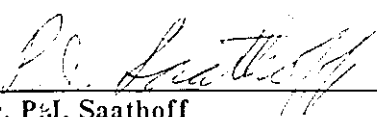
Signed by the final examining committee:

  
\_\_\_\_\_  
Dr. M.N.S. Swamy Chair

  
\_\_\_\_\_  
Dr. Chia Yu Shaw External Examiner

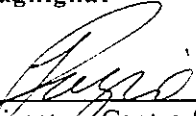
  
\_\_\_\_\_  
Dr. R. Neemeh External-to-Program

  
\_\_\_\_\_  
Dr. R. Guy Examiner

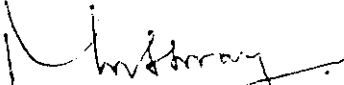
  
\_\_\_\_\_  
Dr. P.J. Saathoff Examiner

  
\_\_\_\_\_  
Dr. R. Zmeureanu Examiner

  
\_\_\_\_\_  
Dr. F. Haghighat Thesis Supervisor

Approved by   
\_\_\_\_\_  
Director, Centre for Building Studies

March 8 19 93

  
\_\_\_\_\_  
Dean of Faculty of Engineering  
and Computer Science

# **ABSTRACT**

## **Assessment of the Effect of Mean and Fluctuating Wind-Induced Pressures on Air Infiltration and Ventilation in Buildings: A System Theoretic Approach**

**Jiwu Rao, Ph.D.**

**Concordia University, 1993**

Energy and indoor air quality concerns have motivated extensive research on air infiltration and ventilation in buildings. Airflow models have been developed to study the problem and to assist in the building design process. Existing research concentrates on measurements, modelling and predictions of steady-state airflow caused by wind-induced pressures, thermal buoyancy and mechanical ventilation systems. Wind-induced pressures on building envelopes have temporal variations due mainly to the wind gustiness. The resultant airflow has both mean and fluctuating components. Existing research shows discrepancies between the current steady-state airflow predictions and the actual air exchanges influenced by fluctuations.

This thesis is devoted to the development of a comprehensive framework and methodology for airflow analysis and design assistance for buildings under both mean and fluctuating driving forces. A building airflow system is seen as two subsystems: steady-state and fluctuating. In the fluctuating airflow system, the temporal variations in wind pressures are taken as driving forces. The predictions of the resultant fluctuating airflow and internal pressures are based on the statistical linearization of flow relations, proper

considerations of large openings, the system theoretic approach to governing equation formulations, and, frequency and spectral analyses for solutions. By combining both fluctuating and mean airflow solutions, the total air exchange in a building is obtained. Three types of validation strategies are employed. Numerical simulations are carried out to evaluate the effects of the statistical linearization on solutions. Laboratory experiments are designed, implemented and conducted to validate the fundamental relations. The theoretical predications are also compared to field experimental data. The fluctuating airflow model provides correct predictions for the simulation conditions and the experimental setups. In addition, modelling and sensitivity analysis procedures for steady-state airflow systems using a system theoretic approach are developed to calculate the influences on airflow results of the variations in building and climatic conditions, and to facilitate error analysis and building ventilation designs.

Future research directions include: the incorporation into the existing research paradigm of the developed sensitivity analysis procedure and fluctuating airflow model, and the acquisition of more suitable data on characteristics of fluctuating driving forces.

# ACKNOWLEDGEMENTS

The author wishes to thank Dr. F. Haghighat, thesis supervisor, for his help and guidance during this Ph.D. program.

The author would like to thank Mr. J. Payer, Mr. Z. Ghonaim, Mr. J. Zilkha, Mr. J. Hrib, and Mr. H. Obermeir for their assistance in setting up the experimental work.

The author is in debt to the following person for their invaluable advices: C.Y. Shaw, James Reardon, Francis Allard, Richard Guy, and T. Stathopoulos.

The author wants to thank the Department of Energy, Mines and Resources Canada which partially financed this thesis program.



# TABLE OF CONTENTS

<b>LIST OF FIGURES</b> .....	x
<b>LIST OF TABLES</b> .....	xii

## CHAPTER I

<b>INTRODUCTION</b> .....	1
<b>1.1. DEFINITION OF THE PHYSICAL PROBLEM</b> .....	4
<b>1.2. IMPORTANCE AND APPLICATIONS OF FLUCTUATING AIRFLOW</b> .....	7
<b>1.3. OBJECTIVES AND PLAN</b> .....	9

## CHAPTER II

<b>LITERATURE REVIEW</b> .....	13
<b>2.1. STEADY-STATE AIRFLOW MODELLING</b> .....	13
2.1.1. Mechanism of Air Infiltration and Ventilation .....	14
2.1.1.1. Openings and Flow Equations .....	14
2.1.1.2. Driving Forces .....	15
2.1.2. Roles and Structures of Mathematical Models .....	18
2.1.2.1. Modelling Steady-State Airflow Systems .....	19
2.1.2.2. Governing Equation Formulation for Steady-State Airflow	20
2.1.2.3. Solution Algorithm for Steady-State Airflow .....	20
2.1.3. Related Studies .....	21
<b>2.2. FLUCTUATING AIRFLOW MODELLING</b> .....	22
2.2.1. Wind Characteristics in the Frequency Domain .....	22
2.2.1.1. Fluctuating Wind Velocity .....	23
2.2.1.2. Wind-Induced Fluctuating Pressures .....	25
2.2.1.3. Correlations Between Wind-Induced Pressures .....	26
2.2.2. Phenomena and Mathematical Descriptions of Fluctuating Airflow	27
2.2.3. Existing Fluctuating Airflow Models and Correlations .....	30
2.2.4. Inadequacies of Existing Research .....	31

## **CHAPTER III**

### **SYSTEM THEORETIC APPROACH TO**

#### **AIRFLOW MODELLING AND DESIGN . . . . . 40**

##### **3.1. MODELLING BUILDING AIRFLOW SYSTEMS . . . . . 42**

###### **3.1.1. Building Airflow Systems . . . . . 42**

###### **3.1.2. Assumptions . . . . . 43**

##### **3.2. SYSTEM THEORETIC APPROACH TO STEADY-STATE AIRFLOW MODELLING . . . . . 44**

###### **3.2.1. Modelling Components of a Building and Its Ventilation System . 45**

###### **3.2.2. Governing Equations of Steady-State Airflow Systems . . . . . 48**

###### **3.2.3. Automatic Formulation Procedure for the Steady-State Airflow Model . . . . . 57**

##### **3.3. SENSITIVITY ANALYSIS OF AIRFLOW IN BUILDINGS . . . . . 58**

###### **3.3.1. Derivation of Sensitivity Calculation . . . . . 60**

###### **3.3.2. Sensitivity Calculation for a Case Study . . . . . 64**

###### **3.3.3. Error Analysis and Design Assistance . . . . . 66**

###### **3.3.4. Further Discussion on Sensitivity Analysis . . . . . 71**

## **CHAPTER IV**

### **FLUCTUATING AIRFLOW MODEL . . . . . 84**

#### **4.1. AN OVERVIEW OF THE FLUCTUATING AIRFLOW MODEL . . 85**

#### **4.2. COMPONENT MODELLING . . . . . 88**

##### **4.2.1. Flow Equation and Statistical Linearization . . . . . 89**

##### **4.2.2. Inertia Force . . . . . 92**

##### **4.2.3. Compressibility of Air . . . . . 93**

#### **4.3. FLUCTUATING AIRFLOW MODELLING AND SOLUTION . . . . 94**

##### **4.3.1. Pressure Balance: Loop Formulation . . . . . 95**

##### **4.3.2. Mass Conservation: Nodal Formulation . . . . . 97**

##### **4.3.3. Spectral Analysis . . . . . 98**

#### **4.4. MODELLING LARGE OPENINGS . . . . . 99**

<b>4.5. COMBINED EFFECT OF MEAN AND FLUCTUATING AIRFLOW</b>	102
4.5.1. The Effect of Hidden Air	102
4.5.2. The Effect of Mixing	104
4.5.3. The Effect of Flow Reversal	105
<b>4.6. CASE STUDIES</b>	106
4.6.1. Single-Opening Enclosure	106
4.6.1.1. Modelling and Solution Approach for a Single-Opening Enclosure	106
4.6.1.2. Quantitative Analysis for the Single-Opening Case	109
4.6.1.3. Theoretical Results for the Single-Opening Case	110
4.6.2. Two-Opening Building	112
4.6.2.1. Modelling and Solution Approach for a Two-Opening Building	112
4.6.2.2. Calculation Results for the Two-Opening Building	114

## **CHAPTER V**

### **FLUCTUATING AIRFLOW MODELLING:**

<b>SYSTEM-THEORETIC APPROACH</b>	125
<b>5.1. MODELLING OF FLUCTUATING AIRFLOW SYSTEMS</b>	126
5.1.1. Graphic and Network Representation	126
5.1.2. Mathematical Representations and Notations	128
<b>5.2. FORMULATION OF NODAL GOVERNING EQUATIONS</b>	130
5.2.1. Basic Equations	130
5.2.2. Nodal System Equation and Solution	134
5.2.3. Examples of Nodal Formulation	136
5.2.4. Automatic Formulation of Nodal System Equations	138
5.2.5. Properties of the Matrix F	140
<b>5.3. FORMULATION OF LOOP GOVERNING EQUATIONS</b>	140
5.3.1. Basic Equations	141
5.3.2. Loop System Equation and Solution	144
5.3.3. Examples of Loop Formulation	144
5.3.4. Automatic Formulation of Loop System Equations	145

<b>CHAPTER VI</b>	
<b>VALIDATION OF FLUCTUATING AIRFLOW MODEL . . . .</b>	<b>153</b>
<b>6.1. EVALUATION OF LINEARIZATION ASSUMPTION . . . . .</b>	<b>153</b>
6.1.1. Numerical Simulation Method . . . . .	155
6.1.2. Computer Program of Numerical Simulation . . . . .	157
6.1.3. Numerical Simulation Results . . . . .	159
<b>6.2. LABORATORY EXPERIMENTAL COMPARISONS . . . . .</b>	<b>160</b>
<b>6.3. VALIDATION WITH FIELD EXPERIMENTAL DATA . . . . .</b>	<b>166</b>
6.3.1. Test Set-up of BOUIN House . . . . .	166
6.3.2. Comparison of Results . . . . .	167
<b>6.4. DISCUSSION OF THE MODEL VALIDATIONS . . . . .</b>	<b>170</b>
 <b>CHAPTER VII</b>	
<b>CONCLUSIONS . . . . .</b>	<b>194</b>
 <b>REFERENCES . . . . .</b>	
 <b>APPENDIX A</b>	
<b>EXPERIMENTAL SETUP AND PROCEDURE . . . . .</b>	<b>205</b>
<b>A.1. LABORATORY EXPERIMENTAL SETUP . . . . .</b>	<b>205</b>
<b>A.2. EXPERIMENTAL PROCEDURE . . . . .</b>	<b>210</b>

# LIST OF FIGURES

1.1.	Eddy Flow and Pulsating Flow . . . . .	12
2.1.	Influence of Driving Forces on Airflow . . . . .	33
2.2.	Wind-Induced Pressures on Building Envelopes . . . . .	34
2.3.	Role of Mathematical Models in Building Ventilation Design . . . . .	35
2.4.	A Wind Velocity Spectrum Sample . . . . .	36
2.5.	A Sample of Davenport Wind Spectrum . . . . .	37
2.6.	A Sample of Coherence Function . . . . .	37
3.1.	A Two-Opening Building . . . . .	73
3.2.	A Four-Room Building . . . . .	74
3.3.	Graph Representation of the Four-Room Building . . . . .	75
3.4.	Calculated Airflow and Pressures for the Four-Room Building . . . . .	75
3.5.	Schematic Graph of an Opening for Steady-State Airflow . . . . .	76
3.6.	Indication of Discrepancy Between Sensitivity Calculation and Simulation . . . . .	76
4.1.	Schematic Diagram of an Opening for Fluctuating Airflow . . . . .	116
4.2.	Effects of Fluctuating Airflow to Air Exchange . . . . .	117
4.3.	Related Spectra and Transfer Functions of a One-Opening Enclosure . . . . .	118
4.4.	Positions of Related Spectra and Transfer Function for a One-Opening Enclosure . . . . .	119
4.5.	Related Spectra in a Two Opening Enclosure . . . . .	120
4.6.	Decomposition of Airflow Spectrum . . . . .	121
4.7.	Difference between Two Airflow Spectra . . . . .	121
5.1.	An Example of Graph Representation of a Building Fluctuating Airflow System . . . . .	148
5.2.	A Single-Enclosure Multiple Opening Building . . . . .	149
5.3.	MEGA House and Graph Representations . . . . .	150
5.4.	A Two-Room and Four-Opening Building . . . . .	151
5.5.	A Two-Room and Six-Opening Building . . . . .	151
6.1.	Flow Chart of Numerical Simulation Program . . . . .	174
6.2.	Simulation Results of the Single Opening Case . . . . .	175
6.3.	Flow Equation Estimation for Data Set JUN05 . . . . .	176

6.4. Experimental Data in the First Minute .....	177
6.5. Related Spectra for Data Set JUN05 .....	178
6.6. Related Transfer Functions for Data Set JUN05 .....	179
6.7. Tracer Gas Decay for Data Set JUN05 .....	180
6.8. Related Transfer Functions for Data Set JUL22 .....	181
6.9. Related Transfer Functions for Data Set JUL23 .....	182
6.10. Related Transfer Functions for Data Set APR29 .....	183
6.11. Related Transfer Functions for Data Set MAY12 .....	184
6.12. Related Transfer Functions for Data Set MAY19 .....	185
6.13. Related Transfer Functions for Data Set MAY22 .....	186
6.14. BOUIN Test House .....	187
6.15. Results of Pulsating Model for Data Set VB1312 .....	188
6.16. Coherence Functions as Aerodynamic Admittance Function from Data Set VB1312 .....	188
6.17. Results of Aerodynamic Admittance Approach for Data Set VB1312 ....	189
6.18. Results of Multi-Path Approach for Data Set VB1312 .....	189
A.1. Experimental Setup .....	214
A.2. Damper Unit .....	214
A.3. Tracer Gas Measurement System .....	215
A.4. Calibration Curve of the GC Analyzer .....	216

# LIST OF TABLES

2.1.	Current Research on Airflow and Related Studies . . . . .	38
2.2.	Approaches to Fluctuating Airflow Modelling . . . . .	39
3.1.	Symbols and Notations Used in Chapter III . . . . .	77
3.2.	Calculation Formulae of Basic Jacobian Matrices . . . . .	78
3.3.	Basic Jacobian Matrices of the Case Study . . . . .	79
3.4.	Sensitivity Analysis Results of the Case Study . . . . .	80
3.5.	Error Analysis from Single Parameter Variations . . . . .	81
3.6.	Error Analysis from Multiple Parameter Variations . . . . .	82
3.7.	Comparison between Sensitivity and Monte Carlo Approaches . . . . .	83
4.1.	Statistical Linearization Formulae for Power Law Equation . . . . .	122
4.2.	Parameters and Results of the Single-Opening Case . . . . .	123
4.3.	Parameters and Results of the Two Opening Case . . . . .	124
5.1.	Matrix, Dimensions, and Notations . . . . .	152
6.1.	List of Parameters for Single-Opening Case . . . . .	190
6.2.	Summary of Results for Laboratory Experiments . . . . .	191
6.3.	Comparison Results for Data Set VB1312 . . . . .	192
6.4.	Airflow Through Slot Opening for Data Set VB1312 . . . . .	193

# CHAPTER I

## INTRODUCTION

The trend in modern construction towards more airtight buildings and increased use of synthetic materials in construction, furnishings, and maintenance operations have increased the indoor airborne contaminant concentration levels. This, in addition to concerns about moisture transport and accumulation indoors, has raised concerns about indoor air quality in modern buildings from both health and durability perspectives. The transport of airborne contaminants throughout a building is caused by air movement driven by pressure differences between individual zones. The concern for better indoor environments and energy conservation requires the implementation of the best ventilation system and its optimal operation. This goal calls for an improved understanding of airflow circulation patterns within and through buildings, for procedures for simulations of buildings and ventilation systems with respect to airflow behaviour, and for the evaluation of their performance under different operating conditions.

Theoretical airflow models are important analytical tools for studying air infiltration and ventilation in buildings. It is closely related to research on indoor air quality and thermal analysis. Research has drawn international attentions from the



scientific community and governments of both industrial and developing countries. The research is also reaching into and drawing more participation from the industry and public. For example, the international research project COMIS (Conjunction Of Multizone Infiltration Specialists) has been organized by the Energy Performance of Building Group at Lawrence Berkeley Laboratory (LBL) and has drawn participation and support from 12 countries. Here in Canada, NRC (National Research Council Canada), CMHC (Canadian Mortgage and Housing Corporation), Public Works of Canada, EMR (Energy, Mines and Resources), and other organizations have been carrying out or sponsoring research related to airflow and air quality in buildings.

Airflow models predict air infiltration and ventilation of buildings resulting from combinations of three driving forces: wind-induced pressures, thermal buoyancy and mechanical ventilation systems. The results are used for building energy analyses and indoor air quality evaluations. Due to the complexity of weather conditions, building structure and occupant behaviour, the phenomenon poses a challenging task for its prediction. Many predictive models and estimation procedures have been developed.

The current research efforts on theoretical airflow models concentrate on predicting the steady-state airflow for single or multi-zone buildings. This leaves two aspects which lack much research. One is to develop the procedures for assistance in designing a building airflow system. The other is to predict the dynamic or fluctuating aspect of the building airflow.

The existing airflow models calculate airflow from given building characteristics. In practice, more information is required as to design a building for predefined goals. In

retrofitting a building, one would like to know, for example, how tight the building envelope should be to obtain the desired reductions in the air infiltration and ventilation rates and the associated energy consumption. In designing a building with low energy use while maintaining required ventilation rate and an acceptable indoor air quality, one needs to find the optimal design parameters. The solution lies in developing a sensitivity analysis procedure to assist the ventilation design process.

Temporal variations in driving forces, especially wind-induced pressures, cause fluctuating airflow in addition to the mean values. In many situations, single-sided ventilation for example, the fluctuations are the dominant forces in providing or causing natural ventilation. This aspect of the problem has drawn much attention recently.

With the emphasis on the fluctuating aspect, this thesis research is devoted to the development of a comprehensive framework for building airflow analyses and design. In dealing with temporal variations of driving forces, a fluctuating airflow model has been developed. Combined with the existing airflow models and contaminant transport models, the research provides a general methodology for airflow analysis, indoor air quality evaluation, energy analysis and building design assistance. A procedure for airflow sensitivity analysis has been developed to calculate the relation between a building as well as weather parameters and the resultant airflow of the building. Combined with the existing airflow model, the procedure can perform error analysis and facilitate the design of natural and mechanical ventilation systems. Both parts of the research will be carefully disseminated and modelled in this thesis, preceded by a literature survey on the status quo of related fields and areas. In the remainder of this chapter, the definition of the problem,

its practical value, the main objectives and thesis planning of the outlined research are identified.

## **1.1. DEFINITION OF THE PHYSICAL PROBLEM**

When air flows around a building with openings, airflow through the openings is induced by a variety of factors which can be broadly classified into two groups; those which induce steady-state airflow by virtue of their mean values, and those whose effect is due to a fluctuating nature. Factors which fall into the first group include mean wind pressures on the building surfaces, the effect of temperature differences between the inside and outside of the building, and the mechanical ventilation systems. Factors in the second group mainly include the fluctuating wind-induced pressures acting on external surfaces of buildings.

Airflow through individual openings can also be divided into the steady-state airflow and the fluctuating airflow. Steady-state airflow is caused by the mean pressure difference. For isolated individual openings, the mechanisms of airflow are complex under microscopic (fluid mechanical) examinations, and are different for different flow conditions or types of openings (Kronvall, 1980). However, as far as the relations between the airflow rate and the pressure difference are concerned, the existing research indicates that the power-law or quadratic-law can be used for crack type openings, while other relations are obtained for other types of openings (Walton, 1989; Feustel and Raynor-Hoosen, 1990). For airflow in an entire building, the calculation is further

complicated by many parameters, such as, the weather conditions, the interference among driving forces, building configurations, and occupant behaviour. The steady-state aspect has received much attention. The contribution of this research is to develop an airflow modelling and sensitivity analysis procedure for error analysis and design assistance. This is presented in Chapter III. In the rest of this chapter and thesis, the presentation is concentrated on the fluctuating aspect of building airflow systems.

Fluctuating airflow through individual openings is caused by the fluctuations in pressure differences. The phenomena can be divided into two types: pulsating flow and the penetration of eddies (Figure 1.1). Pulsating flow results from wind fluctuations and the compressibility of air in the building internal space. When the temporal variations in the wind cause simultaneous positive or negative pressure fluctuations on an opening, the inside air is either pressurized or depressurized. This results in incoming and outgoing airflow through the opening (Figure 1.1b).

Eddy flow is due to turbulence in the air stream. Eddies create a rotational effect on the inside air. This leads to a consistent exchange between inside air and outside air (Figure 1.1a). Eddies with dimensions of approximately the same size as the opening give the maximum fluctuating effect of inflow and outflow (Cockroft and Robertson, 1976). Eddy flow can also be viewed as a result of imperfectly synchronized pressures on the opening area. At any instant, the pressures are not uniform on the opening, thus, in addition to the mean airflow and the pulsating flow, eddies are produced which in turn cause extra air exchanges between the two sides of the opening.

In the case of multi-zone buildings, the pulsating flows also arise due to the lack of perfect correlations among fluctuating wind pressures acting on different locations of the building envelope (Figure 1.1c). At any instance and the following infinitesimal time lag, the fluctuating pressures may be increasing at one location while decreasing at other locations. If the internal zones are connected, this imperfect correlation would cause flows at both openings, as well as, at the related internal openings.

In a building with more than one opening, both types of fluctuating airflow exist at the same time. Eddy flow depends mainly on local turbulence field near the individual openings and is not significantly affected by the state of the other openings. On the other hand, the pulsating flows are more related to the flows and pressures at other openings. Therefore, eddy flow can be studied under more isolated conditions, while pulsating flow should be studied for the whole building.

Fluctuating airflow in a (multi-zone) building is further complicated by many factors. The fluctuating wind-induced pressures on building external surfaces are the primary driving forces, and their frequency characteristics directly influence the airflow. Although many field and laboratory (wind tunnel) measurements have been made for the mean values of the wind-induced pressure on building envelopes, little research has contributed to evaluate the frequency characteristics of wind pressures for the airflow study.

In addition, the steady-state airflow affects the fluctuating airflow. For each individual opening, the relationship between the pressure difference and the airflow is non-linear. The resultant fluctuating airflow of the same fluctuating pressure difference

is different for different mean pressure differences. The steady-state and fluctuating components are two interconnected aspects of a building airflow system.

In this thesis, a model for predicting fluctuating airflow in multi-zone buildings is developed. Both pulsating and eddy flows are accounted for. Inputs to this model include: building airflow system (rooms, openings, and connections); frequency characteristics of wind-induced pressures and their correlations; and output from a steady-state airflow model. The model is able to describe and predict the behaviour of fluctuating airflow through buildings. The output is the fluctuating airflow through all the openings and the internal pressure fluctuations.

## **1.2. IMPORTANCE AND APPLICATIONS OF FLUCTUATING AIRFLOW**

The fluctuating aspect of airflow becomes very important in certain situations, especially when the mean pressure differences are small while the fluctuations in the pressure differences are large.

The effects of wind turbulence on airflow are particularly important in the case of single-sided ventilation or when the wind direction is parallel to openings in two parallel facades. This is because in both cases the mean airflow rates are zero, while the fluctuating pressure differences are present (Liddament, 1986).

When the wind effect and stack effect are negating each other, situations arise when the net pressure differences across openings are zero or very small. Fluctuating airflow

will play a dominant role, and the predictions based on steady-state models will not be able to provide an adequate solution (Etheridge, 1984; Wouters, 1981).

For low-rise buildings that are surrounded by tall buildings, the mean wind pressures on building envelopes are small, while the fluctuating components can be large. The assessment of the air exchange requires analysis of the fluctuating aspect.

In calm weather, the main source of infiltration for naturally ventilated houses comes from the fluctuations in wind. It is of concern whether the resultant fluctuating infiltration is able to provide sufficient fresh air exchange into the building and remove pollutant effectively. This requires the assessment of the effect of fluctuating driving forces on natural ventilation rates.

CMHC (Canadian Mortgage and Housing Corporation) had sponsored several projects to investigate heating system failures and the consequences on indoor air quality. One report stated that "the failure of residential heating systems to properly expel their products of combustion from the interior of houses is an emerging problem in Canadian housing with potential detrimental effects on indoor air quality" (CMHC, 1987). The results of the investigation showed that the backdrafting due to house depressurization is one major failure mechanism. Wind-induced pressures on top of the chimney and around the building envelope partially contribute to the pressurization/depressurization. Due to the lack of definite knowledge on the fluctuating aspect of wind pressures, analysis was based on mean values. Solutions to the fluctuating aspect of airflow could furnish better understanding of the mechanism.

Pollutants are transported along with airflow. The predictions of contaminant migration through buildings require accurate calculations of airflow, and in many cases, of both mean values and fluctuating components.

Some other building phenomena, which depend on the fluctuating characteristics of airflow and internal pressures, such as double dashed windows (Sasaki et al., 1987), pressure equalized rainscreen walls (Baskaran, 1992) and dynamic walls (Morrison, 1992), will have to be studied together with the fluctuating airflow systems. This naturally requires models for the combined building structural and fluctuating airflow systems.

As a research domain itself, solutions to fluctuating air infiltration and ventilation remain largely unsolved. Many research efforts, such as an on-going international collaborate research project IEA-Annex 23 (IEA-Annex, 1992), are still under way in searching for solutions.

All these practical situations and the need for theoretical solutions demand more study and new models to predict fluctuating airflow caused by temporal variations in wind-induced pressures.

### **1.3. OBJECTIVES AND PLAN**

The objective of this thesis research is to develop a comprehensive framework and methodology for airflow analyses and design assistance for buildings under both mean and fluctuating driving forces. The research effort is concentrated on the development and validation of a fluctuating airflow model to predict the effects of temporal variations



in wind-induced pressures. Efforts have also been made to develop a procedure for airflow sensitivity analysis to assist in the building design process.

**Specific objectives are:**

- to apply system theory to the modelling processes for both steady-state and fluctuating aspects of airflow models;
- to develop a formulation procedure for airflow sensitivity analysis;
- to study the characteristics of fluctuating driving forces and to understand the mechanism of fluctuating airflow;
- to examine the relationship between fluctuating driving forces and resultant airflow, and to employ the statistical linearization method;
- to introduce the spectral analysis method to provide solutions to the fluctuating airflow system;
- to develop formulation procedures for the governing equations using the system theoretic approach; and
- to evaluate and validate the developed fluctuating airflow model.

The remainder of the thesis is arranged into six chapters. In the next chapter, a literature review of air infiltration and ventilation on both steady-state and fluctuating aspects is presented.

In Chapter III, the steady-state airflow modelling using a system theoretic approach and airflow sensitivity analysis are presented.

In Chapter IV, the fluctuating airflow model is presented. This includes: the component modelling, the statistical linearization method, and the basic concepts of spectral analysis. Two hypothetical cases are solved to demonstrate the procedure of the proposed method.

In Chapter V, system theoretic formulation procedures for governing equations of fluctuating airflow in multi-zone buildings are presented.

In Chapter VI, the validation of the fluctuating airflow model is presented. Three validation schemes are employed: numerical simulations, laboratory experiments and field experiments.

In the last chapter, conclusions and future research directions are presented.

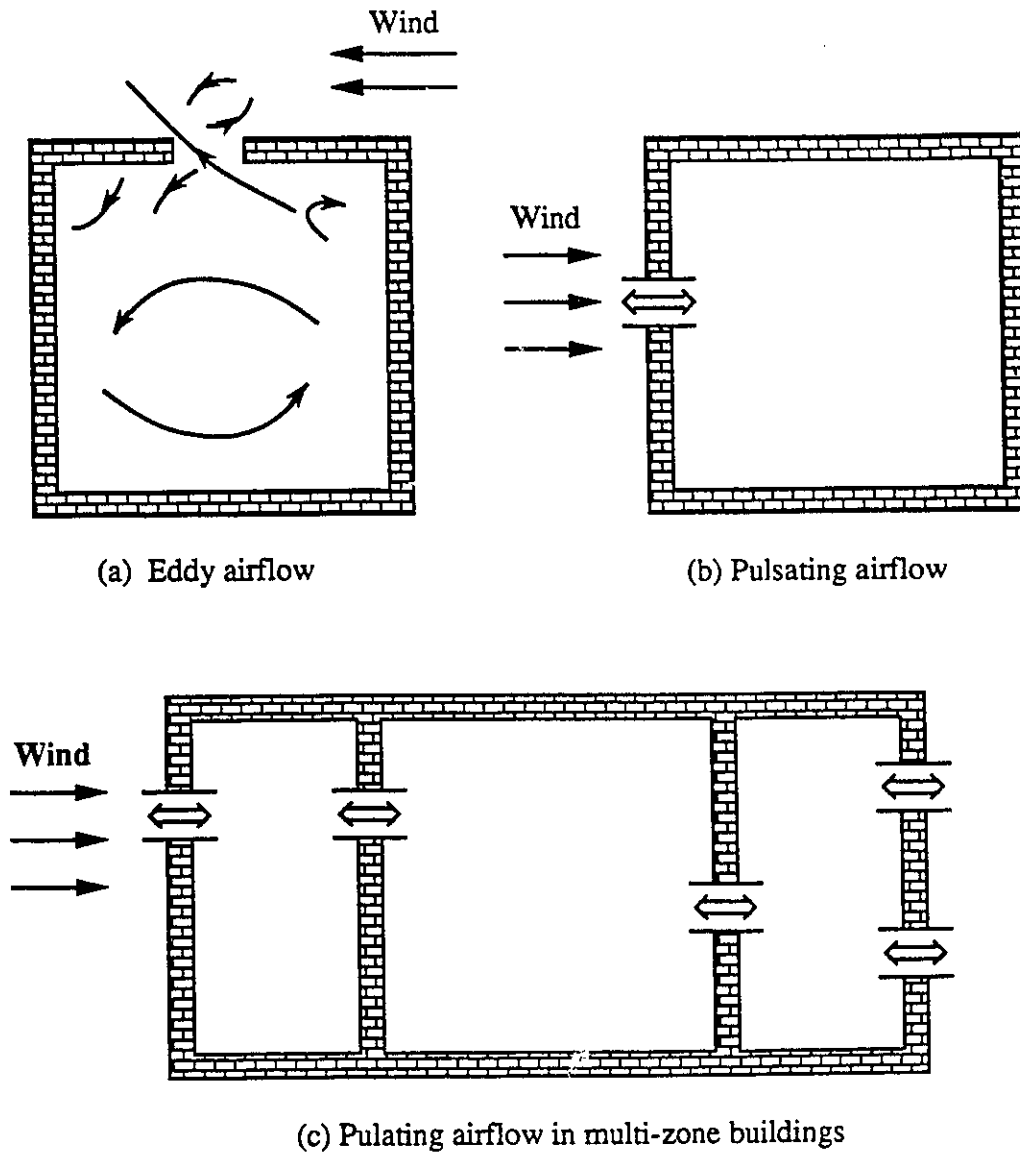


**Figure 1.1. Eddy Flow and Pulsating Flow**

# **CHAPTER II**

## **LITERATURE REVIEW**

The growing concerns about indoor air quality and energy conservation, as well as global environmental risks of excess energy use, have motivated extensive research on various aspects of building environments. The study on air infiltration and ventilation of buildings is one of the fastest growing fields that contribute to designing buildings with healthier indoor environments and minimum energy demands.

As a central theme of this thesis, the airflow through building openings is considered to consist of two parts: steady-state and fluctuating. The two parts are dealt with separately, and then are combined to predict the total airflow rates.

In this chapter, the review is divided into two sections. In Section §2.1, the general mechanisms of air infiltration and ventilation, and general roles and structure of airflow models are outlined with emphasis on the network approach to the steady-state airflow modelling. In Section §2.2, pertinent information and existing research related to the modelling and predictions of fluctuating airflow are reviewed.

### **2.1. STEADY-STATE AIRFLOW MODELLING**

Extensive research has been carried out on various aspects of the steady-state airflow models (Table 2.1). The driving forces of air infiltration and ventilation in

buildings are identified as wind-induced pressures, thermal buoyancy, and mechanical ventilation systems. The airflow models are developed as analytical tools to assist the building ventilation design process and to provide necessary information for energy calculations, indoor pollutant dispersion analysis and related studies. Modelling, formulation and solutions are the basic constituents of an airflow model.

### **2.1.1. Mechanism of Air Infiltration and Ventilation**

#### **2.1.1.1. Openings and Flow Equations**

Buildings have many openings in their envelope surfaces and within the partitions that separate rooms. In most literature, openings are placed into three categories: (1) purpose-provided openings such as air vent, windows, etc.; (2) component openings which are identifiable cracks that occur around doors and windows; (3) background leakage areas which are the openings that remain after the first two types of openings are sealed, such as cracks between walls and floors. The geometry of the first two openings can be measured while the third type of openings cannot be easily identified. The last two types of openings are collectively referred to as *adventitious openings*. Fresh air entry through these openings is called *infiltration*. The term *ventilation* is used for the airflow through the purposed-provided openings (Etheridge and Gale, 1983). In this thesis, however, the term airflow is used as a general term for describing air movement through openings due to both air infiltration and ventilation.

In general, pressure drops may occur due to flow resistances along flow paths. Two forms of flow equations are commonly used to describe the flow through component

openings and background cracks: the quadratic form and the power law form. Many other forms and types of flow equations had been used in other airflow models for cracks, large opening, ducts and fans (Feustel and Dieris, 1992).

The power law form is written as:

$$Q = K \Delta P^n, \quad (2-1)$$

where the component permeability,  $K$ , is a function of Reynold's number and the ratio of the opening size to the entire surface. The value of exponent  $n$  is in the range of 0.5 to 1.0 depending on the type of the flow;  $n = 0.5$  for inertia flow, and  $n = 1$  for viscous flow. Values of  $K$  and  $n$  can be measured by the fan pressurization technique (DC) or the AC pressurization technique (Roulet and Vandaele, 1991; Liddament 1986).

#### **2.1.1.2. Driving Forces**

Air infiltration and ventilation is a complex phenomena due to the nature of the airflows and the complexity of building structures. Generally, air infiltration and ventilation are the airflows through openings on building structures and are due to the action of pressure differences across openings.

There are three sources of pressure differences: wind-induced pressures, thermal buoyancy and mechanical ventilation systems. Wind produces a pressure distribution over the external surfaces of the building. The buoyancy of air within the building leads to vertical pressure gradients. The mechanical fans affects the internal pressure distribution. The influence of these three driving forces on airflow in buildings is shown in Figure 2.1.

### Wind-Induced Pressure

Wind within the lower region of the earth's atmosphere is characterised by random fluctuations in the velocity which, when averaged over a fixed period of time, poses a mean value of speed and direction. On impinging the surface of a building, the wind deflection induces a positive pressure on the windward face. The flow separates at sharp edges of the building, giving rise to negative pressures along the sides. Negative pressures are also experienced with the wake region on the leeward face. Figure 2.2 shows some examples of pressure distribution on the walls and roof of a building, for different wind incidence angles.

In general, the time averaged pressure acting at any point on the surface of a building is related to the static pressure of the free wind, and may be represented by the equation:

$$P^w = C_p \frac{1}{2} \rho V_h^2, \quad (2-2)$$

where  $P^w$  is the surface pressure due to wind (unit: Pa),  $C_p$  is the mean pressure coefficient, and  $V_h$  is the mean wind velocity at the building height (m/s).

The pressure coefficient,  $C_p$ , is an empirically derived parameter and is a function of the pattern of flow around the building. It is normally assumed to be independent of wind speed but varies according to wind direction and position on the building surface. It is also significantly affected by neighbouring obstructions. A similar building subjected to different surrounding may be expected to exhibit markedly different pressure coefficient patterns. Accurate evaluation of this parameter is one of the most difficult

aspects of airflow modelling, and it is not possible by theoretical means alone. Although pressure coefficients can be determined by direct measurements of real buildings, most information is based on scale models in wind tunnels.

Based on a large set of data, Swami and Chandra (1988) studied, using nonlinear regression techniques, the effects of wind incident angle and building side ratio on the pressure coefficient distribution over building external surfaces, and proposed an improved procedure for calculating wind driven natural ventilation rates. Grosso (1992) proposed parametrical correlations to express the wind pressure distribution around buildings by factors such as terrain roughness, surrounding buildings, aspect ratios, and wind directions. A data base of wind coefficients is also available (Allen, 1984).

Research has been carried out to calculate wind pressure distributions around the external surfaces of a building by means of CFD (Computational Fluid Dynamics) (Jones and Whittle, 1992; Baskaran and Stathopoulos, 1989; Haggkvist, et al., 1989; Murakami and Mochida, 1989; Paterson and Apelt, 1989; and Mathews, 1987).

### Stack Effect

The difference in air temperature and hence densities between two sides of a wall affects airflow through the building. The pressure difference across an opening,  $\Delta P^S$ , due to the stack effect can be calculated by:

$$\Delta P^S = g(\rho_j h_j - \rho_i h_i). \quad (2-3)$$

where  $\rho_i$  and  $\rho_j$  are the air density in rooms  $i$  and  $j$ , respectively, and  $h_i$  and  $h_j$  are the opening heights with respect to reference heights of rooms  $i$  and  $j$ . Using the ideal gas



law, equation (2-3) can be rewritten as:

$$\Delta P^s = g \frac{P_a}{R_a} \left( \frac{h_j}{T_j} - \frac{h_i}{T_i} \right), \quad (2-4)$$

where  $T_i$  and  $T_j$  are the air temperature in zones  $i$  and  $j$ ,  $P_a$  is the atmospheric pressure,  $R_a$  is the characteristic gas constant and  $R_a = 287$  (J/Kg·K).

### **Mechanical Ventilation Systems**

Mechanical ventilation systems are installed in buildings to provide additional outside air, to remove indoor pollutants, or to provide "total" man-made indoor environments. Mechanical systems are usually modelled as airflow paths. The cubic polynomial (Walton, 1989) and other forms of relations (Feustel and Dieris, 1992) have been used to describe the fan performance.

#### **2.1.2. Roles and Structures of Mathematical Models**

The role of airflow models as an aid in the building ventilation design process has been discussed by Liddament (1986). Using information concerning climate, shielding and terrain parameters, combined with design details as input data; the mathematical/theoretical airflow models are used to predict the corresponding air change rates, airflow patterns, energy requirements, and cost benefits. The variables over which the designers have control can then be optimized to best suit their requirement (Figure 2.3).

Steady-state airflow models have received much attention. There are basically two approaches: network modelling and correlation. Network modelling assumes that

buildings are composed of nodes interconnected by elements of openings, and the system theoretic method can be used to formulate system equations (Haghighat and Rao, 1991). The correlation approach attempts to establish an empirical relation between air exchange rates and information of the building characteristics, surroundings and climate data (Liddament, 1986).

The structure of any airflow model should include three basic components: modelling, formulation and solutions. The three basic components of airflow models are related but each component is independent as to what specific method is chosen for that individual component. This independence makes it possible for modularity in computer implementations such as the modular airflow model COMIS (COMIS, 1989).

#### **2.1.2.1. Modelling Steady-State Airflow Systems**

The modelling process is the characterization of components by mathematical relations. The primary concern of modelling lies in the translation of physical properties and geometric design specifications of every component in a building airflow system into the mathematical formulation. The modelling process involves forming assumptions to simplify reality into manageable problems. For example, the assumption that all physical properties are measurable at discrete points of a component has been implicitly used by most researchers in developing their airflow models.

Modelling represents processes and methods used to transform the physical building airflow system into a conceptual model. In the network approach to steady-state airflows, a building is represented by a network of nodes interconnected by flow

elements. The nodes and elements are chosen in such a way so as to closely simulate the real airflow system of the building. Each node is assumed to have a uniform temperature and pressure. One flow element usually represents an airflow path and is assumed to transport air instantly.

#### **2.1.2.2. Governing Equation Formulation for Steady-State Airflow**

In the formulation process, a set of equations describing the overall building airflow system is developed from the conceptual model of the real building system. In the network approach, the set of system equations is usually derived from air mass conservation in each zone (node) of a building. The nodal pressures are unknown in the equations. A detailed derivation of the system equations is presented in Chapter III. An alternative formulation derives the set of equations from loop equations (known as circuit postulate in network theory). This method also reaches a set of nonlinear equation but with the loop airflow rates being the unknown variables.

#### **2.1.2.3. Solution Algorithm for Steady-State Airflow**

Solution algorithms are mathematical procedures of determining solutions to the system equations. The nonlinear dependency between the air flow rate and pressure difference results in solving a set of non-linear mass balance equations. The solution is obtained by an iterative technique, which progressively adjusts the nodal pressures until the convergence criterion is satisfied. Different types of algorithms for calculating the adjustment or correction term have been used in airflow models (Herrlin and Allard,

1992). Most models use the well-known "Newton-Raphson" technique, or its modified versions. As an example, the standard Newton-Raphson algorithm is used in the Oscar Faber model (Irving, 1979), while the Relaxed Newton-Raphson is used in the NBS airflow model (Walton, 1983).

### **2.1.3. Related Studies**

Determination of air infiltration and ventilation rates in buildings represents only a part of the overall ventilation design need. Having satisfactorily predicted the ventilation performance of a building, it is necessary to determine the impact of air infiltration and ventilation on both the building heat loss, and the desired ventilation strategy (Liddament, 1986).

The heating load calculation is a major objective for predicting airflow in buildings, and has been incorporated in major energy consumption analysis programs, such as BLAST and TARP (Hittle, 1978; Hittle, 1979). Air infiltration and ventilation greatly influence the heating requirements and performance of buildings (Okuyama, 1990; Bielek and Cemik, 1987). Integrated models for predicting the coupled problem of airflow and heating calculations have also been developed (Axley, 1989).

Contaminant transport and dispersion analysis models are used to study the behaviour of indoor pollutant generation and migration in building, so as to devise better ventilation strategies to remove or dilute the pollutants inside buildings or working spaces (Axley, 1988a; 1988b).

Most airflow and contaminant transport models assume uniform air and contaminant distributions, while, in reality, fresh air and pollutants are not uniformly distributed. The study of air exchange efficiency and ventilation effectiveness requires the examination of the room air replacement efficiency and pollutant removal effectiveness (Haghighat, et al., 1990). Liddament (1987) provided a comprehensive review on this subject.

Many research efforts have been devoted to the development of air measurement techniques. The most widely used experimental methods are the building pressurization techniques and the tracer gas techniques (Roulet and Vandaele, 1991; ASHRAE, 1989; Charlesworth, 1988; and Can/CGSB-149.10-M86, 1986).

## **2.2. FLUCTUATING AIRFLOW MODELLING**

Fluctuating airflow through buildings is a complex process, and has yet to be fully studied. Temporal variations in the wind-induced pressures on building external envelopes have been recognized ever since the start of airflow studies. However, due to the complexity of the problem, assumptions were made to consider only mean values. Only a few studies have attempted to model the fluctuating air infiltration caused by variations in the wind driving forces (Haghighat, et al., 1991).

### **2.2.1. Wind Characteristics in the Frequency Domain**

Fluctuations in wind-induced pressures on the surfaces of a building are due to the gustiness of the wind and the interactions between the wind and the building envelope.

These fluctuations display statistical regularity (Simiu and Scanlan, 1986). Although frequency characteristics of wind and the induced pressures have been studied in wind engineering (Simiu and Scanlan, 1986; Stathopoulos, 1980) and have been used for wind load calculations, their applications in the field of air infiltration and ventilation studies require more research efforts. Nevertheless, the importance of the frequency characteristics of driving forces and the resultant airflow has been recognized.

#### 2.2.1.1. Fluctuating Wind Velocity

The instantaneous wind speed is a random variable. The features of concern within the fluctuations are: the turbulence intensity, the integral scales of turbulence, the spectra of velocity fluctuations, and the cross-spectra between velocity fluctuations. For the longitudinal wind velocity, the *turbulence intensity* is defined as the ratio of the RMS value to the mean wind speed. The value is around 0.16 for the wind speed high above the ground and increases near the ground (Simiu and Scanlan, 1986). Similarly, the *turbulence intensity of the wind-induced pressure* can be defined as the ratio of the RMS to the mean pressure. For the windward facade this value is about 2 times the value for the oncoming velocity. For the wind pressures on low-rise buildings, turbulence intensity values around unity have been reported (Gusten, 1989)

The *integral scales of turbulence* are measures of the average sizes of turbulent eddies, which, in turn, influence the eddy flow through building openings. There are nine integral scales of turbulence, corresponding to the three dimensions of eddies associated with longitudinal, traverse, and vertical components of the fluctuating velocity.

The *power spectrum* of the fluctuating wind velocity indicates the energy distributions of different eddy sizes, and is a function of the frequency. Figure 2.4 shows a plot of the wind velocity spectrum from van der Hoven (1957). Four peaks exist on the figure, corresponding to: (a) the year variations of wind, (b) quadra-daily (4 days) variations, (c) bi-daily variations, and (d) turbulence (or gustiness) of wind. The fluctuation corresponding to the fourth peak due to wind gustiness and its effects on building airflow are of main interest to this thesis. The corresponding frequency range of this peak varies between 0.002 to 0.02 Hz (Lumley and Panofsky, 1964). It has been demonstrated that no more peaks occur at higher frequencies, and the fluctuations become exclusively random at higher frequencies (Kronvall, 1980).

Davenport (1961) proposed an empirical expression for the wind velocity spectrum,  $S_u(f)$ , in lower frequency ranges, which is expressed as:

$$S_u(f) = \frac{4.0 \cdot u_*^2}{f} \times \frac{x^2}{(1 + x^2)^{4/3}}, \quad (2-5)$$

where  $f = \omega/2\pi$  is the frequency,  $x = 1200f/U(10)$ ,  $U(10)$  is the wind velocity at 10m above ground,  $u_*^2 = (1/6)\sigma_u^2$  is the frictional velocity, and  $\sigma_u$  is the RMS value of the wind velocity. A sample plot for this spectrum is shown in Figure 2.5. Davenport's spectrum tends to underestimate the velocity turbulence at frequencies lower than the frequency where the peak of the spectrum occurs, and overestimate the turbulence at frequencies higher than the peak frequency.

The *cross-spectrum* of two velocities  $u_1(t)$  and  $u_2(t)$  is a measure of the degree to which the two velocities are correlated. It is related to the coherence function. In a

homogeneous turbulence flow, the cross-spectrum is defined as:

$$S_{u_1 u_2}^c(r, f) = S_{u_1}^{1/2}(z_1, f) \cdot S_{u_2}^{1/2}(z_2, f) \cdot coh(r, f). \quad (2-6)$$

The term  $Coh(r, f)$  is called the *coherence function*. For two velocities on windward facades, it can be expressed by an empirical relation (Vickery, 1970):

$$Coh(r, f) = e^{-\hat{f}}, \quad \hat{f} = \frac{f [C_z^2(z_1 - z_2)^2 + C_y^2(y_1 - y_2)^2]^{1/2}}{\frac{1}{2}[U(z_1) + U(z_2)]}, \quad (2-7)$$

where  $y_1, z_1$  and  $y_2, z_2$  are the (vertical and horizontal) coordinates of two points where velocities  $u_1(t)$  and  $u_2(t)$  are measured, and they are on the same plane perpendicular to the direction of mean wind.  $C_z$  and  $C_y$  are coefficients determined by experiments. Figure 2.6 shows the coherence function as a function of the frequency.

#### 2.2.1.2. Wind-Induced Fluctuating Pressures

Pressures induced by the wind on external walls of buildings depend on both meteorological parameters and parameters which are characteristics of the building (Stathopoulos, 1980; Baechlin, 1987). These parameters include: incoming wind speed and directions, (longitudinal) velocity turbulence intensity, turbulence length, surrounding terrain type, building dimension and shape, opening size and position.

Wind is unsteady in nature, so the wind-induced pressure is expected to be unsteady. The sources of unsteadiness can be placed into three categories: a) turbulence or gustiness of wind, b) turbulence caused by the building structure itself such as wake shedding, and, c) turbulence induced by movements of the building structures. It has



been shown through wind tunnel tests that a similarity exists between the oncoming turbulent energy spectra and surface pressure spectra; and suggested that the upstream turbulence plays a dominant role in producing the pressure fluctuations on the windward face of a bluff body (Cermak and Sadeh, 1971). Therefore, the pressure spectrum,  $S_p(f)$ , may be expressed in an approximate proportion to the wind velocity spectrum,  $S_u(f)$ , in:

$$S_p(f) \propto \left( \frac{2P^w}{U(z)} \right)^2 \cdot S_u(f) \quad (2-8)$$

where  $P^w$  is the mean wind-induced pressure and  $U(z)$  is the mean wind velocity.

### 2.2.1.3. Correlations Between Wind-Induced Pressures

The correlations between the wind pressures at different locations of a building envelope also influence the fluctuating airflow. A correlation between two fluctuating pressures indicates the "spontaneity" between the pressure in pressing or pulling on the building envelope.

For pressures on the windward facade, the cross-spectrum of two pressures is given as:

$$S_{p_1 p_2}^c(r, f) = S_{p_1}^{1/2}(z_1, f) \cdot S_{p_2}^{1/2}(z_2, f) \cdot Coh(r, f), \quad (2-9)$$

where  $Coh(r, f)$  is given by equation (2-7).

For the correlation between pressures on the windward side and pressures on a side face, Vellozzi and Cohen (1968) proposed a relation as:

$$Coh(f) = Coh(r, f) \cdot N(f) \quad (2-10)$$

where

$$N(f) = \frac{1}{\xi} - \frac{1}{2\xi^2}(1 - e^{-2\xi^2}), \quad \xi = \frac{15.4 f \Delta x}{U} \quad (2-11)$$

where  $U$  is the mean wind speed at elevation  $(2/3)H$ ;  $\Delta x$  is the minimum of the building width, height and depth; and  $Coh(r, f)$  is coherence function given by equation (2-7).

### 2.2.2. Phenomena and Mathematical Descriptions of Fluctuating Airflow

The temporal variations in the wind-induced pressures on a building envelope cause fluctuations in the resultant airflow through the building. This phenomenon has been observed by previous research. Mathematical descriptions are searched for to depict the involved variables and to characterize the relationship among them. Research has also been conducted to identify the discrepancy between the steady-state airflow prediction and the air exchange influenced by pressure fluctuations.

Crommelin and Vriens (1988) conducted a laboratory experiment on pulsation flow of single-opening enclosures. Observations from test results indicate that airflow through an opening depends on the local turbulence and the turbulence intensity of the wind. The frequency power spectra must be taken into account in order to obtain accurate predictions. The turbulence of the wind pressure can be contributed by several factors a) eddies in the stagnant zone, b) eddies caused by interaction between the airflow and the building, and c) eddies caused by interactions between the airflow in the boundary layer and the inside air near the window opening (Malinowski, 1971). The second factor is considered as the most significant.

Gusten (1989) measured wind pressure spectrum on four real low-rise buildings,

and recognized the necessity of spectrum considerations in the calculation of fluctuating infiltration. Haghighat et al. (1988) developed a stochastic method to investigate the stochastic nature of forcing functions on the quality of indoor air.

Lay and Bragg (1988) attempted to employ statistical tools in representing data from experiments to study dynamic airflow. They noticed the stochastic nature of the parameters involved and used probability density functions, mean, standard deviation, autocorrelation and power spectrum to describe the measurements made concerning pressures and airflow rates. They concentrated on identifying fluctuating characteristics at very low frequencies corresponding to time scales of 6 to 24 hours.

Certain assumptions have been made regarding the frequency characteristics of pressure variations and airflow fluctuations. Etheridge and Alexander (1980) assumed that the fluctuating pressure distribution with respect to time has a Gaussian distribution.

Identification of the dynamic flow relation between fluctuating pressure difference and resultant airflow is an important aspect of fluctuating airflow modelling, and requires to be fully explored. Most researchers, when needed, employ the steady-state flow relations in studying dynamic situations. Studies by Kronvall (1980) showed that for individual openings, the relationship between the fluctuating pressure differences and the flow rate is only slightly affected by fluctuations at high frequencies, and is hardly affected at low frequencies. Sahin et al. (1988) investigated, through experiments and theoretical model the pulsating (without reversal) flow through orifices under superimposed pressure differences of mean value and single sine wave. The experimental tests were performed on a laboratory scale model in a wind tunnel in order to investigate

unsteady flows through apertures. The exact relationship has not been fully revealed. As pointed out by Vandaele and Wouters (1989) in their review paper, very few correlations have been proposed and most of them concern very particular configurations.

Pressure fluctuations influence in the air exchanges in buildings. The effect is especially significant when the mean pressure differences across openings are low while their fluctuating components are large. This happens in several types of situations, such as: single-opening enclosures (Potter, 1979), two parallel openings, when wind effect and stack effect are neutralizing each other (Wouters, 1987), and flow reversal (Etheridge and Gale, 1983), etc. A few field experiments (Gusten, 1989; Riberon, et al., 1989; Etheridge and Nolan, 1979; Potter, 1979; Hill and Kusuda, 1975) have been conducted to investigate the effects of wind fluctuations in air exchanges. Discrepancies were found between measured air exchange values and those calculated by steady-state prediction procedures or models.

Hill and Kusuda (1975) conducted some field experimental tests on pulsation flow in a single-opening room, and found discrepancies between measured air flow rates due to wind and the predicted values calculated by ASHRAE procedures. Potter (1979) conducted several field experiments to quantify the difference between actual dynamic ventilation rates and the natural ventilation rates predicted using a steady-state model. Results from field experiments showed that measured values of air change rates were generally 20 to 30 percent higher than the predicted values by steady-state calculations. These findings indicate the significance of the dynamic aspect of natural ventilation.

### 2.2.3. Existing Fluctuating Airflow Models and Correlations

The existing modelling approaches can be divided into several categories (Table 2.2). Cockroft and Robertson (1976) studied the pulsating flow of a single-opening enclosure subjected to a fluctuating impinging air stream. They derived a simple theoretical pulsation model to assist in understanding the physical phenomena causing airflow through the opening. Solutions were compared to limited experimental data. Narasaki et al. (1987) also studied this pulsation model and designed more comprehensive (tracer gas) experiments to evaluate the effect of the wind incidence angle on the amount of fluctuating airflow. This special case of single-opening buildings has also been studied by Cermak and Sadeh (1971), Vrins (1986), Crommelin and Vrins (1988), and van der Mass et al. (1991).

Sasaki et al. (1987) employed a dynamic analysis method to account for the fluctuating airflow caused by wind turbulence. A building was modelled by its corresponding mechanical system consisting of mass, resistance and elastic forces. The resultant second order differential equations were solved to obtain responses excited by a sine-wave wind pressure. The model was applied to multiple room buildings and to other problems such as the buffering effect of double sashed windows. A specially designed testing method was used to provide data for experimental comparison.

Holmes (1979) used second-order non-linear differential equations (Helmholtz resonator) to model the internal pressure fluctuations due to wind. Equations were solved numerically with a lumped-impulse method. Results showed good agreements in the frequency domain with the wind tunnel scale-model testing data. Kazic and Novak

(1989) derived similar equations using fluid mechanical principles (continuity equation, energy equation, Bernoulli's equation and ideal gas equation). Saathoff and Liu (1983) extended the Helmholtz model for studying the problem of pressure variations with suddenly-opened windows in a multi-zone building. Davenport and Surry (1984) made some valuable analysis on the Helmholtz resonator model, for example, the condition of resonance.

Etheridge and his colleagues (Etheridge and Gale, 1983; Etheridge and Alexander, 1980) developed a multi-zone model which accounts for the pressure fluctuations due to wind turbulence. The fluctuating airflow is assumed to be proportional to the RMS value of the fluctuating wind pressure. The coefficients depend on the opening characteristics and empirical constants. Phaff and De Gidds (1980) proposed a simple empirical correlation which describes the airflow rate through an open window as a function of the temperature, wind velocity and fluctuating terms that account for the additional air exchange when the influence of wind and temperature is zero.

#### **2.2.4. Inadequacies of Existing Research**

The inadequacies of the existing approaches and models are: (1) Most of them use numerical simulation methods, which are time consuming and require large amounts of computations. The simulation also requires large amount of wind pressure data with reasonable accuracy in representing typical characteristics of wind pressures. (2) The dynamic characteristics of the wind pressures are not been utilized except for the implicit use of time data. The frequency characteristics are more stable measures of the

fluctuating pressures compared to the time data, which changes every time pressures are measured. (3) Most of the models do not separate the steady-state from the fluctuating components (except from Etheridge's correlation, Etheridge and Alexander, 1980), thus can not be easily incorporated into the existing steady-state airflow models.

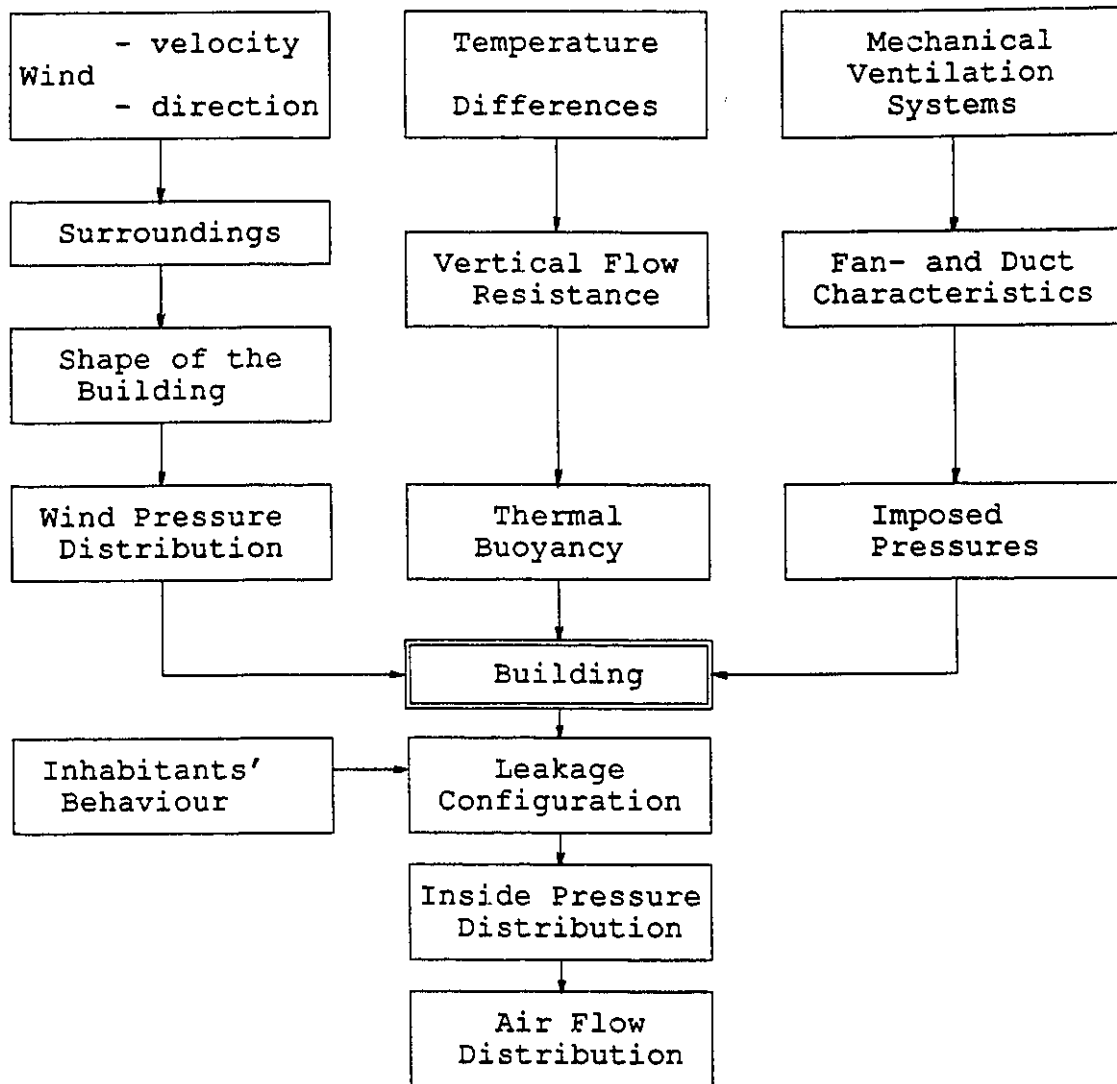


**Figure 2.1. Influence of Driving Forces on Airflow**  
(Adapted from Feustel and Dieris, 1992)



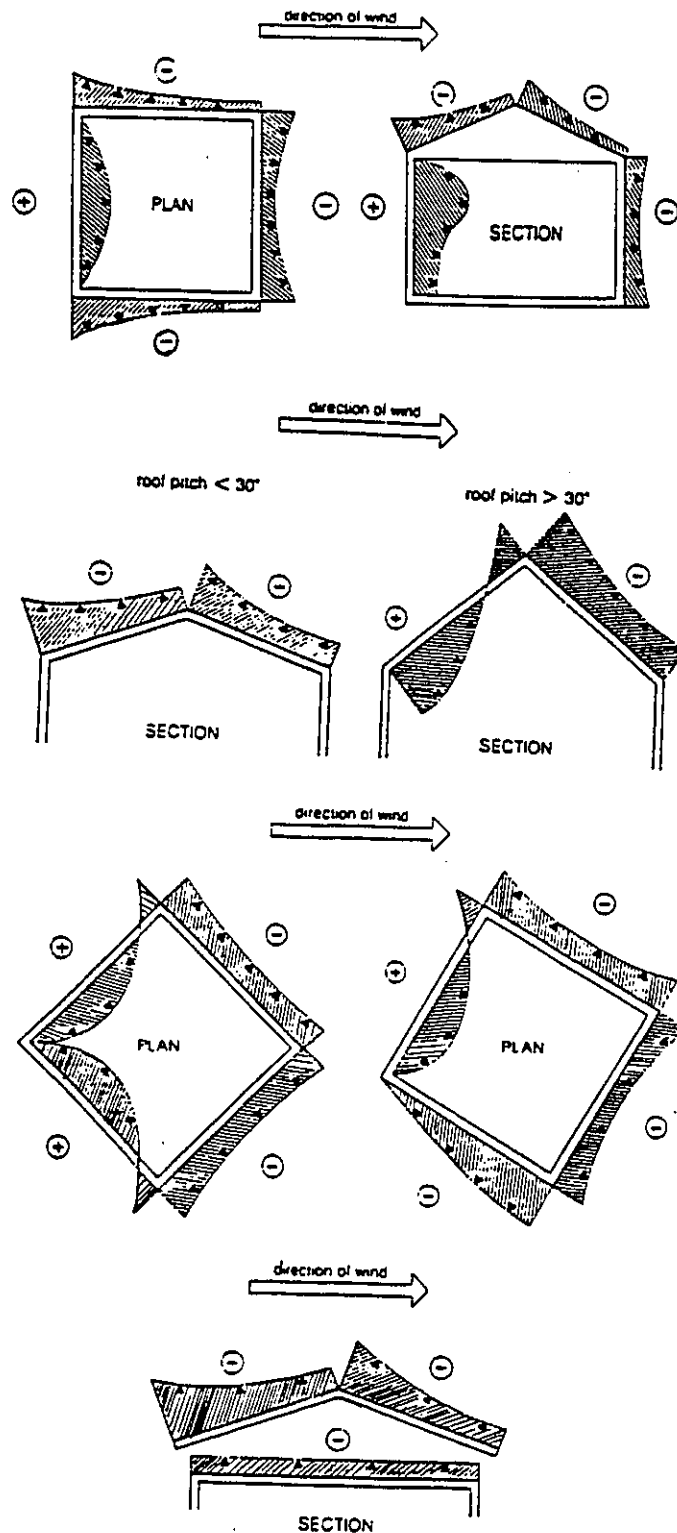
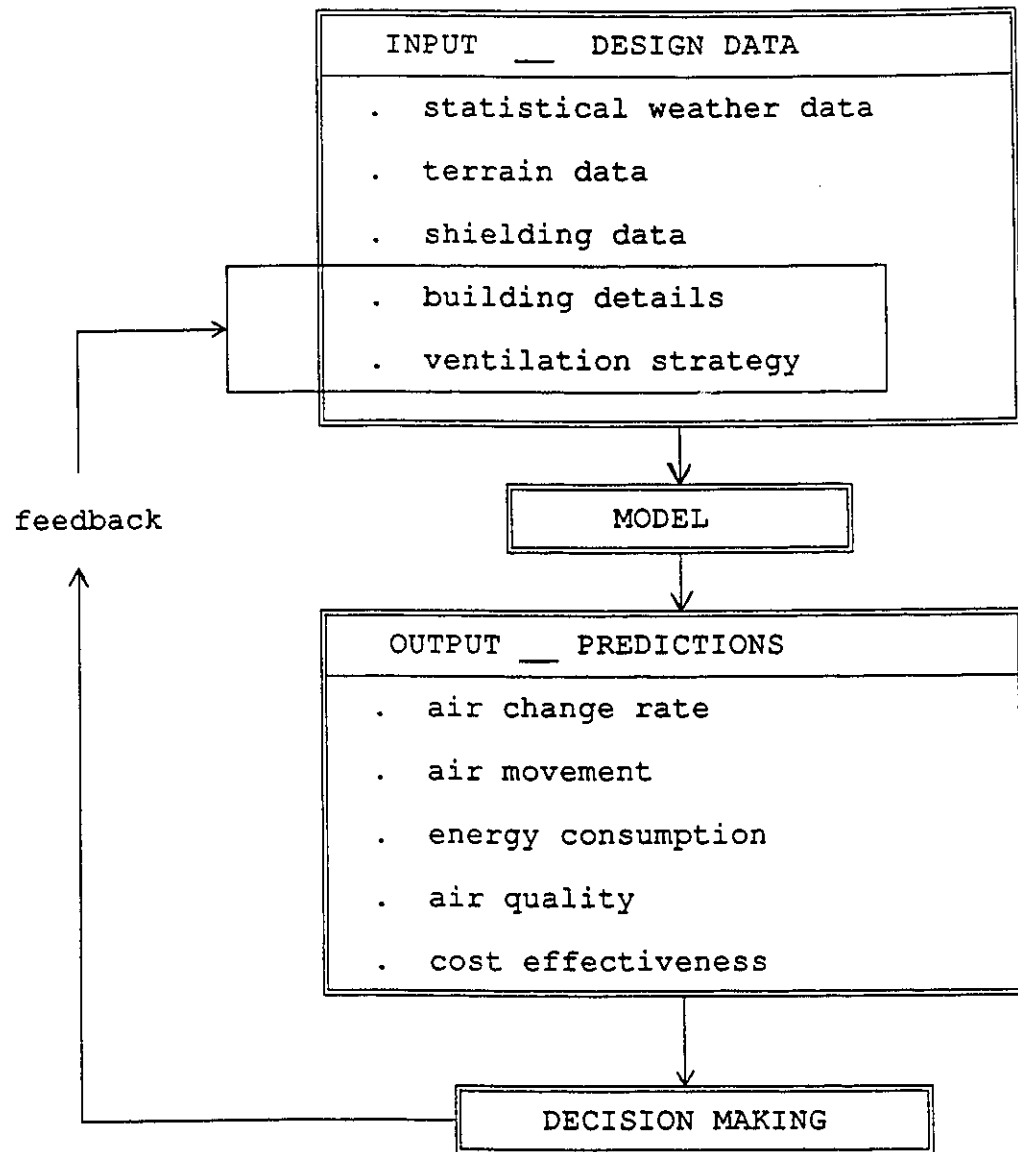
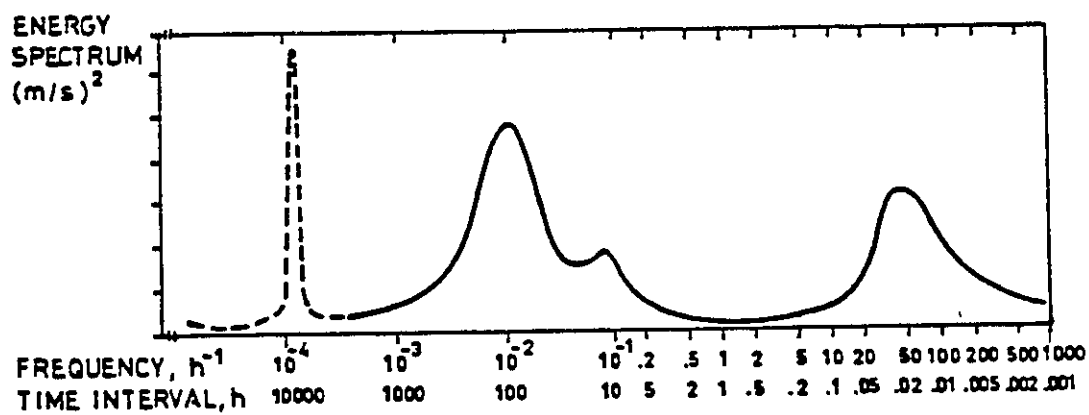


Figure 2.2. Wind-Induced Pressures on Building Envelopes  
(Liddament, 1986)



**Figure 2.3. Role of Mathematical Models in Building Ventilation Design** (adapted from Liddament, 1986)



Energy spectrum of the horizontal wind velocity component  
100 m above ground at Brookhaven, N.Y., USA. After  
van der Hoven (1957).

Figure 2.4. A Wind Velocity Spectrum Sample  
(From Kronvall, 1980)

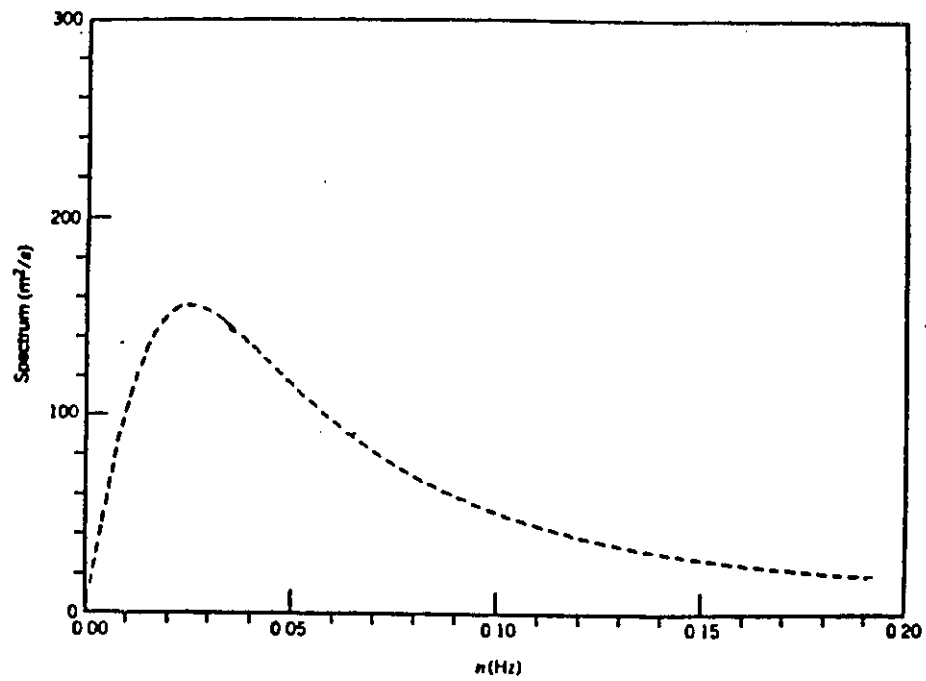


Figure 2.5. A Sample of Davenport Wind Spectrum  
(Copied from Simiu & Scanlan, 1986)

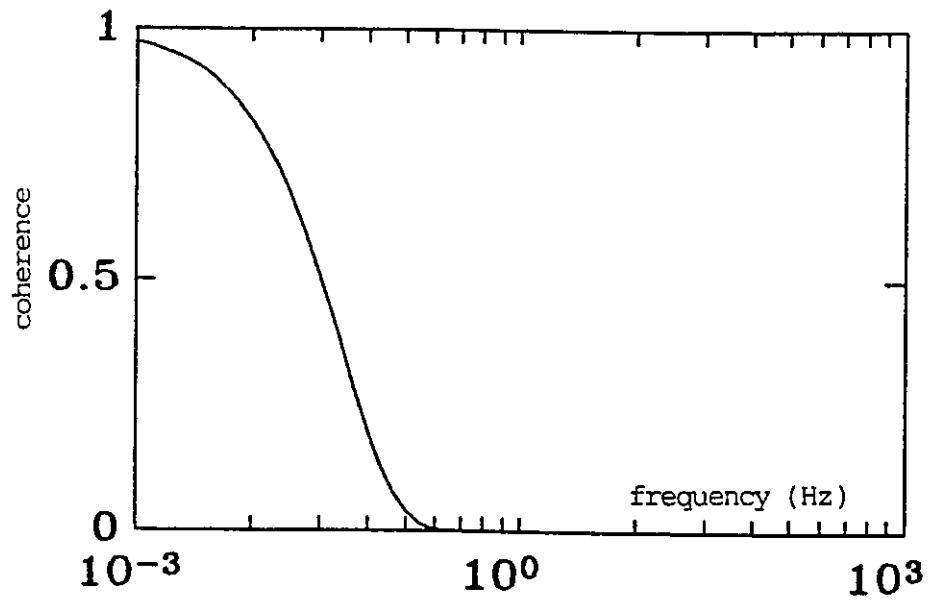


Figure 2.6. A Sample of Coherence Function

**Table 2.1. Current Research on Airflow and Related Studies**

Authors	Contents	Year
Limb	Survey of the world-wide research on measurements, simulations, modelling and other aspects of airflow and air quality related problems, based on questionnaire results	1990
Liddament	handbook for consensus techniques in airflow modelling and measurements	1986
Feustel and Dieris	survey of 50 airflow models on structures and compositions	1992
Haghighat	review on 10 airflow and indoor air quality models	1989
Liddament and Allen	validation of 10 airflow models with three sets of experimental data	1983
Colthorpe	ventilation standards for 13 AIVC participating countries, 3 non-AIVC countries, and many international organizations	1990
Roulet and Vandaee	handbook on measurement techniques for airflow in building	1991
Swami and Chandra	review of data bases on pressure coefficient distributions on building surfaces	1988
Allen	data base of wind pressure distributions	1984
Blacknell	bibliographic data base: AIRBASE of AIVC, currently 4,000 entries, updated monthly, available on diskettes	1989
Collett et al.	building performance data base on energy use, ventilation, lighting, acoustics, indoor air pollutant levels and reported effects on health and comfort of occupants	1987

**Table 2.2. Approaches to Fluctuating Airflow Modelling**

Model	Main Features	Authors
Pulsation Flow	Pulsating airflow of a single-opening enclosure was caused by longitudinal fluctuations of wind and the compressibility of air within the enclosure. Limited experiments.	Cockroft & Robertson (1976)
	Effects of wind incident angles.	Narasaki, et al. (1987)
Mechanical System	Airflows through openings were modelled as mechanical systems and calculated for pressures at a single frequency. Analysis was incorporated into building mechanical systems. With special designed tests.	Sasaki, et al. (1987)
Helmholtz Resonator	Fluctuating internal pressure for single opening enclosure was obtained numerically from second-order non-linear differential equations. Compared with wind tunnel test data in the frequency domain.	Holmes (1979)
	Extended to predict the internal pressure changes after sudden window break in multi-zone buildings.	Saathoff & Liu (1983)
	Condition of resonance.	Davenport & Surry (1984)
	Governing equations were derived from fundamental fluid mechanical equations and were solved numerically.	Kazic & Novak (1989)
Parametrical Coefficient	Fluctuating airflow was assumed to be proportional to RMS value of wind pressures, the coefficients depend on opening characteristics and empirical constants. Used in a multi-zone airflow model.	Etheridge, et al. (1980)
	Empirical formula.	Phaff and Gidds (1980)

# **CHAPTER III**

## **SYSTEM THEORETIC APPROACH TO AIRFLOW MODELLING AND DESIGN**

Air infiltration and ventilation system of a building is considered to be independent and time-invariant. The internal rooms or separable spaces and openings are the basic physical components. Three-types of driving forces serve as inputs or excitations. The outputs are the airflow rates through openings between internal rooms and between the inside and outside of the building. Like any other system, the airflow system can be modelled mathematically, and system techniques can be applied.

Existing studies have concentrated on the mean value predictions. However, wind-induced pressures have a stochastic nature and may be inadequately represented by mean values. In such cases, the total building airflow system can be considered as two subsystems: the steady-state airflow system and fluctuating airflow system. The emphasis of this chapter is to present modelling and sensitivity analysis procedures for steady-state airflow systems using a system theoretic approach. Both procedures have been published in journals (Haghighat and Rao, 1991; Rao and Haghighat, 1993).

The system theory is a major theme of this thesis. The system theoretic approach is used in the modelling of building airflow systems. System techniques are employed in deriving the general formulation procedures for governing equations. The system theory offers an intuitive way of thinking and assorted proven techniques. There are, however, certain assumptions associated with the application of the system theory. These assumptions are generally acceptable and are similar to those involved when other physical problems are modelled. The presentation of these assumptions will be included in Section §3.1. References on the fundamentals and applications of system theory can be found in (Swamy and Thulasiraman, 1981; Haghighat and Chandrashekar, 1987; and Roe, 1966).

In Section §3.2, the modelling and analysis of building ventilation systems are presented. The emphasis is on presenting a theoretical derivation of nodal governing equations for the steady-state building airflow systems and on obtaining efficient procedures for automatic formulations and solutions of the system equations. The matrix representation form of airflow systems can facilitate further theoretical analyses.

In Section §3.3, a general procedure for analyzing airflow sensitivities with respect to input parameter variations is presented. The derivation is based on the developed matrix representation. The sensitivity analysis provides both valuable insight into the effects of input parameter variations on the accuracy of multi-zone airflow models and necessary information for additional analyses. A case study is used to show the procedure for the airflow sensitivity calculation, and to demonstrate how to use sensitivity information in error analysis and design assistance.



### 3.1. MODELLING BUILDING AIRFLOW SYSTEMS

#### 3.1.1. Building Airflow Systems

The entity of air infiltration and ventilation of a building is assumed to be an independent system, in the sense that this system can be divided into interconnected components. These components include the airflow paths (openings) and the separated spaces (rooms) of the building. Each component can be independently described by a mathematical relation.

Although its input and output are of stochastic nature, the airflow system of a building is deterministic and time-invariant. Given a pressure difference, the airflow through an opening is known and unique. For every input (combination of the driving forces) into the entire system, there are unique outputs of the airflow rates among internal rooms and between the inside and outside of the building.

Air infiltration and ventilation through a building is caused by three types of driving forces. Wind-induced pressures upon the building envelope are considered to be non-deterministic and change over time. Although the thermal buoyancy and mechanical ventilation systems have temporal variations, they are assumed to be deterministic and time-invariant in this thesis research. A further assumption is made for the wind pressures so that each pressure can be deemed as a superposition of a deterministic constant (the mean value) and a random term (the fluctuating pressure). Airflow through any opening can be considered to consist of two parts: 1) a deterministic constants to indicate the mean values, and 2) random values which have predictable stochastic properties. The airflow system can thus be divided into two subsystems: a deterministic

system which has the steady-state or mean driving forces as input and mean airflow rates as outputs; and a fluctuating airflow system in which both inputs and outputs are changing with time. These two subsystems will be referred to as the steady-state airflow system and the fluctuating airflow system of a building. The prediction of the whole airflow system requires predictions of both mean and fluctuating systems.

### 3.1.2. Assumptions

More formally, the above discussion on the requirements of a building airflow system can be expressed in several assumptions. Some of these assumptions are used in both this chapter for steady-state airflow modelling and design, and in later chapters for fluctuating airflow modelling. These assumptions are:

1. The airflow system of a building is equivalent to the sum of two subsystems: the steady-state airflow system and the fluctuating airflow system.
2. The airflow system is independent. Components of the system can be independently described by mathematical relations.
3. The airflow system is deterministic and time-invariant. Given an input, the output is unique.

Although the assumption 1 divides an airflow system into two subsystems, the total output (airflow) of the system is not a simple summation of outputs from the two subsystems, it is obtained from the outputs of the subsystems using a combinatory calculation

procedure presented in Section §4.5. Other assumptions are specific for the modelling of fluctuating airflow systems.

4. The dynamic flow equations of openings can be approximated by linear relations, and the volume change of the room air due to compressibility is proportional to the internal pressure change.
5. The wind-induced pressure is a stationary process. The thermal and mechanical forces are deterministic.

### **3.2. SYSTEM THEORETIC APPROACH TO STEADY-STATE AIRFLOW MODELLING**

Computer simulations of airflow in buildings are valuable research tools with which ventilation performance is studied. The modelling process involves the breaking of the airflow system (building and HVAC systems) into components (rooms, duct and fan), and formulating flow equations for each component. The set of governing equations is derived from air mass continuity in any space of a building. Typical input data for these simulators are: meteorological data, building and HVAC characteristics. Typical output data from these simulators are airflow rates, either throughout the building or in selected zones.

In this section, the system theoretic approach is used to model the air infiltration and ventilation systems of buildings. A building airflow system is decomposed into the

elementary components. The system theory is used to formulate a set of governing equations. A detailed analysis of the process and results is then given to show an efficient procedure for the formulation of system equations.

### 3.2.1. Modelling Components of a Building and Its Ventilation System

In the system theoretic approach, the steady-state airflow system of a building can be considered as a collection of several types of components which are interconnected in a predetermined manner, called *terminal graph*. The graph consists of a set of points and lines. A line connecting a pair of points is called an *edge*. The edges in a graph are connected to their end points called *nodes*. In a building airflow system, individual driving forces and airflow resistances are modeled as edges.

A two-opening building is chosen as an example to demonstrate the modelling and formulation procedure. This building can be represented by a graph of 6 nodes and 6 edges (Figure 3.1b). Node 1 represents the single rooms, nodes 2 to 5 represent the four end points of the two openings, and node 0 is the atmosphere outside of the building. The reference heights of a node is chosen at the floor level of a room or at the ground level for the atmosphere node. Each opening is considered as a flow resistance and is represented by an edge (edges 1 and 2). In the inside of the building, the pressure differences due to stack effect from the floor level to the heights of the openings, are known and are represented by separate edges (edges 5 and 6). At the outside, the pressure difference between the end of an opening and the ground, which is the sum of stack effect and wind-induced pressure, is represented as one edge (edges 3 and 4).

The state of each edge is described by a pair of measurements called *across variable* and *through variable*. In a steady-state airflow system, pressure differences are considered as the across variables and the airflow rates as the through variables. The mathematical relations between the across and through variables associated with an edge are called *terminal equations*. For edges that represent openings (edges 1 and 2), this relationship can be expressed in flow equations. Edges that represent driving forces have known pressure differences and are referred to as the known pressure edges (edges 3 to 6).

In addition to terminal equations, two topological relationships exist which are necessary to fully describe the airflow system. These equations are based on the oriented linear graph and, in system-theoretic terms, are called vertex postulates (conservation of mass) and circuit postulates (compatibility law). The *vertex equation* in matrix form is:

$$\mathbf{I}^* \mathbf{Q} = \mathbf{0}, \quad (3-1)$$

where  $\mathbf{Q}$  is the airflow vector and  $\mathbf{I}^*$  is the *incidence matrix* derived from the topology of the graph. See Table 3.1 for the symbols and notations used in this chapter. The incidence matrix has  $v$  rows and  $e$  columns corresponding to  $v$  nodes and  $e$  edges in the graph. Elements of the incidence matrix are defined as follows:

$$I_{ij}^* = \begin{cases} 1 & \text{if edge } j \text{ is connected to node } i \text{ and oriented away from it,} \\ -1 & \text{if edge } j \text{ is connected to node } i \text{ and oriented towards it, and,} \\ 0 & \text{otherwise.} \end{cases} \quad (3-2)$$

Each column of the incidence matrix has one +1 and one -1. Thus, the rows of the incidence matrix are linearly dependent. To obtain a linearly independent set of rows,

one of the rows is deleted. The resulting matrix with  $(v-1)$  rows is called the *reduced incidence matrix*  $\mathbf{I}$ , and:

$$\mathbf{I} \mathbf{Q} = \mathbf{0}. \quad (3-3)$$

The vertex which corresponds to the row of  $\mathbf{I}^*$  and which is not in  $\mathbf{I}$  is called the *reference vertex* or *node*, and is usually chosen to be the one that represents the atmosphere (the outside of the building).

Equation (3-3) is the matrix form of mass balance equations for all the nodes (excepts for node 0). For the example building, it is written as:

$$\begin{bmatrix} 0 & 0 & 0 & 0 & 1 & 1 \\ 1 & 0 & -1 & 0 & 0 & 0 \\ 0 & -1 & 0 & -1 & 0 & 0 \\ -1 & 0 & 0 & 0 & -1 & 0 \\ 0 & 1 & 0 & 0 & 0 & -1 \end{bmatrix} \begin{bmatrix} Q_1 \\ Q_2 \\ Q_3 \\ Q_4 \\ Q_5 \\ Q_6 \end{bmatrix} = \begin{bmatrix} 0 \\ 0 \\ 0 \\ 0 \\ 0 \\ 0 \end{bmatrix}$$

Nodal variables refer to measurements made at each node. In the steady-state airflow system, nodal variables are the nodal (or zonal) pressures of nodes with respect to the atmospheric pressure. System theory (Swamy and Thulasiraman, 1981) shows that any across variable can be expressed as a linear combination of nodal variables. This relation is called the *nodal transformation equation*, and takes the following form:

$$\mathbf{X} = \mathbf{I}^T \Phi, \quad (3-4)$$

where  $\mathbf{X}$  (alias of  $\Delta P$ ) is the vector of pressure differences across all the edges,  $\Phi$  is the vector of nodal pressures and the superscript  $T$  denotes the matrix transpose operation.

For the example building, the above equation can be written as:

$$\begin{bmatrix} X_1 \\ X_2 \\ X_3 \\ X_4 \\ X_5 \\ X_6 \end{bmatrix} = \begin{bmatrix} 0 & 1 & 0 & -1 & 0 \\ 0 & 0 & -1 & 0 & 1 \\ 0 & -1 & 0 & 0 & 0 \\ 0 & 0 & -1 & 0 & 0 \\ 1 & 0 & 0 & -1 & 0 \\ 1 & 0 & 0 & 0 & -1 \end{bmatrix} \begin{bmatrix} \Phi_1 \\ \Phi_2 \\ \Phi_3 \\ \Phi_4 \\ \Phi_5 \end{bmatrix}$$

The nodes can be divided into those which represent rooms, n-nodes, and the remaining s-nodes. This partitions the nodal variable vector into:

$$\Phi = [\Phi_n \ \Phi_s]^T \quad (3-5)$$

For the example building, this division is:

$$\Phi_n = [\Phi_1], \quad \Phi_s = [\Phi_2 \ \Phi_3 \ \Phi_4 \ \Phi_5]^T$$

### 3.2.2. Governing Equations of Steady-State Airflow Systems

In a building airflow system, the pressure differences across an edge that represents a driving force, such as the stack effect, or a combination of stack and wind pressure is given and known. The pressure differences across the flow resistance edges, on the other hand, are unknown. Accordingly, edges are partitioned into f-edges and s-edges. Edges in the graph of Figure 3.1b, for example, can be divided into two sets of 1 to 2 and 3 to 6. The corresponding partitions of the across and through variable vectors are expressed as:

$$X = \begin{bmatrix} X_f \\ X_s \end{bmatrix}, \quad Q = \begin{bmatrix} Q_f \\ Q_s \end{bmatrix}. \quad (3-6)$$

The vertex equation (3-3) can then be written in a partitioned form as:

$$\begin{bmatrix} \mathbf{I}_{nf} & \mathbf{I}_{ns} \\ \mathbf{I}_{nf} & \mathbf{I}_{ss} \end{bmatrix} \begin{bmatrix} \mathbf{Q}_f \\ \mathbf{Q}_s \end{bmatrix} = \mathbf{0}. \quad (3-7)$$

The row of the reduced incidence matrix is partitioned according to equation (3-5).

The partitioned incidence matrix can be simplified if the following conventions are used in assigning orientations and numbering of nodes and edges. The orientations of the known pressure edges at the outside of the building are chosen so that they are all oriented away from the reference node (e.g. edges 3 and 4 are all oriented away from node 0 in Figure 3.1b). The edges that represent inside stack effects are assigned orientations away from n-nodes (e.g., edges 5 and 6 are oriented away from node 1 in Figure 3.1b). The edges of openings can have arbitrary orientations. The numbering for nodes and edges is related. The n-nodes and flow resistance edges (f-edges) are numbered first, in consecutive order, respectively (node 1 and edges 1 and 2 in Figure 3.1b). The s-nodes can then be numbered in any consecutive order, but preferably with the outside (of the building) s-node (nodes 2 and 3) before the s-node inside the building (nodes 4 and 5). The numbering of the s-edges must be in accordance with the numbering of the s-nodes, so that the order of s-edges and the order of s-nodes are the same (edges 3 to 6).

With the above conventions concerning orientations and numbering of nodes and edges, the sub-matrix  $\mathbf{I}_{nf}$  will be equal to a zero matrix (since any f-edge is not directly incident on any n-node), and the sub-matrix  $\mathbf{I}_{ss}$  will be a negative identity matrix (diagonal elements are equal to -1 and off-diagonal elements are equal to zero). Let



$I_1 = I_{ns}$  and  $I_2 = I_{sf}$ , then the vertex equation (3-7) can be simplified to:

$$\begin{bmatrix} 0 & I_1 \\ I_2 & -U \end{bmatrix} \begin{bmatrix} Q_f \\ Q_s \end{bmatrix} = 0. \quad (3-8)$$

For the example case, the two matrices  $I_1$  and  $I_2$  are

$$I_1 = \begin{bmatrix} 0 & 0 & 1 & 1 \end{bmatrix}, \quad I_2 = \begin{bmatrix} 1 & 0 \\ 0 & -1 \\ -1 & 0 \\ 0 & 1 \end{bmatrix} \quad (3-9)$$

The lower part of equation (3-8) is:

$$I_2 Q_f - Q_s = 0, \quad (3-10)$$

and it can be rewritten as:

$$Q_s = I_2 Q_f \quad (3-11)$$

Substituting  $Q_s$  into the upper part of the vertex equation (3-8) yields:

$$(I_1 \ I_2) Q_f = 0. \quad (3-12)$$

Let

$$\Pi = I_1 I_2, \quad (3-13)$$

then the set of vertex equations is obtained as:

$$\Pi Q_f = 0. \quad (3-14)$$

The number of rows in this equation is equal to the number of room nodes. This equation provides the minimum set of equations, and will be referred to as the *reduced vertex equation*.

For the case study, equation (3-14) is written as:

$$\begin{bmatrix} -1 & 1 \end{bmatrix} \begin{bmatrix} Q_1 \\ Q_2 \end{bmatrix} = 0$$

or

$$-Q_1 + Q_2 = 0$$

which is simply the mass balance equation for the building. A general observation about matrix  $\Pi$  is that this matrix is the reduced incidence matrix of the graph of the building's physical connection (Figure 3.1c), with the atmosphere node as the reference node. This physical connection graph consists of rooms (plus atmosphere) as nodes and openings as edges. The orientations of the edges are the same as those of the flow resistance edges of Figure 3.1b.

Using the same division of edges and nodes, the nodal transformation equation can be written as:

$$\begin{bmatrix} X_f \\ X_s \end{bmatrix} = I^T \Phi = \begin{bmatrix} \mathbf{0} & I_2^T \\ I_1^T & -U \end{bmatrix} \begin{bmatrix} \Phi_n \\ \Phi_s \end{bmatrix}. \quad (3-15)$$

From the lower part, the relation between the known across variables and the nodal variables can be written as:

$$X_s = I_1^T \Phi_n - \Phi_s. \quad (3-16)$$

From this equation the nodal variable  $\Phi_s$  of s-nodes is expressed as:

$$\Phi_s = I_1^T \Phi_n - X_s, \quad (3-17)$$

that is,  $\Phi_s$  can be expressed as linear combinations of  $X_s$  and  $\Phi_n$ . For the example building, equation (3-17) is expressed as:

$$\begin{bmatrix} \Phi_2 \\ \Phi_3 \\ \Phi_4 \\ \Phi_5 \end{bmatrix} = \begin{bmatrix} 0 \\ 0 \\ 1 \\ 1 \end{bmatrix} \Phi_1 - \begin{bmatrix} X_3 \\ X_4 \\ X_5 \\ X_6 \end{bmatrix}$$

Substituting equation (3-17) into the upper part of equation (3-15), a reduced nodal transformation equation can be obtained as:

$$X_f = I_2^T \Phi_s = I_2^T (I_1^T \Phi_n - X_s) = (I_1 I_2)^T \Phi_n - I_2^T X_s \quad (3-18)$$

or:

$$X_f = \Pi^T \Phi_n - I_2^T X_s \quad (3-19)$$

The second term on the right hand side of the above equation can be calculated for the example building as:

$$-I_2^T X_s = \begin{bmatrix} X_5 - X_3 \\ X_4 - X_6 \end{bmatrix} \quad (3-20)$$

Comparing it to the graph in Figure 3.1b, it can be concluded that each element of the vector on the right hand side of the above equation represents the combination effect of wind and stack driving forces exerted on an opening. Let the vector of those combinatory driving forces be:

$$P_f = -I_2^T X_s, \quad (3-21)$$

then, the nodal transformation of equation (3-19) can be replaced by:

$$X_f = \Pi^T \Phi_n + P_f \quad (3-22)$$

For an opening  $l$  which connects rooms  $l_i$  and  $l_j$ , the stack effect acting on the opening is calculated as:

$$[P_f]_l = \frac{P_a}{R_a} g \left( \frac{h_{lj}}{T_{lj}} - \frac{h_{li}}{T_{li}} \right). \quad (3-23)$$

While for an opening  $l$  which connects the inside and the outside of the building, the combination of wind and stack forces is:

$$[P_f]_l = P_l^w + \frac{P_a}{R_a} g \left( \frac{h_{lj}}{T_{lj}} - \frac{h_{li}}{T_{li}} \right). \quad (3-24)$$

where  $P_l^w$  is the wind-induced pressure acting on the opening. For the example building in Figure 3.1a, equation (3-22) is written as:

$$\begin{bmatrix} X_1 \\ X_2 \end{bmatrix} = \begin{bmatrix} -1 \\ 1 \end{bmatrix} \Phi_1 + \begin{bmatrix} P_1^w + \frac{P_a}{R_a} g \left( \frac{h_{11}}{T_i} - \frac{h_{10}}{T_o} \right) \\ -P_2^w + \frac{P_a}{R_a} g \left( \frac{h_{20}}{T_o} - \frac{h_{21}}{T_i} \right) \end{bmatrix}$$

Flow equations (or vertex equations) of the flow-resistance edges are represented by:

$$Q_f = F(X_f), \quad (3-25)$$

where  $F()$  is a vector and each element represents a function of the corresponding flow equation. For the example case, the flow equations can be written as:

$$\begin{bmatrix} Q_1 \\ Q_2 \end{bmatrix} = \begin{bmatrix} K_1 X_1^{n_1} \\ K_2 X_2^{n_2} \end{bmatrix} = \begin{bmatrix} K_1(\cdot)^{n_1} \\ K_2(\cdot)^{n_2} \end{bmatrix} \begin{bmatrix} X_1 \\ X_2 \end{bmatrix}$$

Combining the minimum set of vertex equation (3-14), the reduced nodal transformation equation (3-22) and the flow equation (3-25), the system equation in matrix form can finally be obtained as:

$$\Pi \eta \{F(\Pi^T \Phi_n + P_f)\} = 0. \quad (3-26)$$

The symbol  $\eta$  is a diagonal matrix and each diagonal element  $\eta_{ll} = \gamma_l$  is the air densities of the air flowing in the opening  $l$ . Equation (3-26) is the matrix form of the governing equations for the steady-state airflow system of a building. The unknowns in the equation are the nodal pressures. For the example building, this matrix form is written in:

$$\begin{bmatrix} -1 & 1 \end{bmatrix} \begin{bmatrix} \gamma_1 & 0 \\ 0 & \gamma_2 \end{bmatrix} \begin{bmatrix} K_1(\cdot)^{n_1} \\ K_2(\cdot)^{n_2} \end{bmatrix} \begin{pmatrix} -\Phi_1 + P_1^w + \frac{P_a}{R_a} g \left( \frac{h_{11}}{T_i} - \frac{h_{10}}{T_o} \right) \\ \Phi_1 - P_2^w + \frac{P_a}{R_a} g \left( \frac{h_{20}}{T_o} - \frac{h_{21}}{T_i} \right) \end{pmatrix} = 0$$

where  $\gamma_1$  and  $\gamma_2$  are the air densities of air in the two openings. This equation can be simplified to:

$$-\gamma_1 K_1 \left[ -\Phi_1 + P_1^w + \frac{P_a}{R_a} g \left( \frac{h_{11}}{T_i} - \frac{h_{10}}{T_o} \right) \right]^{n_1} + \gamma_2 K_2 \left[ \Phi_1 - P_2^w + \frac{P_a}{R_a} g \left( \frac{h_{20}}{T_o} - \frac{h_{21}}{T_i} \right) \right]^{n_2} = 0$$

Equation (3-26) is a set of non-linear equations and is solved by iterative algorithms. The most popular solution approach is Newton's method. Basically, this method calculates new values of the unknowns, at each iteration by linearization of the flow function  $F()$  and by solving for the resultant set of linear equations. Each iteration brings the set of unknown variables closer to the actual values. Although a guarantee for convergence has not been mathematically proven, solutions can be obtained for most realistic situations (Walton, 1989).

According to Newton's method, the iteration algorithm is given by:

$$\Phi_n^{k+1} = \Phi_n^k - \left[ \frac{\partial}{\partial \Phi_n} \{F(\Pi^T \Phi_n^T - I_2^T X_s)\} \right]^{-1} [\Pi \eta F(\Pi^T \Phi_n^k - I_2^T X_s)]. \quad (3-27)$$

The partial derivatives of functions  $F()$  with respect to nodal pressure at  $\Phi_n = \Phi_n^k$  is:

$$\begin{aligned} J &= \frac{\partial}{\partial \Phi_n} \{ \Pi \eta F(\Pi^T \Phi_n^k - I_2^T X_s^k) \} = \Pi \eta \frac{\partial}{\partial \Phi_n} \{ F(\Pi^T \Phi_n^k - I_2^T X_s) \} \\ &= \Pi \eta \left\{ \frac{\partial F(X_s^k)}{\partial X_s} \times \frac{\partial}{\partial \Phi_n} (\Pi^T \Phi_n^k - I_2^T X_s^k) \right\} = \Pi \times \eta \times \left\{ \frac{\partial F(X_s^k)}{\partial X_s} \right\} \times \Pi^T, \end{aligned} \quad (3-28)$$

or:

$$J = \Pi \eta D \Pi^T, \quad (3-29)$$

where  $D = \frac{\partial F(X_s^k)}{\partial X_s}$  is a diagonal matrix. Each diagonal element  $D_{ii} = \frac{\partial F_i(X_s^k)}{\partial X_i}$  is called the dynamic admittance of the flow opening  $i$ .

Matrix  $J$  of equation (3-29) is called the *dynamic nodal-admittance matrix*. The following relation between the nodal-admittance matrix and the topology of the physical connection graph for the building exist:

- the diagonal elements  $J_{ii}$  are composed of the sum of the dynamic admittance of edges that are connected to the  $i$ th (room) node, the sign is positive, and
- the off-diagonal elements  $J_{ij}$  are composed of the sum of the dynamic admittance of edges that connect between (room) nodes  $i$  and  $j$ , the sign is negative.

The symmetric and non-singular properties of the nodal-admittance matrix  $J$  ensure the solution to the update equation (3-29). For the example building, matrix  $J$  is a scale since only one room exist, and at the  $k^{\text{th}}$  iteration is written as:

$$J = n_1 \gamma_1 K_1 (X_1^k)^{n_1-1} + n_2 \gamma_2 K_2 (X_2^k)^{n_2-1}$$

The iterative formula (equation 3-28) can be expressed in update form:

$$\Phi_n^{k+1} = \Phi_n^k + C^k, \quad (3-30)$$

where the update (or correction) vector  $C^k$  is computed by:

$$\Pi \eta D \Pi^T C^k = -\Pi Q_f^k. \quad (3-31)$$

The initial value for the nodal across variable,  $\Phi_n^0$ , is obtained by approximating each airflow component as a linear relation. This is equivalent to letting the vertex equation be:

$$Q_f = F(X_f) = A + B X_f. \quad (3-32)$$

The vertex equation is thus a set of linear equations of the form:

$$\Pi \eta [A + B (\Pi^T \Phi_n^0 - I_2^T X_s)] = 0 \quad (3-33)$$

which leads to:

$$\Phi_n^0 = -[\Pi \eta B \Pi^T]^{-1} \Pi \eta [A - B I_2^T X_s]. \quad (3-34)$$

The procedure given herein is called the *Nodal Tableau Formulation Method*. It considers the fundamental driving forces and resistance forces. The influence of each component is clearly indicated in the procedure and the final set of equations. Therefore, it leads to a better understanding of the mechanism and modelling process of airflow in buildings.

A four-room building (Figure 3.2) is modelled using the presented modelling procedure. The graph representation of the building is shown in Figure 3.3. The calculated airflow rates are shown in Figure 3.4. Comparing these values to the results of Walton's model (Walton, 1989), the difference in airflow rates are within 0.02 percent.

### 3.2.3. Automatic Formulation Procedure for the Steady-State Airflow Model

The above procedure shows the system-theoretic formulation and solution method for the governing equations of the steady-state airflow system of a building. It utilizes a graph which is composed of the fundamental driving forces and resistance forces. The influence of each individual component is clearly indicated in the formulation.

Analysis of equation (3-27) indicates that it can be formulated from the physical connecting graph of the building airflow system. Therefore, in computational implementation, inputs only require the physical connection data and opening characteristics (which include the flow equations and locations of openings).

The formulation can be further "automated" by taking advantage of the regular composition of the **J** matrix (equation 3-29) in the iterative update calculation. Since the elements of the **J** matrix can be assembled by simple rules, this matrix can be automatically generated from flow equations and the physical connection data.

In summary, it has been demonstrated that the building airflow system can be modeled as a graph which has the fundamental driving forces and flow resistances as edges. The Nodal Tableau method is used to formulate a minimum set of non-linear governing equations with room nodal pressures as unknown variables. The analysis of resultant equations concludes that, due to inherent properties of the airflow systems, the graph has certain patterns which enable direct formulation of the governing equations without consulting the complete graph. Governing equations can be derived from the physical connection data and opening characteristics.



The introduction of general graph helps in understanding the mechanism of the airflow caused by the driving forces. The presented analysis on nodal equations clearly exhibits the formulation procedure of the system equations for building airflow systems, and the influence of driving forces and flow resistance of the airflow. The obtained matrix representation form of the airflow system and solution process enables further analytical analyses, such as the sensitivity analysis presented in the next section.

### **3.3. SENSITIVITY ANALYSIS OF AIRFLOW IN BUILDINGS**

There has been considerable interest over the past few years in the development of models for building airflow analysis, due mainly to energy and indoor air quality considerations. Most of these airflow models are based on the steady-state assumption, and calculate the mean air flow rates due to average values of driving forces (Haghighat and Rao, 1991; Haghighat, 1989). Nevertheless, validations and applications of airflow models have been slow and difficult. One of the major reasons can be attributed to the lack of studies on the influence of input parameter variations on the models and the simulation results.

Variations of input parameters arise in several categories. First, the modelling assumptions and approximations employed to transfer a physical building into a multi-zone airflow network introduce errors between the actual systems and the conceptual models. Second, in analyzing existing buildings the input data from measurements or

estimations have errors due to measurement techniques (Liddament, 1986). Third, when these airflow models are used in the design process, the input parameters are based on estimations using standard procedures and/or manufacturer's specifications. They can be affected by inaccuracy of estimation procedures, manufacturing tolerances, and installation disparities. Fourth, seasoning of building components due to erosions and abrasions can also cause changes in the input parameters. In addition, effects of intentional parameter variations on airflow are analyzed for designing building airflow systems. Changes of input parameters due to any of these or other reasons may cause the predictions of airflow models to be erroneous or even invalid. Therefore, it is important to examine the influence of the input parameter variations on airflow models and their simulation results.

One possible technique to study the influence of parameter variations is the application of *parametric analysis*. In this approach tentative changes in some input parameters are assigned and airflow models are applied to observe the responses. This necessitates considerable data handling and computational efforts. In addition, when the effects of many parameters are concerned, the interpretation of the numerous simulation results can be difficult and time consuming.

A more feasible approach is the use of *sensitivity analysis* methods. The *sensitivity* (or *sensitivity function* as used in the sensitivity theory, Frank, 1978) of airflow with respect to individual input parameters is calculated. Then, additional analyses such as error analysis and airflow system design assistance can be carried out based on the sensitivity information. The airflow sensitivities are obtained at a particular point as

defined by the values of input parameters and the airflow simulation results based on these input values. This method is also referred to as the *perturbation method*.

The emphasis of this section is to present a procedure for calculating airflow sensitivities with respect to input parameters. The derivation is based on the matrix representation form of the modelling process for airflow models using the system theoretic approach, presented in the previous section §3.2. The application of the sensitivity information for error analysis and design assistance is briefly discussed in a case study. In the following sections, the derivation of the airflow sensitivity calculation procedure, sensitivity calculation for a case study, and additional analyses are presented.

### 3.3.1. Derivation of Sensitivity Calculation

Values of input parameters used in the above calculation are called *nominal values*. When there are small changes around the nominal values in one or more of these parameters, the mass balance equations will be interrupted. Consequently, the zonal pressures and airflow through openings will tend to move away from the steady-state solution obtained from multi-zone airflow models. The *sensitivity analysis* examines the relationship between small variations in input parameters and the potential change of the airflow through buildings.

The *input parameters* considered by this sensitivity analysis method can be separated into two types: the driving forces and the opening characteristics. The *driving*

*force parameters* are related to pressure differences across openings, including wind-induced pressures, zonal temperatures and opening locations. The *opening characteristic parameters* are related to flow equations, an example can be the discharge coefficient for the flow equation of an orifice type opening. Variations of both types of input parameters should not affect the structure of the building airflow system.

Let the vector  $\theta$  be the  $M$  mutually independent parameters to be studied,  $\theta^p$  for the driving forces parameters and  $\theta^f$  for the opening characteristic parameters. The *sensitivity* of an air flow rate  $Q_l$  to the variation of a parameter  $\theta_j$  is usually defined as the first order partial derivative:  $\frac{\partial Q_l}{\partial \theta_j}$  (Frank, 1978).

Since  $\theta^p$  and  $\theta^f$  are related to the airflow in different ways, the calculations are carried out separately before a general form is analyzed. The parameters  $\theta^p$  are related to the pressure differences across openings. Figure 3.5 shows the schematic diagram of a general opening  $l$ , which connects zones  $i$  and  $j$ . The expression for the driving force acting on the opening  $l$  is:

$$(P_f)_l = P_i^w + \frac{P_a}{R_a} g \left( -\frac{h_{ii}}{T_{ii}} + \frac{h_{jj}}{T_{jj}} \right) - \frac{P_a}{R_a} g \frac{h_l}{T_l} \quad (3-35)$$

where the wind-induced pressure can be obtained from the given pressure coefficient  $(C_p)_l$  and the wind velocity at roof height  $V_h$  as:  $P_i^w = (C_p)_l \frac{1}{2} \rho_0 V_h^2$ . The derivatives of  $Q$  with respect to  $\theta^p$  are calculated as follows:

$$\frac{\partial Q}{\partial \theta^p} = \frac{\partial}{\partial \theta^p} \{ F(\Pi^T \Phi + P_f) \} = D \Pi^T \frac{\partial \Phi}{\partial \theta^p} + D \frac{\partial P_f}{\partial \theta^p} \quad (3-36)$$

The left hand side is called the Jacobian matrix of  $Q$  at  $\theta^p$ . It is a  $N$  by  $M$  matrix and its elements are  $\left[ \frac{\partial Q}{\partial \theta^p} \right]_i = \frac{\partial Q_i}{\partial (\theta^p)_j}$ . The case is similar for matrices  $\frac{\partial \Phi}{\partial \theta^p}$  and  $\frac{\partial P_f}{\partial \theta^p}$ .

Equation (3-36) indicates that the relative changes of airflow rates with respect to input parameters  $\theta^p$  depends on both matrices  $\frac{\partial \Phi}{\partial \theta^p}$  and  $\frac{\partial P_f}{\partial \theta^p}$ . Since the zonal pressures  $\Phi$  are implicit functions of  $\theta^p$  through mass balance equation (3-26), the Jacobian matrix of  $\Phi$  can be obtained by applying partial derivatives to equation (3-26) with respect to  $\theta^p$ , it yields:

$$\Pi \frac{\partial \Upsilon}{\partial \theta^p} \cdot Q \chi + \Pi(\eta D) \Pi^T \frac{\partial \Phi}{\partial \theta^p} + \Pi(\eta D) \frac{\partial P_f}{\partial \theta^p} = 0 \quad (3-37)$$

where  $\chi$  is a row vector of 1's. Therefore,

$$\frac{\partial \Phi}{\partial \theta^p} = - [\Pi(\eta D) \Pi^T]^{-1} \Pi \left( \frac{\partial \Upsilon}{\partial \theta^p} \cdot Q \chi + (\eta D) \frac{\partial P_f}{\partial \theta^p} \right) \quad (3-38)$$

The matrix that requires the inverse operation in this equation is the same as that used in the steady-state airflow calculation (equation 3-26), and should exist if the steady-state solution of airflow can be obtained.

The Jacobian matrix,  $\frac{\partial P_f}{\partial \theta^p}$ , is obtained by directly applying partial differentiations to equation (3-35). The composition of  $(P_f)_i$  depends on connections among zones of the building (represented by the  $\Pi$  matrix) and the directions of airflow (represented by the signs of  $Q$ ). Table 3.2 shows the elements of this Jacobian matrix for different parameters under various conditions.

For the opening characteristic related input parameters, the sensitivity of  $Q$  with respect to  $\theta^f$  can be represented by the Jacobian matrix:

$$\frac{\partial Q}{\partial \theta^f} = \frac{\partial}{\partial \theta^f} F(\Pi^T \Phi + P_f) = D \Pi^T \frac{\partial \Phi}{\partial \theta^f} + \frac{\partial F}{\partial \theta^f} \quad (3-39)$$

The elements of  $\frac{\partial F}{\partial \theta^f}$  are the derivatives of the flow equations to the flow equation related parameters, such as:  $\left(\frac{\partial F}{\partial \theta^f}\right)_{ij} = \frac{\partial(K_i \Delta P_i^{n_i})}{\partial K_i}$  if  $F_i = K_i \Delta P_i^{n_i}$  and  $\theta_j^f = K_i$ . The Jacobian matrix for  $\Phi$  can be obtained in a similar manner as in equations (3-37 & 3-38):

$$\frac{\partial \Phi}{\partial \theta^f} = -[\Pi(\eta D)\Pi^T]^{-1} \Pi \eta \frac{\partial F}{\partial \theta^f} \quad (3-40)$$

For a mixed set of input parameters, made up of driving forces and opening characteristics,  $\theta = [\theta^p \ \theta^f]^T$ , the zonal pressures and airflow are functions of these parameters, defined as the mass balance equation (3-26) and the opening flow equations. The general form for the Jacobian matrix for  $\Phi$  can be obtained by combining the analysis performed on  $\theta^p$  and  $\theta^f$ , as:

$$\frac{\partial \Phi}{\partial \theta} = -[\Pi(\eta D)\Pi^T]^{-1} \Pi \Lambda \quad (3-41)$$

where  $\Lambda$  is composed of:

$$\Lambda = \left[ \frac{\partial \gamma}{\partial \theta^p} \cdot Q \chi + (\eta D) \frac{\partial P_f}{\partial \theta^p} \quad \eta \frac{\partial F}{\partial \theta^f} \right] \quad (3-42)$$

The sensitivity matrix can, then, be calculated from:

$$\frac{\partial Q}{\partial \theta} = \frac{\partial}{\partial \theta} \{F(\Pi^T \Phi + P_f)\} = \left[ 0 \quad \frac{\partial F}{\partial \theta^f} \right] + D \Pi^T \frac{\partial \Phi}{\partial \theta} + \left[ D \frac{\partial P_f}{\partial \theta^p} \quad 0 \right] \quad (3-43)$$

Matrices  $\frac{\partial P_f}{\partial \theta^p}$ ,  $\frac{\partial F}{\partial \theta^f}$ , and  $\frac{\partial \gamma}{\partial \theta^p}$  are basic Jacobian matrices, and can be calculated

directly by employing the procedures in Table 3.2.

Usually, we are interested in the percentage change of airflow due to parameter variations. This is called the *semi-relative sensitivity* and can be obtained through  $\frac{(\partial Q)/Q}{\partial \theta}$ . In addition, changes in airflow out of one zone or into the entire building is more informative. The sensitivities of the total airflow out of zones or into the building are calculated by summations in:

$$\frac{\partial Q_i^T}{\partial \theta_j} = \sum_l \frac{\partial Q_l}{\partial \theta_j}, \quad i = 0, 1, \dots, N. \quad (3-44)$$

where the summation is over all of opening  $l$  so that air in opening  $l$  is flowing away from zone  $i$ .

### 3.3.2. Sensitivity Calculation for a Case Study

The airflow sensitivity analysis for input parameters has been presented. The inputs to this analysis are data for and solutions of steady-state airflow models, and the set of parameters of interest. In the following, the example from the previous section §3.2 is used to demonstrate the sensitivity calculation procedure. The case study building, its opening characteristics, and the incidence matrix  $\Pi$  are shown in Figure 3.1. By using the calculations presented in the previous section, the steady-state solutions are obtained (Figure 3.4).

Let  $\theta = [T_0 \ T_4 \ h_{30} \ C_{p1} \ P_4^w \ V_h \ K_4 \ n_3 \ n_1]^T$  be an arbitrary set of input parameters of interest. The first six parameters are related to driving forces, while the last

three are related to opening characteristics. The calculations are as follows. Table 3.3 shows the expressions of individual elements in the basic Jacobian matrices  $\frac{\partial P_f}{\partial \theta^p}$ ,  $\frac{\partial F}{\partial \theta^f}$  and  $\frac{\partial Y}{\partial \theta^p}$ , obtained by using Table 3.2. The  $\Lambda$  matrix can be calculated according to equation (3-42).

Matrix  $[\Pi(\eta D)\Pi^T]^{-1}$  can be obtained from the last iteration of the steady-state calculation in equation (3-29). Then, the Jacobian matrix of zonal pressures,  $\frac{\partial \Phi}{\partial \theta}$ , can be obtained from equation (3-41). Finally, using equation (3-43), the sensitivities of airflow  $Q$  with respect to the set of parameters  $\theta$  can be calculated.

Table 3.4 shows the results of the sensitivity calculation. The sensitivities of air flow rates through openings with respect to the 9 parameters are shown in the first 8 rows. Displayed in the next 8 rows are the semi-relative sensitivities. The semi-relative sensitivities of total airflow out of individual zones and into the entire building due to input parameter variations are shown in the last 5 rows.

Values in Table 3.4 indicate the tendency of airflow changes as a result of small input parameter variations around their nominal values. For example, the entry on row 1 and column 1 indicates that if the outside temperature were to increase one unit, i.e., 1°C, the air flow rate in opening 1 would tend to increase 0.44 m<sup>3</sup>/hr, or 0.53% of the nominal value (82.6 m<sup>3</sup>/hr) as indicated by the entry on row 9 and column 1. The same 1°C increase of the outside temperature would cause the air flow rate out of room 1 to increase 0.164% (column 1 and row 5 from bottom), and the natural ventilation rate into the entire building to decrease 0.17% (column 1 and the last row).



The sensitivities calculated by the above procedure indicate the potential influence of parameters on the airflow at **only** one specific point defined by the nominal values of the input parameters.

### 3.3.3. Error Analysis and Design Assistance

Airflow sensitivities provide information about potential changes in airflow due to input parameter variations. This information can be used for further analyses such as error analysis and design assistance. The *error analysis* provides information about deviations in airflow calculations due to errors in input parameters. Given general information regarding error ranges in the input data, this analysis can calculate the accuracy of the predications by airflow models. In assisting building airflow system designs, the sensitivity information is used for designing building airflow systems to achieve desired specifications. In this section, the case study is used to briefly show the procedures of these two additional analyses.

The potential changes of airflow due to input parameter variations in one or more input parameters can be estimated based on the airflow sensitivity values. If a single parameter  $\theta_j$  increases by  $\Delta\theta_j$  to a new value of  $\theta_j^*$ , the airflow changes can be calculated by:

$$\Delta Q = \frac{\partial Q}{\partial \theta_j} \times \Delta \theta_j \quad (3-45)$$

When two or more parameters have small variations, the predicted airflow changes can

be obtained by summing the individual effects, as:

$$\Delta Q = \sum_j \frac{\partial Q}{\partial \theta_j} \times \Delta \theta_j \quad (3-46)$$

When the standard deviations of input parameters,  $\sigma_{\theta_j}$ , are given, the standard deviations of airflow as a result of the uncertainty in input parameters can be obtained as:

$$\sigma_Q = \left\{ \sum_j \left[ \left| \frac{\partial Q}{\partial \theta_j} \right| \times \sigma_{\theta_j} \right]^2 \right\}^{\frac{1}{2}} \quad (3-47)$$

In order to verify the results of the calculations performed in equations (3-45 and 3-46), the predictions of airflow change potentials based on airflow sensitivities are compared with the airflow changes obtained through multiple simulations using airflow models. Let  $\Delta Q^*$  be the actual airflow change between the calculated airflow by substituting  $\theta_j + \Delta \theta_j$  into the airflow models and the nominal values of airflow. The relation between the prediction and the actual simulation result, for a single input parameter, is illustrated in Figure 3.6.

Both equations (3-45 and 3-46) use linear extrapolation to approximate the potential changes of airflow due to input parameter variations. Theoretically, equations (3-45 and 3-46) are only the first order terms in the power expansion of airflow with respect to input parameters. The expansion for single parameter variations is expressed as:

$$\Delta Q = \sum_j \frac{\partial Q}{\partial \theta_j} \Delta \theta_j + \frac{1}{2} \sum_j \frac{\partial^2 Q}{\partial \theta_j^2} \Delta \theta_j^2 + o(3) \quad (3-48)$$

and for variations of two or more parameters in:

$$\Delta Q = \sum_j \frac{\partial Q}{\partial \theta_j} \Delta \theta_j + \frac{1}{2} \left\{ \sum_j \frac{\partial^2 Q}{\partial \theta_j^2} \Delta \theta_j^2 + \sum_i \sum_{j \neq i} \frac{\partial^2 Q}{\partial \theta_i \partial \theta_j} \Delta \theta_i \Delta \theta_j \right\} + o(3) \quad (3-49)$$

where  $o(3)$  are higher order errors, which are normally smaller than the first and second order terms.

The accuracy of equations (3-45 and 3-46) depends mainly on the degree of linearity of  $Q$  as a function of the parameter  $\theta_j$  and the magnitude of parameter variations. For the multiple parameter variations, the accuracy of equation (3-46) is further influenced by the second-order cross partial differentials among the parameters.

For the case study, the calculations in equation (3-45) for selected single parameters are listed in Table 3.5, together with the relative discrepancies between the predictions made by equation (3-45) and the actual airflow simulations. The parameter variations are 3°C for temperatures, 0.5 m for opening locations, and 10% for the remaining variables. Each entry in Table 3.5 contains two numbers, the first one is the predicted potential airflow change due to one parameter variation. The second number corresponds to the relative discrepancy,  $\frac{\Delta Q - \Delta Q^*}{\Delta Q^*}$ , with positive numbers indicating over prediction. For example, the entry of  $T_o$  and  $Q_1^{-1}$  is 0.44/7.36, which indicates that if the outdoor temperature were to drop 3°C, the airflow out of room 1 would increase by 0.44 (m<sup>3</sup>/hr). This prediction is over estimated by 7.36% compared to the actual simulation results.

Table 3.5 shows that the prediction and simulation results are in very good agreement. Most of the discrepancies are under 2%, only very few are larger than 5%. The same analysis for other individual parameters shows similar results.

One main advantage of using the sensitivity analysis method is that it requires much less computational efforts than the simulations using airflow models. In the implementation of the case study, each simulation needed approximately 10 to 15 iterations to converge to a relative precision of  $10^{-5}$ , while the calculation using sensitivities was performed in one run without iterations. For the calculations of Table 3.5, the method using airflow sensitivities needed less than 5% of the computing time required by the simulation method.

Table 3.6 shows similar analyses (as in Table 3.5) for variations of two or more parameters. Most of the relative discrepancies are around 5% and a few (6 out of 100) are over 10%. Only for a few cases (7 out of 100), are there larger discrepancies, but these only happen when the relative changes of airflow  $\Delta Q'/Q'$  are very small (less than 1% of the nominal air flow rates).

Equation (3-47) describes quantitatively the propagation of errors from input parameters to the airflow simulation results. It can be used to obtain the standard deviations (STDs) of airflow for given error ranges of input parameters. In the course of verifying this relation, the *Monte-Carlo method* (Hamersly and Handscomb, 1964) is employed. In this method, the statistics of airflow are calculated from multiple simulations using combinations of randomly chosen input parameters. Results based on

both the sensitivity approach (equation 3-47) and the Monte-Carlo method are shown in Table 3.7. Taking the first row for example, if a STD of 3°C exists in outdoor and zonal temperatures, the calculation using equation (3-47) shows a STD of 1.21 m<sup>3</sup>/hr in the ventilation rate into the building. The Monte-Carlo method based on 100 airflow simulations, with each temperature independently and randomly chosen according to a normal distribution of 3°C STD, yields a STD of 1.18 m<sup>3</sup>/hr. Similar comparisons for other selected groups of parameters in Table 3.7 indicate compatible results from both methods, however the sensitivity approach requires much less computational efforts.

Information from airflow sensitivities can also be used to assist in the design of building airflow systems. Design goals can be to achieve specified ventilation rates, to obtain specifications for retrofitting of existing buildings, to limit airflow into or out of a zone, etc. For the case study building, we assume that the nominal values of input parameters represent a protocol design of a building and the typical outdoor weather conditions during the winter. The design goal is to reduce the building natural ventilation rate down to 100 m<sup>3</sup>/hr by air-tightening the building.

The variations of the four openings on the building envelope are of interest. The sensitivity information on these four openings should be obtained and used for guidance in the selection of new opening sizes. Calculations show that the sensitivity of the air flow rate into the building with respect the K values of these four openings are:

$$\left\{ \frac{\partial Q_0'}{\partial K_j} \times K_j \right\} = [ 35.41 \quad 32.72 \quad 31.82 \quad 24.06 ] \quad (3-50)$$

Since all values for the four sensitivities are positive, their  $K$  values should be reduced to achieve any reduction in the ventilation rate. Assuming  $\beta\%$  variations in the  $K$  values will bring about the required reduction, the following equation holds:

$$100 - 159.1 \text{ (m}^3\text{/hr)} - \left\{ \sum_j^4 \frac{\partial Q_0^t}{\partial K_j} K_j \right\} \times \beta\% \quad (3-51)$$

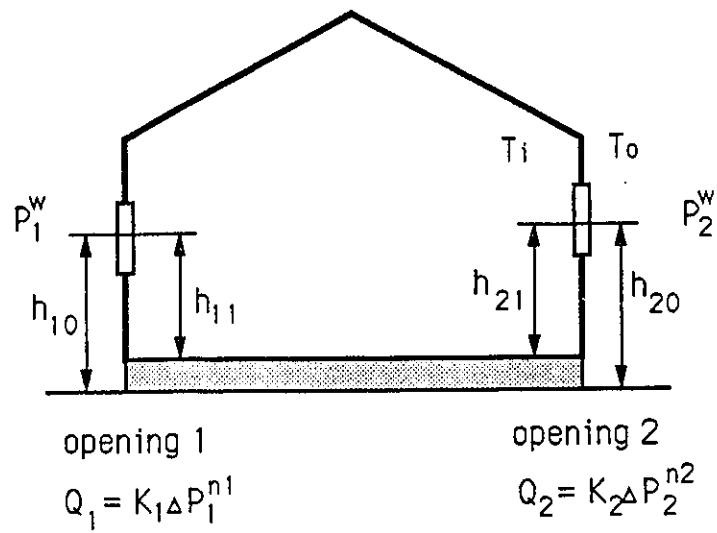
This yields  $\beta = (100-159.1)/124.02 \times 100 = -47.68$ . That is, each of the  $K$  values should be reduced by 47.68 percent to bring the building ventilation rate down to 100 m<sup>3</sup>/hr. The airflow simulation with the reduced new  $K$  values yields an actual ventilation rate of 90.98 m<sup>3</sup>/hr. This indicates that the new  $K$  values based on sensitivity information overestimated the ventilation reduction by 15%. Therefore, we correct the  $\beta$  value to  $47.68\% \times (1-15\%) \approx 40\%$ . One more simulation shows that the airflow into the building is reduced to 102.5 m<sup>3</sup>/hr. By using the sensitivity information in combination with the airflow simulations, we have been able to quickly find the required  $K$  values to achieve the design goal.

### 3.3.4. Further Discussion on Sensitivity Analysis

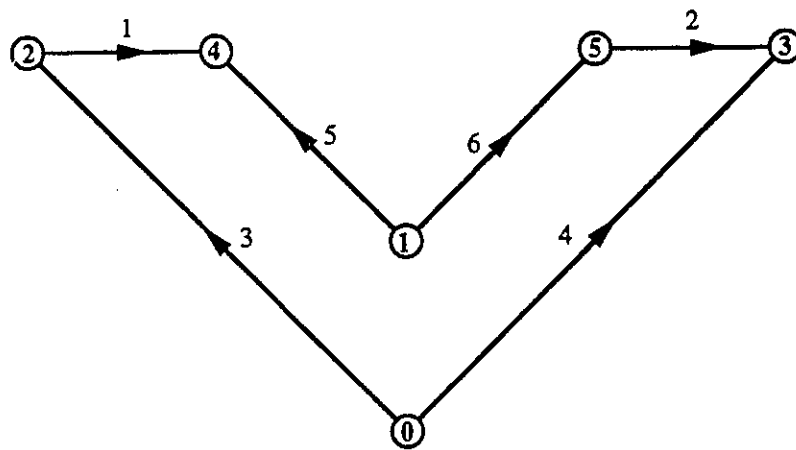
A general procedure for the sensitivity analysis of airflow in multi-zone buildings has been presented. The sensitivity of an air flow rate to a specific input parameter is defined as the corresponding partial derivative. The airflow sensitivities indicate potential changes of airflow, due to variations in mutually independent input parameters, at the point defined by the nominal values of input parameters and the airflow simulation

results. By utilizing the matrix representation form of a multi-zone airflow model, a general form of the sensitivity calculation is derived.

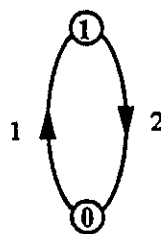
The sensitivity analysis provides useful information for error analysis and design assistance, furnishes further insights into the accuracy of existing airflow models, and requires minimum computational effort. The calculation procedure can be easily integrated into existing steady-state airflow models, such as the COMIS (1989) model. Further research is needed to use the sensitivity information for more comprehensive procedures in error analysis and building airflow system design.



(a) Building and Parameters



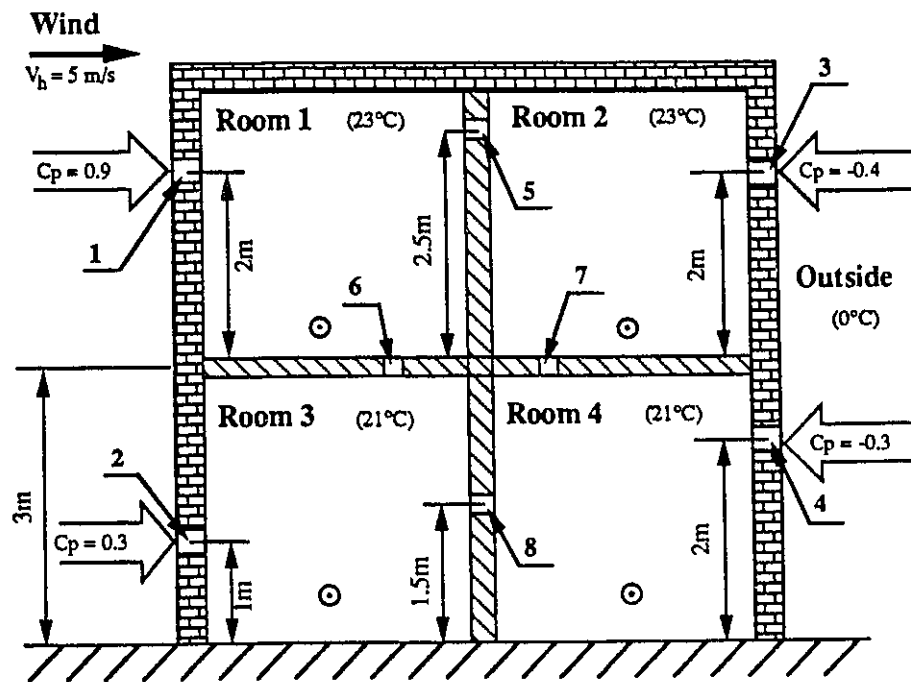
(b) Graph Representation



(c) Building Connection Graph

**Figure 3.1. A Two-Opening Building**





a) A Four Room Building

$$\Pi = \begin{bmatrix} -1 & 0 & 0 & 0 & 1 & -1 & 0 & 0 \\ 0 & 0 & 1 & 0 & -1 & 0 & 1 & 0 \\ 0 & -1 & 0 & 0 & 0 & 1 & 0 & 1 \\ 0 & 0 & 0 & 1 & 0 & 0 & -1 & -1 \end{bmatrix}$$

b)  $\Pi$  Matrix

#	n	K	#	n	K
1	.65	.005	5	.5	.015
2	.65	.008	6	.5	.020
3	.65	.007	7	.5	.020
4	.65	.009	8	.5	.015

c) Opening Parameters

Figure 3.2. A Four-Room Building

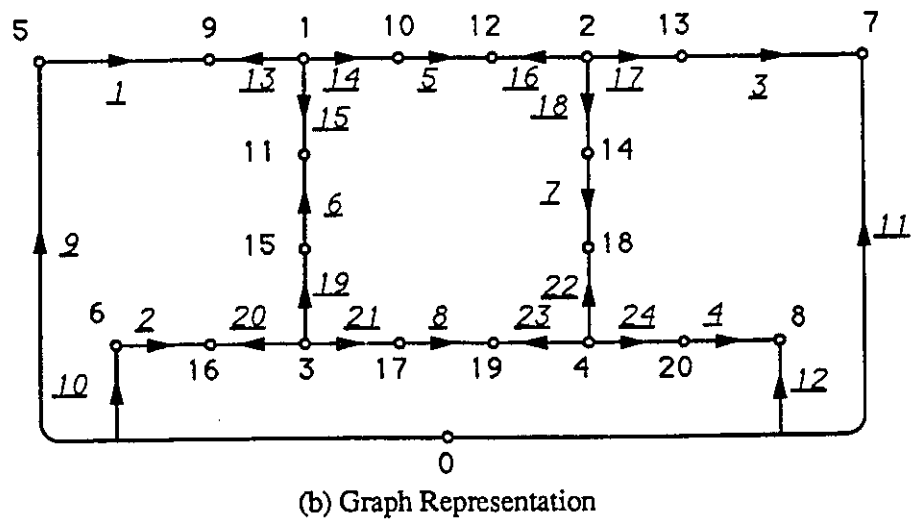


Figure 3.3. Graph Representation for the Four-Room Building

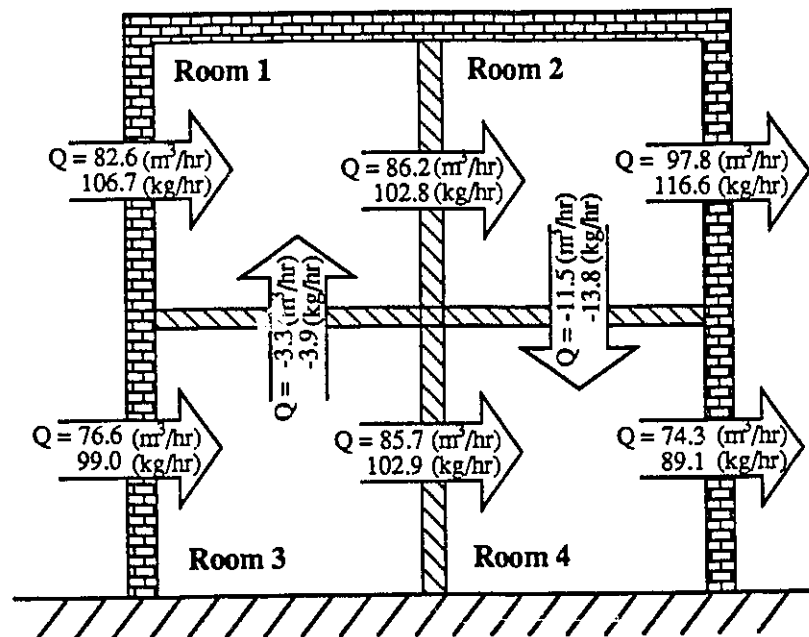


Figure 3.4. Calculated Airflow and Pressures for the Four-Room Building

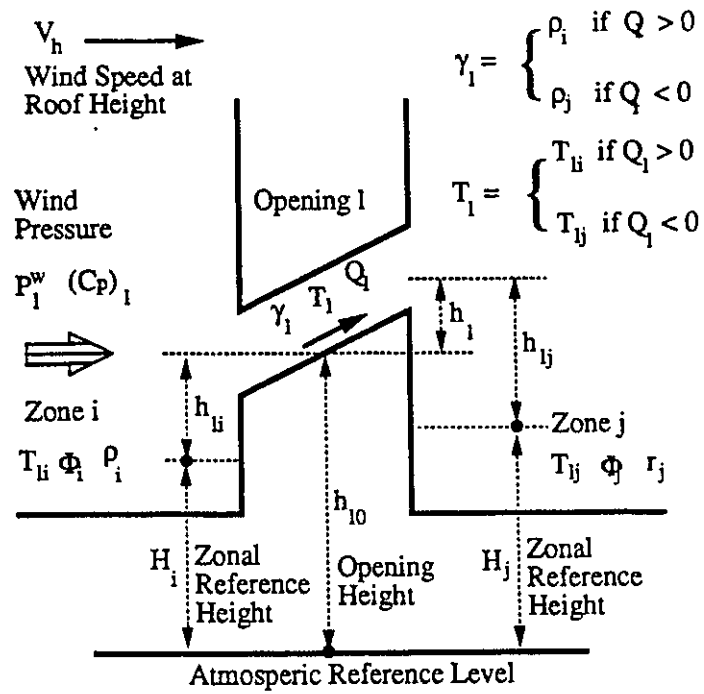


Figure 3.5. Schematic Graph of an Opening for Steady-State Airflow

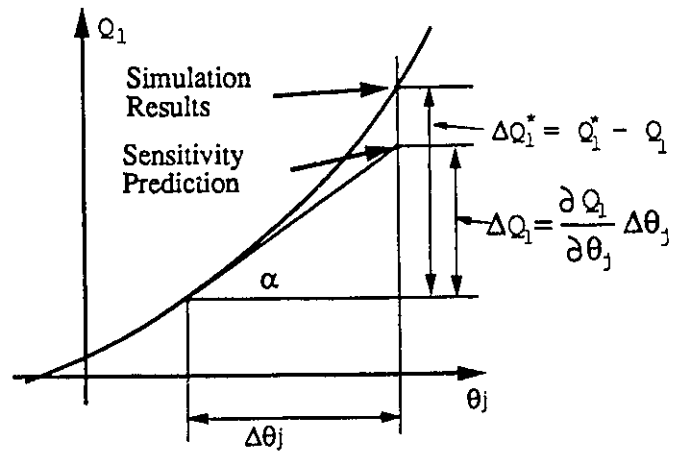


Figure 3.6. Indication of Discrepancy between Sensitivity Calculation and Simulation

Table 3.1. Symbols and Notations Used in Chapter III

---



---

$C$	update vector in airflow calculation
$C_p$	pressure coefficient
$D_{ii}$	dynamic admittance of an opening
$F()$	flow equation vector for all openings
$h$	height of openings to floor levels
$I$	incidence matrix
$J$	dynamic nodal-admittance matrix
$K$	flow coefficient of the power law equation
$n$	power law exponent
$P_f$	driving forces on an opening
$P_a$	atmospheric pressure
$P^w$	wind-induced pressure
$R_a$	gas constant for air
$T$	temperature
$U$	identity matrix
$V_h$	wind velocity at the roof height
$X$	across variable (pressure difference) vector of an edge, alias of $\Delta P$
$\gamma$	air density of an opening
$\eta$	opening air density matrix
$\theta$	input parameters about driving forces ( $\theta^p$ ) and opening characteristics ( $\theta^f$ )
$\Pi$	incidence matrix of physical connection graph
$\rho$	air density of a node
$\Phi$	nodal pressure vector
$\chi$	vector with all elements as 1s

---



---

Table 3.2. Calculation Formulae for Basic Jacobian Matrices

Elements	Calculation Formulae
$\frac{\partial (P_f)_i}{\partial T_i}$	$\Pi_{i1} \frac{\rho_i g}{T_i} \left\{ h_{i1} + u \left[ \frac{\Pi_{i1} + \xi(Q_i)}{2} \right] \times h_{i1} \right\}$
$\frac{\partial (P_f)_i}{\partial h_{i1}}$	$(-\rho_i + \rho_j) g \cdot u \left[ \frac{\Pi_{i1} - \xi(Q_i)}{2} \right]$
$\frac{\partial (P_f)_i}{\partial h_{i0}}$	$(-\rho_i + \rho_j) g$
$\frac{\partial (P_f)_i}{\partial (P^v)_i}$	$\Pi_{01}$
$\frac{\partial (P_f)_i}{\partial (C_p)_i}$	$\Pi_{01} \frac{(P^v)_i}{(C_p)_i}, \quad \text{or} \quad \Pi_{01} \frac{\rho_0}{2} v_h^2$
$\frac{\partial (P_f)_i}{\partial V_h}$	$2 \Pi_{01} \frac{(P^v)_i}{V_h}, \quad \text{or} \quad \Pi_{01} (C_p)_i \rho_0 V_h$
$\frac{\partial F_i}{\partial (\theta^f)_j}$	derivatives of flow equation to $(\theta^f)_j$
$\frac{\partial \gamma_i}{\partial T_i}$	$-\frac{\rho_i}{T_i} \quad \text{if} \quad \gamma_i = \rho_i$

Notes:

1. The function  $u()$  is equals to the nearest integer value toward negative infinity,
2.  $\Pi_{01} = -\sum_{i=1}^N \Pi_{i1}$  and  $\rho_0$  is the density of the outdoor air,
3.  $\xi(v) = 1$  if  $v > 0$ ;  $\xi(v) = -1$  if  $v < 0$ ;  $\xi(v) = 0$  if  $v = 0$ .

Table 3.3. Basic Jacobian Matrices of the Case Study

$$\frac{\partial \mathbf{P}_f}{\partial \theta^P} = \begin{bmatrix} \rho_0 g \frac{h_{10}}{T_0} & \rho_0 g \frac{h_{20}}{T_0} & -\rho_0 g \frac{h_{30}}{T_0} & -\rho_0 \frac{g_{40}}{T_0} & 0 & 0 & 0 & 0 \\ 0 & 0 & \rho_4 g \frac{h_{44}}{T_4} & 0 & 0 & -\rho_4 g \frac{h_{24}}{T_4} & 0 & 0 \\ 0 & 0 & (-p_2 + \rho_0) g & 0 & 0 & 0 & 0 & 0 \\ \frac{P_1^w}{C_{p1}} & 0 & 0 & 0 & 0 & 0 & 0 & 0 \\ 0 & 0 & 0 & -1 & 0 & 0 & 0 & 0 \\ \frac{P_1^w}{V_h} & \frac{P_2^w}{V_h} & -\frac{P_3^w}{V_h} & -\frac{P_4^w}{V_h} & 0 & 0 & 0 & 0 \end{bmatrix}^T$$

$$\frac{\partial \mathbf{P}}{\partial \theta^F} = \begin{bmatrix} 0 & 0 & 0 & \frac{Q_4}{K_4} & 0 & 0 & 0 & 0 \\ 0 & 0 & n_3 \frac{Q_3}{\Delta P_3} & 0 & 0 & 0 & 0 & 0 \\ n_1 \frac{Q_1}{\Delta P_1} & 0 & 0 & 0 & 0 & 0 & 0 & 0 \end{bmatrix}^T$$

$$\frac{\partial \gamma}{\partial \begin{bmatrix} T_0 \\ T_4 \end{bmatrix}} = \begin{bmatrix} -\frac{\rho_0}{T_0} & -\frac{\rho_0}{T_0} & 0 & 0 & 0 & 0 & 0 & 0 \\ 0 & 0 & 0 & 0 & 0 & 0 & -\frac{\rho_4}{T_4} & -\frac{\rho_4}{T_4} \end{bmatrix}^T$$

where

$$\theta = [T_0 \ T_4 \ h_{30} \ C_{p1} \ P_4^w \ V_h \ K_4 \ n_3 \ n_1]^T$$

$$\theta^P = [T_0 \ T_4 \ h_{30} \ C_{p1} \ P_4^w \ V_h]^T \quad \text{and} \quad \theta^F = [K_4 \ n_3 \ n_1]^T$$

Table 3.4. Sensitivity Analysis Results of the Case Study

Sensitivity of Individual Air Flow Rates									
	$\frac{\partial Q_1}{\partial T_0}$	$\frac{\partial Q_1}{\partial T_4}$	$\frac{\partial Q_1}{\partial h_{30}}$	$\frac{\partial Q_1}{\partial CP_1}$	$\frac{\partial Q_1}{\partial P_4^*}$	$\frac{\partial Q_1}{\partial V_h}$	$\frac{\partial Q_1}{\partial K_4}$	$\frac{\partial Q_1}{\partial n_3}$	$\frac{\partial Q_1}{\partial n_1}$
$Q_1(82.6)$	0.438	-0.016	0.808	67.93	-1.391	25.40	851.5	21.17	157.77
$Q_2(76.6)$	-0.714	-0.028	1.725	-32.20	-2.975	11.73	1821.9	45.20	-74.78
$Q_3(97.8)$	-1.055	0.258	5.834	14.36	3.133	18.08	-1918.4	152.91	33.36
$Q_4(74.3)$	0.123	-0.052	-3.067	24.20	-7.813	22.03	4784.6	-80.39	56.22
$Q_5(86.2)$	-0.478	-0.500	1.519	19.63	-2.148	20.02	1315.2	39.81	45.61
$Q_6(-3.3)$	0.625	0.483	-0.643	54.01	0.640	7.52	-391.8	-16.85	125.45
$Q_7(-11.5)$	-0.573	0.792	4.286	-5.23	5.245	-1.92	-3211.8	112.32	-12.16
$Q_8(85.7)$	-0.451	0.449	1.219	18.97	-2.568	20.11	1572.8	31.93	44.06
Semi-Relative Sensitivity of Individual Air Flow Rates									
	$\frac{(\partial Q_1)/Q_1}{\partial T_0}$	$\frac{(\partial Q_1)/Q_1}{\partial T_4}$	$\frac{(\partial Q_1)/Q_1}{\partial h_{30}}$	$\frac{(\partial Q_1)/Q_1}{\partial CP_1}$	$\frac{(\partial Q_1)/Q_1}{\partial P_4^*}$	$\frac{(\partial Q_1)/Q_1}{\partial V_h}$	$\frac{(\partial Q_1)/Q_1}{\partial K_4}$	$\frac{(\partial Q_1)/Q_1}{\partial n_3}$	$\frac{(\partial Q_1)/Q_1}{\partial n_1}$
$Q_1(82.6)$	0.530	-0.020	0.979	82.28	-1.684	30.77	1031.5	25.67	191.11
$Q_2(76.6)$	-0.933	-0.037	2.252	-42.05	-3.885	15.32	2379.2	59.03	-97.66
$Q_3(97.8)$	-1.079	0.264	5.967	14.69	3.204	18.49	-1962.2	156.39	34.12
$Q_4(74.3)$	0.165	-0.070	-4.131	32.60	-10.521	29.67	6443.0	-108.25	75.71
$Q_5(86.2)$	-0.554	-0.580	1.762	22.78	-2.491	23.22	1525.5	46.18	52.90
$Q_6(-3.3)$	18.926	14.620	-19.488	1636.55	19.390	228.06	-11874.0	-510.74	380.00
$Q_7(-11.5)$	-4.994	6.900	37.325	-45.61	45.676	-16.77	-27970.9	978.24	-105.00
$Q_8(85.7)$	-0.526	0.524	1.421	22.12	-2.995	23.45	1834.3	37.24	51.3
Semi-Relative Sensitivity of Zonal Ventilation Rates									
	$\frac{(\partial Q_1^T)/Q_1^T}{\partial T_0}$	$\frac{(\partial Q_1^T)/Q_1^T}{\partial T_4}$	$\frac{(\partial Q_1^T)/Q_1^T}{\partial h_{30}}$	$\frac{(\partial Q_1^T)/Q_1^T}{\partial CP_1}$	$\frac{(\partial Q_1^T)/Q_1^T}{\partial P_4^*}$	$\frac{(\partial Q_1^T)/Q_1^T}{\partial V_h}$	$\frac{(\partial Q_1^T)/Q_1^T}{\partial K_4}$	$\frac{(\partial Q_1^T)/Q_1^T}{\partial n_3}$	$\frac{(\partial Q_1^T)/Q_1^T}{\partial n_1}$
$Q_1^T(89.5)$	0.164	-0.020	0.979	82.28	-1.684	30.77	1031.5	25.650	191.11
$Q_2^T(97.8)$	-1.079	0.264	5.967	14.69	3.204	18.49	-1962.1	156.396	34.12
$Q_3^T(85.7)$	-0.526	0.524	1.421	22.12	-2.995	23.45	1834.3	37.247	51.39
$Q_4^T(85.7)$	-0.526	0.864	1.421	22.12	-2.995	23.45	1834.3	37.247	51.38
$Q_0^T(159.1)$	-0.174	-0.028	1.592	22.45	-2.744	23.34	1680.0	41.713	52.14

Note: Units for air flow rates are m<sup>3</sup>/hr.

Table 3.5. Error Analysis for Single Parameter Variations

$\theta$	$\Delta\theta$	$Q_1^t$ 89.5	$Q_2^t$ 97.8	$Q_3^t$ 85.7	$Q_4^t$ 85.7	$Q_0^t$ 159.1
$T_0$	3°C	0.44/ 7.36	-3.17/ 0.25	-1.35/-0.26	-1.35/-0.26	-0.83/-2.12
$T_4$	3°C	-0.05/-3.78	0.77/ 2.13	1.35/ 2.01	2.22/ 0.59	-0.13/-1.43
$h_{30}$	0.5	0.44/ 0.84	2.92/ 0.69	0.61/ 2.10	0.61/ 2.11	1.27/ 0.95
$C_{D_1}$	10%	6.63/ 1.79	1.29/ 1.95	1.71/ 4.41	1.71/ 4.41	3.22/ 2.20
$P_4^v$	10%	0.73/ 0.97	-1.52/-0.07	1.25/ 2.05	1.25/ 2.05	2.12/ 1.10
$V_h$	10%	13.77/-0.61	9.04/-1.86	10.06/-0.80	10.06/-0.80	18.57/-1.00
$K_4$	10%	0.83/ 4.97	-1.73/ 3.73	1.42/ 6.14	1.42/ 6.14	2.41/ 5.10
$n_3$	10%	1.49/ 0.63	9.94/ 0.05	2.08/ 4.95	2.08/ 4.95	4.31/ 0.95
$n_1$	10%	11.12/-2.05	2.17/-1.76	2.86/ 2.37	2.86/ 2.37	5.39/-1.27

Note: Units for air flow rates are m<sup>3</sup>/hr.



**Table 3.6. Error Analysis for Multiple Parameter Variations**

Varying Parameters	Sensitivity Prediction/Relative Discrepancy				
	$Q_1^t$	$Q_2^t$	$Q_3^t$	$Q_4^t$	$Q_0^t$
$T_0, T_4$	0.39/ 9.71	-2.39/ 0.41	-0.01/-30.78	0.87/ 0.28	-0.96/ -1.89
$T_0, h_{30}$	0.88/ 11.95	-0.25/-60.27	-0.74/ -9.71	-0.74/ -9.71	0.44/ 67.11
$T_0, C_{p1}$	7.07/ 4.70	-1.87/ -1.53	0.36/ 64.18	0.36/ 64.18	2.39/ 5.33
$T_0, V_h$	14.21/ 1.95	5.88/ -3.12	8.70/ 0.51	8.70/ 0.51	17.74/ -1.12
$T_0, K_4$	1.27/ 6.41	-4.89/ 0.60	0.06/-335.2	0.06/-335.2	1.58/ 6.67
$T_0, n_1$	11.56/ -3.52	-1.00/ 14.51	1.51/ 3.92	1.51/ 3.92	4.57/ -5.11
$C_{p1}, V_h$	20.40/ -3.54	10.33/ -2.82	11.76/ -1.04	11.76/ -1.04	21.79/ -2.02
$C_{p1}, K_4$	7.46/ 2.17	-0.43/ -4.28	3.12/ 3.63	3.12/ 3.65	5.62/ 2.03
$C_{p1}, K_3$	7.73/ 2.28	8.62/ 1.71	3.24/ 3.74	3.24/ 3.74	6.40/ 2.09
$C_{p1}, n_1$	17.75/ -8.14	3.46/ -7.62	4.57/ -1.02	4.57/ -1.02	8.61/ -6.86
$V_h, K_4$	14.61/ -0.95	7.31/ 0.86	11.47/ -1.51	11.47/ -1.51	20.98/ -1.91
$V_h, n_1$	24.89/-11.88	11.21/ -6.66	12.92/ -4.33	12.92/ -4.33	23.96/ -6.32
$K_4, n_4$	1.52/ 7.35	-3.16/ 5.17	2.59/ 9.61	2.59/ 9.61	4.40/ 7.73
$K_4, n_1$	11.95/ -3.42	0.44/ -9.40	4.28/ 0.30	4.28/ 0.30	7.80/ -2.50
$T_5, C_{p1}, V_h, K_4$	21.67/ -1.16	5.44/ 0.55	11.83/ -0.63	11.83/ -0.62	23.36/ -3.13
$T_0, T_1, T_2, T_3, T_4$	-0.54/ 0.74	-0.86/ 1.06	-0.64/ 0.94	-0.64/ 0.94	-1.06/ 0.85
$C_{p1}, C_{p2}, C_{p3}, C_{p4}$	6.89/ 2.14	4.52/ 1.48	5.03/ 2.04	5.03/ 2.04	9.29/ 1.91
$K_1, K_2, K_3, K_4$	7.74/ 1.76	8.34/ 1.96	6.65/ 3.40	6.65/ 3.40	12.40/ 3.29
$n_1, n_2, n_3, n_4$	11.84/ -4.23	11.96/ -3.27	7.90/ 0.54	7.90/ 0.54	14.90/ -0.12
$T_0, T_4, h_{30}, C_{p1},$ $V_h, K_4, n_3, n_1$	34.67/-14.92	21.24/-11.73	18.72/ -5.46	19.60/ -6.14	34.21/-10.63

Note: Units for air flow rates are  $\text{m}^3/\text{hr}$ .

**Table 3.7. Comparisons between Sensitivity and Monte-Carlo Approaches**

Varying Parameters	STD	STD of $Q_0'$		
		SENSI <sup>1</sup> (m <sup>3</sup> /hr)	MONTE <sup>2</sup> (m <sup>3</sup> /hr)	RELDIS <sup>3</sup> (percent)
$T_0$ $T_1$ $T_2$ $T_3$ $T_4$	3°C	1.21	1.18	2.54%
$h_{10}$ $h_{20}$ $h_{30}$ $h_{40}$	0.5m	3.40	3.19	6.58%
$C_{p1}$ $C_{p2}$ $C_{p3}$ $C_i$	10%	4.84	4.88	-0.83%
$K_1$ $K_2$ $K_3$ $K_4$	10%	6.82	6.48	5.25%
$n_1$ $n_2$ $n_3$ $n_4$	10%	8.13	7.80	4.23%
$V_h$	10%	18.81	19.86	-5.29%
All of Above		22.43	22.08	1.58%

Note:

1. Results based on sensitivity approach, equation (19),
2. Results using the Monte-Carlo method,
3. Relative discrepancy between the above two approaches.

# **CHAPTER IV**

## **FLUCTUATING AIRFLOW MODEL**

Fluctuating airflow in buildings is caused by temporal variations in wind-induced pressures on building envelopes. The phenomenon is a complex one, and depends upon characteristics of the building and openings, and characteristics of fluctuating wind-induced pressures.

In this Chapter, the fluctuating airflow model will be presented. The emphasis is to present fundamental ideas and concepts about the approach, component modelling, governing equation formulations, solution approach and combinatory effect assessment used in this model. More mathematically rigorous procedures for formulating governing equations for fluctuating airflow in multi-zone buildings is presented in Chapter V. The validation of the model is given in Chapter VI.

In Section §4.1, the approach used in the fluctuating airflow model is introduced. In Section §4.2, fundamentals of the governing equation formulation are presented. Three factors are analyzed: the flow resistance, compressibility of the room air and the inertia of the air in openings. The statistical linearization method, which is a major component of the fluctuating airflow model, and which makes it possible for fluctuating airflow to be studied in the frequency domain, is also presented. In Section §4.3, the frequency

analysis that is based on linear governing equations and utilizes the spectral analysis method is outlined. The modelling approach to account for large openings is presented in Section §4.4. In Section §4.5, factors that influence the effect of fluctuating airflow to total air exchanges across an opening or in a building are identified and analyzed. In Section §4.6, two case studies, one for a single-opening enclosure and the other for a two-opening building, are analyzed, modelled and solved using the presented methods.

#### **4.1. AN OVERVIEW OF THE FLUCTUATING AIRFLOW MODEL**

The fluctuating aspect of air infiltration and ventilation in a building is modelled by a fluctuating airflow system. This system consists of zones as rooms or internal spaces of the building, and openings as airflow paths through the building envelope and internal partitions. Time varying variables in this building airflow system include wind-induced pressures, airflow through openings and internal pressures. Other variables such as temperatures and mechanical ventilation systems are assumed to be steady-state and remain deterministic. The time-varying variables are divided into two parts, the mean values and the fluctuating components. The fluctuating airflow model calculates the fluctuating components of airflow and internal pressures caused by the temporal variations in wind-induced pressures.

Wind-induced pressures can be viewed as stationary processes having temporal fluctuations. The mathematical study of random processes reveals that a fluctuating pressure, as a random variable, can be considered as composed of an infinite series of

simple sine waves at different frequencies. Wind engineering finds out that the contribution of the sine wave at a particular frequency to the total fluctuating pressure is stable with time for a given combination of wind type and building configuration. This weight or power at each frequency to the total pressure can be more precisely represented by the concept of the power spectrum function. Fluctuating characteristics of a pressure can be fully described and represented by its power spectrum function. The calculation of the resultant airflow may be based on the spectral information of wind-induced pressures.

In light of the power spectrum concept, the complex problem of calculating the resultant airflow due to fluctuating pressures can be decomposed into an infinite series of simple problems, each one calculating the corresponding portion of airflow caused by the simple sine wave pressure at a single frequency. The total fluctuating airflow can then be obtained by summing up all these infinitesimal portions of airflow at single frequencies.

Theoretically, the above "divided" and "sum up" solution approach is the method of spectral analysis. In this method, the fluctuating airflow system in a building has spectra of wind-induced pressures as input. The output spectra of airflow are calculated from the system characteristics (the transfer functions) and the spectral information of wind pressures. Statistical information on the fluctuating airflow such as RMS (root-mean-square) values can then be obtained by spectral relations.

Further consideration is made to account for the air exchange across openings due to eddy penetrations. The pressure spectra as input represent the "point" forces of wind

fluctuations at individual points on the building envelope. The wind pressures over the area of openings are, however, not uniform and not perfectly synchronized. The pushing in and pulling out action by pressures on the air in the opening are not simultaneous at all points. Eddy flows, thus, occur in the opening.

This imperfect synchronization is solved using two approaches: the aerodynamic admittance approach and multi-path approach. In the first approach, an aerodynamic function is used to modify each wind pressure (spectrum) to obtain the net effect of all the "point" pressures on a large opening. In the second approach, each large opening is modelled by several airflow paths, and each path is assumed to allow pulsating airflow only. In either approach, the imperfect synchronization of pressures on an opening is considered and the fluctuating airflow due to eddy penetration is, therefore, accounted for.

The frequency and spectral analysis method requires implicit assumptions of the building airflow systems. The system must be deterministic, and the system parameters (such as window crack sizes) should be constant during the analysis. This poses no real restrictions since most airflow models assume deterministic or quasi-deterministic conditions on the building and climate. A simple solution is to perform separate analyses for different building and climate conditions.

Another implicit assumption by the spectral analysis method is that the system must be linear (a simple definition of a linear system is that the output for the sum of two inputs is equal to the sum of outputs for individual inputs, Roe, 1966). However, the airflow system of a building is non-linear due to the inherent nonlinearity of flow relations. In this thesis, a statistical linearization method is employed to solve this

problem by converting the nonlinear flow equations to equivalent linear relations. The "equivalence" is in a statistical sense (thus the name of the method). The variances of airflow calculated by both nonlinear and linear flow equations are made to be the same for each individual opening. With the flow equation linearized, the airflow in a building can be modelled by a linear system, and its transfer functions can be obtained by system techniques.

## 4.2. COMPONENT MODELLING

In describing the behaviour of a fluctuating airflow system, governing equations are formulated. These equations relate the inputs of pressures to outputs of airflow, and form the basic relation for later analysis. The fluctuating airflow in an opening is assumed to consist of pulsating flows only until Section §4.4 where this restriction is relaxed and eddy penetrations are included in the analysis.

For each airflow path through an opening, there are three basic components involved: the flow resistance of the opening, the inertia of air in the opening, and the compressibility of air in the zone. These three components are the major factors that affect the airflow through an opening. The component modelling process analyzes these components and forms analytic relationships among the involved variables, namely the pressures and the airflow rates.

#### 4.2.1. Flow Equation and Statistical Linearization

The opening (Figure 4.1) has a cross sectional area of  $A$  and a depth of  $L$ . The opening cross sectional area measures  $h$  in height by  $b$  in width.  $\bar{Q} + q(t)$  is the total airflow rate and  $\Delta\bar{P} + \Delta p(t)$  is the pressure difference.  $\bar{X}(t) + x(t)$  represents the imaginary distance between the position of a slug of air at any time  $t$  and the initial position (at  $t=0$ ), if the air is imagined to flow in a straight line along the opening's (imaginal) central axis. In the following, the  $(t)$  of fluctuating components of the variables are omitted.

The total volumetric airflow rate,  $Q(t)$ , and the total pressure difference across the opening,  $\Delta P(t)$ , are bounded by the flow relation  $F(\cdot)$ , i.e.:

$$Q(t) = F(\Delta P(t)) \quad (4-1)$$

Generally, the flow relation  $F(\cdot)$  is nonlinear. For example, when the power law relation is used for the opening,

$$Q(t) = K[\Delta P(t)]^n \quad (4-2)$$

where  $K$  is the flow coefficient,  $n$  is the exponent, and  $Q(t)$  is the volumetric airflow rate.

The same flow relation should also hold for the mean variables as:

$$\bar{Q} = F(\Delta\bar{P}) \quad (4-3)$$

Subtracting equation (4-3) from equation (4-1), the flow equation between fluctuating components of airflow and pressure difference can be obtained by:

$$q = Q(t) - \bar{Q} = F(\Delta P(t)) - F(\Delta\bar{P}) = F(\Delta\bar{P} + \Delta p) - F(\Delta\bar{P}) \quad (4-4)$$



Let  $G(\cdot)$  be the reverse relation of the general flow equation (4-1), then, the pressure difference across an opening can be expressed in terms of the mean and fluctuating airflow, as:

$$\Delta p = \Delta P(t) - \Delta \bar{P} = G(\bar{Q} + q) - G(\bar{Q}) \quad (4-5)$$

For the power law equation, it is:

$$\Delta p = K^{-\frac{1}{n}} \left[ (\bar{Q} + q)^{\frac{1}{n}} - \bar{Q}^{\frac{1}{n}} \right] \quad (4-6)$$

This is the required force (pressure actually) to overcome the fluctuating component of the flow resistance. The nonlinear relationship can be approximated by a linear relationship using a method called statistical linearization. In this method, the nonlinear relationship in equation (4-5) is transformed into a linear one as:

$$\Delta p = \lambda q \quad (4-7)$$

where  $\lambda$  is the linear coefficient. This  $\lambda$  is chosen in such a way so that the variances of  $\Delta p$  in both equations (4-5 and 4-7) are the same. The calculation is expressed in:

$$\lambda = \left[ \frac{\langle \Delta p^2 \rangle}{\langle q^2 \rangle} \right]^{\frac{1}{2}} \quad (4-8)$$

where the brackets  $\langle \rangle$  denote the variances of the enclosed variables. The statistical linearization method have also been successfully applied to other nonlinear dynamic systems (Ziegler and Schueller, 1987).

In most other previous studies (e.g.: Etheridge and Alexander, 1980; Lay and Bragg, 1988; etc.), the normal distribution is found to be adequate in describing the probabilistic characteristics of the given airflow rate data. In the statistical linearization method, the normal distribution is assumed for all fluctuating airflow. The coefficient can

then be expressed as:

$$\lambda = \frac{1}{\sigma_q} \left\{ \int_{-\infty}^{\infty} [G(\bar{Q}+q) - G(\bar{Q})]^2 \frac{1}{\sqrt{2\pi}\sigma_q} e^{-\frac{q^2}{2\sigma_q^2}} dq \right\}^{\frac{1}{2}} \quad (4-9)$$

If more accurate distribution functions of airflow are known, the linear coefficients can be calculated accordingly.

For the power law case, the temperatures on both sides of the opening are different, and the air densities are  $\rho_1$  and  $\rho_2$ . The air density in the opening ( $\rho_i$ ) equals  $\rho_1$  if the total airflow  $Q(t)$  is positive, or  $\rho_2$  if otherwise. The total and mean airflow rates (in mass flow rates) are expressed in:

$$Q(t) = \rho_i K [\Delta P(t)]^n, \quad \bar{Q} = \rho_1 K \Delta \bar{P}^n$$

The nonlinear relationship between the fluctuating components of airflow and pressure for the flow resistance through a power law opening can be derived from the above two equations as:

$$\begin{aligned} \Delta p &= \rho_i^{-\frac{1}{n}} K^{-\frac{1}{n}} (\bar{Q}+q)^{\frac{1}{n}} - \rho_1^{-\frac{1}{n}} K^{-\frac{1}{n}} \bar{Q}^{\frac{1}{n}} \\ &= \rho_1^{-\frac{1}{n}} K^{-\frac{1}{n}} \left[ \left( \frac{\rho_i}{\rho_1} \right)^{\frac{1}{n}} (\bar{Q}+q)^{\frac{1}{n}} - \bar{Q}^{\frac{1}{n}} \right] \end{aligned} \quad (4-10)$$

where the mean air mass rate  $\bar{Q}$  is positive.

The derivation of  $\lambda$  by equation (4-9) provides a expression for the linear coefficient of the power law relation in:

$$\lambda = \rho_1^{-\frac{1}{n}} K^{-\frac{1}{n}} \sigma_q^{\frac{1}{n}-1} \beta_v \quad (4-11a)$$

where  $\beta$  is calculated in:

$$\beta_v = \left\{ \frac{1}{\sqrt{2\pi}} \int_{-\infty}^{\infty} \left[ \left( \frac{p_i}{p_1} \right)^{\frac{1}{n}} \left( \frac{1}{I} + \eta \right)^{\frac{1}{n}} - \left( \frac{1}{I} \right)^{\frac{1}{n}} \right] e^{-\frac{\eta^2}{2}} d\eta \right\}^{\frac{1}{2}} \quad (4-11b)$$

where  $I = \frac{\sigma_q}{\bar{Q}}$  is the turbulence intensity of the airflow rate.

These two equations (4-11a and 4-11b) show clearly that the linear coefficient  $\lambda$  is a function of the turbulence intensity of the airflow rate, or a function of the RMS value of the airflow rate if the mean airflow rate is a constant, i.e.:

$$\lambda = \lambda(\sigma_q) \quad (4-12)$$

The calculation formulae of  $\lambda$  for the power law case, whether in a simple arithmetic expression or in an analytic integration, are listed in Table 4.1 for different conditions. The calculation for other types of flow equations can be done either by applying the general expression (equation 4-9) or by deriving simplified formulae as in Table 4.1, if computational speed is of a major concern.

#### 4.2.2. Inertia Force

When the airflow through an opening is fluctuating, the air is either accelerated or decelerated. By Newton's second law of motion, a force is required to cause this fluctuating change in the airflow rate. The source of this force is part of the pressure difference across the opening:

$$(\Delta p \cdot A) = (\text{mass in the opening}) \times (\text{acceleration rate}) = (\rho A L) \cdot \frac{d(q/A)}{dt} \quad (4-13)$$

The pressure difference across the opening required to overcome this inertial force can be expressed as:

$$\Delta p = M \frac{dq}{dt} \quad (4-14)$$

where  $M = \rho LA$ .

#### 4.2.3. Compressibility of Air

The air in each node/room is assumed to be an ideal gas and is compressible. Initially, the room air has a volume of  $V$  at a pressure of  $P_0$ . When the pressure  $P$  ( $P - P_0 = \Delta p$ ) is applied to the air, the volume of the original air in the room is compressed to a smaller volume,  $V - \Delta v$ . The volume decrement,  $\Delta v$ , equals the amount of outside air that is pressurized into the room, and therefore, an air exchange is taking place in the process.

From the ideal gas law for adiabatic processes, it follows:

$$P_0 V^\gamma = (P_0 + \Delta p)(V - \Delta v)^\gamma \quad (4-15)$$

or

$$P_0 = (P_0 + \Delta p) \left(1 - \frac{\Delta v}{V}\right)^\gamma$$

where  $\gamma=1.4$  is a constant. Assume  $|\Delta v/V| \ll 1$ , which is true in actual cases since the variations in driving forces are very small compared to  $P_0$ , then:

$$P_0 = P_0 + \Delta p - P_0 \gamma \frac{\Delta v}{V} - \Delta p \gamma \frac{\Delta v}{V} \quad (4-16)$$

The term  $\Delta p \gamma (\Delta v / V)$  is very small compared to the term  $P_o \gamma (\Delta v / V)$ , since  $|\Delta p / P_o| \ll 1$ . Therefore, the relation between the pressure change and the volume change can be expressed in a linear function as:

$$\Delta p = \frac{\gamma P_o}{V} \Delta v = \frac{\gamma P_a}{V} \Delta v \quad (4-17)$$

where  $P_a$  is the standard atmospheric pressure.

In a single opening enclosure, the volume change  $\Delta v$  equals the integration of the airflow rate into the enclosure. If the initial pressure  $P_0$  is chosen as the mean internal pressure  $\bar{p}^i$ , then  $\Delta p$  in equation (4-17) is equal to the fluctuating internal pressure and:

$$p^i = \frac{\gamma P_a}{V} \int_0^t q dt = B \int_0^t q dt \quad (4-18)$$

where  $B = \gamma P_a / V$ . For a zone with more than one opening, the above equation is expressed as:

$$p^i = B \int_0^t \sum_k q_k dt \quad (4-19)$$

The summation of airflow rates into the building is over openings,  $k$ , that are connected to the zone.

### 4.3. FLUCTUATING AIRFLOW MODELLING AND SOLUTION

Governing equations for the entire fluctuating airflow system of a building can be formulated using system techniques: the loop and nodal formulation procedures. The loop formulation relies on the pressure conservation in complete airflow loops, for example,

the loop formed by a wind pressure, an opening and the room air compressibility. This pressure conservation can also be viewed as pressure balance across the openings. The pressure difference across an opening between the wind-induced pressure and internal pressure should be balanced by the forces required to overcome the flow resistance through and inertia of air in the opening. The nodal formulation procedure relies on the well-known mass conservation of the air in a room. For the fluctuating airflow system, however, airflow due to compressibility of the room air has to be considered.

#### 4.3.1. Pressure Balance: Loop Formulation

The fluctuating airflow through an opening is influenced by three forces: inertia/mass, resistance and air compressibility forces. The equation which governs the fluctuating airflow through an opening is obtained from the pressure/force balance. For each opening, the fluctuating difference across the opening is balanced by resistance and inertial forces of the air flowing through the opening. Thus for each opening, the nonlinear governing equation is expressed as:

$$M_k \frac{dq_k}{dt} + [G(\bar{Q}_k + q_k) - G(\bar{Q}_k)] - p_k^w - B_i \int_0^t \sum_i q_i dt \quad (4-20)$$

where the subscript  $k$  is the index for the opening under analysis, and the subscript  $i$  in  $B_i$  indicates the zone to which the opening  $k$  is connected.

Through statistical linearization, the nonlinear term is approximated by a linear relation:

$$[G(\bar{Q}_k + q_k) - G(\bar{Q}_k)] \sim \lambda_k q_k \quad (4-21)$$

The linear equation is obtained as:

$$M_k \frac{dq_k}{dt} + \lambda_k q_k = P_k^w - B_i \int_0^t \sum_i q_i dt \quad (4-22)$$

The value of  $\lambda_k$  is chosen such that the variance of the nonlinear term in equation (4-20) is equal to the variance of the linear term in equation (4-22). The airflow  $q_k$  is assumed to have a normal distribution, and:

$$\lambda_k = \int_0^t \left[ G(\bar{Q}_k + q_k) - G(\bar{Q}_k) \right]^2 \frac{1}{\sqrt{2\pi} \sigma_{qk}} e^{-\frac{q_k^2}{2\sigma_{qk}^2}} dq_k \quad (4-23)$$

$\lambda_k$  is a function of the RMS value of the airflow rate.

The linear equation (4-22) is transformed into the frequency domain by applying the Fourier transformation as:

$$j\omega M_k Q_k(\omega) + \lambda_k Q_k(\omega) = P_k^w(\omega) - \frac{B_i}{j\omega} \sum_i Q_i(\omega) \quad (4-24)$$

where  $j = \sqrt{-1}$ . Separating the input variables from the outputs, it yields:

$$(\lambda_k + j\omega M_k) Q_k(\omega) + \frac{B_i}{j\omega} \sum_i Q_i(\omega) = P_k^w(\omega) \quad (4-25)$$

If the above formulation (equation 4-20 to 4-25) is applied to each of the openings, then, a set of (linear) equations can be obtained in the frequency domain. The inputs are the wind-induced pressures, and airflow through openings are the outputs. Solving the set of equations, a transfer function matrix can be obtained and each airflow can be calculated from input excitations, by:

$$Q_k(\omega) = \sum_i \left[ H_{qki}(\omega) \times P_i^w(\omega) \right] \quad (4-26)$$

where  $H_{qki}(\omega)$  is the transfer function of airflow in the opening  $k$  with respect to the wind pressure  $i$ .

#### 4.3.2. Mass Conservation: Nodal Formulation

There are two types of air mass sources/sinks in a room: the air mass transported by the airflow through openings and the air mass stored in a room due to pressurization and depressurization of the room air. For airflow through an opening ( $k$ ), the airflow rate through the opening can be expressed in relation to the pressure difference between two sides of the opening. In the case where the opening connects to the outside to a room ( $i$ ), the relation can be derived from equation (4-24) as:

$$Q_k(\omega) = \frac{1}{\lambda_k + j\omega M_k} [P_k^w(\omega) - P_i^i(\omega)] \quad (4-27)$$

The pressurization and depressurization of air in a room result in air mass variations in the room. If the air mass in the room is assumed to be constant, then, the variations can be attributed to an imaginary airflow path that connects the room with the outside. This airflow is referred to as the compressibility airflow and is denoted by the letter  $Q$  with a superscript  $i$ . The relation between the compressibility airflow and the internal pressure (which is the pressure difference across the imaginary airflow path) has been described by equation (4-18). Applying a Fourier transformation, the fluctuating airflow equation for the compressibility airflow path can be written in the frequency domain as:

$$Q_i^i(\omega) = \frac{j\omega}{B_i} P_i^i(\omega) \quad (4-28)$$



Mass conservation of the room air can be expressed in the frequency domain as:

$$\sum_k Q_k(\omega) - Q_i^i(\omega) = 0$$

or

$$\sum_k \frac{P_k^w(\omega) - P_i^i(\omega)}{\lambda_k + j\omega M_k} - \frac{j\omega}{B_i} P_i^i(\omega) = 0 \quad (4-29)$$

where the summation is over all the openings ( $k$ ) that are connected to room  $i$ .

Once the above mass conservation equation is applied to each room in a building, a set of equations is obtained as the nodal governing equations. The unknown variables are the internal pressures. Transfer functions of internal pressures can be obtained. Each internal pressure can be expressed in a linear combination of the excitation pressures. The internal pressure of room ( $i$ ), for example can be written as:

$$P_i^i(\omega) = \sum_k [H_{p^i k}(\omega) \times P_k^w(\omega)] \quad (4-30)$$

where  $H_{p^i k}(\omega)$  is the transfer function of the internal pressure in room ( $i$ ) with respect to wind pressure ( $k$ ).

#### 4.3.3. Spectral Analysis

If the spectra and co-spectra of all the fluctuating wind pressures are given, then, together with the relation in equation (4-26), the spectra of the airflow can be calculated. The airflow spectrum is equal to the summation of the contributions made by all the individual wind-induced pressures, with the effects of correlations between every two excitation forces being eliminated (or added). The formula can be expressed as:

$$S_{q_k}(\omega) = \sum_i \left\{ \|H_{qk}(\omega)\|^2 \cdot S_{p_i}(\omega) \right\} \pm \sum_{\substack{i,j \\ i \neq j}} \left\{ \|H_{qk}(\omega)\| \cdot \|H_{qk'}(\omega)\| \cdot S_{p_i p_j}^{(c)}(\omega) \right\} \quad (4-31)$$

where the symbol  $\|\cdot\|$  denotes the magnitude of the complex number. By using stochastic properties of the spectrum, the variance of airflow can be calculated by the integral of the airflow spectrum over the entire frequency range, i.e.:

$$\sigma_{q_k}^2 = 4\pi \int_0^\infty S_{q_k}(\omega) d\omega. \quad (4-32)$$

The obtained RMS values of airflow and the linear coefficients are functions of each other. Iterative procedures are employed to obtain the solutions. Initial values of airflow RMS are given at first. The calculation are performed to obtain a new set of  $\sigma_{qk}$  values. If the new values are equal (within a predefined precision) to the initial values, the calculation ends, and the obtained values are the solution. Otherwise, the new  $\sigma_{qk}$  values are taken as the initial values and the calculation repeats again until a solution is reached.

#### 4.4. MODELLING LARGE OPENINGS

In the approach presented so far, fluctuating airflow through an opening includes only the pulsation airflow. Air moves as a rigid body through the opening in a piston-like action. The pressures on the external opening are uniform and act on the whole area of the opening simultaneously with the same force. The model considers only the turbulence characteristics of the wind-induced pressure along the longitudinal direction (perpendicular

to the wall of the opening). Information on the turbulence intensity, integral scales of turbulence, spectra and co-spectra of the longitudinal wind pressure fluctuations are used in the model to calculate the resultant airflow.

In reality, however, the spatial variations in wind-induced pressures exists on the transverse (parallel to the wall and on the horizontal) and vertical ( parallel to the wall and on the vertical) directions in addition to temporal variation on the longitudinal direction (perpendicular to the wall). Therefore, the fluctuating pressures are not perfectly correlated with each other and are different at various points of the opening. This local pressure variation in pressures and imperfect correlation may cause penetration of eddies through the opening. The air movements are not piston-like actions through the opening, rather they may differ from location to location. In this case, the eddy penetration through the opening occurs, and the opening of concern is considered as a *large opening* in this thesis.

To correctly model this phenomenon, two approaches have been developed in this thesis: the multi-path approach and the aerodynamic admittance approach. The multi-path approach uses an equivalent technique that has been successfully employed to study deterministic airflow through large openings (Allard and Utsumi, 1992). A large opening is divided into several smaller airflow paths. Each path is modelled separately by the presented pulsating airflow model. The pressures on the portion of the opening corresponding to each airflow path are uniform and well correlated. The airflow through each path is piston-like pulsating only. However, the pressures are different and not well correlated on different airflow paths of the opening.

The multi-path approach is advantageous for modelling situations where substantial differences exist in the pressures on the large openings. It is flexible since the number of the smaller airflow paths can be chosen to appropriately represent any situation. This approach, however, requires more input data and computational effort due to additional airflow paths in the model.

In the other approach, the pressures are modified to reflect the imperfect correlations and the presence of eddies. This modifying function is the aerodynamic admittance. The aerodynamic admittance is a function of the characteristics of the building, the opening configuration, and the characteristics of the wind gustiness. For a given wind condition and a building with its opening configuration, the aerodynamic admittance is thus a frequency-dependent function. This function decreases with increasing frequency because the small turbulent eddies have shorter wavelengths. Those eddies with higher frequencies will suffer loss of coherence more rapidly than do the larger eddies at lower frequencies (Simiu and Scanlan, 1986).

Let  $\chi(f)$  be the aerodynamic admittance function for the pressure on an opening, then the spectrum of the pressures is modified by the relation:

$$\hat{S}_{p_k}(\omega) = S_{p_k}(\omega) \cdot \chi_k^2(\omega) \quad (4-33)$$

To calculate fluctuating airflow by this approach, the same procedure presented in Sections §4.1 to §4.3 is followed, except the input pressure spectra are replaced by the modified ones for large openings.

The aerodynamic admittance approach is suitable for situations where the pressures on the opening, though not perfectly correlated, have same spectra, and the modified spectra are adequate in representing the effective pressures.

#### **4.5. COMBINED EFFECT OF MEAN AND FLUCTUATING AIRFLOW**

In this chapter and Chapter III, the resultant steady-state airflow and fluctuating airflow are obtained. The steady-state results represent the mean airflow rates due to the action of the average driving forces. The fluctuating components are the results of temporal variations in the wind-induced pressures. Generally, both components of airflow exist, and the total air exchanges across the openings and through the building depend on both components.

The contribution of fluctuating airflow to total air exchange for each individual opening is assessed. Previous studies have indicated three factors: the hidden air, mixing effect and flow reversal (Etheridge and Alexander, 1980; Cockroft and Robertson, 1976). However, the existing research did not use information of the turbulent characteristics of wind pressures, and had no detailed information about the airflow. The estimation of these three factors had to be experimental or simple correlations.

The fluctuating airflow model, on the other hand, calculates detailed solutions of the fluctuating characteristics of airflow (and internal pressures) in the frequency domain. The spectra of airflow can be obtained by considering the building airflow system characteristics and the pressure spectral information. Much information may be extracted or calculated from the available airflow spectra.

##### **4.5.1. The Effect of Hidden Air**

The "hidden air" is the air in an opening that has not travelled from one side of the opening to the other side. This could happen when the direction of airflow changes

rapidly. For the air exchange in this situation, the airflow has to be kept in one direction long enough so that the air flowing from one side reaches and mixes with the air on the other side.

Two methods are proposed in this thesis to calculate the reduction (to the RMS value of the airflow rate) in air exchange due to the hidden air effect: the zero-crossing rate and statistical probability. The zero-crossing rate method calculates the rates of the directional changes of the airflow through an opening, and subtracts the amount of the hidden air according to the directional change rate. The amount of hidden air equals to the product of the rate of the airflow directional change and the volume of the opening, i.e.:

$$Q = v \cdot AL \quad (4-34)$$

where  $A$  and  $L$  are the area and depth of the opening respectively, and  $v$  is the zero-crossing rate. The value of  $v$  can be calculated from the power spectrum of the airflow rate in (Simiu and Scanlan, 1986):

$$v = 2 \left[ \frac{\int_0^\infty f^2 S_q(f) df}{\int_0^\infty S_q(f) df} \right]^{\frac{1}{2}} \quad (4-35)$$

The statistical method calculates the STD (Standard Deviation) of the air displacement distance. The percentage of the air that does cross the opening and exchange with the air on the other side is then calculated by assuming a normal distribution. The air displacement distance is defined in Section §4.1, and is related to the airflow rate by the equation:

$$x_k(t) = \frac{1}{A_k} \int_0^t q_k(t) dt \quad (4-36)$$

or by the corresponding relation in the frequency domain:

$$X_k(\omega) = \frac{1}{j\omega A_k} Q_k(\omega) \quad (4-37)$$

Therefore the air displacement spectrum can be obtained from the airflow spectrum in:

$$S_{x_k}(\omega) = \frac{1}{(\omega A_k)^2} S_{q_k}(\omega) \quad (4-38)$$

The STD of the air displacement can be calculated by:

$$\sigma_{x_k}^2 = 4\pi \int_0^\infty S_{x_k}(\omega) d\omega = \frac{4\pi}{A_k^2} \int_0^\infty \frac{S_{q_k}(\omega)}{\omega^2} d\omega \quad (4-39)$$

The probabilistic distribution of the air displacement distance is assumed to be normal with an STD of  $\sigma_{x_k}$  calculated in equation (4-39). In the case when the mean airflow rate is zero (such as the case of single sided ventilation), the portions of air trapped in the opening or crossing to other side can be calculated easily by the probabilities of air displacement, smaller or greater than the opening depth.

#### 4.5.2. The Effect of Mixing

Once the air flows from one side (say side 1) of an opening to the other side (side 2), the air will eventually mix with the air on that side. When fluctuations exist in the airflow, the airflow direction changes. The air from side 1 may not have enough time to be completely mixed with the air from side 2 before the airflow direction changes. The

not-well mixed air is moved back to side 1. Thus, not all the air that crossed the opening takes part in the air exchange.

The exact effect of mixing on the air exchange is a very complex problem, and depends on many local variables such as the opening shape, opening location relative to the room, and the air movement pattern in the room. Analytical solutions cannot be easily found. This problem exists for deterministic airflow as well, and has been studied by means of air exchange efficiency (Haghighat, et al., 1990). In the fluctuating airflow model, the effect due to mixing is excluded.

#### 4.5.3. The Effect of Flow Reversal

The actual effect of fluctuating airflow on the total air exchange, when mean airflow rates are not zero, can fall into two cases, as shown in Figure 4.2. In the case of Figure 4.2a, the fluctuating component is small and the total airflow rate is in one direction. The total air exchange is equal to the mean airflow rate. In the case of Figure 4.2b, the fluctuating component is large and the total airflow rate changes direction. Flow reversal occurs. The reversed airflow, indicated by the shaded area in Figure 4.2b, presents an additional air exchange across the opening.

Given the mean and RMS values of the fluctuating airflow rate through an opening and assuming a normal distribution for the fluctuating airflow rate, the percentage of reversely flowing air can be calculated by:

$$\beta = \int_{\frac{\bar{q}}{\sigma_q}}^{\infty} \frac{1}{\sqrt{2\pi}} e^{-\frac{1}{2}\eta^2} d\eta \quad (4-40)$$



The air exchange in the reverse direction (relative to the direction of the mean airflow rate) is  $\beta \sigma_q$ . The air exchange in the positive direction is  $\bar{Q} + \frac{1}{2}\beta \sigma_q$ . Therefore, the total air exchange across this opening is the summation of airflow in both directions, and can be calculated to be:

$$\bar{Q} + \frac{3}{2}\beta \sigma_q \quad (4-41)$$

## 4.6. CASE STUDIES

### 4.6.1. Single-Opening Enclosure

The case of the fluctuating airflow in a single-opening enclosure is special. The mean airflow rate through the opening is zero. In reality, air exchange does occur between the inside and outside. Several studies have been conducted to examine this case with similar findings (van der Maas, et al., 1991; Cockroft and Robertson, 1976; Hill and Kusuda, 1975).

#### 4.6.1.1. Modelling and Solution Approach for a Single-Opening Enclosure

The case study building has a volume of  $1000 \text{ m}^3$  and an opening with a cross sectional area  $A$  and a depth  $L$  located on the windward facade. The wind is blowing perpendicular to the opening. The opening conforms with to the power law flow relation. Let  $p^w$ ,  $p^i$ ,  $\Delta p$  and  $q$  be the fluctuating components of wind-induced pressure, internal pressure inside the enclosure, pressure difference across the opening, and the flow rate through the opening, respectively.

The loop governing equation is derived from the pressure/force balance across the opening. The pressure difference across the opening between external wind pressure and internal pressure,  $(p^w - p^i)$ , is balanced by the force required to overcome the flow resistance and the inertia of air in the opening. This pressure balance relation can be obtained from equation (4-22) as:

$$M \frac{dq}{dt} + \lambda q + B \int_0^t q dt = p^w \quad (4-42)$$

where  $M = \rho L/A$  and  $B = \gamma P_a/V$ . The coefficient of statistical linearization for the single opening can be calculated from the formulae in Table 4.1.

Applying Fourier transformations to both sides of the above equation, the system equation can be written in the frequency domain as:

$$(\lambda + j\omega M + \frac{B}{j\omega})Q(\omega) = P^w(\omega)$$

For a given wind-induced pressure  $P^w(\omega)$ , the resultant airflow through the opening can be expressed by:

$$Q(\omega) = \frac{1}{\lambda + j\omega M + B/j\omega} \times P^w(\omega) = H_q(\omega) \cdot P^w(\omega). \quad (4-43)$$

where  $H_q(\omega)$  is the transfer function of the airflow.

When the spectrum of the wind pressure at the opening is known, the airflow spectrum can be calculated as:

$$S_q(\omega) = \|H_q(\omega)\|^2 \cdot S_p^w(\omega).$$

The root-mean-square (RMS) value of the fluctuating airflow can be calculated by integrations of the spectrum over the frequency:

$$\sigma_q^2 = 4\pi \int_0^\infty S_q(\omega) d\omega$$

Using the iterative procedure outlined in Section §4.3.2, the solution can be obtained.

The nodal governing equation is derived from the air mass conservation in the enclosure. Applying equation (4-29), this equation can be expressed as:

$$\frac{P^w(\omega) - P^i(\omega)}{\lambda + j\omega M} - \frac{j\omega}{B} P^i(\omega) = 0 \quad (4-44)$$

The transfer function of the internal pressure is written as:

$$H_{pi}(\omega) = \frac{1/(\lambda + j\omega M)}{j\omega/B + 1/(\lambda + j\omega M)} \quad (4-45)$$

Therefore, the internal pressure spectrum can be calculated by the spectral relation:

$$S_{pi}(\omega) = \|H_{pi}(\omega)\|^2 \times S_{pw}(\omega)$$

When the opening is large, there are eddy penetrations through the opening as well as pulsation airflow. An aerodynamic admittance function can be used to attenuate the wind pressure spectrum. The coherence function of equation (2-6) is used for this purpose. Substituting appropriate parameter from the case enclosure, the function can be expressed as:

$$\chi(\omega) = e^{\frac{-9.43\sqrt{A}}{V_z} 2\pi\omega} \quad (4-46)$$

The wind pressure spectrum as input can be obtained either experimentally or by means of empirical formulae. To simplify the calculation procedure, it is assumed that the fluctuations in wind pressure are caused only by the gustiness in wind velocity, and the empirical formula for the wind velocity spectrum by Davenport (1961), shown in equation (2-5), is employed.

#### 4.6.1.2. Quantitative Analysis for the Single-Opening Case

Before going into the detailed calculations, it is valuable to estimate the maximum pulsating airflow into the enclosure. Assuming the opening is very large (but still permits only pulsating airflow), the internal pressure follows the external wind pressure instantly without delay, and the inertia of the air is zero. The air exchange should be equal to the number of times fluctuating airflow changes direction multiplied by the (average) amount of air exchange during each direction change, i.e.:

$$Q^* = v \times \sigma_v \quad (4-47)$$

where  $v$  is the zero crossing rate of the airflow. The changes in the RMS values of the air volume in the enclosure, due to pressurization or depressurization, can be calculated by:

$$\sigma_v = \frac{\sigma_{pi}}{\gamma P_a / V} = \frac{\sigma_{pi}}{B}$$

Since the internal pressure is assumed to be equal to the external pressure, it follows that:

$$\sigma_v = \frac{\sigma_{pw}}{B}$$

The zero crossing rate of airflow should be the same as that of the wind pressure, and be calculated as:

$$v = 2 \sqrt{\frac{\int_0^\infty f^2 S_p(f) df}{\int_0^\infty S_p(f) df}} \quad (4-48)$$

If the fluctuations under 10 cycles per second (since Davenport's spectrum over estimated the energy content at high frequencies) are of interest, this rate for the case study is

calculated at  $v = 1.18$  (1/s). The upper bound of the air exchange across the opening is calculated at  $Q^* = 1.18 \cdot 0.087 = 0.0934$  (m<sup>3</sup>/s).

#### 4.6.1.3. Theoretical Results for the Single-Opening Case

For the given values listed in Table 4.2, the RMS value for the fluctuating airflow rate is  $\sigma_q = 0.0554$  m<sup>3</sup>/s = 199.3 m<sup>3</sup>/hr. The internal pressure has an RMS value almost as large as that of the external wind pressure acting on the opening,  $\sigma_{pi}/\sigma_{pw} = 10.80/11.20 = 96\%$ . The internal pressure is also about one fourth of the mean free-stream wind pressure at the roof height and about one third of the mean wind pressure at the opening.

The related frequency information reveals more detailed information. Figure 4.3 shows the spectra and transfer functions involved. The wind pressure spectrum ranges from  $10^{-4}$  to  $10^{-1}$ , which means that the pressure fluctuation is more intense for the cycles between 10000 seconds and 10 seconds. The peak occurs at about 0.008 Hz, which indicates the wind fluctuation has an approximate return period of 120 seconds (Figure 4.3a). The transfer function  $H_q(\omega)$ , shown in Figure 4.3b, indicates the relationship between airflow and pressure. It represents the characteristics of the opening combined with the space of the enclosure.  $\|H_q(\omega)\|$  has a peak at a frequency of about 8 Hz, which is much higher compared to the wind pressure spectrum. The "band width" of  $\|H_q(\omega)\|$  ranges from 0.2 Hz to 3 Hz. The airflow spectrum is determined by the interaction between the pressure spectrum and the airflow transfer function. Since the pressure spectrum and the transfer function do not occupy the same frequency range, and only

overlap in a narrow band width, the resultant airflow spectrum is small (Figure 4.3d). The  $S_q(\omega)$  sits between peaks of  $S_{pw}(\omega)$  and  $\|H_q(\omega)\|^2$  (Figure 4.4). Compared to wind fluctuations, the frequency of the airflow fluctuation is higher. The fluctuating pressure difference across the opening is about one-fourth of that of  $p^w$ , although  $\sigma_{pi}$  is approximately equal to  $\sigma_{pw}$ . This is because the wind pressure and internal pressure do not change simultaneously. There is a phase difference between  $p^w$  and  $p^i$  (Figure 4.3c). This creates a pressure difference and thus the air exchange.

The calculated RMS value of fluctuating airflow is only a theoretical flow rate. The opening depth may affect the actual air exchange across the opening. The air in the opening must be displaced by at least the depth of the opening to enable the outside air to enter the building or the inside air to leave the building. The relationship between the actual air exchange and the RMS value of fluctuating airflow is complex and depends on the airflow spectrum and opening characteristics. Using the zero-crossing rate method of Section §4.5.1 (equations 4-34 and 4-35), the zero-crossing rate is calculated at 0.94 and the reduction due to hidden air effect is  $0.0094 \text{ m}^3/\text{s}$ , or 17% of the RMS value of fluctuating airflow. The calculation based on the air displacement spectrum results in an RMS value of 1.54 m for the air displacement distance. The percentage of reduction due to the hidden air effect is calculated from the probability that the air displacement is less than the opening depth. Calculations show that this is 15%.

When the aerodynamic admittance approach is applied in a recalculation, the air flow rate has an RMS value of  $0.0595 \text{ m}^3/\text{s}$ , or approximately 7% more than the results from the pulsating airflow only.

#### 4.6.2. Two-Opening Building

##### 4.6.2.1. Modelling and Solution Approach for a Two-Opening Building

A building with the dimensions of  $8 \times 8 \times 8 \text{ m}^3$  has two openings which are located on the windward facade. For the steady-state calculations, the mass conservation of this building is governed by:

$$K_1(\bar{P}_1^w - \bar{P}^i)^{n_1} + K_2(\bar{P}_2^w - \bar{P}^i)^{n_2} = 0 \quad (4-49)$$

For the analysis of fluctuating components in the pressures and airflow, the pressure balances for both openings result in two nonlinear governing equations:

$$\frac{\rho L_i}{A_i} \frac{dq_i}{dt} + K_i \left[ (\bar{Q}_i + q_i)^{\frac{1}{n_i}} - \bar{Q}_i^{\frac{1}{n_i}} \right] = P_i^w - \frac{\gamma P_a}{V} \int_0^t (q_1 + q_2) dt$$

where  $i = 1, 2$ . The nonlinear flow relations can be statistically linearized and a set of linear governing equations can be obtained as:

$$M_i \frac{dq_i}{dt} + \lambda_i q_i = p_i^w - B \int_0^t (q_1 + q_2) dt$$

where  $B = \gamma P_a / V$  and  $M_i = \rho L_i / A_i$ . The linear coefficients have values such that the variances of the linear and nonlinear terms in the latter two sets of equations above are the same. The transfer functions of airflow can be obtained by applying Fourier transformation to the linear set of equations, as:

$$H_q(\omega) = \begin{bmatrix} H_{q11}(\omega) & H_{q12}(\omega) \\ H_{q21}(\omega) & H_{q22}(\omega) \end{bmatrix} = \begin{bmatrix} \lambda_1 + j\omega M_1 + B/j\omega & B/j\omega \\ B/j\omega & \lambda_2 + j\omega M_2 + B/j\omega \end{bmatrix}^{-1} \quad (4-50)$$

When the spectra of wind pressures and the co-spectrum between them are known, the spectra for the fluctuating airflow can be expressed as:

$$S_{q_i}(\omega) = \|H_{q_i1}\|^2 \cdot S_{p_1}(\omega) + \|H_{q_i2}\|^2 \cdot S_{p_2}(\omega) - 2 \|H_{q_i1}\| \cdot \|H_{q_i2}\| \cdot S_{p_1 p_2}^{(c)}(\omega) \quad (4-51)$$

The RMS values of the airflow are obtained through integration of the corresponding spectra over the frequency.

In deriving the nodal governing equations, two types of airflow paths are considered: the openings and the compressibility airflow. For the two openings, the fluctuating airflow equations in the frequency domain can be expressed as:

$$Q_i(\omega) = \frac{1}{\lambda_i + j\omega M_i} [p_i(\omega) - P^i(\omega)]$$

The compressibility airflow is an imaginary path. It represents the air mass increments due to pressurization of the air volume in the building and decrements due to depressurizations. Its airflow rate is related to the fluctuating internal pressure as:

$$Q^i(\omega) = \frac{j\omega}{B} P^i(\omega)$$

The airflow system of the two-opening building, therefore, can be modelled by three openings in the frequency domain: the two openings and the imaginary airflow path for air compressibility. The nodal governing equation can be obtained from air mass conservation. By mathematical manipulations, the transfer functions for the internal pressure can be calculated as:

$$H_{p^i i}(\omega) = \left\{ \frac{1}{\lambda_i + j\omega M_i} \right\} / \left\{ \frac{j\omega}{B} + \sum_{i=1,2} \frac{1}{\lambda_i + j\omega M_i} \right\} \quad (4-52)$$

When the spectra and co-spectrum of wind pressures are known, the spectrum for the fluctuating internal pressure is calculated by the spectral relation:

$$S_{p^i}(\omega) = \|H_{p^i 1}\|^2 S_{p_1}(\omega) + \|H_{p^i 2}\|^2 S_{p_2}(\omega) + 2 \|H_{p^i 1}\| \|H_{p^i 2}\| S_{p_1 p_2}^{(c)}(\omega) \quad (4-53)$$

In turn, the RMS value and other statistical information of the fluctuating internal pressure can be derived from the spectrum.



#### 4.6.2.2. Calculation Results for the Two-Opening Building

The above modelling processes are valid for buildings having two openings. The inputs may differ depending on the specific opening locations and weather conditions. For the case study, the single-room building has two openings on the windward facade. The related parameters are listed in Table 4.3. To simplify the data input procedure, the power spectra of (longitudinal) wind velocities are assumed to comply with Davenport's (1961) correlation. The fluctuations in wind pressures are caused by gustiness in the wind speed only, and equations (2-5 and 2-8) are used to obtain the pressure spectra. The co-spectrum is affected by the correlation between the two wind pressures, and is assumed to comply with the relation proposed by Vickery (1970):

$$S_{p_1 p_2}^{(c)}(f) = \sqrt{S_{p_1}(f) \times S_{p_2}(f)} \times Coh(f)$$

where the coherence function in equation (2-7) is used.

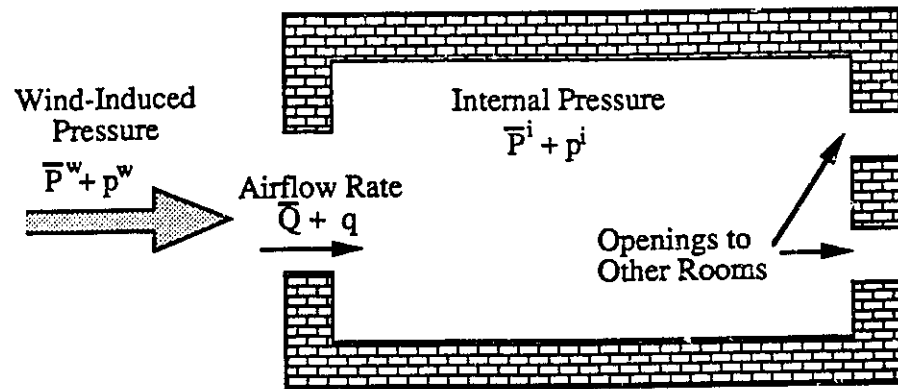
The fluctuating airflow through each opening is affected by the two fluctuating pressures and the correlation between them. The exact relationship depends on the transfer function matrix  $\mathbf{H}_q(\omega)$ .

Figure 4.5 shows the spectra and co-spectrum of wind pressures and the spectra for the fluctuating airflow. Table 4.3 lists the parameters used in the calculation and the steady-state solutions to the airflow of the building. The two spectra for airflow through two openings are almost the same. The maximum, of the spectra  $S_{q1}(\omega)$  and  $S_{q2}(\omega)$ , occurs at a frequency of 0.007 Hz, almost the same as those of the pressure spectra.

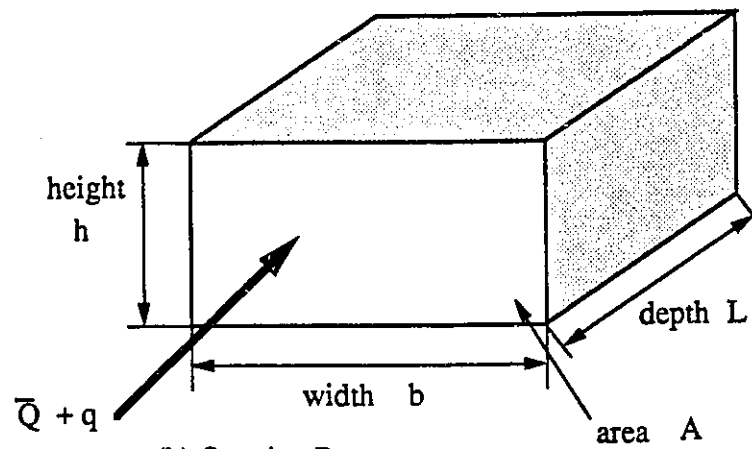
The power spectrum of the fluctuating airflow through each opening is composed of or affected by three terms: the effects of the two pressure spectra and the effects of the co-spectrum. In Figure 4.6 the three terms of the spectrum  $S_{qI}(\omega)$  are plotted. The first two terms contribute positively to the spectrum  $S_{qI}(\omega)$ ; the third term, related to the co-spectrum, contributes negatively. The spectrum  $S_{qI}(\omega)$  would be equal to the sum of the first two terms if the two wind pressures were totally un-correlated. However, since the two pressures on the same windward surface are correlated positively only to a certain extent, the actual spectrum  $S_{qI}(\omega)$  should be smaller than the sum of the first two terms by an amount given by the third term. In other words, the third term denotes the effect of correlation between the two pressures on the overall (spectrum of) fluctuating airflow.

Figure 4.7 shows that the two spectra of airflows through the two openings are not equal. The difference is due to the storage effect of the room air compressibility. When the airflow through one opening increases (or decreases) the airflow through the other opening does not necessarily need to be decreased (or increased). The room serves as a buffer for the differences between the two airflows.

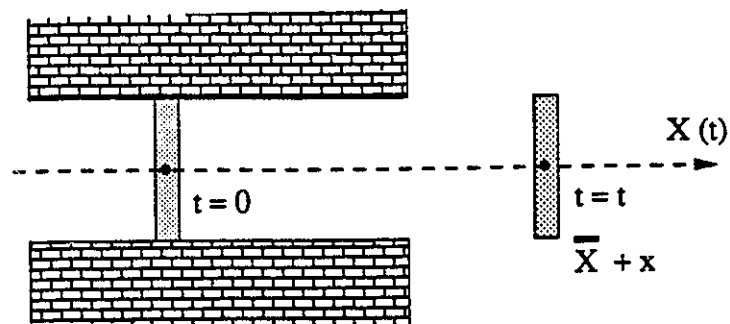
The RMS values for fluctuating airflows can be obtained by integration of the corresponding spectra. The results in Table 4.3 show that the RMS values of airflow rates are about 84% of the mean airflow rates (for the given conditions). This is to say that on average, the fluctuating components of airflow are about 84% of the mean values. Assuming normal distributions for airflow, the reversed airflow is about 11.7% of the RMS values. By using the relation in equation (4-41), the fluctuating airflow contributes to a 14.7% increase in air exchange over the mean values.



(a) Opening in Relation to Zones



(b) Opening Parameters



(c) Air Displacement Distance

**Figure 4.1. Schematic Diagram of an Opening for Fluctuating Airflow**

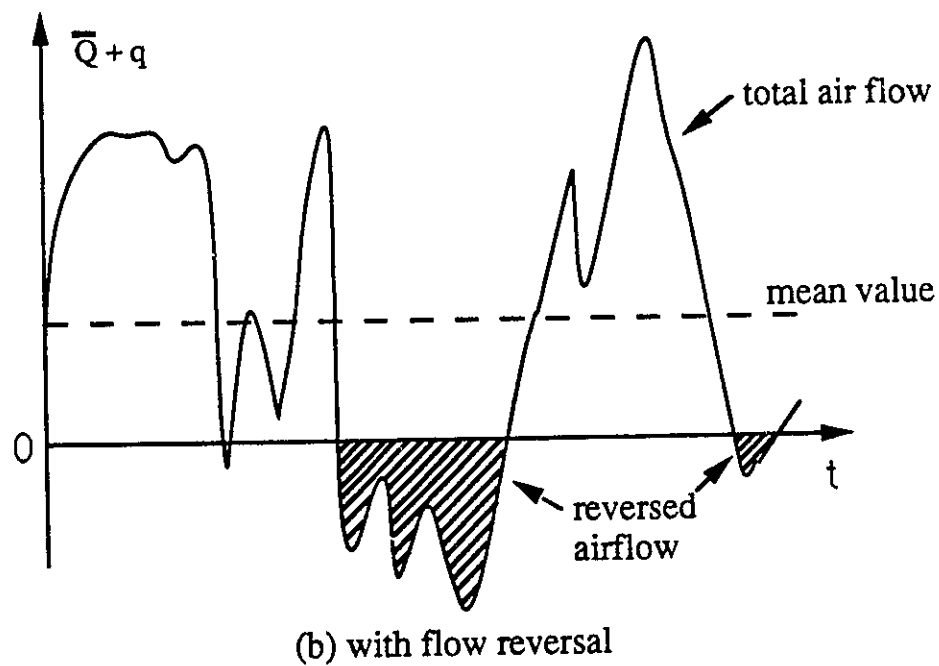
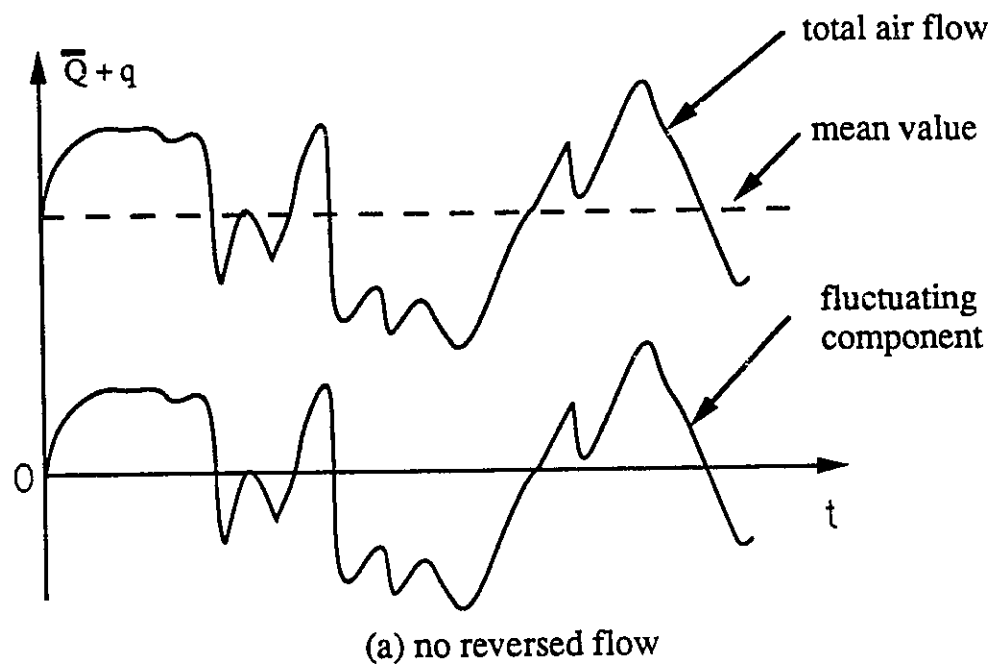


**Figure 4.2. Effects of Fluctuating Airflow to Air Exchange**

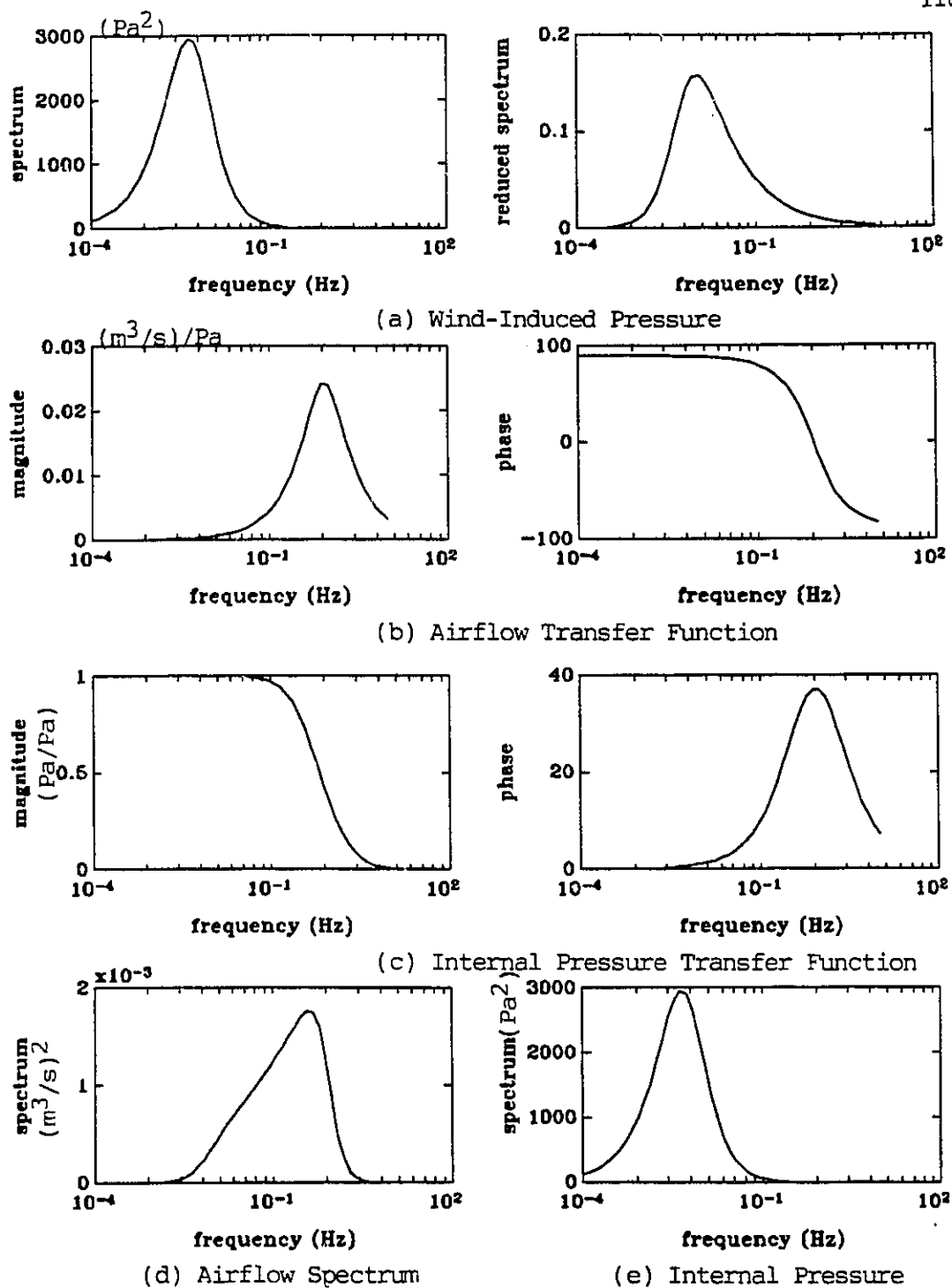


**Figure 4.3. Related Spectra and Transfer Functions for a One-Opening Enclosure**

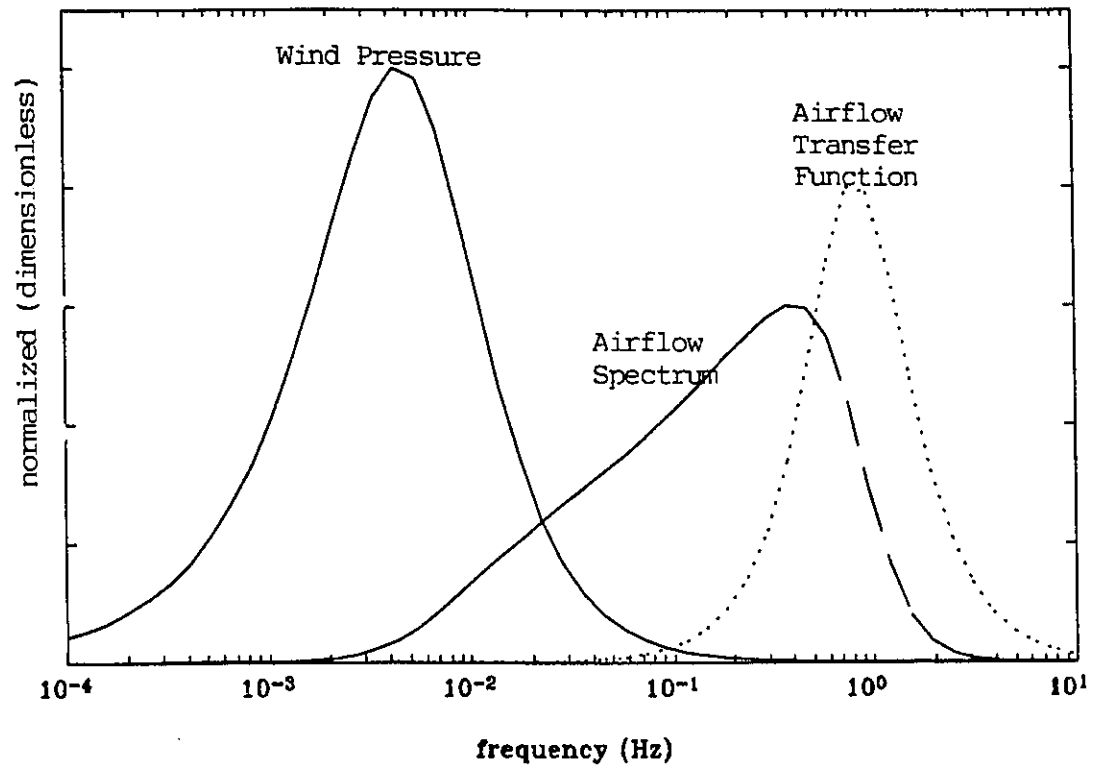
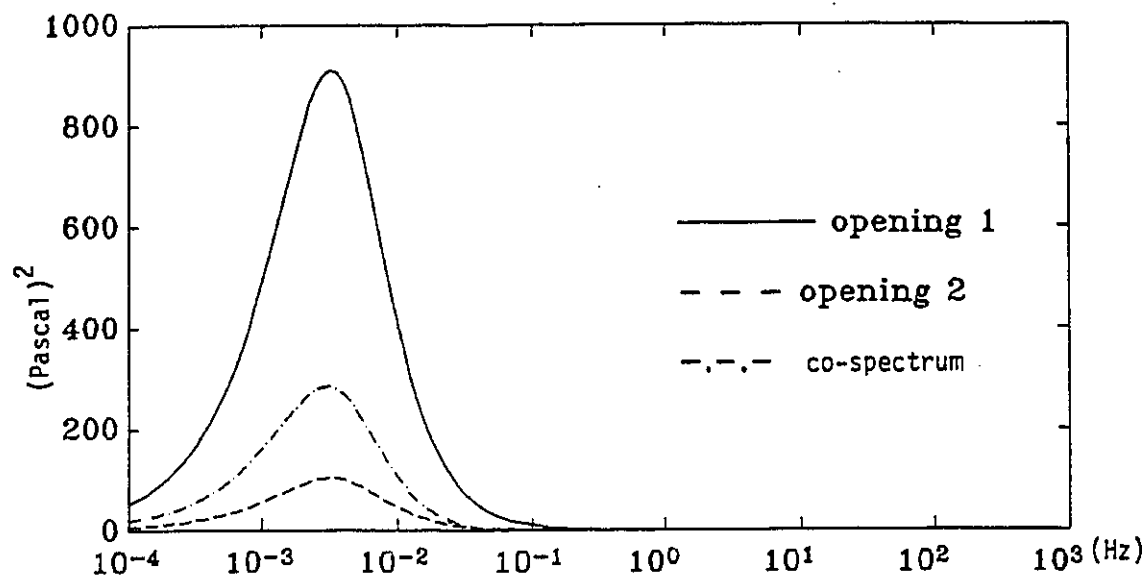
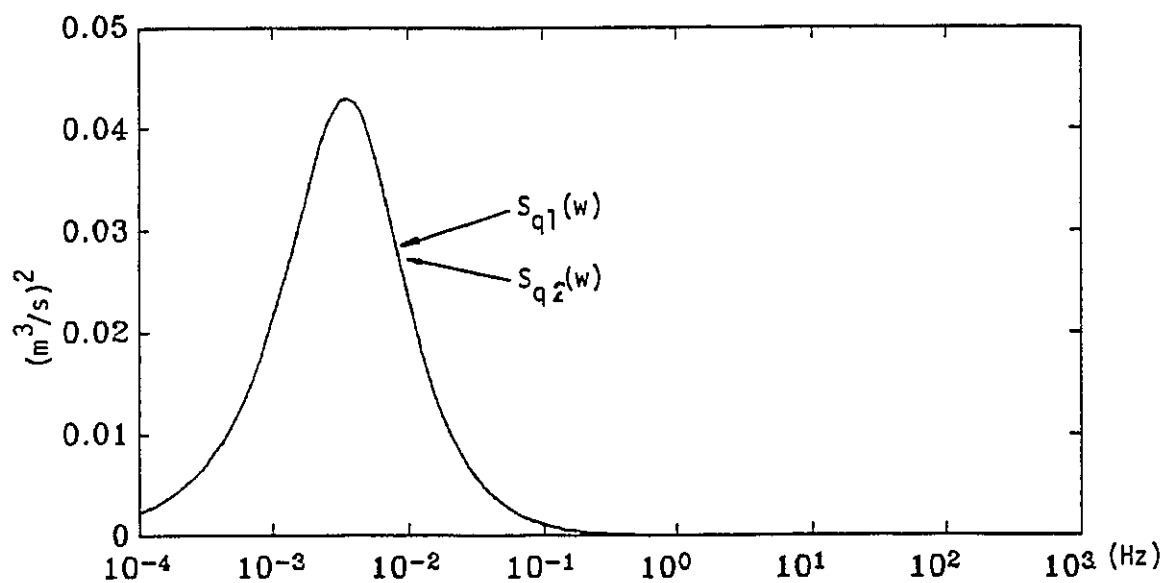


**Figure 4.4. Positions of Related Spectra and Transfer Function for A One-Opening Enclosure**



(a) Pressure Spectra and Co-spectrum



(b) Airflow Spectra

Figure 4.5. Related Spectra in Two Opening Enclosure

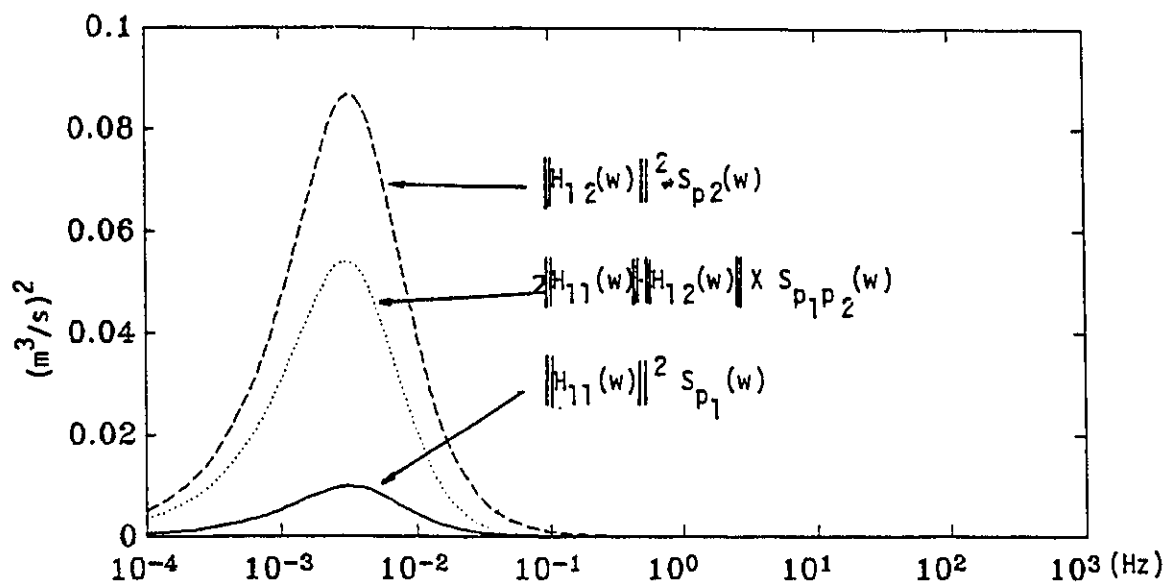
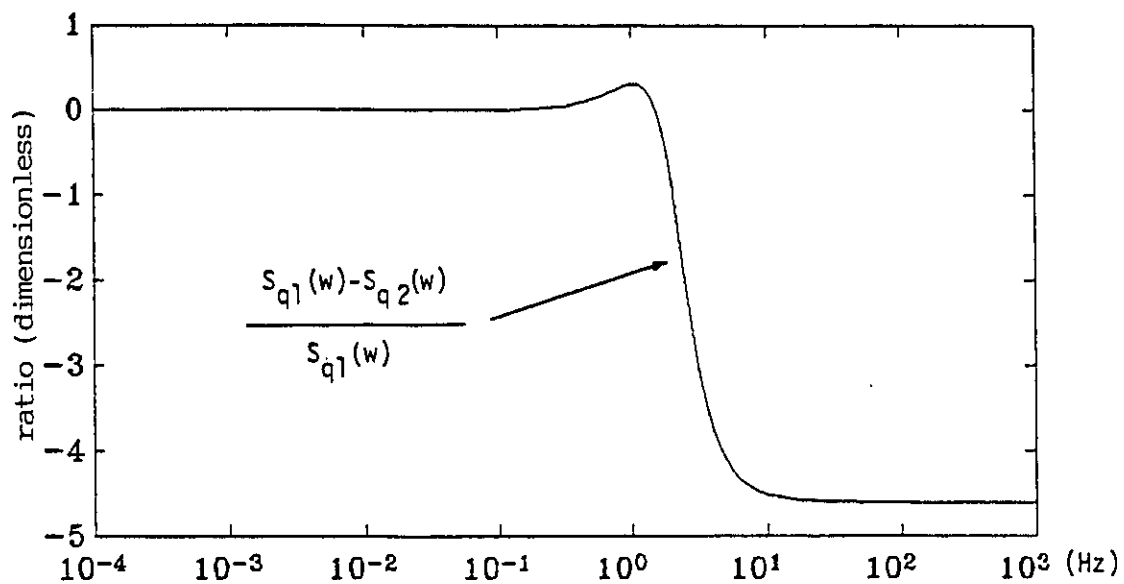
Figure 4.6. Decomposition of  $S_{q1}(w)$ 

Figure 4.7. Difference between Two Flow Spectra



**Table 4.1. Statistical Linearization Formulae for Power Law Equation**

Conditions	$\rho_1^{-\frac{1}{n}} K^{-\frac{1}{n}} \sigma_q^{\left(\frac{1}{n}-1\right)}$	$\beta_v$
General Case	$\rho_1^{-\frac{1}{n}} K^{-\frac{1}{n}} \sigma_q^{\left(\frac{1}{n}-1\right)}$	Equation (4-11b)
$\bar{Q} = 0$	$\frac{1}{2}(\rho_1^{-\frac{2}{n}} + \rho_2^{-\frac{2}{n}})^{\frac{1}{2}} K^{-\frac{1}{n}} \sigma_q^{\left(\frac{1}{n}-1\right)}$	$\left[ \frac{2}{\sqrt{2\pi}} \int_0^\infty \eta^{\frac{2}{n}} e^{-\frac{\eta^2}{2}} d\eta \right]^{\frac{1}{2}}$
$\rho_1 = \rho_2$ $\bar{Q} = 0$	$\rho_1^{-\frac{1}{n}} K^{-\frac{1}{n}} \sigma_q^{\left(\frac{1}{n}-1\right)}$	$\left[ \frac{2}{\sqrt{2\pi}} \int_0^\infty \eta^{\frac{2}{n}} e^{-\frac{\eta^2}{2}} d\eta \right]^{\frac{1}{2}}$
$\rho_1 = \rho_2$ $n = 0.5$ $\bar{Q} = 0$	$\rho^{-2} K^{-2} \sigma_q$	1.162099167
$\rho_1 = \rho_2$ $n = 0.5$ $\bar{Q} \neq 0$	$\rho_1^{-2} K^{-2} \sigma_q$	$\left[ \frac{4}{\sqrt{2\pi}} e^{-\frac{1}{2}\left(\frac{\bar{Q}}{\sigma_q}\right)^2} + 2\left(\frac{\bar{Q}}{\sigma_q}\right)^2 e^{-\frac{1}{2}\left(\frac{\bar{Q}}{\sigma_q}\right)^2} \right]^{\frac{1}{2}}$

Table 4.2. Parameters and Results for the Single-Opening Case

**Building Parameters**

Volume	$V = 1000 \text{ m}^3$ ,
	$\gamma = 1.4$ , $P_a = 101,325 \text{ Pascals}$
Temperature	$T_{in} = 22^\circ\text{C}$ , $T_{out} = 0^\circ\text{C}$ ,
Roof height	$H = 6 \text{ m}$

**Opening Characteristics**

Type: Orifice,	
Crack area:	$A = 0.05 \text{ m}^2$ , Depth: $L = 0.2 \text{ m}$
Discharge coefficient:	$C_d = 0.6$ ,
Opening position:	$Z = 4 \text{ m}$

**Wind Data**

Velocity at weather station:	$V_{10} = 10 \text{ m/s}$
Pressure coefficient:	$C_p = 0.8$
Turbulence intensity:	$I = 0.16$
Wind speed at roof height	$V_H = 8,76 \text{ m/s}$

**Pressure at the Opening**

Mean wind pressure	$\bar{P}^w = 39.4 \text{ Pascals}$
RMS of wind pressure	$\sigma_{pw} = 11.20 \text{ Pa}$

**Results of Fluctuating Airflow Model**

Airflow through the opening:	$\sigma_q = 0.0554 \text{ m}^3/\text{s}$
Internal pressure:	$\sigma_{pi} = 10.80 \text{ Pa}$
$\frac{\sigma_{pi}}{\sigma_{pw}} = 0.96$ , $\frac{\sigma_{pi}}{\bar{P}_H^w} = 0.25$ , $\frac{\sigma_{pi}}{\bar{P}^w} = 0.31$	

Pressure difference across opening:

$$\sigma_{\Delta p} = 2.47 \text{ Pa} \quad \sigma_{\Delta p}/\sigma_{pw} = 0.22$$

**Results with Aerodynamic Admittance Approach**

Airflow through the opening:	$\sigma_q = 0.0595 \text{ m}^3/\text{s}$
Internal pressure:	$\sigma_{pi} = 10.82 \text{ Pa}$

**Table 4.3. Parameters and Results of the Two Opening Case****Building Parameters**

Building dimension:	8×8×8	Volume = 500 m <sup>3</sup>
Temperatures:	$T_{in} = 23^{\circ}\text{C}$ ,	$T_{out} = 0^{\circ}\text{C}$
Roof Height:	H = 8 m	

**Opening Characteristics**

Type:	orifice openings	
Opening areas:	$A_1 = 0.05 \text{ m}^2$ ,	$A_2 = 0.04 \text{ m}^2$
Opening depth:	$L_1 = 0.2 \text{ m}$ ,	$L_2 = 0.2 \text{ m}$
Discharge coefficient:	$C_d = 0.6$	
Opening positions:	$Z_1 = 2 \text{ m}$ ,	$Z_2 = 6 \text{ m}$
Distance in between:	$\Delta Z = 4 \text{ m}$ ,	$\Delta Y = 6 \text{ m}$

**Wind Data**

Velocity at weather station:	$V_{10} = 5 \text{ m/s}$	
Pressure coefficients:	$C_{p1} = 0.5$ ,	$C_{p2} = 0.9$
Turbulence intensity:	$I = 0.16$	

**Derived Values**

Wind speed at roof height:	$V_H = 4.72 \text{ m/s}$	
Mean wind pressures:	$\bar{P}_1^w = 7.18 \text{ Pa}$ ,	$\bar{P}_1^w = 12.92 \text{ Pa}$
Stack effect:	$P_s = 3.93 \text{ Pa}$	
Mean airflow rates:	$\bar{Q}_1 = \bar{Q}_2 = 0.031 \text{ m}^3/\text{s}$ ,	$\text{ach} = 0.23$
RMS of wind pressure:	$\sigma_{pw1} = 1.25 \text{ Pa}$ ,	$\sigma_{pw2} = 3.71 \text{ Pa}$
K values:	$K_1 = 2.252$ ,	$K_2 = 2.816$

**Results of the Fluctuating Airflow Model**

$\sigma_{q1} = 0.026 \text{ m}^3/\text{s}$ ,	$\sigma_{q2} = 0.026 \text{ m}^3/\text{s}$
$\sigma_{q1}/\bar{Q}_1 = 84.2\%$ ,	$\sigma_{q2}/\bar{Q}_2 = 84.3\%$
$\sigma_{p1} = 1.14 \text{ Pa}$ ,	$\sigma_{p1}/\bar{P}_H = 7.9\%$
$\sigma_{p1}/\sigma_{ph} = 27\%$	

# **CHAPTER V**

## **FLUCTUATING AIRFLOW MODELLING:**

### **SYSTEM-THEORETIC APPROACH**

Fluctuating airflow systems can be modelled and predicted as shown in the previous chapter. The governing equations for simple cases can be derived by applying pressure balances and mass conservation principles on a case-by-case basis. For multi-zone buildings, however, the formulation for the fluctuating airflow system would be too complicated to be done in this fashion. In this chapter the general formulation procedures for both nodal and loop governing equations using the system theoretic approach are presented. Automatic formulation procedures are derived through detailed examinations of the system equations. With the results of this chapter, the system equations for any fluctuating airflow system can be obtained automatically. The automatic formulation procedure also makes it possible for computer implementation. Fundamentals of the system theory and its applications can be found in (Swamy and Thulasiraman, 1981; Haghighat, et al., 1988).

In this Chapter, the modelling procedure, graph and network representation and mathematical notations are explained in Section §5.1. Systematic formulations of nodal and loop governing equations are presented in Sections §5.2 and §5.3, respectively.

## 5.1. MODELLING OF FLUCTUATING AIRFLOW SYSTEMS

### 5.1.1. Graphic and Network Representation

A fluctuating airflow system is defined by its openings and internal rooms. This system can be modeled as a graph of nodes and edges. The *nodes* represent three types of physical entities: the separable room or space within a building, the location at the outside end of an opening upon which the wind-induced pressure acts, and the outside atmosphere. They are named as: room node (r-node), wind node (w-node) and atmospheric node (0-node). The reference height of each r-node is chosen the same as that in the corresponding steady-state model. Therefore, the stack effects and mechanical forces (if assumed to be deterministic) will not appear in the fluctuating airflow model.

*Edges* represent three types of physical entities. The first type is those openings that offer a resistance to the airflow. The second type models the imaginary airflow of each room due to the compressibility of the room air. This type of edge is represented by a link between the room nodes and atmospheric node. The third type of edge represents the fluctuating wind-induced pressures. These three types of edges are named as: flow-resistance edge (or f-edge for short), room-air edge (r-edge) and wind edge (w-edge), respectively.

*Orientations* of all the r-edges and w-edges are assigned in a way such that they are all incident into the atmospheric node. The orientations of the f-edges are arbitrary and can be defined by users.

Fluctuating components of the pressure difference and airflow rate are considered as the *across and through variables* of an edge, and they completely define the state of

the edge. The pressure difference is defined to be positive whenever the pressure drop across an edge is in the direction of the edge. The airflow rate in the direction of an edge is defined as positive for a through variable.

The *spanning tree*, which includes all the nodes and no circuit, of the graph for a building fluctuating airflow system is defined as the subgraph that contains exactly all the r-edges and w-edges. The f-edges will make up the *cospanning tree*. Each *fundamental cutset* contains only one node (either an r-node or w-node), and has an orientation away from the node. Since there is only one node in each cutset and it has an orientation away from the node, the fundamental cutset matrix is identical to the (reduced) incidence matrix with atmospheric node as *reference node*.

For the same spanning tree defined above, the *fundamental set of circuits* can be formed. Due to the definition of the spanning tree, each circuit contains exactly three edges: one f-edge and two r-edges or one f-edge, one r-edge and one w-edge. The direction of each fundamental circuit is defined as the direction that agrees with that of the chord edge (f-edge).

The graph of a (fluctuating) airflow system can also be represented by its network analogue. Two types of elements appear in the network, the resistors (which are f-edges and r-edges) and the (voltage) drivers or sources which are the fluctuating components of the wind-induced pressures (the w-edges). Two fundamental laws, Kirchhoff's current law and voltage law form the basic governing relations.

Figure 5.1a shows a building with two rooms and five openings. The fluctuating airflow system of this building can be represented by a graph in Figure 5.1b. In this

graph, there are five nodes and ten edges. The fundamental tree of this graph is shown as the bold lines in Figure 5.1c. The fundamental circuits consist of five loops, each having exactly one f-edge (Figure 5.1c).

Nodes are numbered by consecutive numbers starting from zero. The number zero is reserved for the atmospheric node. The room node are numbered from one. Then the w-nodes are numbered. The numbering of edges, starting from number one, begins with the f-edges, then the r-edges, and finally the w-edges. The numbering for f-edges is arbitrary. The numbering of r-edges and w-edges follows the orders of the numbering of r-nodes or w-nodes to which the edges are connected. The complete graph of the building fluctuating airflow system for the building of Figure 5.1a, with numbering, orientations and the fundamental tree, is shown in Figure 5.1d.

### 5.1.2. Mathematical Representations and Notations

Let  $N$  be the number of separated spaces depicted as nodes (r-nodes) in a building,  $M$  the number of openings,  $M^e$  the number of openings which have one end exposed to the outside and subjected to wind-induced pressures,  $M^i$  the number of openings that connect two rooms inside the building, and  $L$  the number of w-nodes (which equals the number of wind-induced pressures acting on the building envelope) (Table 5.1). The total number of nodes equals  $(N+L+1)$  and the total number of edges equals  $(M+N+L)$ .

The pressure difference and airflow rate of each edge are denoted by letters with subscripts such as  $p_i$  and  $q_i$ , and they are stochastic in nature:

$$p_i = p_i(t), \quad q_i = q_i(t).$$

The power spectra of these random variables are denoted by the letter  $S$  with subscripts of corresponding variable denotations:

$$S_{p_i}(f) = 2 \int_0^{\infty} e^{-j\omega \tau} R_{p_i}(\tau) d\tau$$

$$S_{q_i}(f) = 2 \int_0^{\infty} e^{-j\omega \tau} R_{q_i}(\tau) d\tau$$

where  $R_{p_i}(\tau)$  and  $R_{q_i}(\tau)$  are autocorrelation functions and  $j = \sqrt{-1}$ .

Vectors of across and through variables are associated with a set of edges, and are indicated by small bold letters as:

$$\mathbf{p} = \mathbf{p}(t), \quad \mathbf{q} = \mathbf{q}(t)$$

The elements of vectors are the variables of individual edges, so that:  $p_i = p_i$ ;  $q_i = q_i$ .

*Nodal variables* refer to measurements made at each node with respect to the datums or reference node. In the airflow graph or network, nodal variables are pressures at nodes with respect to the reference node (the atmospheric node), and are denoted by  $\phi$ . The circuit through variables are denoted by  $\psi$ .

In this chapter, the analysis is carried out in the frequency domain. The formulation involves the Fourier transformation of variables. Fourier transformations are denoted by capitals of corresponding letters, such as,  $P$ ,  $Q$ ,  $\Phi$ , and  $\Psi$ .

Edges are grouped into f-edges, r-edges and w-edges. Accordingly, the variables associated with edges can be partitioned into:

$$\mathbf{P} = [\mathbf{P}_f \quad \mathbf{P}_r \quad \mathbf{P}_w]^T; \quad \mathbf{Q} = [\mathbf{Q}_f \quad \mathbf{Q}_r \quad \mathbf{Q}_w]^T. \quad (5-1)$$



Similarly, the nodal variable  $\Phi$  can be partitioned into two parts:

$$\Phi = \begin{bmatrix} \Phi_r \\ \Phi_w \end{bmatrix} \quad (5-2)$$

according to the division between r-nodes and w-nodes.

## 5.2. FORMULATION OF NODAL GOVERNING EQUATIONS

The set of nodal governing equations is based on the Kirchhoff's current law (KCL), and is derived from three sets of equations: vertex equations, nodal transformation equations and flow equations.

### 5.2.1. Basic Equations

Let the *reduced incidence matrix* of the graph for a building fluctuating airflow system be  $\mathbf{I}$  and the airflow rates (in Fourier transform) of all edges be vector  $\mathbf{Q}$ , the *vertex equation* expresses Kirchhoff's current law for all the nodes and can be written as:

$$\mathbf{I}\mathbf{Q} = \mathbf{0} \quad (5-3)$$

The incidence matrix  $\mathbf{I}$  has  $(N+L)$  rows and  $(M+N+L)$  columns corresponding to the number of nodes and number of edges in the graph.

If the spanning tree is chosen to be composed of all the r-edges and w-edges, the incidence matrix  $\mathbf{I}$  is equivalent to the cutset matrix and the set of vertex equations is identical to the fundamental cutset equations. Therefore, if the reduced incidence matrix  $\mathbf{I}$  is partitioned by the columns according to the division between branch and chord edges:

$$\mathbf{I} = [\mathbf{I}_c \ \mathbf{I}_b] \quad (5-4)$$

then the submatrix  $I_b$  is an identity matrix of dimension  $(N+L)$ , that is:

$$I_b = U. \quad (5-5)$$

The condition for the above identity property to be true is described in Section §5.1.1.

The incidence matrix can further be divided within its columns and rows. In the partition of columns, the matrix is divided according to three types of edges; f-, r- and w-edges. The partition of nodes into r- and w-nodes divides the rows of matrix  $I$ .

$$I = \begin{bmatrix} I_{rf} & I_{rr} & I_{rw} \\ I_{wf} & I_{wr} & I_{ww} \end{bmatrix} \quad (5-6)$$

Compared to the identity property of the equation (5-5), the above partitioned matrix  $I$  in equation (5-6) can be simplified into:

$$I = \begin{bmatrix} I_{rf} & U & 0 \\ I_{wf} & 0 & U \end{bmatrix} \quad (5-7)$$

The vertex equation (5-3) can, thus, be rearranged into partitioned form as:

$$\begin{bmatrix} I_{rf} & U & 0 \\ I_{wf} & 0 & U \end{bmatrix} \begin{bmatrix} Q_f \\ Q_r \\ Q_w \end{bmatrix} = 0, \quad (5-8)$$

or into two parts as:

$$[I_{rf} \quad U] \begin{bmatrix} Q_f \\ Q_r \end{bmatrix} = 0, \quad (5-9)$$

and

$$I_{wf}Q_f + Q_w = 0$$

The flow rates of f-edges and r-edges are of primary concern for airflow studies. Equation (5-9) provides a relation confining  $Q_f$  and  $Q_r$ , and is referred to as the reduced vertex equation.

Nodal variables are pressures at the nodes with respect to the reference node (the atmosphere). The system theory shows that any across variable can be expressed as a linear combination of nodal variables (i.e. the pressure difference across any opening can be expressed by the internal pressures). The second equation set, necessary for the derivation of governing equations, is the nodal transformation equation. Let  $P$  be the vector of all across variables and  $\Phi$  the vector of nodal variables, the relation then takes the form:

$$P = I^T \Phi = T \Phi \quad (5-10)$$

where  $T = I^T$  is the transpose of the reduced incidence matrix. Using the similar partitions as for the vertex equations, the nodal transformation equation (5-10) can be re-written in the form of:

$$\begin{bmatrix} P_f \\ P_r \\ P_w \end{bmatrix} = \begin{bmatrix} T_{fr} & T_{fw} \\ T_{rr} & 0 \\ 0 & T_{ww} \end{bmatrix} \begin{bmatrix} \Phi_r \\ \Phi_w \end{bmatrix} = \begin{bmatrix} T_{fr} & T_{fw} \\ U & 0 \\ 0 & U \end{bmatrix} \begin{bmatrix} \Phi_r \\ \Phi_w \end{bmatrix}, \quad (5-11)$$

The last row of the above equation shows that:

$$P_w = \Phi_w \quad (5-12)$$

By substituting equation (5-12) into the first two rows of equation (5-11), it yields:

$$\begin{bmatrix} P_f \\ P_r \end{bmatrix} = \begin{bmatrix} T_{fr} \\ U \end{bmatrix} \Phi_r + \begin{bmatrix} T_{fw} \\ 0 \end{bmatrix} P_w. \quad (5-13)$$

This equation expresses across variables of the concerning edges as the summation of the linear combination of r-nodal variable and the linear combination of excitation forces. Since it is derived directly from equation (5-10), it is referred to as the reduced nodal transformation equation.

The relation between across and through variables of an edge is called the flow equation and has been examined in the last chapter. For the f-edges and r-edges, the flow equations can be expressed as:

$$Q_f = C P_f \quad (5-14)$$

and

$$Q_r = D P_r \quad (5-15)$$

where **C** and **D** are diagonal matrices. Therefore, the flow equation of f-edges and r-edges can be expressed in the matrix form of:

$$\begin{bmatrix} Q_f \\ Q_r \end{bmatrix} = \begin{bmatrix} C & 0 \\ 0 & D \end{bmatrix} \begin{bmatrix} P_f \\ P_r \end{bmatrix} \quad (6-16)$$

According to Chapter IV, the relationship between the fluctuating airflow rate and fluctuating pressure difference of a flow resistance edge in the time domain is:

$$M \frac{dq}{dt} + \lambda q = p$$

where  $M = \rho L / A$ ,  $\rho$  is air density in the corresponding opening,  $A$  is the opening area,  $L$  is the opening depth, and  $\lambda$  is the coefficient of statistical linearization. By applying Fourier transformation to the above equation, the flow relation in the frequency domain can be written as:

$$Q = \frac{1}{\lambda + j\omega M} P \quad (5-17)$$

Therefore, each element of the **C** matrix is given by:

$$C_i = \frac{1}{\lambda + j\omega M} \quad (5-18)$$

The time domain relationship for the r-edge, between the compressibility airflow and the pressure difference, is:

$$p = \frac{\gamma P_o}{V} \int_0^t q dt = B \int_0^t q dt$$

and can be expressed in the frequency domain as:

$$Q(\omega) = \frac{j\omega}{B} P(\omega) \quad (5-19)$$

so that an individual element of the **D** matrix is defined as follows:

$$D_i = \frac{j\omega}{B} \quad (5-20)$$

### 5.2.2. Nodal System Equation and Solution

Combining the reduced vertex equation (5-9), the reduced nodal transformation equation (5-13) and the flow equation (5-16), yields:

$$[I_{fr} \ U] \begin{bmatrix} C & 0 \\ 0 & D \end{bmatrix} \left\{ \begin{bmatrix} T_{fr} \\ U \end{bmatrix} \Phi_r + \begin{bmatrix} T_{fw} \\ 0 \end{bmatrix} P_w \right\} = 0,$$

By substituting **T** with **I<sup>T</sup>**,

$$[I_{fr} \ U] \begin{bmatrix} C & 0 \\ 0 & D \end{bmatrix} \left\{ \begin{bmatrix} I_{fr}^T \\ U \end{bmatrix} \Phi_r + \begin{bmatrix} I_{fw}^T \\ 0 \end{bmatrix} P_w \right\} = 0, \quad (5-21)$$

This equation contains the input  $P_w$  of the wind-induced pressures and the unknown nodal pressures  $\Phi_r$ .

With simplifications, equation (5-21) is changed to:

$$\begin{bmatrix} I_{rf} & C & D \end{bmatrix} \begin{bmatrix} I^T \\ U \end{bmatrix} \Phi_r + \begin{bmatrix} I_{rf} & C & D \end{bmatrix} \begin{bmatrix} I_{wf}^T \\ 0 \end{bmatrix} P_w = 0$$

Therefore, the relationship between  $\Phi_r$  and the excitation  $P_w$  can be expressed in the following equation:

$$\begin{bmatrix} I_{rf} & C & I_{rf}^T + D \end{bmatrix} \Phi_r = - \begin{bmatrix} I_{rf} & C & I_{wf}^T \end{bmatrix} P_w \quad (5-22)$$

Let

$$F = \begin{bmatrix} I_{rf} & C & I_{rf}^T + D \end{bmatrix} \quad (5-23)$$

$$E = - \begin{bmatrix} I_{rf} & C & I_{wf}^T \end{bmatrix} \quad (5-24)$$

then, the final set of governing equations can be written as:

$$F \cdot \Phi_r = E \cdot P_w \quad (5-25)$$

Generally, this equation can be solved as:

$$\Phi_r = F^{-1} \cdot E \cdot P_w \quad (5-26)$$

According to equations (5-13) and (5-16), the flow rates  $Q_f$  of the flow resistance edges, i.e. the airflow through openings, can be expressed as:

$$\begin{aligned} Q_f &= C \cdot P_f = C \left\{ I_{rf}^T \Phi_r + I_{wf}^T P_w \right\} \\ &= C \left[ I_{rf}^T F^{-1} E + I_{wf}^T \right] P_w \end{aligned} \quad (5-27)$$

The airflow due to compressibility of air can be expressed as:

$$Q_r = D P_r = D \Phi_r = D F^{-1} E P_w \quad (5-28)$$

### 5.2.3. Examples of Nodal Formulation

#### 5.2.3.1. Single Room Enclosure

Let's first consider a single room enclosure with an arbitrary number of openings which connect the room to the outside (Figure 5.2a). Let  $M$  be the total number of openings. The graph representation is given in Figure 5.2b. The submatrix  $\mathbf{I}_{ff}$  is formed as a row vector of  $M$  number of ones, and the  $\mathbf{I}_{wf}$  matrix is a negative identity matrix.

The vertex equation has only one row and can be written according to equation (5-9) as:

$$\left( \sum_{i=1}^M Q_i \right) + Q_{M+1} = 0.$$

The reduced transformation equation is:

$$\begin{bmatrix} P_f \\ P_r \end{bmatrix} = \begin{bmatrix} 1 \\ 1 \\ \vdots \\ 1 \end{bmatrix} \Psi_1 + \begin{bmatrix} U \\ 0 \end{bmatrix} P_w.$$

Through simplifications, the matrix  $F$  can be obtained as:

$$F = I_{ff} C I_{ff}^T + D_1 = D_1 + \sum_{i=1}^M C_i.$$

The excitation matrix  $E$  is:

$$\begin{aligned} E &= -I_{ff} C I_{wf}^T = -I_{ff} C (-U) = I_{ff} C \\ &= [C_1 \ C_2 \ \dots \ C_M]. \end{aligned}$$

Therefore, the system equation that governs the fluctuating airflow system of the single room enclosure is:

$$\left( D_1 + \sum_{i=1}^M C_i \right) \Phi_1 = [C_1 \ C_2 \ \dots \ C_M] P_w. \quad (5-29)$$

The solution can be obtained as:

$$\Phi_1 = \frac{[C_1 \ C_2 \ \dots \ C_M] P_w}{\left(D_1 + \sum_{i=1}^M C_i\right)} = \frac{\sum_{i=1}^M (C_i P_i)}{\left(D_1 + \sum_{i=1}^M C_i\right)} \quad (5-30)$$

Airflow rates of openings are given by:

$$Q_f = C(I_{ff}^T F^{-1} E + I_{wf}^T) P_w.$$

The flow rate of an individual opening is given by:

$$Q_i = C_i(\Psi_i - P_i) = C_i \times \frac{\sum \{C_j(P_j - P_i)\} - D_i P_i}{D_1 + \sum C_j} \quad (5-31)$$

A special case is the single-opening enclosure. The internal pressure and the flow rate can be calculated by:

$$\Phi_1 = \frac{C_1}{D_1 + C_1} \times P_w, \quad Q_1 = -\frac{C_1 \cdot D_1}{D_1 + C_1} \times P_w$$

### 5.2.3.2. Multiple Room Building

The first floor of the MEGA house (Haghighat, et al., 1989) contains three rooms and six openings (Figure 5.3a). This airflow system can be modeled as a graph of 8 nodes and 13 edges (Figure 5.3b). For the reduced incidence matrix, the submatrix  $I$  can be obtained as:

$$I_{ff} = \begin{bmatrix} -1 & 0 & 1 & 0 & -1 & 1 \\ 0 & -1 & 0 & 0 & 1 & 0 \\ 0 & 0 & 0 & 1 & 0 & -1 \end{bmatrix}; \quad I_{wf} = \begin{bmatrix} 1 & 0 & 0 & 0 & 0 & 0 \\ 0 & 1 & 0 & 0 & 0 & 0 \\ 0 & 0 & -1 & 0 & 0 & 0 \\ 0 & 0 & 0 & -1 & 0 & 0 \end{bmatrix}. \quad (5-32)$$



The set of system equations can be obtained as:

$$\begin{bmatrix} C_1 + C_3 + C_5 + C_6 + D_1 & -C_5 & -C_6 \\ -C_5 & C_2 + C_5 + D_2 & 0 \\ -C_6 & 0 & C_4 + C_6 + D_3 \end{bmatrix} \begin{bmatrix} \Phi_1 \\ \Phi_2 \\ \Phi_3 \end{bmatrix} - \begin{bmatrix} C_1 & 0 & -C_3 & 0 \\ 0 & C_2 & 0 & 0 \\ 0 & 0 & 0 & -C_4 \end{bmatrix} \begin{bmatrix} P_1 \\ P_2 \\ P_3 \\ P_4 \end{bmatrix} \quad (5-33)$$

#### 5.2.4. Automatic Formulation of Nodal System Equations

In Section §5.2.2, the set of system equations that governs the fluctuating airflow system of a building is derived:

$$F \cdot \Phi_r = E \cdot P_w \quad (5-34)$$

where

$$F = [I_{rf} C I_{rf}^T + D], \quad E = -[I_{rf} C I_{wf}^T]$$

The second example in Section §5.2.3. shows that the matrices **F** and **E** of the system equations have certain patterns. The formulation and solution to this set of equations are the central task of establishing input-output relationships for the fluctuating airflow system of a building.

In equation (5-23), the  $I_{rf}$  matrix contains only 1, 0 and -1's, and matrices **C** and **D** are diagonal matrices.  $I_{rf}$  is part of the incidence matrix which represents the interconnection of f-edges to r-nodes. In other word, the  $I_{rf}$  matrix indicates the connections of openings to rooms. A physical connection graph can be built, it has only rooms as nodes and openings as edges. The orientations and numbering of nodes and edges in this graph is the same as those of the corresponding r-nodes and f-edges in the graph of the fluctuating airflow system. The MEGA house example building has a

physical connection graph as in Figure 5-3c. The  $L_{rr}$  matrix will, therefore, be the (reduced) incidence matrix of the physical connection graph.

$F$  is a  $N \times N$  matrix, where  $N$  is the number of rooms in the building. The analysis shows that the relationship between the elements of this matrix and the topology of the physical connection graph are: 1) The  $i^{\text{th}}$  diagonal element is composed of the sum of the  $C$  values of edges which are connected to (incident on) room  $i$ . The sign of the element is positive. 2) The off-diagonal element  $F$  is composed of the sum of the  $C$  values of edges that are incident on both node  $i$  and node  $j$ . The signs are negative.  $E$  is an excitation matrix, it relates excitation forces  $P_w$  to  $\Phi_r$ . The number of rows equals the number of r-nodes or rooms, and the number of column equals the number of wind pressures. It can be formed by:

$$E_{ij} = \xi(i, j) \times C_j \quad (5-35)$$

Each element is either zero or  $C_j$ , where  $j$  is a opening connecting node  $i$  to the outside.

The  $\xi(i, j)$  is a sign function and takes a value as:

$$\xi(i, j) = \begin{cases} 0 & \text{if } j^{\text{th}} \text{ edge connects an r-node } i \text{ to another r-node,} \\ 1 & \text{if } j^{\text{th}} \text{ edge connects a r-node } i \text{ to a w-node,} \\ & \text{and is incident into the node } i, \\ -1 & \text{if } j^{\text{th}} \text{ edge connects a r-node } i \text{ to a w-node, and} \\ & \text{is incident out of the node } i. \end{cases} \quad (5-36)$$

### 5.2.5. Properties of the Matrix $F$

Matrix  $F$  determines whether the system equation (5-25) is solvable. It has the following properties:

- 1). Matrix  $F$  is symmetric. Definition of off-diagonal elements ensures that:

$$F_{ij} = F_{ji}, \quad i \neq j \quad (5-37)$$

since both elements are negative and are composed of  $C$  values of the same edges that connect nodes  $i$  and  $j$ .  $F$  has positive diagonal elements and negative off-diagonal elements.

- 2). Elements of matrix  $F$  are complex. This is because the analysis is carried out in the frequency domain and  $C_i$  and  $D_i$  are complex numbers. The diagonal elements are non-zero.

- 3). Matrix  $F$  is strictly diagonal dominant.

- 4). Matrix  $F$  is non-singular.

Therefore, it can be concluded that the solution to the system equation (5-25) exists.

## 5.3. FORMULATION OF LOOP GOVERNING EQUATIONS

The derivation of loop equations relies on the fundamental tree. As defined in Section §5.1.2., the fundamental tree is chosen to be constituted of all the  $r$ -edges and  $w$ -edges. The co-spanning tree is then composed purely of the  $f$ -edges. Each fundamental circuit consists of exactly one  $f$ -edge, its direction is chosen to agree with that of the  $f$ -edge. There are two types of circuits in terms of its constituent edges: the

f-edge connects a w-node and an r-node and the f-edge connects two r-nodes. The loop system equations are formulated from three sets of equations: the circuit equations, the loop transformation equations and the flow equations.

### 5.3.1. Basic Equations

The *circuit matrix* indicates the interconnecting relationship between edges and circuits. Let **B** be the circuit matrix for the fundamental circuits. Then **B** is an  $M \times (M+N+L)$  matrix. The number of its rows is equal to the number of the fundamental circuits (which in turn equal to the number of flow resistance edges or openings), and the number of its columns is equal to the number of all the edges in the graph. The elements of the **B** matrix are defined as:

$$B_{ij} = \begin{cases} 1 & \text{if } j^{\text{th}} \text{ edge is in the } i^{\text{th}} \text{ circuit and its orientation} \\ & \text{agrees with the circuit orientation,} \\ -1 & \text{if } j^{\text{th}} \text{ edge is in the } i^{\text{th}} \text{ circuit and its orientation} \\ & \text{does not agree with the circuit orientation,} \\ 0 & \text{if } j^{\text{th}} \text{ edge is not in the } i^{\text{th}} \text{ circuit.} \end{cases} \quad (5-38)$$

Each row of **B** is referred to as a circuit vector.

The set of fundamental circuit equations is a direct application of Kirchhoff's voltage law to fundamental circuits. This set of equations expresses the relationship among across variables of edges. Let **P** be the vector of across variables of all edges, the set of fundamental circuit equations can be expressed as:

$$BP = 0. \quad (5-39)$$

Matrix  $B$  and vector  $P$  can be partitioned according to the division among f-edges, r-edges, and w-edges, i.e.:

$$\begin{bmatrix} B_f & B_r & B_w \end{bmatrix} \begin{bmatrix} P_f \\ P_r \\ P_w \end{bmatrix} = 0. \quad (5-40)$$

The f-edges are chords and both r-edges and w-edges are branches of the fundamental tree. If the orientation and numbering conventions in Section §5.1.2 is followed, the fundamental circuits are numbered according to the order of f-edges, and the orientations of fundamental circuits agree with f-edges, then the submatrix  $B_f$  is an identity matrix:

$$B_f = U. \quad (5-41)$$

Thus the set of fundamental circuit equations (5-40) can be rewritten as:

$$\begin{bmatrix} U & B_r \end{bmatrix} \begin{bmatrix} P_f \\ P_r \end{bmatrix} + B_w P_w = 0. \quad (5-42)$$

Let  $\Psi$  be the (Fourier transform of) vector of circuit through variables. The through variable of any edge can be expressed as a linear combinations of circuit through variables. This relation is referred to as the loop transformation equation. Let  $Q$  be the edge through variable vector, the relation then takes the form:

$$Q = B^T \Psi. \quad (5-43)$$

Applying the same partition scheme as used in the manipulation of the fundamental circuit equation (5-40), the loop transformation equation can be rewritten as:

$$\begin{bmatrix} Q_f \\ Q_r \\ Q_w \end{bmatrix} = \begin{bmatrix} U \\ B_r^T \\ B_w^T \end{bmatrix} \Psi,$$

or can be divided into two parts:

$$Q_w = B_w^T \Psi, \quad (5-44)$$

and

$$\begin{bmatrix} Q_f \\ Q_r \end{bmatrix} = \begin{bmatrix} U \\ B_r^T \end{bmatrix} \Psi. \quad (5-45)$$

From (5-45),  $Q_f = \Psi$  indicates that the circuit through variables are equal to edge through variables. Substituting this relation into equation (5-45), it yields:

$$\begin{bmatrix} Q_f \\ Q_r \end{bmatrix} = \begin{bmatrix} U \\ B_r^T \end{bmatrix} Q_f. \quad (5-46)$$

The above equation is referred to as the reduced loop transformation equation.

The flow equation needs to be rearranged so that:

$$P_f = Z Q_f \quad (5-47)$$

$$P_r = R Q_r \quad (5-48)$$

The analysis in Section §5.2.1 shows that:

$$P_f = (\lambda + j\omega M) Q_f$$

and

$$P_r = \frac{B}{j\omega} Q_r$$

Therefore the elements of resistance matrices are:

$$Z_{ii} = \lambda_i + j\omega M_i \quad (5-49)$$

and

$$R_{ii} = \frac{B_i}{j\omega} \quad (5-50)$$

The flow equation of f-edges and r-edges can be expressed in matrix form:

$$\begin{bmatrix} P_f \\ P_r \end{bmatrix} = \begin{bmatrix} Z & 0 \\ 0 & R \end{bmatrix} \begin{bmatrix} Q_f \\ Q_r \end{bmatrix}. \quad (5-51)$$

### 5.3.2. Loop System Equation and Solution

Combining the fundamental circuit equation (5-42), the reduced loop transformation equation (5-46) and the flow equation (5-51), the loop system equation can be obtained as:

$$\begin{bmatrix} U & B_r \end{bmatrix} \begin{bmatrix} Z & 0 \\ 0 & R \end{bmatrix} \begin{bmatrix} U \\ B_r^T \end{bmatrix} Q_f + B_w^T P_w = 0,$$

or

$$F \cdot Q_f = E \cdot P_w \quad (5-52)$$

where

$$F = Z + B_r R B_r^T, \quad E = -B_w^T$$

The solution can be obtained in a similar manner as in Section §5.2.2.

### 5.3.3. Examples of Loop Formulation

**Example 1.** For the building in Figure 5.4a, there are two rooms and four openings. The graph representation of this building airflow system is drawn in Figure 5.4b. The circuit matrix can be written as:

$$B = \begin{bmatrix} 1 & 0 & 0 & 0 & 1 & 0 & -1 & 0 \\ 0 & 1 & 0 & 0 & -1 & 1 & 0 & 0 \\ 0 & 0 & 1 & 0 & 1 & -1 & 0 & 0 \\ 0 & 0 & 0 & 1 & 0 & -1 & 0 & 1 \end{bmatrix}$$

The system equation can be formed according to equation (5-52) as:

$$\begin{bmatrix} Z_1 & 0 & 0 & 0 \\ 0 & Z_2 & 0 & 0 \\ 0 & 0 & Z_3 & 0 \\ 0 & 0 & 0 & Z_4 \end{bmatrix} + \begin{bmatrix} 1 & 0 \\ -1 & 1 \\ 1 & -1 \\ 0 & -1 \end{bmatrix} \begin{bmatrix} R_1 & 0 \\ 0 & R_2 \end{bmatrix} \begin{bmatrix} 1 & -1 & 1 & 0 \\ 0 & 1 & -1 & -1 \end{bmatrix} \begin{bmatrix} Q_1 \\ Q_2 \\ Q_3 \\ Q_4 \end{bmatrix} = - \begin{bmatrix} -1 & 0 \\ 0 & 0 \\ 0 & 0 \\ 0 & 1 \end{bmatrix} \begin{bmatrix} P_1^w \\ P_2^w \end{bmatrix}$$

By simplification, it arrives at:

$$\begin{bmatrix} Z_1+R_1 & -R_1 & R_1 & 0 \\ -R_1 & Z_2+R_1+R_2 & -R_1-R_2 & -R_2 \\ R_1 & -R_1-R_2 & Z_3+R_1+R_2 & R_2 \\ 0 & -R_2 & R_2 & Z_4+R_2 \end{bmatrix} \begin{bmatrix} Q_1 \\ Q_2 \\ Q_3 \\ Q_4 \end{bmatrix} = \begin{bmatrix} 1 & 0 \\ 0 & 0 \\ 0 & 0 \\ 0 & -1 \end{bmatrix} \begin{bmatrix} P_1^w \\ P_2^w \end{bmatrix}$$

**Example 2.** For the building and its graph representation in Figure 5.5, the loop system equation (5-52) can be formulated by:

$$\begin{bmatrix} Z_1 & 0 & 0 & 0 & 0 & 0 \\ 0 & Z_2 & 0 & 0 & 0 & 0 \\ 0 & 0 & Z_3 & 0 & 0 & 0 \\ 0 & 0 & 0 & Z_4 & 0 & 0 \\ 0 & 0 & 0 & 0 & Z_5 & 0 \\ 0 & 0 & 0 & 0 & 0 & Z_6 \end{bmatrix} \begin{bmatrix} 1 & 0 \\ -1 & 0 \\ -1 & 1 \\ 1 & -1 \\ -1 & 1 \\ 0 & -1 \end{bmatrix} + \begin{bmatrix} R_1 & 0 \\ 0 & R_2 \end{bmatrix} \begin{bmatrix} 1 & -1 & -1 & 1 & -1 & 0 \\ 0 & 0 & 1 & -1 & 1 & -1 \end{bmatrix} \begin{bmatrix} Q_1 \\ Q_2 \\ Q_3 \\ Q_4 \\ Q_5 \\ Q_6 \end{bmatrix} = \begin{bmatrix} -1 & 0 & 0 \\ 0 & 1 & 0 \\ 0 & 0 & 0 \\ 0 & 0 & 0 \\ 0 & 0 & 0 \\ 0 & 0 & 0 \end{bmatrix} \begin{bmatrix} P_1^w \\ P_2^w \\ P_3^w \end{bmatrix}$$

The final loop system equation is:

$$\begin{bmatrix} Z_1+R_1 & -R_1 & -R_1 & R_1 & -R_1 & 0 \\ -R_1 & Z_2+R_1 & R_1 & -R_1 & R_1 & 0 \\ -R_1 & R_1 & Z_3+R_1+R_2 & -R_1-R_2 & R_1+R_2 & -R_2 \\ R_1 & -R_1 & -R_1-R_2 & Z_4+R_1+R_2 & -R_1-R_2 & R_2 \\ -R_1 & R_1 & R_1+R_2 & -R_1-R_2 & Z_5+R_1+R_2 & -R_2 \\ 0 & 0 & -R_2 & R_2 & -R_2 & Z_6+R_1+R_2 \end{bmatrix} \begin{bmatrix} Q_1 \\ Q_2 \\ Q_3 \\ Q_4 \\ Q_5 \\ Q_6 \end{bmatrix} = \begin{bmatrix} 1 & 0 & 0 \\ 0 & -1 & 0 \\ 0 & 0 & 0 \\ 0 & 0 & 0 \\ 0 & 0 & 0 \\ 0 & 0 & -1 \end{bmatrix} \begin{bmatrix} P_1^w \\ P_2^w \\ P_3^w \end{bmatrix}$$

#### 5.3.4. Automatic Formulation of Loop System Equations

In Sections §5.3.1 and §5.3.2, the set of loop system equations (5-52) is derived.

The examples in Section §5.3.3 indicate certain patterns in this final set of equations.



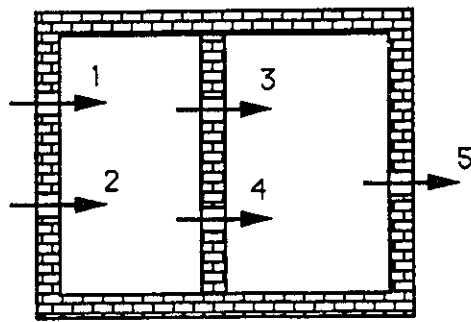
The final set of loop system governing equations (5-52) is determined by two matrices: the flow matrix  $F$ , and excitation matrix  $E$ . The central task of automatic formulation of loop system equations is to formulate these two matrices.

The elements of the  $F$  matrix are composed of  $Z_k$  and  $R_j$  -- the resistances of f-edges and r-edges respectively. The elements on the diagonal are positive and are composed of the  $Z$  and  $R$  terms. The  $Z$  terms are the resistances of the f-edges in the corresponding circuit. If the f-edge connects two r-nodes (rooms), then the  $R$  term equals the summation of the resistances of the two r-nodes. If this f-edge connects an r-node to an w-node (i.e. it represents the opening of the building envelope), the  $R$  term has only one value and is equal to the resistance of the only r-edge with which the f-edge shares a node.

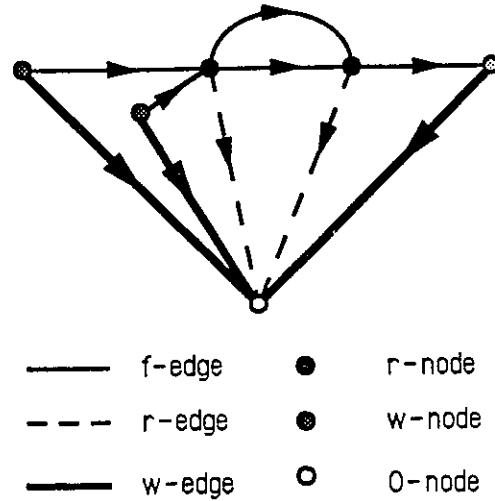
Off-diagonal elements of the matrix  $F$  are composed of only  $R$  terms.  $F_{kl}$  depends upon the relationship between the terminals of f-edges  $k$  and  $l$ . If  $k$  edge and  $l$  edge do not share a common node,  $F_{kl}$  equals zero. If edges  $k$  and  $l$  share a common node, the value of  $F_{kl}$  equals the resistance of the r-edge on that node. The sign depends upon the relationship between the two f-edges and their common node(s). If both f-edges are incident on or out of the node, the sign is positive, otherwise the sign is negative. If f-edges  $k$  and  $l$  are incident on two same nodes, then  $F_{kl}$  equals the summation of the resistances of the two r-edges. The sign is positive if the orientations of the two f-edges are the same, negative otherwise.

Since the  $F$  matrix depends only on the interconnection of openings (f-edges) and rooms (r-nodes), it can be obtained without referring to the graph representation. For a building having  $N$  rooms and  $M$  openings, the  $F$  matrix is an  $M$  by  $M$  square matrix. Elements of  $Z$  and  $R$  matrices are formed by equations (5-49) and (5-50).

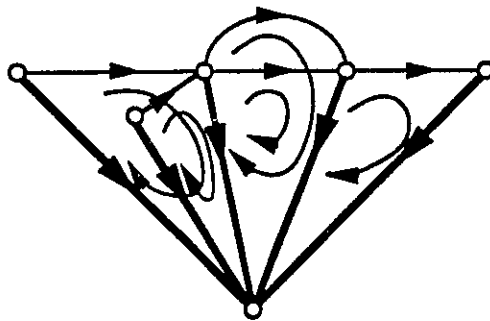
The  $E$  matrix includes only 0, 1 and -1s. The number of rows equals to the number of openings, and the number of columns equals to the number of wind-induced pressures or the number of openings that are on the building envelope. The value of each element,  $E_{kj}$ , depends upon whether the wind pressure  $j$  acts on the opening  $k$  or not.



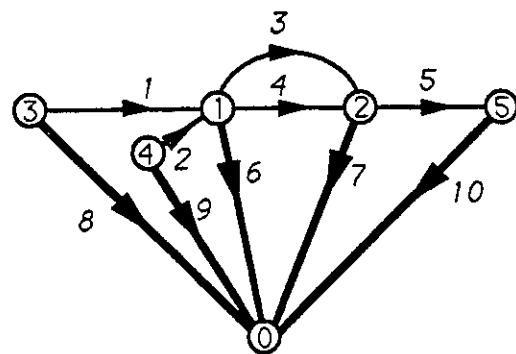
(a) A Two Room Building



(b) Graph Representation



(c) Fundamental Tree and Circuit



(d) Node and Edge Numbering

**Figure 5.1. An Example of Graph Representation of a Building Fluctuating Flow System**

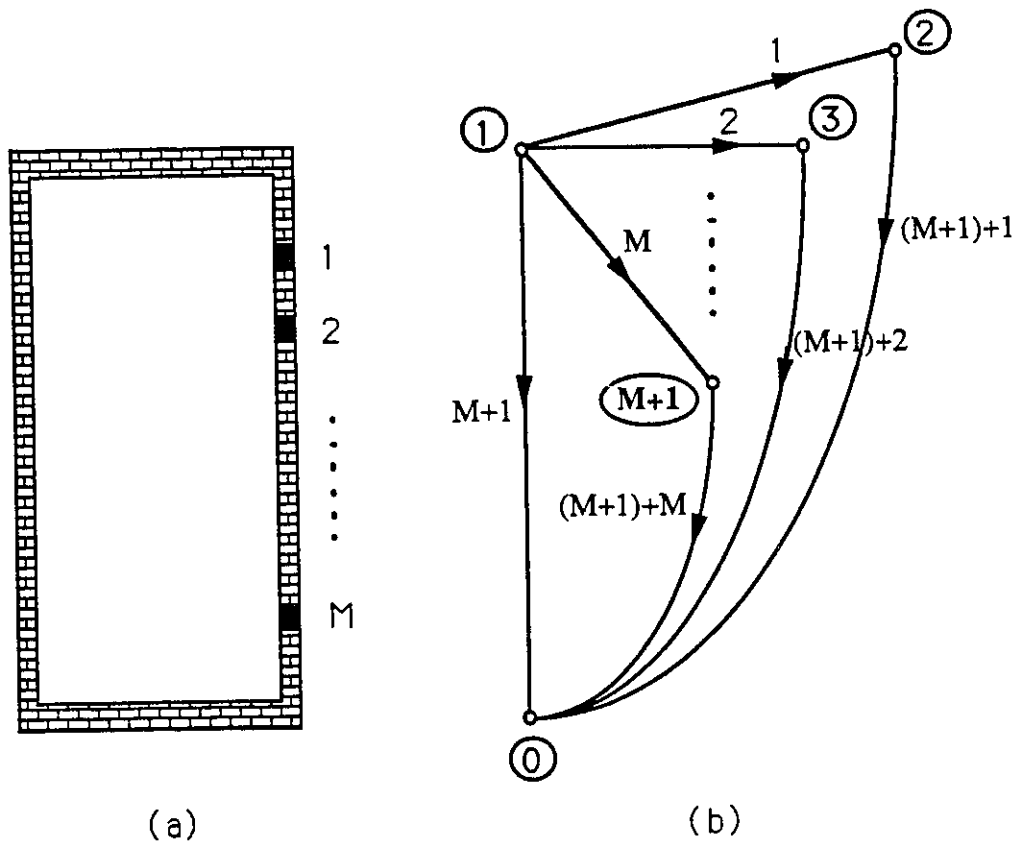
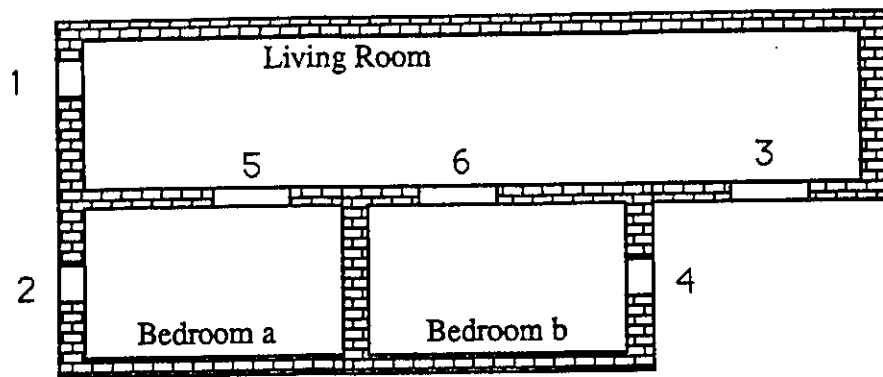
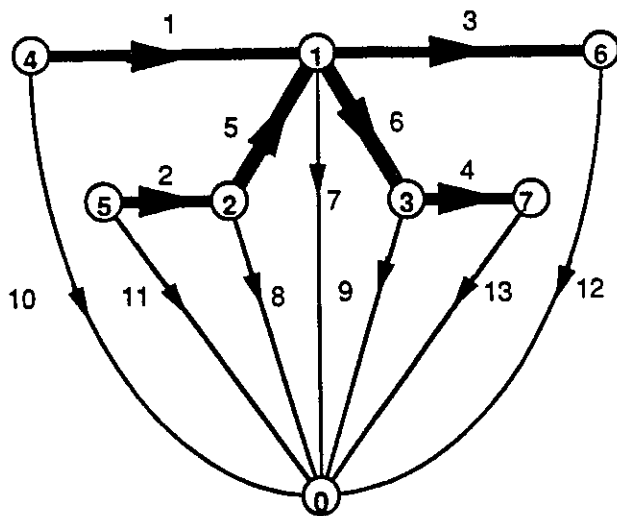


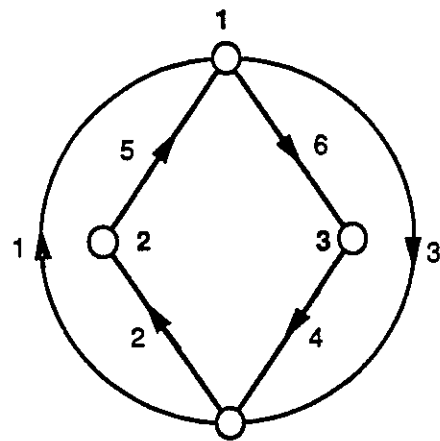
**Figure 5.2. A Single-Enclosure Multiple Opening Building**



(a) MEGA House



(b) Graph Representation



(c) Physical Connection Graph

**Figure 5.3. MEGA House and Graph Representations**

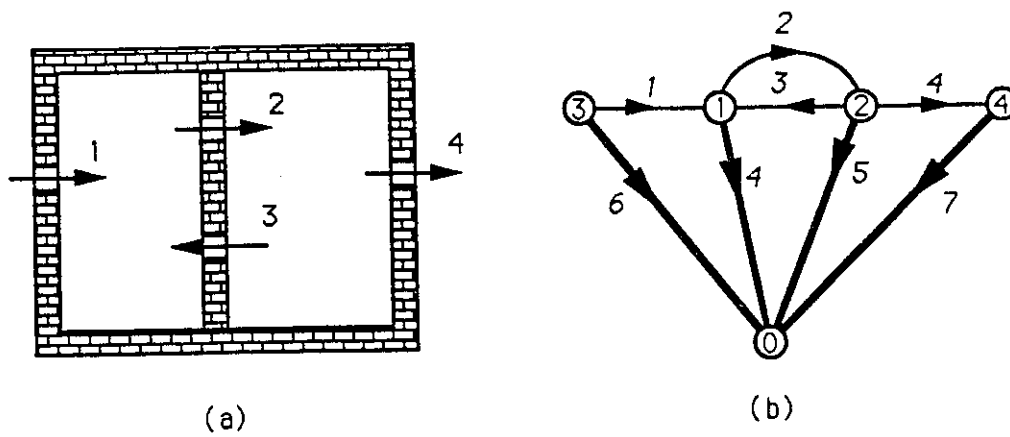


Figure 5.4. A Two-Room and Four-Opening Building

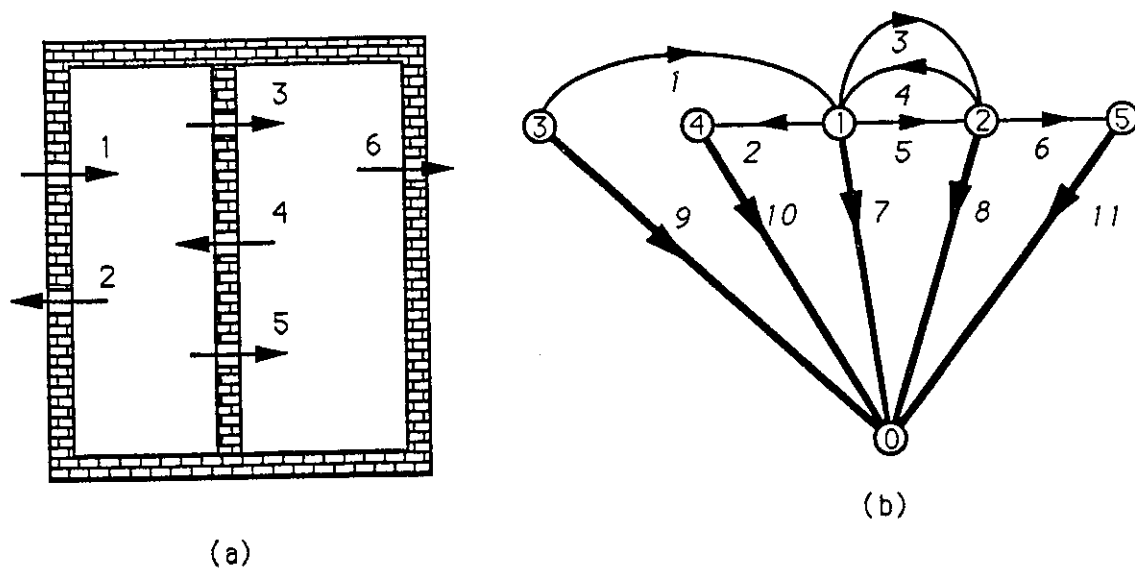


Figure 5.5. A Two-Room and Six-Opening Building

Table 5.1 Matrix, Dimension, and Notations

**Numbers in the Graph**

N = number of internal zones

M = number of flow paths

L = number of wind pressures

 $M^e$  = number of flow paths with external pressure $M^i$  = number of flow paths with both ends being internal zones $M = M^e + M^i$ **Edges:**

f: flow path or openings (M) f-edge

r: compressible of room air (N) r-edge

w: wind-induced pressure (L) w-edge

**Nodes:**

r: room node r-node

w: pressure acting location w-node

**Variables:**

p: across variable

q: through variable

 $\phi$ : nodal across variable $\psi$ : circuit through variable $\mathbf{p}, \mathbf{q}, \boldsymbol{\phi}, \boldsymbol{\psi}$ : the vectors of corresponding variables $\mathbf{P}, \mathbf{Q}, \boldsymbol{\Phi}, \boldsymbol{\Psi}$ : the vectors of Fourier transformation of corresponding variables.**Matrix Notations:** $\times$  element product, if  $\mathbf{C} = \mathbf{A} \times \mathbf{B}$ , then  $C_{ij} = A_{ij} \times B_{ij}$

# **CHAPTER VI**

## **VALIDATION OF**

### **FLUCTUATING AIRFLOW MODEL**

The validation of the developed fluctuating airflow model is presented in this chapter in three steps. First, a computer simulation program is used to estimate the effects of the statistical linearization. Since the linearization forms the basis for the theoretical analyses in the presented model, it is important to evaluate the linearization assumption. Second, a laboratory experiment validation program is conducted to validate the fluctuating airflow model in cases of two-opening enclosures. The experiments are performed in an indoor chamber. The third means of validation is through the use of field experimental data collected by other researchers working in related areas. The data from the BOUIN House in France (van der Mass, et al., 1991) are used. This offers a realistic data set for verifying the fluctuating airflow model with consideration of large openings. Results of the experimental comparisons have also been published in (Haghighat, et al., 1992; Rao, et al., 1992; Rao and Haghighat, 1991).

#### **6.1. EVALUATION OF LINEARIZATION ASSUMPTION**

The statistical linearization technique presented in Section §4.2.1 ensures the linearity of the governing equations of the fluctuating airflow system, and therefore,



makes it possible for further frequency analysis methods to be applied. Although the technique has been used for the random vibration study (Ziegler and Schueller, 1987), the effects and validity of introducing linearization into the governing equations need to be evaluated.

The numerical simulation method is used to compare the simulation results with and without statistical linearization. The governing equations are a set of differential equations. The nonlinear governing equations are assumed to be the true equations. An appropriate numerical simulation method is applied to both the nonlinear equation and the linear equations. The results are compared to indicate the effect of linearization on the solutions.

The intention of the statistical linearization is to make the results from the nonlinear and linear governing equations to be the same on statistical average. Whether they provide the same results on other aspects, such as the airflow as a function of time, is of no importance. Therefore, the comparison of the results should also be carried out by statistical means instead of by values at instantaneous times.

In obtaining the results from the differential governing equations (both non-linear and linear), numerical simulations with a Runge-Kutta integration scheme (Gordon, 1978; Kochenburger, 1972) are employed. The wind pressures as input are generated by a routine to inverse the spectrum back to time domain signals.

This section is not intended for a comprehensive examination and validation. Instead, numerical simulations for the fluctuating airflow in a single-opening enclosure

are performed. The purpose is to show that the linearization introduces insignificant statistical departures from the original nonlinear equations and that further analyses can be based on the linearized governing equations.

### 6.1.1. Numerical Simulation Method

For a single-opening enclosure, the steady-state flow equation for the opening is assumed to conform with the power law flow relation, i.e.:

$$\bar{Q} = K(\Delta\bar{P})^n \quad (6-1)$$

where the unit for the airflow rate is  $\text{m}^3/\text{s}$  and the unit for the pressure difference is Pascal. The non-linear differential equation that governs the fluctuating airflow through the opening is expressed as:

$$M \frac{dq}{dt} + \left(\frac{1}{K}\right)^{\frac{1}{n}} q^{\frac{1}{n}} = p^w - B \int_0^t q dt \quad (6-2)$$

where  $M = \rho \frac{L}{A}$ ,  $B = \frac{\gamma P_a}{V}$ , and units for  $L$ ,  $A$ ,  $V$ , and  $\rho$  is  $\text{m}$ ,  $\text{m}^2$ ,  $\text{m}^3$ , and  $\text{Kg}/\text{m}^3$ , respectively.

Employing the statistical linearization technique, the nonlinear term in the above equation is approximated by a linear relation. The linear coefficient is obtained from the fluctuating airflow model in Chapter IV. The nonlinear differential governing equation can, thus, be converted into a linear one as:

$$M \frac{d\hat{q}}{dt} + \lambda \hat{q} = p^w - B \int_0^t \hat{q} dt \quad (6-3)$$

where (^) indicates that the airflow by the linear equation is different from that of the non-linear equation.

For these two differential equations to be solved by the numerical simulation method, they have to be converted into two sets of first-order differential equations. A substitution of variables changes the second-order differential equations into sets of first-order equations. For the non-linear equation (6-2), let  $y_1 = \int_0^t q dt$ ,  $y_2 = q$ , then,

$$\begin{cases} \dot{y}_1 = y_2 \\ \dot{y}_2 = \frac{dq}{dt} = \frac{1}{M} \left[ p^w - \left( \frac{1}{K} \right)^{\frac{1}{n}} y_2^{\frac{1}{n}} - B y_1 \right] \end{cases} \quad (6-4)$$

This is the set of first-order equations that are equivalent to the second-order governing equation (6-2). Similarly, for the linear equation (6-3), let  $\hat{y}_1 = \int_0^t \hat{q} dt$ ,  $\hat{y}_2 = \hat{q}$ , and the set of first-order differential equations can be obtained as:

$$\begin{cases} \dot{\hat{y}}_1 = \hat{y}_2 \\ \dot{\hat{y}}_2 = \frac{d\hat{q}}{dt} = \frac{1}{M} [p^w - \lambda \hat{y}_2 - B \hat{y}_1] \end{cases} \quad (6-5)$$

Numerical simulations by integrations are carried out on these two sets of first-order differential equations. In the simulation, initial values (normally zeros) of airflow and its derivatives are given first, the values at a latter time  $\Delta t$  are obtained by integrations based on the initial values, the derivatives and the first-order differential equations. Then, the obtained new values are taken as initial values and the calculation repeats.

Take the first equation of (6-4) for example. At any iteration  $n$  and time  $t(n) = (n-1)\Delta t = 0, \Delta t, 2\Delta t, \dots$ , the new values of  $y_1$  are calculated by the Runge-Kutta

integration method for time at  $t(n+1) = n\Delta t$ . For variable  $y_1$ , let  $y = y_1$ ,  $z = \dot{y}_1$ , the Runge-Kutta integration scheme is as follows:

$$y(n+1) = y(n) + \frac{1}{6}(k_1 + 2k_2 + 2k_3 + k_4) \quad (6-6a)$$

where:

$$\begin{cases} k_1 = z(t(n), y(n)) \Delta t \\ k_2 = z(t(n + \frac{1}{2}), y(n) + \frac{k_1}{2}) \Delta t \\ k_3 = z(t(n + \frac{1}{2}), y(n) + \frac{k_2}{2}) \Delta t \\ k_4 = z(t(n+1), y(n) + k_3) \Delta t \end{cases} \quad (6-6b)$$

The error of the Runge-Kutta integration scheme is of the fifth order  $o(\Delta t^5)$ .

### 6.1.2. Computer Program of Numerical Simulation

The solution of equations (6-2 and 6-3) by the simulation method is implemented into a computer program. The program is in the FORTRAN language and is executed on a VAX machine.

The flow chart of the program is shown in Figure 6.1, and has the following steps:

1. **Initialization:** The initial values and characteristics of the building are set. Program execution control parameters, such as the step length, simulation duration and output control are entered (at the keyboard or from a batch file).

2. Updating: The interested variables (time, wind-induced pressure, airflow rates) are printed on the screen or into a text file. The simulation time is increased by one step length.
3. Terminating Logical: If the designated simulation duration is reached, the simulation is terminated. Otherwise, continue to the next step.
4. Calculation of the wind-induced pressure at the new time.
5. Integration: The values at the new time are calculated using the Runge-Kutta integration scheme.
6. Continue from step 2.

The selection of the step length is of great importance. A large step length may induce too much error in each iteration and thus cause erroneous simulation results, or may even cause a divergence of the simulation results. A small step length, on the other hand, will require longer computational time. In addition, too many integrations due to a too small step length may introduce errors in simulation results due to the round-off errors. A decision is made to select a step length so that the convergence is guaranteed and the minimum error is allowed. In the simulation for the single-opening enclosures, the step length is chosen, by trial and error, as one-hundredth of a second.

The calculation of the fluctuating wind-induced pressure is generated by a subroutine according to the equation (Papoulis, 1965):

$$p(t) = A \sum_{n=1}^N \cos(2\pi f_n t + \phi_n) \quad (6-7)$$

where  $N$  is the number of cosine terms used to approximate the spectrum, a number of 200 is used in the simulation. The  $f_n$  and  $\phi_n$  are independent random variables;  $\phi_n$  has a uniform distribution over  $[0, 2\pi]$  and  $f_n$  has a distribution specified by the normalized power spectrum of the wind-induced pressure  $S_p(t)/\sigma_p^2$ ; and the value of  $A^*$  is obtained in the relation:

$$\sigma_p = \left[ \sqrt{\frac{N}{2}} A^* \right] \quad (6-8)$$

### 6.1.3. Numerical Simulation Results

The parameters used in the simulation are given in Table 6.1. The linear coefficient  $\lambda$  of the statistical linearization is obtained from the fluctuating airflow model (Table 4.1).

Figure 6.2 shows the simulation results for both the non-linear and linear differential equations. Figure 6.2a shows the two airflow rates in the first 50 seconds. It can be observed that the two flow rates follow each other closely and that the agreement is good.

The difference between the results from non-linear and linear equations can be shown more clearly in Figure 6.2b and c. In Figure 6.2b, the flow relations used by non-linear and linear governing equation is illustrated. The curved line is the power law flow equation (equation 6-1). The straight line is the linearized flow relation. The slope ( $\lambda$ )

is chosen in such a way that the variance of the corresponding terms in the two governing equations are the same. The formulae are given in Table 4.1. The discrepancy of the instantaneous values of the airflow rates does exist and is expected to be large when the two lines of Figure 6.2b remain distant. Figure 6.2c shows the airflow rates in a shorter time duration (for the same simulation run as Figure 6.2a). The differences and similarities between the instantaneous values of the two airflow rate are shown more clearly.

In Figure 6.2d, the spectra estimated from the two airflow data and the 95% confidence intervals are shown. The relative discrepancy between the two spectra is less than 3%. When taking the confidence interval into consideration, these two sample spectra can be considered identical. There is no statistical evidence indicates that the two spectra are from two different signals having distinct spectra. Therefore, the introduction of the statistical linearization method causes no significant departures from the nonlinear relations.

## 6.2. LABORATORY EXPERIMENTAL COMPARISONS

Laboratory experiments have been designed, set-up, and performed to provide data for validating the model. The primary variables of interest are the excitation pressures and the resultant airflow. Since the fluctuating airflow model studies the statistical and stochastic properties and relationship in the building airflow system, the experiments are of a dynamic nature. The excitation pressure must be varying with time in a similar manner as the wind-induced pressure on the real building envelopes. The primary

frequency range of interest is approximately from 0.001 to 1 Hz, where the energy of wind gustiness concentrates.

The primary objective of the laboratory validation is to verify that the theoretical transfer functions calculated from the fluctuating airflow model agree with the frequency characteristics estimated from experimental data. The experiments are conducted in an indoor chamber. The experimental setup and procedure are described in detail in Appendix A. The experimental results of seven tests are presented in the following.

Results from test JUN05 is taken here as an example to explain the details of the experiments and data processing. This experiment was a one-directional test without operation of the fan #2 (as described in Appendix A, same for other details concerning the experimental setup and procedure).

The data from the flow equation estimation are used to estimate the flow relations of the purposed-provided opening and the chamber porosity. Figure 6.3 shows the experimental data and the least-square fitting results. The power law relation was used as the protocol. The fitting results for this test and all other tests are also listed in Table 6.2. Due to both variations in the chamber conditions (e.g. how tightly is the door closed) and the planned parameter changes (refill the opening with straws), the  $K$  and  $n$  values of the flow equations vary from test to test. The flow equation estimation in the test step 4 serves both as backup data (in case of errors in the test step 2) and for the verification purpose (whether the opening characteristics remain the same before and after the experiment).



The chamber is modelled as a single-zone building with two openings: the purpose-provided opening and the chamber porosity. The mean values of test step 3 are used as input to the steady-state calculations. The mass conservation, for uniform indoor and outdoor temperatures, for the chamber is:

$$K_1(\bar{P}_1^w - \bar{P}^i)^{n_1} - K_2(\bar{P}^i)^{n_2} = 0$$

where  $\bar{P}_1^w$  is the mean pressure generated by the damper unit on the outside of the opening, and  $\bar{P}^i$  is the mean internal pressure of the chamber. The predicted internal pressure and the airflow rate are listed in Table 6.2 against corresponding values from experiments.

The fluctuating airflow data come from the test step 3 of the experiment. The damper control signal is generated according to a certain spectrum. The collected data of external pressure, internal pressure, airflow rate and the control signal varies with time (Figure 6.4). The time domain data show little information about the relations among involved variables. Spectral estimation methods are used to obtain the correspond power spectra and transfer functions. In processing the experimental data to obtain spectral information, a mean smoothed spectral estimator is used. The estimator uses a truncation length of 1024 data points and a Hanning spectral window. The obtained information lie in the frequency range from 0.005 to 2.5 Hz due to the selected truncation length and the sampling rate. With the sampling length of approximate 14,000, a degree of freedom of 36 is achieved. The design of the spectral estimator follows the guidelines of Jenkins and Watts (1968). The program implementation is done in MATLAB (Moler, et al., 1987).

The theoretical calculation for this test set-up is the same as presented in Section §4.6.2.1 for the case study of the two opening building. The transfer functions for airflow in the opening and for the internal pressure are:

$$H_{q11}(\omega) = \frac{\lambda_2 + j\omega M_2 + B/j\omega}{(\lambda_1 + j\omega M_1 + B/j\omega)(\lambda_2 + j\omega M_2 + B/j\omega) + B^2/\omega^2} \quad (6-9)$$

$$H_{p11}(\omega) = \frac{\frac{1}{\lambda_1 + j\omega M_1}}{-\frac{j\omega}{B} + \frac{1}{\lambda_1 + j\omega M_1} + \frac{1}{\lambda_2 + j\omega M_2}} \quad (6-10)$$

The spectra for airflow and internal pressure are calculated by equations:

$$S_{q1}(\omega) = \|H_{q11}(\omega)\|^2 \cdot S_{p1}^w(\omega) \quad (6-11)$$

$$S_{p1}(\omega) = \|H_{p11}(\omega)\|^2 \cdot S_{p1}^w(\omega) \quad (6-12)$$

The implementation of the above calculations is also done in MATLAB (Moler et al., 1987) programs. In order to reduce the error in input data of the fluctuating airflow model, parameters for the flow equations use values measured during each experiment. The model also takes as input the measured values of the mean airflow rate and mean internal pressure, instead of the calculated results from a steady-state airflow model. The use of measured data as input eliminates errors in the fluctuating airflow predictions due to the accuracy of the steady-state airflow calculations.

Figure 6.5. shows the related spectra from both estimations (solid lines) of the experiment data and theoretical calculations (dotted lines) by the fluctuating airflow model. The spectra are plotted on the left hand column and the reduced spectra (e.g.:

$f \cdot S_{p_1}(\omega) / \sigma_{p_1}^2$  ) are displayed on the right hand column. The plots indicate that the results of theoretical calculations are very close to those from experimental estimations. The relative discrepancy between the two spectra is within 9%. The 95% confidence interval of the measured airflow transfer function is also shown. The theoretical calculation result is well within this interval. It can be concluded that the model predicts the correct airflow transfer function.

The transfer functions between related variables provide more direct and clear indications about the agreement between the theoretical and experimental results. In the analysis of the data set JUN05 and other sets, the data are examined in pairs of two such as external pressure and airflow, external pressure and internal pressure, and, external pressure and pressure difference.

In Figure 6.6a, the theoretical transfer function of airflow through the opening is plotted against the experimental results. It agrees well with the measured one for frequencies less than 0.3 Hz. At higher frequencies (>0.5 Hz), the measured curve shows very low values instead of reaching the peak as the theoretical results. This may be due to the data quality. The coherence between the external pressure and the airflow is low at higher frequencies, thus, the estimated transfer function is inaccurate (Jenkins and Watts, 1968). A second possible explanation is that the assumption of inertia of the air in the theoretical model is invalid for higher frequencies. Nevertheless, the power density of the wind-induced pressure (external pressure in the experiments) is mainly concentrated at a lower frequency range away from where the discrepancy occurs. The resultant

airflow at the high frequency range generally contributes very little to the total value. Therefore, the poor agreement between the experimental and theoretical transfer functions at the high frequencies would not cause significant deviation in the prediction.

The theoretical and experimental phase plots of the transfer function of airflow (Figure 6.6a) are in good agreement. At low frequencies, the phase lag between airflow and pressure is negligible. Airflow is ahead of the pressure in frequency 0.02 to 1.0 Hz due to the inertia of the air in the opening. At frequencies greater than 2 Hz, the inertia and flow resistance makes the airflow lag behind the pressure.

Above calculations are performed on the other pairs of data. In Figure 6.6b and 6.6c, the plots for both estimated and calculated transfer functions of the internal pressure in the chamber and the pressure difference across the opening also show very good agreements.

The theoretically calculated mean and RMS values of airflow, internal pressure and pressure difference are listed in Table 6.2. The calculated mean values match those of measured ones well. The calculated RMS values of fluctuating components also match within a 7% relative error range with the test results for the data set JUN05.

Figure 6.7 shows the concentration decay of the tracer gas in the chamber during the test step 3 (no mixing fan was used). Using a least-square fitting program, the air exchange per hour is calculated as 0.92 ach (air change per hour). This rate is 83% of the measured mean airflow rate.

Figures 6.8 to 6.13 show the comparisons of transfer functions from other six data set. Test sets JUL22, JUL23 and APR29 have similar setup as the set JUN05. In the other three tests (MAY12, MAY19 and MAY22), the fan #2 was in operation. Similar good agreements between the theoretical solutions and experimental estimations are obtained. The experimental comparisons establish the fluctuating airflow model's ability in predicting the airflow system characteristics, for pulsating only airflow in enclosures with two openings.

### **6.3. VALIDATION WITH FIELD EXPERIMENTAL DATA**

#### **6.3.1. Test Set-up of BOUIN House**

The test house at BOUIN (Figure 6.14a) is a single zone building on an exposed site near the Atlantic coast. The volume of the test house is  $93.6 \text{ m}^3$ . The equivalent air leakage area of the house was measured and is less than  $5 \text{ cm}^2$ . The building is mounted on a turntable, which can be rotated during an experiment to keep the facade with a door facing the wind.

A single opening is introduced into the building envelope on the door and maintained windward. A sharp edged slot of 40 cm in width, 2.5 cm in height and 1 cm in thickness is investigated. The ventilation rate is obtained from the tracer gas concentration decay measured in the room. The wind-induced external pressures, internal pressures, wind speed and direction and tracer gas concentration are all measured

simultaneously, at a rate of 10 Hz. Each test consists of a 10 minute mixing period, with the opening sealed, and then after removing the seal, a 20 minute decay period.

The wind pressure is measured close to the opening. The pressure are also measured at eight points within the opening (Figure 6.14b), both inside and outside the building, allowing the direction of flow to be known locally. Full details of the site and the measuring equipments can be found in Riberon and Villain (1990).

### 6.3.2. Comparison of Results

The BOUIN test set-up is similar to the laboratory test set-up. The house can be modelled as a building with two openings: the slot opening and the house porosity. The information of the wind pressures at the slot opening,  $p^w_1$ , is measured. No measurements are available for the wind pressure at the porosity opening,  $p^w_2$ . Reasonable assumptions are made according to general observations about wind-induced pressure distributions on building envelopes (Grosso, 1992). The pressure spectrum of  $p^w_2$  takes a similar shape of that of  $p^w_1$  but has less energy contents. The RMS value of  $p^w_2$  is assumed to be -0.3 of  $p^w_1$ . The coherence between the two pressures is assumed to comply with the empirical correlations in equations (2-10) and (2-11).

The mean and RMS values of interested variables are displayed in Table 6.3. Figure 6.15 shows the magnitude and phase plots of the transfer function  $H_{p_i}(\omega)$  for both experimental estimation and theoretical calculation based on the pulsating airflow model.

The discrepancy between theoretical and experimental results shown in Figure 6.15 can be attributed to the fact that the pulsating airflow model does not consider the eddy flow due to the spatial variations of wind pressures over the opening. The pressures on the area of the opening are assumed to be simultaneously pushing in or pulling out the air through the opening at all points. In reality, however, the pressures at different points on the opening are not perfectly synchronized or correlated due to the presence of eddies. Two approaches are introduced in Chapter IV: the aerodynamic admittance approach and multi-path approach.

In the first approach, the aerodynamic admittance function is chosen to be the coherence function of wind-induced pressures at two representative points. Figure 6.16 shows the experimental estimation of the coherence function and the regression fitting. The fitting curve was used for the later calculation.

Once the aerodynamic admittance function is obtained, the net effect should be equal to the "point" value modified (multiplied) by the aerodynamic admittance function. In the theoretical calculation the "point" force is the power spectrum of the external pressure at the opening. Therefore, the calculation will take:

$$\hat{S}_{p_1 v}(\omega) = S_{p_1}(\omega) \cdot \chi_1^2(\omega) \quad (6-13)$$

as the input force. A further analysis shows this is equivalent to using a modified transfer function:

$$\hat{H}_{p_1 i}(\omega) = H_{p_1 i}(\omega) \cdot \chi_1(\omega) \quad (6-14)$$

in the theoretical calculation.

The comparison between experimental estimations and theoretical calculations by the modified model is shown in Figure 6.17. The plots show an improvement of the modified model over the pulsating model in predicting the transfer function. Table 6.3 also shows that the predicted RMS value of the internal pressure by the modified model is closer to the experimental results. The new approach also results in a larger RMS of airflow at the slot opening.

The second approach for modelling large openings is to consider airflow through an opening as composed of several separate airflows (sub-flows). Each sub-flow is a pulsating airflow and is modelled as one distinct airflow path using the pulsating airflow model. In this way, the limitation to pulsating airflow is overcome, and eddy flow or multi-path airflow through large openings can be accounted for in the prediction.

The slot opening of the BOUIN house is modelled as two flow paths. The theoretical results based on this modified model is shown in Table 6.3 and Figure 6.18. The predictions of the transfer function and RMS value for the internal pressure, as well as for the fluctuating airflow, show an improvement over the original pulsating airflow model.

The total air exchange across an opening is determined by both the mean and fluctuating airflow rates, using the *combinatory model* presented in Section §4.5. The amount of flow reversal due to contributions from fluctuating components can be calculated from the RMS values and by assuming normal distributions for the temporal variations in the airflow rates. The last column of Table 6.3 shows the percentage of fluctuating airflow that is involved in flow reversal through the slot opening. The



percentages are compatible with the experimental results of 24.0% obtained from the measured pressure differences across the slot opening.

Let the percentage of reversed flows be  $\beta$ , then, the total air exchange across the opening is the summation of the mean airflow rate and 150% of the reversal flow (as expressed in equation 4-41). Calculations (Table 6.4) show that due to fluctuations in the airflow, the air exchange across the slot opening is approximately 50 percent more than the mean value.

Tracer gas measurements during the experiment indicate a ventilation rate of 0.21 air change per hour. This is equivalent to a measured air exchange rate of 5.46 (l/s) between the inside and outside of the house. The theoretical predictions on the total air exchange rate are compatible with the measured value (Table 6.4).

The turbulence intensity of the wind-induced pressures at the slot opening is 0.35, the turbulence intensity of the wind velocity at the top of the BOUIN house is about 0.19. Even with this relative "smooth" wind, the fluctuation causes an increase of 50% in the air exchange of the building. With larger turbulence (turbulence intensities of the wind pressure) around 1.0 as measured in other cases, Gusten 1989), the contribution of the fluctuations to air exchange would be much greater.

#### **6.4. DISCUSSION OF THE MODEL VALIDATIONS**

The objective of the validation is to establish the accuracy of the model in predicting the resultant air exchange in buildings due to both mean and fluctuating wind-

induced pressures. An ultimate validation program that compares the model predictions to the measurements from real buildings is not available at the present stage. Instead, three validation schemes were carried out to compare the model predictions to numerical simulations, and to experimental results from a laboratory chamber and a special designed test house.

The degree to which the experimental parameters (such as wind speeds and types, building characteristics, and opening flow relations) can be controlled is important. Greater controls make it easier for the data collection and result comparisons, but may cause deviation in the experiments from the real buildings. In the numerical comparison, total controls are achieved by assuming the nonlinear equation as the true behaviour of the airflow system. The good agreement between the simulation results from nonlinear and linear equations shows the validity of using the statistical linearization in the fluctuating airflow model. In the laboratory experiments, controls are maintained on the stochastic properties of the wind-induced pressures by the damper unit, on the pulsating airflow through the opening by straws, and on the temperatures by the ventilation system. The experimental comparisons indicate the model can correctly predict the transfer functions of the airflow system and therefore calculate the correct fluctuating airflow and internal pressures. In the field experiments done in the BOUIN test house, controls were maintained on the opening size, location and orientation. The experimental comparisons lead to the development of approaches in dealing with eddy flows through large openings, and subsequently support the proposed two approaches. Since controls were maintained

in all validation schemes, considerations should be taken in the generalization of the validation results.

The validation is achieved by evaluations of the discrepancies between the model predictions and experimental results. Two types of errors cause these discrepancies: the external errors and internal errors. The external errors are not due to the theoretical model. They are caused mainly by the measurement errors in the experiments and affect the input to the model. The internal errors are contributed by the model. They may be due to: (1) the incorrect assumptions of the model, such as pulsating airflow and the inertia of air, and (2) the incorrect calculation algorithms and methods, such as the statistical linearization method. The model validation and error evaluation were also discussed by Herrlin (1992) for steady-state airflow models.

In the numerical simulations, the external errors are eliminated. The discrepancies between model predictions and real values are fully caused by the internal errors. With the simulation design, the only cause of the errors is the introduction of the statistical linearization method. The absence of significant deviations in the simulation results suggests that the statistical linearization method is valid. In the chamber experiments, external errors are minimized by: (1) the controlled chamber environment and simulated wind pressures provide constant temperatures and stationary pressure fluctuations, (2) the special designed test set-up provides pulsating only airflow and direct measurements of pressures and airflow rates, and (3) the use of measured mean airflow and internal pressure values in the fluctuating airflow model eliminates the cumulative error due to the inaccuracy of the steady-state calculations. The good agreement between the predicted

and measured transfer functions shows the success of the experimental set-up in reducing external errors and validity of the fluctuating airflow model. In the field experiments, external errors exist in or are due to: (1) flow relations of the slot opening and house porosity, (2) lack of wind pressure data for other surfaces (other than the one with the slot opening), and (3) no direct measurements of airflow rates. Still, this test house and experimental set-up are more accurate than real cases. Although small discrepancies were found for both steady-state and fluctuating predictions, the theoretical results still agree reasonably well with the experimental results.

The criteria by which the validity is defined are also important for the validation. In validation of the steady-state airflow models against measurement from real buildings, a 25% error is considered to be accepted (Liddament and Allen, 1983). In the three validation programs, a higher accuracy of the model is achieved due to the specially designed experiments and accurate measurements.

Although not a comprehensive validation, this chapter provides an evaluation of the fluctuating airflow model on its assumptions, fundamental relations and approach for eddy flows. Further efforts must be made for more experimental comparisons and real applications.

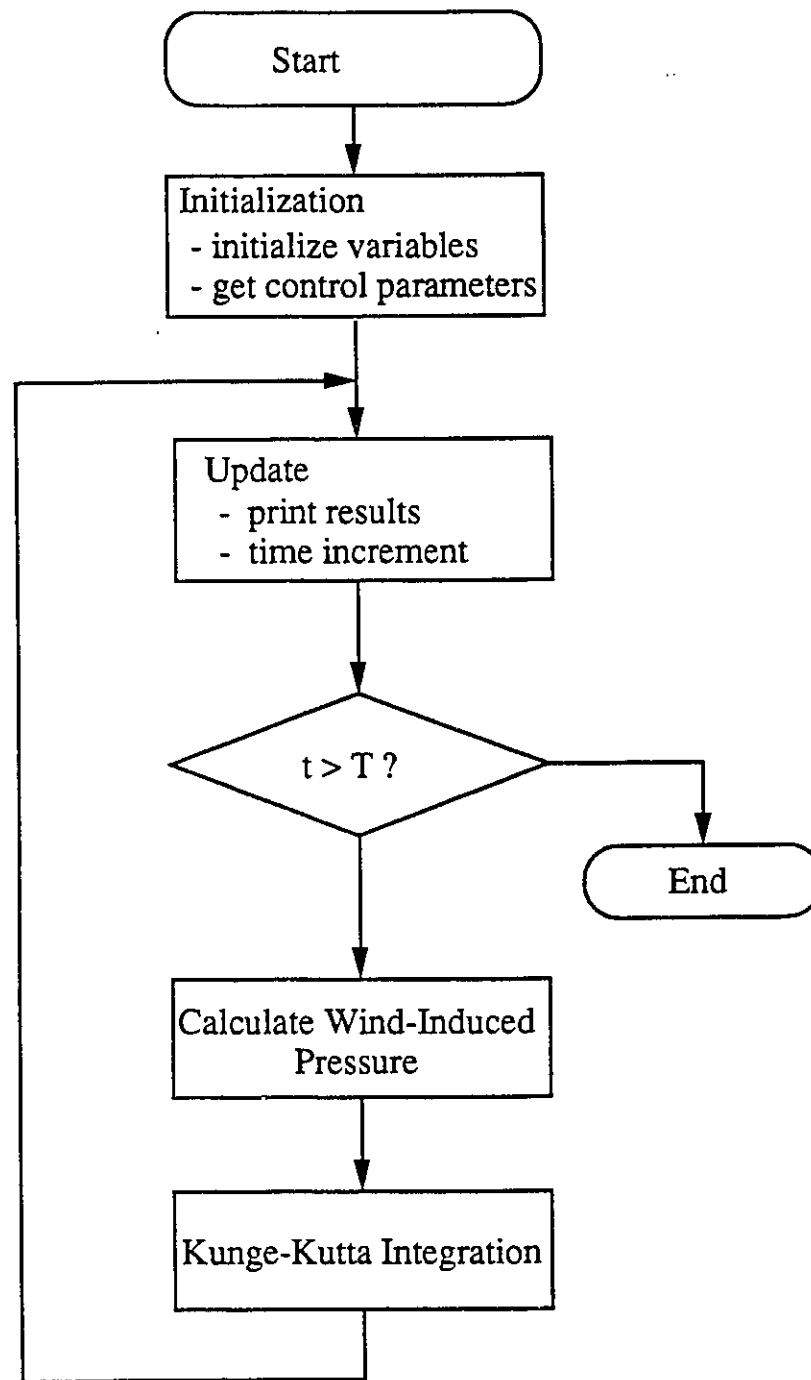
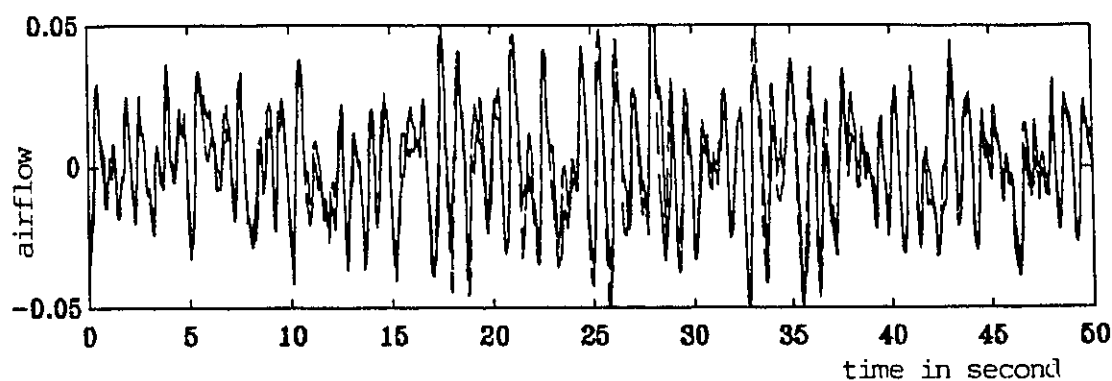
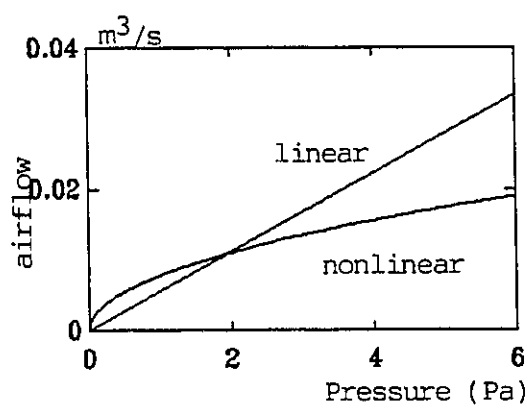


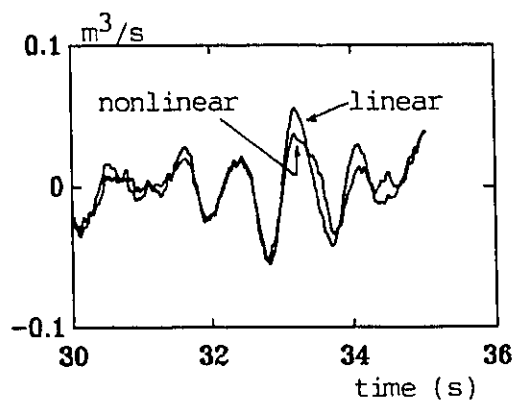
**Figure 6.1. Flow Chart of Numerical Simulation Program**



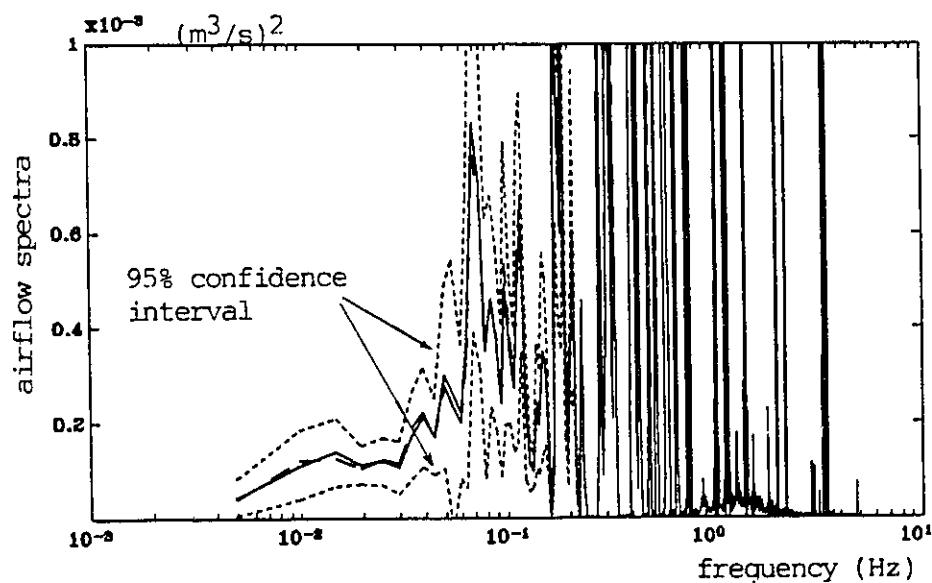
(a) Data Sample



(b) Flow Relations



(c) Data Sample



(d) Airflow Spectra

———— nonlinear equation      - - - - - linear equation

Figure 6.2. Simulation Results of the Single Opening Case

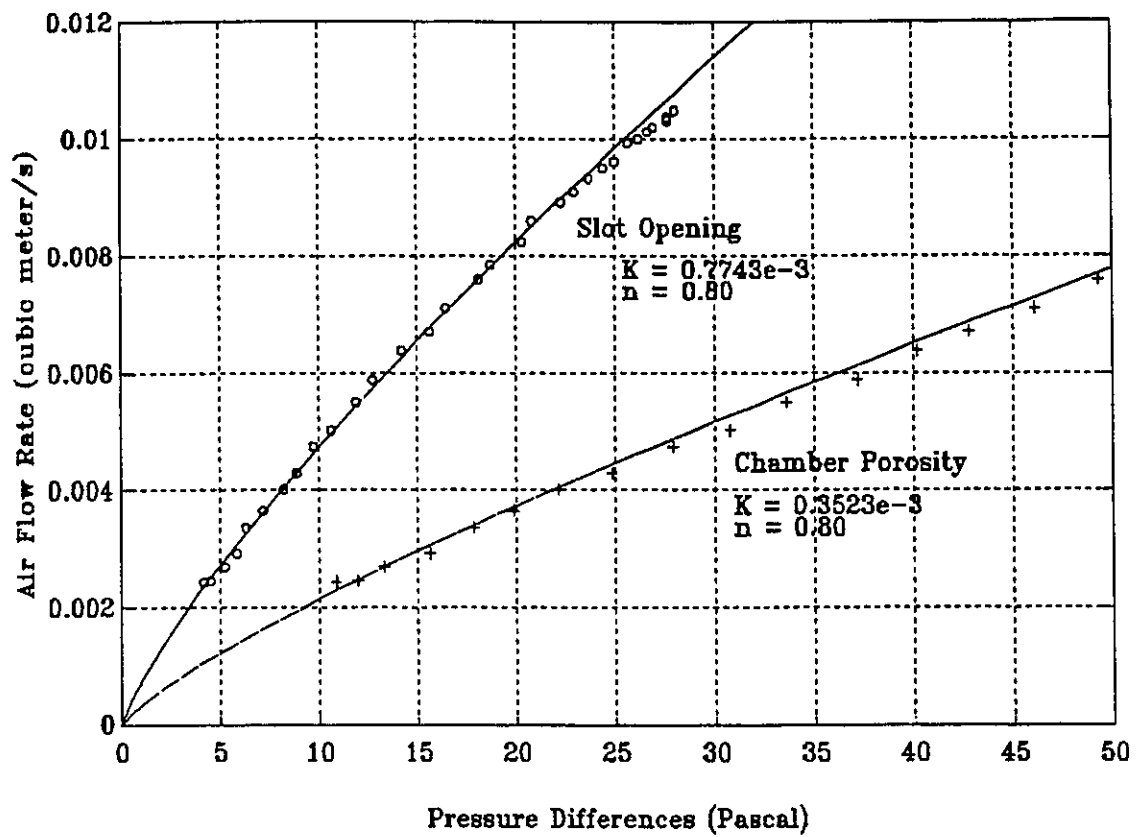
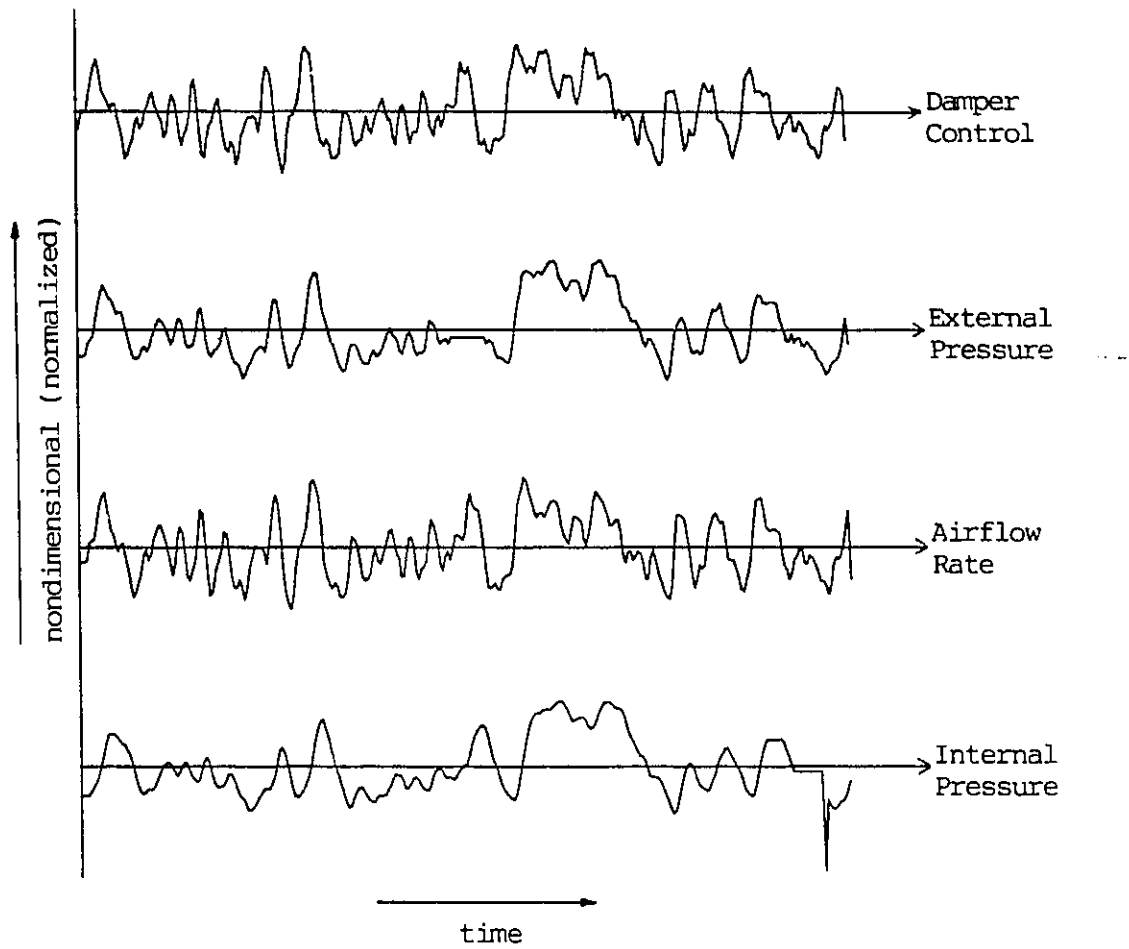
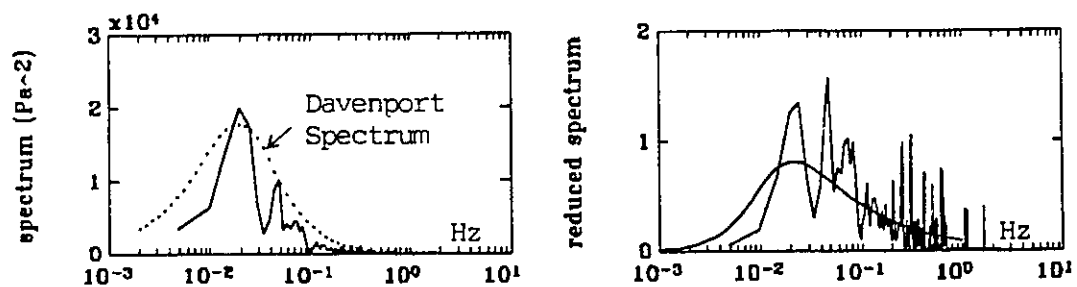


Figure 6.3. Flow Equation Estimation for Data Set JUN05

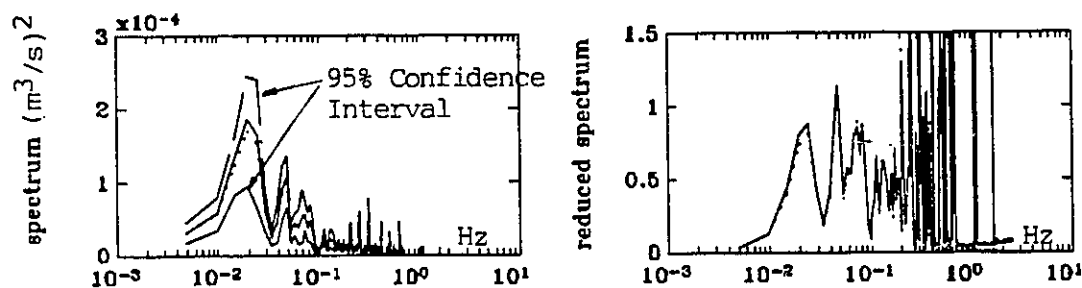


**Figure 6.4. Experimental Data in the First Minute**

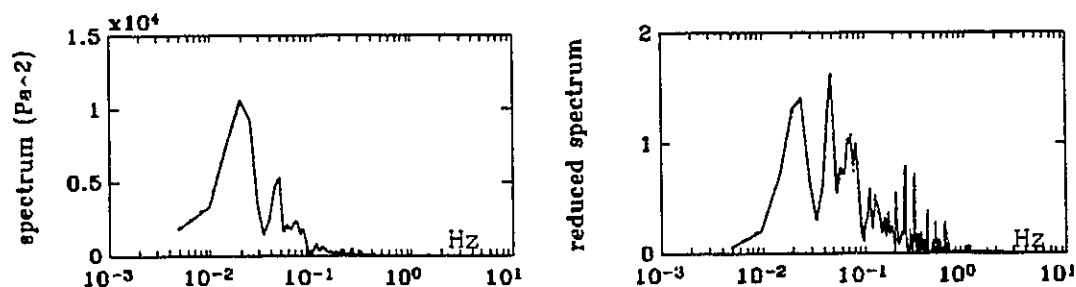




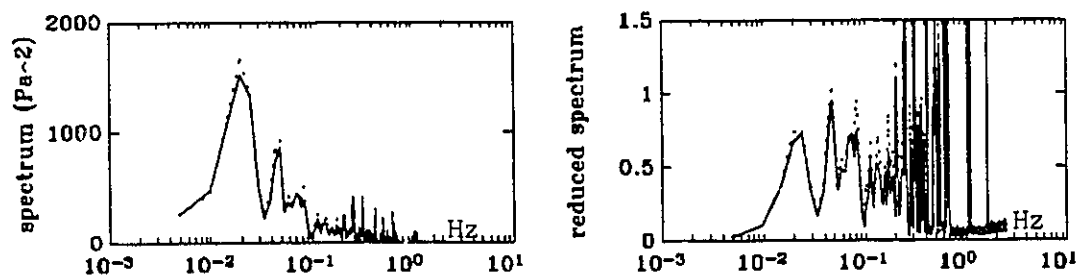
(a) External Pressure Spectrum



(b) Airflow Spectrum



(c) Internal Pressure Spectrum



(d) Pressure Difference Spectrum

———— experimental    ..... theoretical

**Figure 6.5. Related Spectra for Data Set JUN05: (a) External Pressure, (b) Airflow Rate, (c) Internal Pressure, and (d) Pressure Difference**

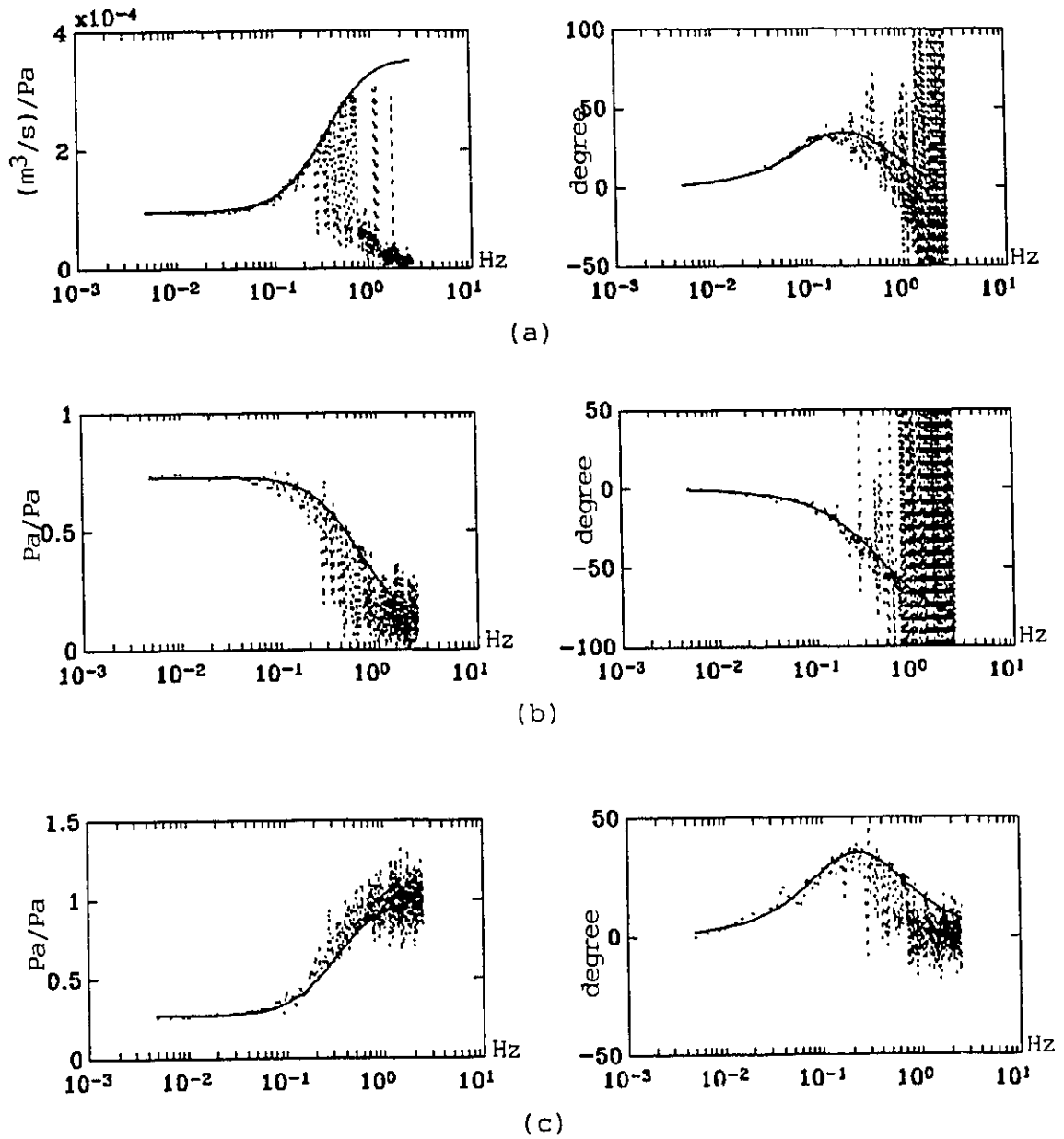


**Figure 6.6. Related Transfer Functions for Data Set JUN05 for  
(a) Airflow Rate, (b) Internal Pressure, and (c) Pressure Difference**

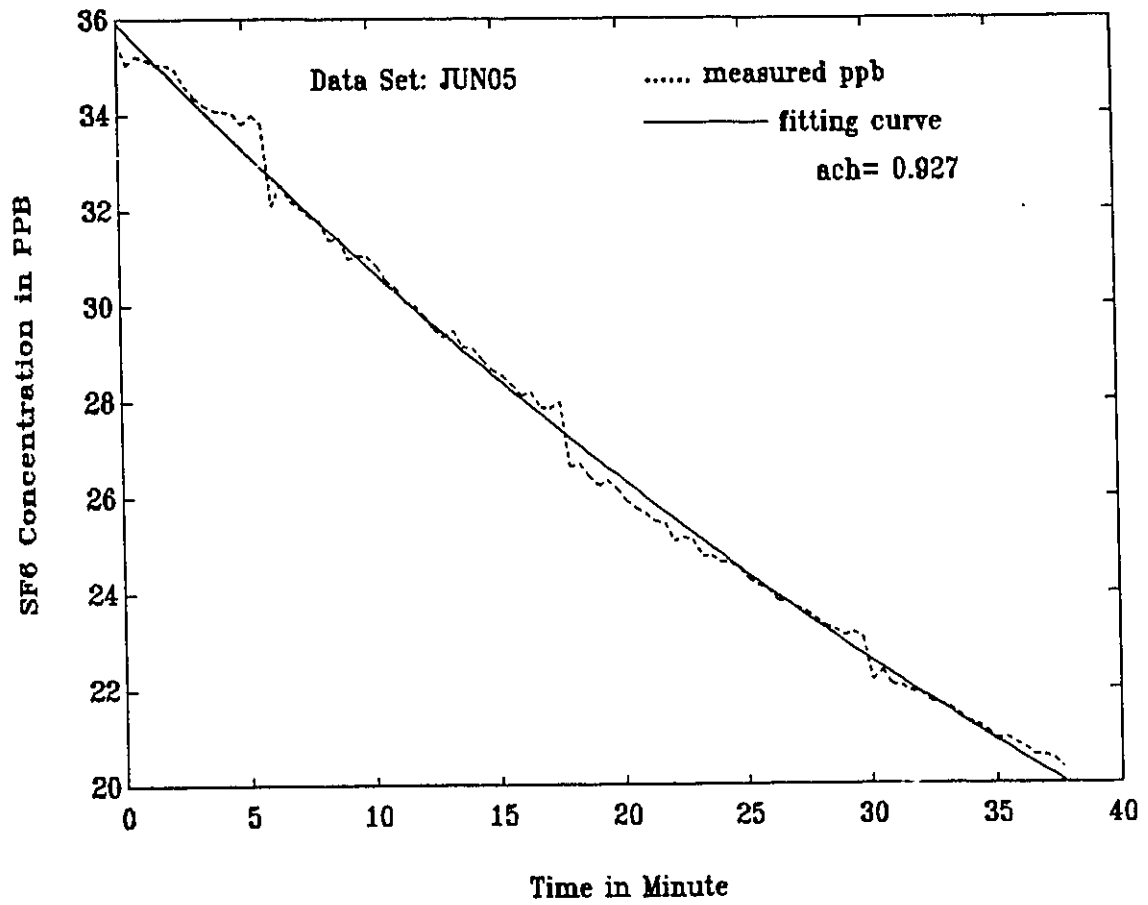
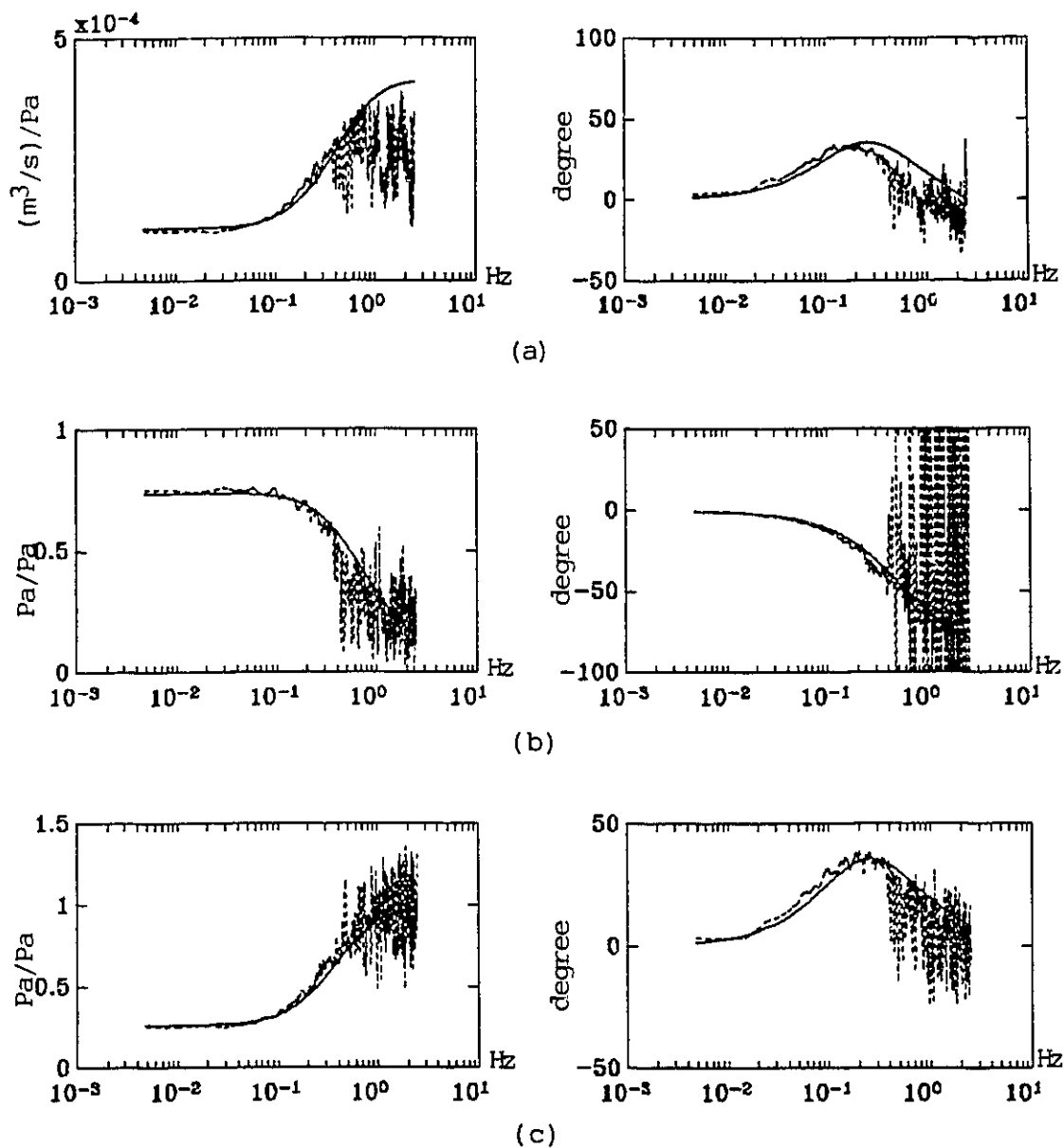
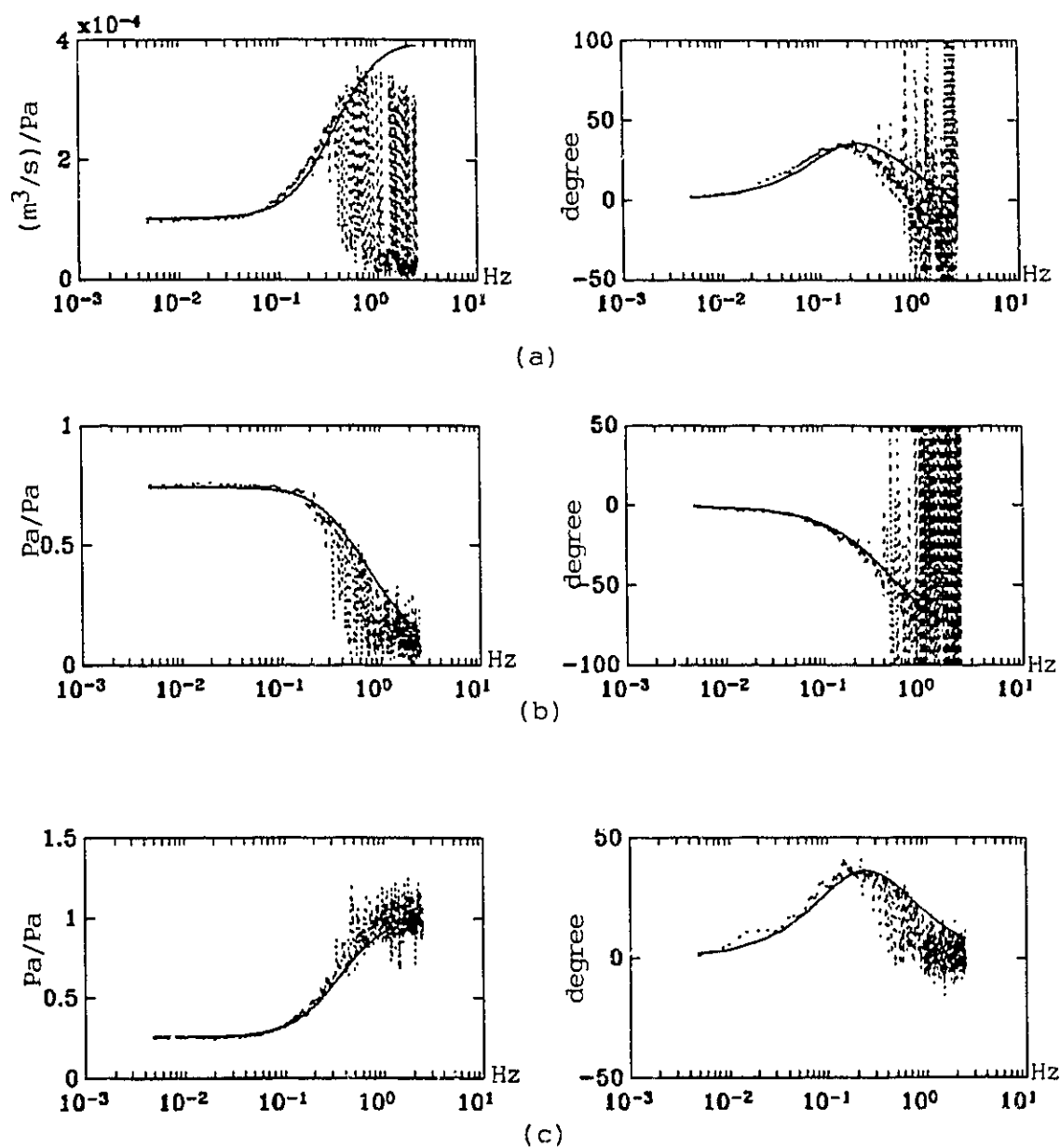


Figure 6.7. Tracer Gas Decay For Data Set JUN05

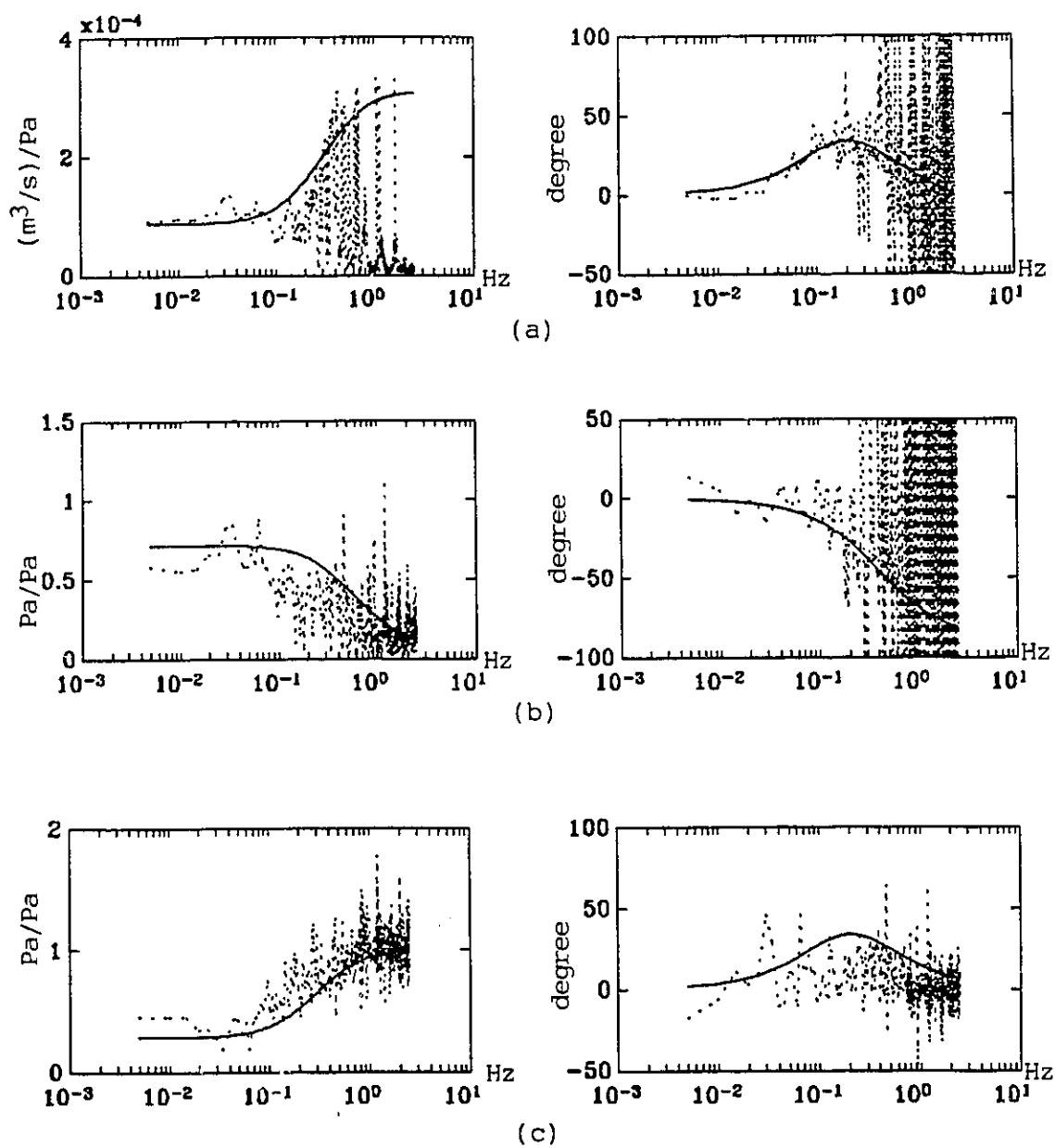


———— theoretical      ..... experimental

**Figure 6.8. Related Transfer Function for Data Set JUY22 for (a) Airflow Rate, (b) Internal Pressure, and (c) Pressure Difference**



**Figure 6.9. Related Transfer Functions for Data Set JUY23 for  
(a) Airflow Rate, (b) Internal Pressure, and (c) Pressure Difference**



———— theoretical ..... experimental

**Figure 6.10. Related Transfer Functions for Data Set APR29 for  
(a) Airflow Rate, (b) Internal Pressure, and (c) Pressure Difference**

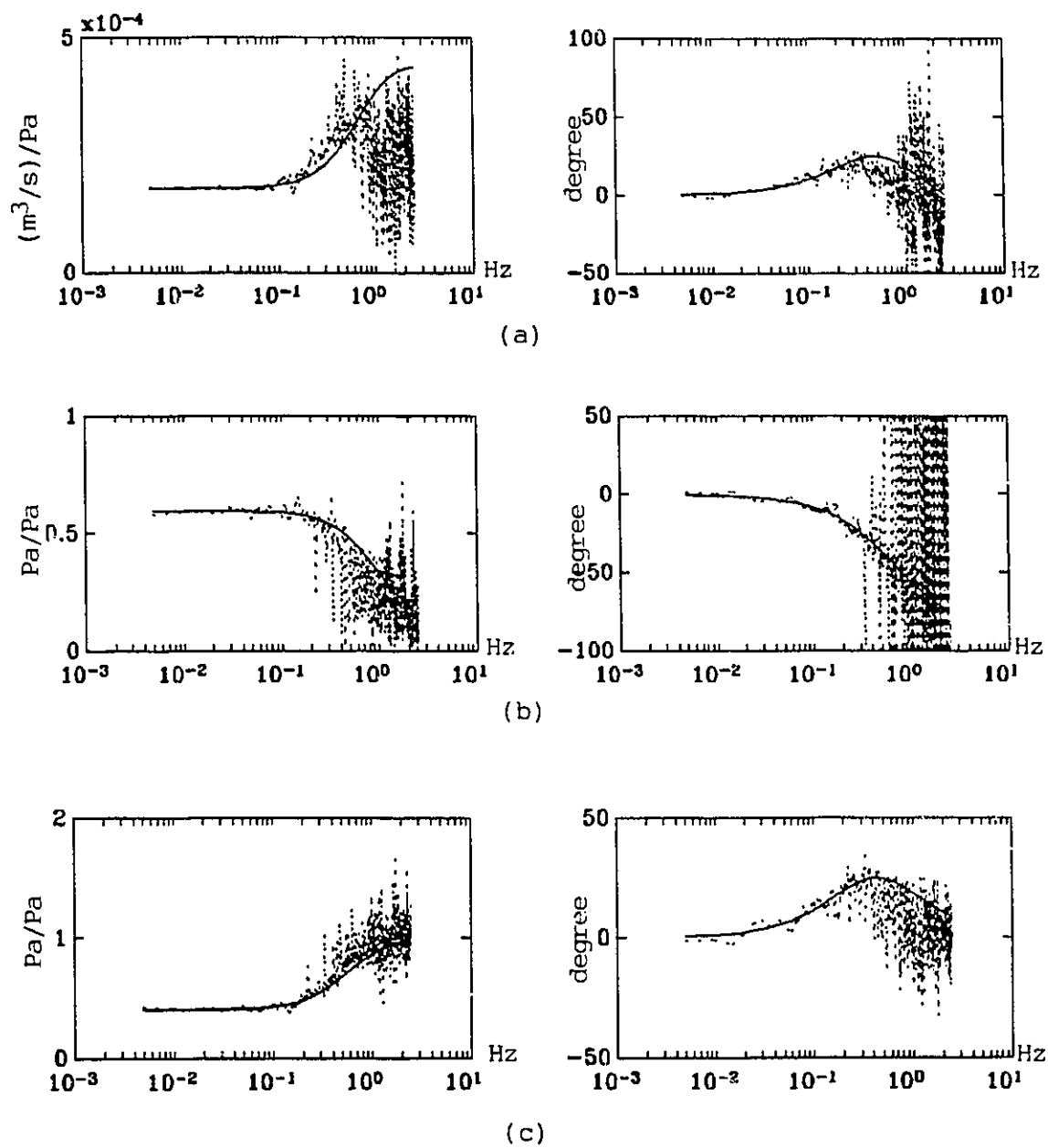


**Figure 6.11. Related Transfer Functions for Data Set MAY12 for  
(a) Airflow Rate, (b) Internal Pressure, and (c) Pressure Difference**

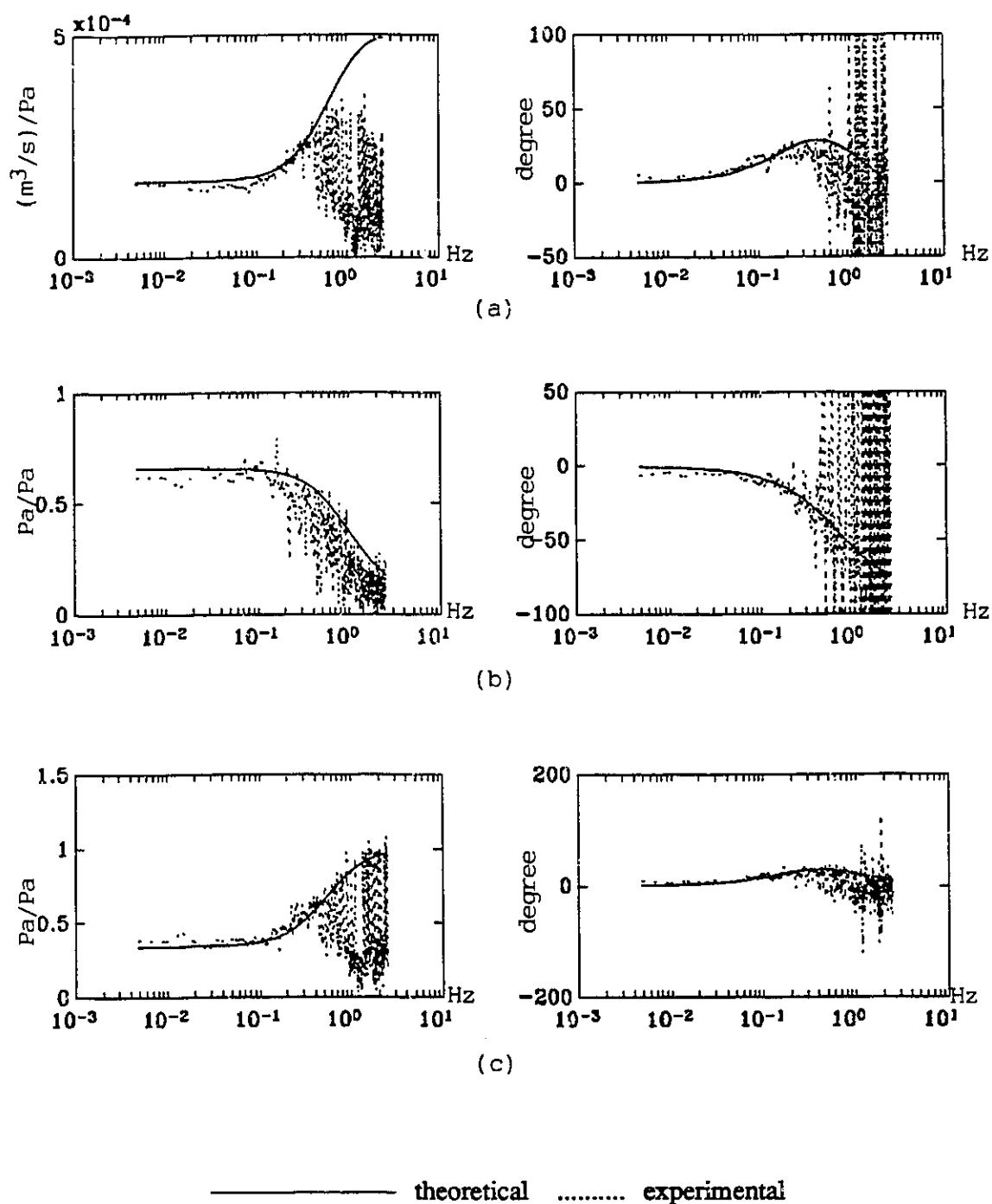


**Figure 6.12. Related Transfer Functions for Data Set MAY19 for  
(a) Airflow Rate, (b) Internal Pressure, and (c) Pressure Difference**



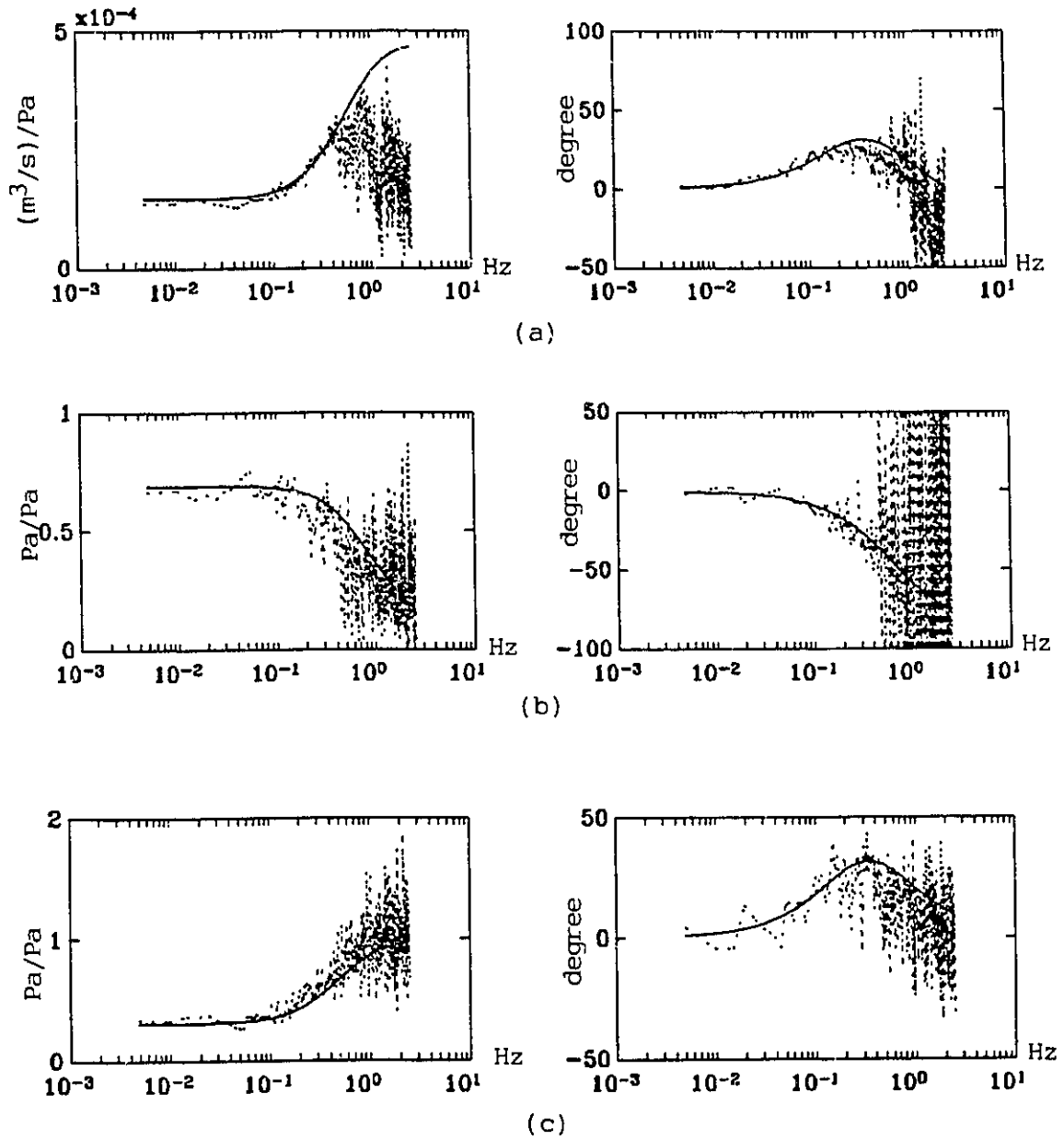
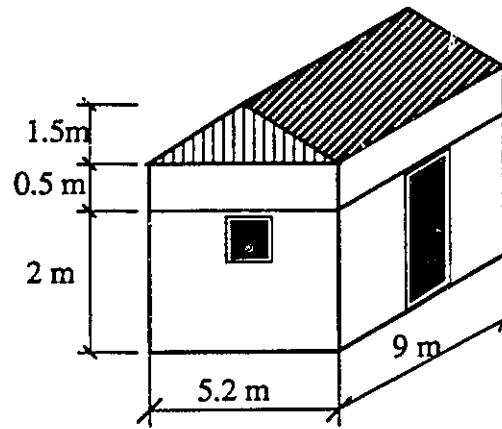
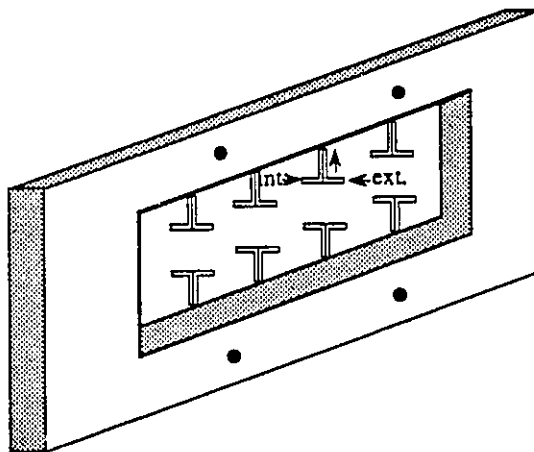


**Figure 6.13. Related Transfer Functions for Data Set MAY22 for (a) Airflow Rate, (b) Internal Pressure, and (c) Pressure Difference**



(a) BOUIN Test House



(b) Pressure Tapping Points

**Figure 6.14. BOUIN Test House**

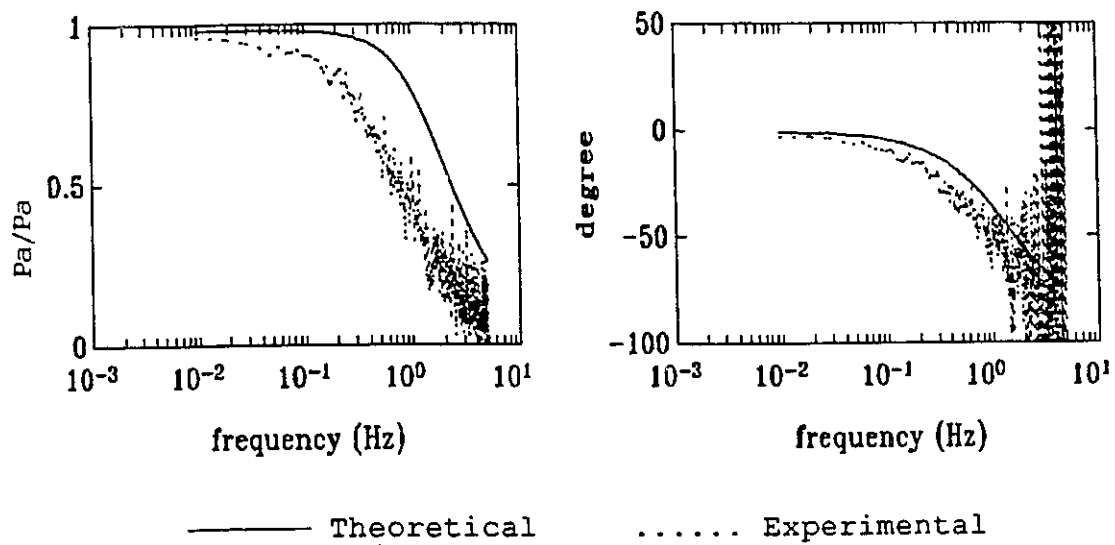


**Figure 6.15. Results of Pulsating Model for Data Set VB1312  
(a) Magnitude and (b) Phase Plots of Transfer Function  
Between External and Internal Pressures**

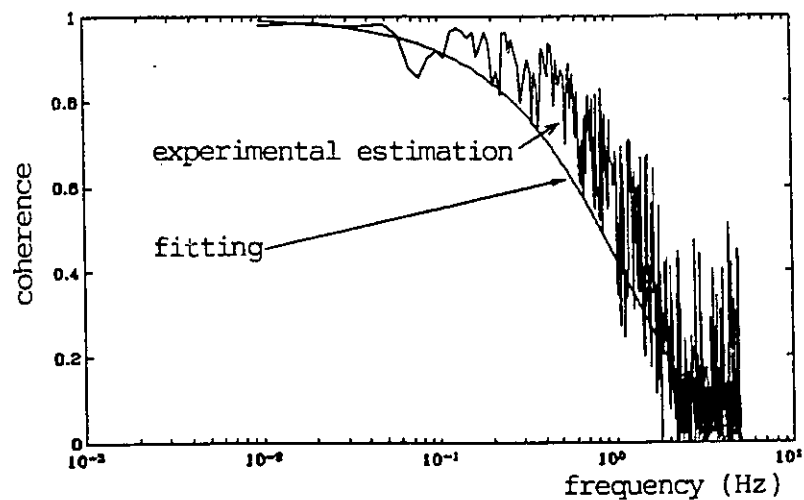


**Figure 6.16. Coherence Functions as Aerodynamic Admittance  
Function from Data Set VB1312**

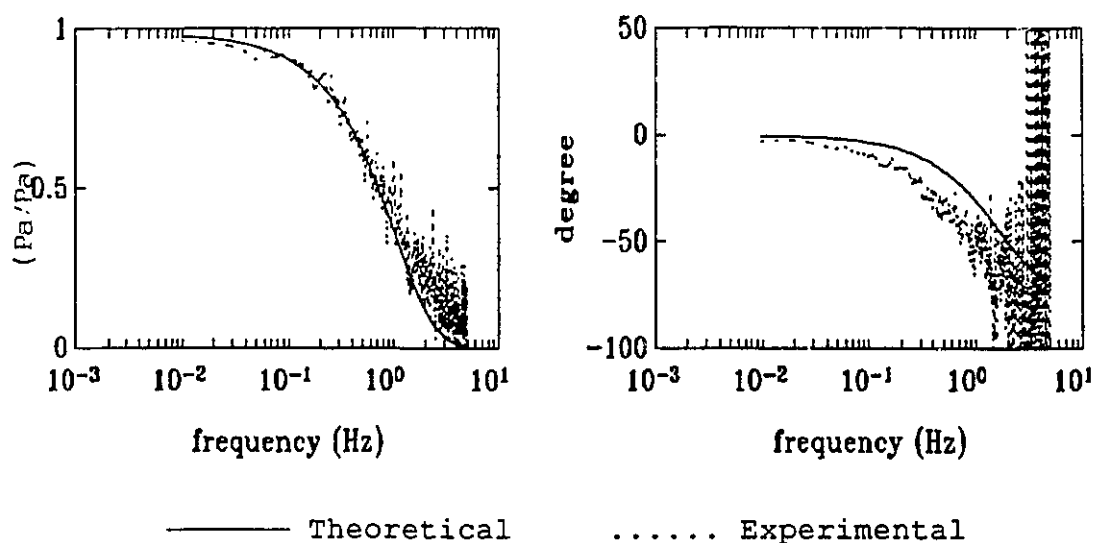


Figure 6.17. Results of Aerodynamic Admittance Approach for Data Set VB1312: (a) Magnitude and (b) Phase Plots of Transfer Function Between External and Internal Pressures

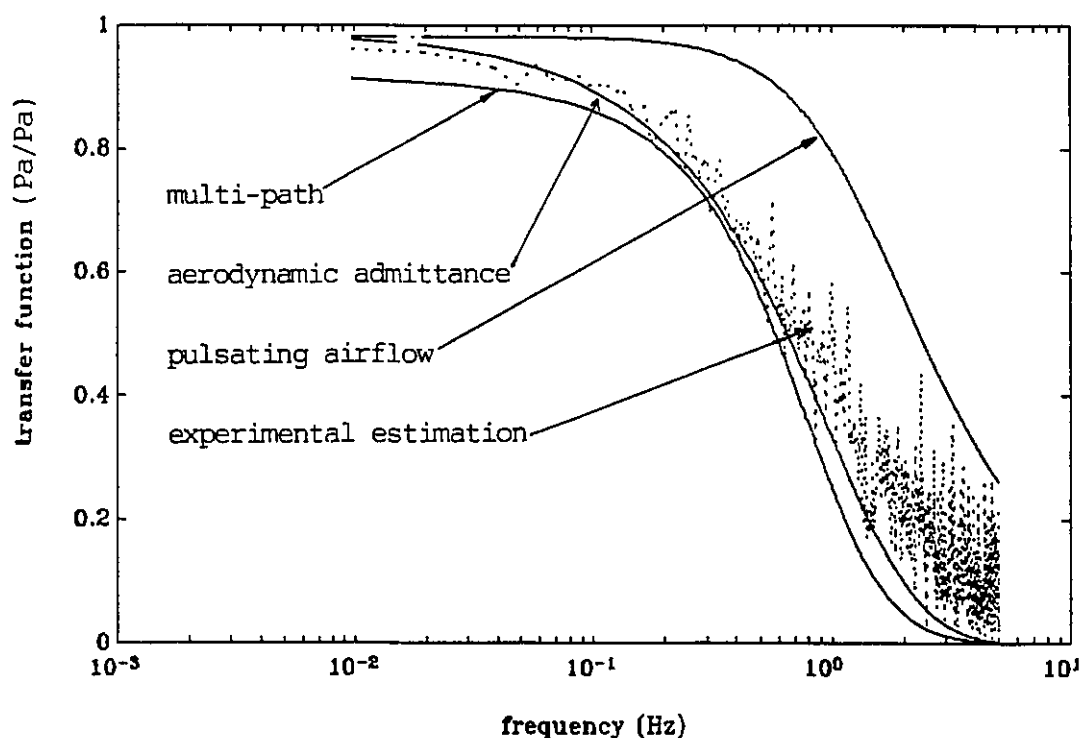


Figure 6.18. Results of Multi-Path Approach for Data Set VB1312: Magnitude Plot of Transfer Function Between External Pressure and Internal Pressure

**Table 6.1. List of Parameters for Single-Opening Case**


---



---

Building Internal Volume: 500 m <sup>3</sup>	
Temperature: Inside 23°C, Outside 23°C	
Opening Characteristics:	
Opening Cross Area:	A = 0.05 m <sup>2</sup>
Opening Depth:	L = 0.2 m
Opening Flow Equation:	$Q = C_d A \sqrt{\frac{2 \Delta P}{\rho}}$
Wind Induced Pressure:	
Spectrum:	Davenport's (1961)
RMS Values:	3.17 Pa
Simulation Controls:	
Time Step:	$\Delta t = 0.01$ sec
Duration:	1800 sec
Output:	every 0.1 second
Statistical Linearization:	
RMS of airflow:	$\sigma_q = 0.01145$ m <sup>3</sup> /s
Linear Coefficient:	$\lambda = \frac{1.162}{K^2} \sigma_q = 8.808808$

---



---

**Table 6.2. Summary of Results for Laboratory Experiments**

		JUN05	JUL22	JUL23	APR29	MAY12	MAY19	MAY22
Opening	$K_1$	0.7743	1.0937	1.0533	0.7152	0.8271	0.6717	0.8437
	$n_1$	0.80	0.75	0.75	0.80	0.75	0.85	0.75
Porosity	$K_2$	0.3523	0.3974	0.3720	0.3412	0.7906	0.5104	0.5507
	$n_2$	0.80	0.80	0.80	0.80	0.65	0.75	0.70
$\bar{P}_1^w$	mean	64.66	65.90	66.74	60.14	-0.61	3.80	16.64
	RMS	17.12	14.55	14.81	18.43	17.37	17.88	19.46
$\bar{P}^I$	expe	47.07	49.19	49.94	43.21	0.05	2.79	11.39
	calc	47.07	49.32	50.30	43.07	0.37	2.29	11.26
$\bar{Q}$	expe	7.68	8.86	8.64	8.76	0.18	0.75	2.40
	calc	7.68	8.99	8.60	6.92	-0.82	0.95	3.00
$q_1$	expe	2.13	2.21	2.18	2.41	3.67	3.34	3.38
	calc	2.24	2.24	2.20	2.32	3.63	3.68	3.66
$p^i$	expe	12.61	10.47	10.72	13.24	10.09	11.23	13.29
	calc	12.51	10.29	10.53	12.72	9.90	11.87	12.92
$\Delta P_1$	expe	6.67	5.67	5.76	8.79	8.92	8.71	9.91
	calc	6.40	5.49	5.61	7.56	8.37	7.24	7.85
$q_2$	calc	1.64	1.51	1.44	1.55	2.99	2.74	2.73
$q_1^I$	calc	2.21	1.82	1.86	2.25	1.76	2.12	2.29

Unit of  $K$ : (l/s)/Pa; pressures: Pascal, Pa; airflow rates: litter per second, l/s;

Notations:

expe: Experimental data or estimation,

calc: Theoretical calculation results,

$K_1$ ,  $n_1$ : Power law coefficient and exponent for the slot opening,

$K_2$ ,  $n_2$ : Power law coefficient and exponent for the chamber porosity.

Table 6.3. Comparison Results for Data Set VB1312

		Experimental		Theoretical		
		Mean	RMS	Mean	RMS	Flow Reversal
Opening		$K_1=7.6771 \times 10^{-3}$ $n_1=0.5$		input		NA
Porosity		$K_2=8.3424 \times 10^{-4}$ $n_2=0.5$		input		NA
$P_1^w$		14.45	5.02	input		NA
$P_2^w$		-4.35	1.51	input		NA
Pulsating Model	$P^i$ (Pascal)	13.60	4.53	14.23	4.85	NA
	$Q_1$ (l/s)	4.93	6.24	3.60	4.72	22.3%
	$Q_2$ (l/s)	3.02	0.59	3.60	0.66	0
Aerodynamic Admittance Approach	$P^i$ (Pascal)	13.60	4.53	14.23	4.50	NA
	$Q_1$ (l/s)	4.93	6.24	3.60	5.17	24.3%
	$Q_2$ (l/s)	3.02	0.59	3.60	0.66	0
Multi-Path Approach	$P^i$ (Pascal)	13.60	4.53	14.23	4.60	NA
	$Q_1$ (l/s)	4.93	6.24	3.60	5.50	25.7%
	$Q_2$ (l/s)	3.02	0.59	3.60	0.31	0

Note:

NA: not available.

Pressure at the porosity opening was not measured.

Table 6.4. Airflow Through Slot Opening for Data Set VB1312

	pulsating model	aerodynamic admittance approach	multi-path approach
mean airflow $\bar{Q}$	3.6		
RMS $\sigma_q$	4.72	5.17	5.50
$\beta$	0.223	0.243	0.257
total airflow $\bar{Q} + \frac{3}{2}\beta\sigma_q$	5.18	5.48	5.72
% over mean $[\frac{3}{2}\beta\sigma_q]/\bar{Q}$	43.3%	52.4%	58.8%
measured air exchange rate by tracer decay	5.46		

Note: the unit of airflow rates is litre per second (l/s).



## **CHAPTER VII**

### **CONCLUSIONS**

A framework and methodology are presented in this thesis to study the building airflow systems under both mean and fluctuating driving forces. Two constituent aspects are addressed: the steady-state airflow modelling and sensitivity analysis, and the fluctuating airflow modelling and prediction. The emphasis is on the assessment of the effect of fluctuating wind-induced pressures on airflow in buildings.

The system concept, as a scientific view point of the real physical world, is incorporated in attacking the solution of a building airflow system. The airflow system is divided into two subsystems: the steady-state and fluctuating airflow systems. Separate analyses are performed to concentrate on the special characteristics of the two subsystems. The system theoretic approach is applied in the modelling and formulation processes. The advantage is that derivation processes are mathematically rigorous, and automatic formulation procedures are derived.

The system theoretic approach to the steady-state airflow modelling and sensitivity analysis advances the existing understanding of the airflow mechanism and expands the ability of airflow models for analysis and design assistance in buildings under

the action of temperature, wind and mechanical forces. The sensitivity analysis also provides tools for evaluating the existing airflow models and therefore accelerate their applications to the real situation.

The fluctuating airflow model resolves another aspect of the airflow problem that have drawn much attention recently: the effects of temporal variations in wind-induced pressures. In searching for a solution approach, knowledge from several disciplines and research areas such as wind engineering, acoustics, signal processing, spectral analysis, and system theory are utilized. An array of techniques and methods such as statistical linearization, frequency analysis, system theoretic approach, spectral analysis, and aerodynamic admittance reduction are employed to model, formulate and solve the fluctuating airflow in buildings due to wind pressure variations. The analyses and calculations are performed in the frequency domain. The spectra information of fluctuating wind pressures are taken as input. The model predicts the airflow spectra and statistical measures, and assesses the total air exchanges in the building due to both mean and fluctuating driving forces.

The developed fluctuating airflow model is evaluated and validated by three strategies. Numerical simulations are used to compare the results of both nonlinear and linear governing equations, and to evaluate the effects of the statistical linearization on the solutions. Laboratory experiments are designed, implemented and conducted. The mechanism of pulsating airflow in a simple two-opening building is simulated to validate the fundamental relations. Field experimental data from other researchers are used to

validate the model with consideration of large openings. The comparison results from all three validation schemes prove the model's ability in providing satisfactory predictions.

The development of the fluctuating airflow model further strengthens the need for dynamic studies of air infiltration and ventilation in buildings. Both the hypothetical case studies in Chapter 4 and the experiments in Chapter 6 show the significance of the contributions from fluctuations. The field experiments in the BOUIN test house, for example, indicates a 50% increase in the air exchange over the mean value due to the variations in the wind.

The conducted research creates opportunities for further research work in implementations, applications and data acquisitions. The sensitivity analysis procedure can be incorporated into well known steady-state airflow models (such as COMIS model, COMIS, 1989) to facilitate the model validations, experimental design, error analyses and design assistance. The fluctuating airflow model could be incorporated into existing airflow models to provide more powerful analytical tools for solving a wider spectrum of airflow related problems. The model can also be linked with the contaminant dispersion models and thermal analysis models to study the effects of wind fluctuations on indoor air quality and energy consumptions (such as the work done by Axley, 1988b and 1989 for the steady-state counterpart). Applications of the fluctuating airflow model can be carried out to study the problems outlined in Section §1.2. The consideration on dynamic aspect may provide improved solutions and further insights into these problems. This process can also provide feedbacks for the model. Data acquisitions of the frequency characteristics of wind-induced pressures from an air infiltration perspective

(such as research done by Gusten, 1989) may also benefit from and provide valuable input to this research work. The development of the fluctuating airflow model clearly identifies the wind parameters that are important for the modelling, and therefore, may guide the experimental designs. Experimental comparisons against the collected data may, in turn, furnish further understanding of the model and/or provide simplifications to the input requirement of the model.

## REFERENCES

Allen, C., (1984), "Wind Pressure Data Requirements for Air Infiltration Calculations", Technical Notes 13, Air Infiltration and Ventilation Center, Warwick, UK.

ASHRAE, (1989), *ASHRAE Standard 62-1989, Ventilation for Acceptable Indoor Air Quality*, Atlanta, Georgia.

Allard, F. and Utsumi, Y., (1992), "Airflow Through Large Openings", *Energy and Building*, vol. 18, pp. 133-145.

Axley, J., (1988a), "Multizone Disposal Analysis by Element Assembly", *Building and Environment*, vol. 24(2), pp. 113-130.

Axley, J.W., (1988b), "Integrating Microscopic and Macroscopic Models of Air Movement and Contaminant Dispersal in Buildings", NSF Symposium: Buildings Systems: Room Air and Air Contaminant Distribution, Illinois, Dec.

Axley, J.W., (1989), "The Coupled Airflow and Thermal Analysis Problem in Building Airflow System Simulation", ASHRAE Symposium on Calculation of Interzonal Transport in Buildings.

Baechlin, W., (1987), "Pressure Inside Buildings-- A Dominant Parameter for Calculating Effective Natural Ventilation", *Indoor Air'87*, Vol 3.

Baskaran, A. (1992), *Review of Design Guideline for Pressure Equalized Rainscreen Walls*, NRC, Internal Report-629.

Baskaran, A. and Stathopoulos, T., (1989), "Computational Evaluation of Wind Effects on Buildings", *Building and Environment*, vol. 24, No. 4.

Bielek, M. and Cernik, P., (1987), "The Influence of Infiltration on the Heating of a Building", *Air Infiltration Review*, vol. 8(4).

Blacknell, J., (1989), "A Subject Analysis of the AIVC's Bibliographic Database - AIRBASE 6th Ed.", Technical Note 25, Air Infiltration and Ventilation Center, Warwick, UK.

CAN/CGSB-149.10-M86, (1986) *Determination of the Equivalent Leakage Area of Building by the Fan Depressurization Method*, Canadian General Standards Board.

Cermack, J.E. and Sadeh, W.Z., (1971), "Pressure Fluctuations on Buildings", *Proc. of Symposium on Urban Climates and Building Climatology*, Brussels, Oct, 1968, Volume II.

Charlesworth, P.S. (1988) *A Guide to Air Exchange Rates and Airtightness Measurement Techniques*, Air Infiltration and Ventilation Center, Warwick, UK.

CMHC, (1987), *Residential Combustion Ventilation Failure: A Systems Approach*, Summary Report, Scanada, Sheltair Consortium.

Cockroft, J.P. and Robertson, P., (1976), "Ventilation of an Enclosure Through a Single Opening", *Building and Environment*, vol. 11(1), pp. 29-35.

Collett, C.W., et al., (1987), "The Building Performance Data Base: an Analytical Tool for Indoor Air Quality Research", *Indoor Air '87*, vol. 2, pp. 482-486.

Colthorpe, K., (1990), *A Review of Building Airtightness and Ventilation Standards*, Technical Note-30, Air Infiltration and Ventilation Centre, Warwick, UK.

COMIS, (1989), "Conjunction of Multizone Infiltration Specialists", COMIS Workshop, Lawrence Berkeley Laboratory, Berkeley, CA.

Crommelin, R.D. and Vriens, E.M.H., (1988), "Ventilation Through a Single Opening in a Scale Model", *Air Infiltration Rev.* vol. 9, No. 3.

Davenport, A.G., (1961), "The Spectrum of Horizontal Gustiness Near the Ground in High Wind", *J. Royal Meteorol. Soc.*, vol. 87.

Davenport, A.G. and Surry, D., (1984), "The Estimation of Internal Pressures due to Wind with Application to Cladding Pressures and Infiltration", Technical Note 13.1, "1984 Wind Pressure Workshop Proceedings", Air Infiltration and Ventilation Center, pp. 1-9.

Etheridge, D.W. and Alexander, D.K., (1980), "The British Gas Multi-Cell Model for Calculating Ventilation", *ASHRAE Trans.*, vol. 86(2), pp. 808-821.

Etheridge, D.W. and Nolan, J.A., (1979), "Ventilation Measurements at Scale Model in a Turbulent Flow", *Building and Environment*, vol. 14, pp. 52-64.

Etheridge, D.W., (1984), "Air Leakage Characteristics of House, A New Approach", *BSE & T*, vol. 5, pp. 32-36.

Etheridge, D.W. and Gale, R., (1983), "Theoretical and Experimental Techniques for Ventilation Research in Buildings", Reprint 1983 International Gas Research Conf. London, June, 1983.

- Feustel, H.E. and Raynor-Hoosen, A. (Ed.), (1990), *Fundamentals of the Multizone Air Flow Model - COMIS*, Technical Note-29, Air Infiltration and Ventilation Centre, Warwick, UK.
- Feustel, H.G. and Dieris, J., (1992), "A Survey of Airflow Models for Multizone Structures", *Energy and Buildings*, vol. 18, pp. 79-100.
- Frank, P.M., (1978), *Introduction to System Sensitivity Theory*, Academic Press, New York.
- Gordon, G., (1978), *System Simulation*, Prentice-Hall Inc., Eaglewood Cliffs, New Jersey.
- Grosso, M., (1992), "Wind Pressure Distribution Around Buildings: A Parametrical Model", *Energy and Buildings*, vol. 18, pp. 101-131.
- Gusten, J., (1989), "Wind Pressure on Low-Rise Buildings. An Air Infiltration Analysis Based on Full-Scale Measurements", Publication 1989:2 Division of Structural Design, Chalmers University of Technology, Sweden, Gothenburg, 1989 ISSN 0281 1863.
- Haggkvist, K., Svenssen, V. and Taeser, R., (1989), "Numerical Simulation of Pressure Fields Around Buildings", *Building and Environment*, vol. 24(1), pp. 65-72.
- Haghighat, F., (1989), "Air Infiltration and Indoor Air Quality Models: A Review", *The International of Ambient Energy*, vol. 10(3), pp. 115-122.
- Haghighat, F. and Rao, J., (1991), "Computer Aided Building Ventilation System Design - A System-Theoretic Approach", *Energy and Buildings*, vol. 17, pp. 145-155.
- Haghighat, F., Rao, J. and Fazio, P., (1991), "The Influence of Turbulent Wind on Air Change Rates - a Modelling Approach", *Building and Environment*, vol. 26, No. 2, pp. 95-109.
- Haghighat, F., Rao, J. and Riberon, J., (1992), "Modelling Fluctuating Airflow through Large Openings", *13th AIVC Conf.*, Nice, France, Sept. 15-18.
- Haghighat, F., Fazio, P. and Rao, J., (1990), "A Procedure for Measurement of Ventilation Effectiveness in Residential Buildings", *Building and Environment*, vol. 25(2), pp. 163-172.
- Haghighat, F., Fazio, P. and Unny, T.E., (1988), "A Predictive Stochastic Model for Indoor Air Quality", *Building and Environment*, vol. 23(3), pp. 195-201.
- Haghighat, F. and Chandrashekar, M., (1987), "System-Theoretic Models for Building Thermal Analysis", *J. of Solar Energy Engineering*, vol. 109, pp. 79-88.

Hammersley, J.M. and Handscomb, D.C., (1964), *Monte Carlo Methods*, Methuen & Co., London.

Herrlin, M.K. and Allard, F., (1992), "Solution Methods for the Air Balance in Multizone Buildings", *Energy and Buildings*, vol. 18, pp. 159-170.

Hill, J.E. and Kusuda, T., (1975), "Dynamic Characteristics of Air Infiltration", *ASHRAE Trans.*, vol. 81, Pt. 4, pp. 168-185.

Hittle, D.C., (1978), "The Building Loads Analysis and System Thermodynamics Program--BLAST", Proc. of the 3<sup>rd</sup> International Symposium on the Use of Computers for Environmental Engineering Related to Building, Banff, Canada.

Hittle, D.C., (1979), *The Building Loads Analysis and System Thermodynamics, BLAST Program, Version 2.0: User's Manual*, U.S. Army Construction Engineering Research Laboratory Technical Report E-153.

Holmes, J.D., (1979), "Mean and Fluctuating Internal Pressures Induced by Wind", *Proc. of 5th Int. Conf. on Wind Engineering*, Colorado, Pergamon, July.

IEA-Annex 23, (1992), Multizone Airflow Modelling: 5th Expert Meeting Minutes, International Energy Agency, Budapest, Hungary, Sep. 10-11.

Irving, G., (1979), "The Computer Simulation of Smoke Movement During Building Fires", *Fire Prevention Science and Technology*, vol. 22, pp. 3-8.

Jenkins, G.M. and Watts, D.G., (1968), *Spectral Analysis and Its Applications*, Golden-Day, San Francisco.

Jones, P.J. and Whittle, G.E., (1992), "Computational Fluid Dynamics for Building Air Flow Prediction - Current Status and Capabilities", *Building and Environment*, vol. 27(3).

Kazic, N. and Novak, P., (1989), "A Dynamic Model of Air Movement in a Building", The 2<sup>nd</sup> Work Congress on Heating, Ventilation, Refrigerating and Air Conditioning - CLIMA 2000, pp. 250-255, Saragero, Yugoslavia.

Kochenburger, R.J., (1972), *Computer Simulation of Dynamic Systems*, Prentice-Hall Inc., Eaglewood Cliffs, New Jersey.

Kronvall, J., (1980), *Air Flows in Building Components*, Doctor Dissertation, Lund Institute of Technology, LUTVDG/(TVBH-1002)/1-194/(1980).

Lay, R.M. and Bragg, G.M., (1988), "Distribution of Ventilation Air -- Measurement and Spectral Analysis by Microcomputer", *Building and Environment*, vol. 23(3), pp. 203-213.



- Liddamend, M.W., (1986), "Air Infiltration Calculation Techniques -- An Applications Guide", AIVC Document AIC-AG-1-86, Air Infiltration and Ventilation Center, Warwick, UK.
- Liddament, M.W. and Allen, C., (1983), "The Validation and Comparison of Mathematical Models of Air Infiltration", Technical Note 11, Air Infiltration Center.
- Liddament, M.W., (1987), "A Review and Bibliography of Ventilation Effectiveness - Definitions, Measurement, Design and Calculation", Technical Note 21, Air Infiltration and Ventilation Centre, Warwick, UK.
- Limb, M., (1990), *1990 Survey of Current Research into Air Infiltration and Related Air Quality Problems in Buildings*, Technical Note 31, Air Infiltration and Ventilation Centre, Warwick, UK.
- Lumley, J.L. and Panofsky, H.A., (1964), *The Structure of Atmospheric Turbulence*, Interscience Publishers, John Wiley and Sons, New York.
- Malinowski, H.K., (1971), "Wind Effect on the Air Movement Inside Buildings", Paper presented at Tokyo conf. on wind load, Tokyo, Japan, Sept 6.
- Mathews, E.H., (1987), "Prediction of the Wind Generated Pressure Distribution Around Buildings", *J. Wind Engng Ind. Aerodynam.*, vol 25, pp. 219-228.
- Moler, C., Little, J., and Bangert, S., (1987), *Pro-MATLAB For VAX/VMS Computers, Version 3.1-VMS*, The Math Works Inc, US.
- Morrison, D., Karagiozis, A.N. and Kumaran, K. (1992), "Thermal Performance of a Residential Dynamic Wall", to be published in the Proc. of ASHRAE/DOE/BTECC.
- Murakami, S. and Mochida, A., (1989), "Three Dimension Numerical Simulation of Turbulent Flow Around Buildings Using the k-e Turbulence Model", *Building and Environment*, vol. 24(1), pp. 51-64.
- Narasaki, M, Yamanaka, T, et al, (1987), "Influence of Turbulent Wind on Ventilation", *Indoor Air'87* Conference, Berlin, 17-21 August 1987, Japan, Osaka University.
- Papoulis, A. (1965), *Probability, Random Variables and Stochastic Processes*, McGraw-Hill, New York.
- Paterson, D.A. and Apelt, C.J., (1989), "Simulation of Wind Flow around Three Dimensional Buildings", *Building and Environment*, vol. 24(1), pp. 39-50.

- Phaff, H. and De Gidds, W., (1980), "Building Ventilation, Investigation of the Consequence of Opening One Window on the Internal Climate of a Room", IMG-TNO Report C448, Delft, Netherland.
- Potter, I.N., (1979), "Effect of Fluctuation Wind Pressures on Natural Ventilation Rates", *ASHRAE Trans.*, vol. 85(2), pp. 445-457.
- Rao, J. and Haghighat, F. (1991) "Wind Induced Fluctuating Airflow in Buildings", *Proc. of the 12<sup>th</sup> AIVC Conference*, Ottawa Canada, vol. 1, pp. 111-122.
- Rao, J. and Haghighat, F., (1993), "A Procedure for Sensitivity Analysis of Airflow in Multi-Zone Buildings", *Building and Environment*, vol. 28, No. 1, pp. 53-62.
- Rao, J., Haghighat, F. and Bienfait, D., (1992), "Fluctuating Airflow in Buildings", *5<sup>th</sup> Jacque Cartier Conf.*, Montreal, Quebec.
- Riberon J. and Villain J., (1990), "Etude en vraie grandeur des débits effectifs de renouvellement d'air", CSTB GEC/DAC-90.101R, Champs-Sur-Marne.
- Riberon, J., Mounajed, R., Barnaud, G., and Vilain, J., (1989), "Turbulence Du Vent et Ventilation", Colloque AFME, Sophia Antipolis, Sept, 1989.
- Roe, P.H., (1966), *Network and Systems*, Addison-Wesley Reading, Mass.
- Roulet, C. and Vandaele, L., (1991), *Airflow Patterns Within Building: Measurement Techniques*, Air Infiltration and Ventilation Centre.
- Saathoff, P.J. and Liu, H., (1983), "Internal Pressure of Multi-Room Buildings", *J. of Engineering Mechanics*, vol. 109, No. 3.
- Sahin, B., Clark, C., Reynolds, A.J., and Wakelin, R., (1988), "Ventilation Generated by a Fluctuating Pressure Differential", 9th AIVC Conf., Gent, Belgium, 12-15 September.
- Sasaki, T., Hayashi, M. and Aratani, N., (1987), "On the Ventilating Characteristics of the Space under the Fluctuating Wind Pressure", Room Vent-87 Session 4 June 12th "Air Distribution in Ventilated Spaces".
- Simiu, E. and Scanlan, R.H., (1986), *Wind Effects on Structures -- An Introduction to Wind Engineering*, John Wiley & Sons, New York.
- Stathopoulos, T., (1980), "PDF of Wind Pressures on Low-Rise Buildings", *J. of the Structural Division*, ASCE, vol. 106(ST5).

- Swami, M.V. and Chandra, S., (1988), "Correlations for Pressure Distribution on Buildings and Calculation of Natural Ventilation Airflow", *ASHRAE Trans.*, vol. 94, pt. 1.
- Swamy, M.N.S. and Thulasiraman, K. (1981), *Graphs, Networks, and Algorithms*, John Wiley & Sons, New York.
- van der Hoven, I., (1957), "Power Spectrum of Horizontal Wind Speed in the Frequency Range from 0.0007 to 900 Cycle per hour", *J. of Meteorology*, vol. 14, pp. 160-167.
- van der Maas, J., Bienfait, D., Vandaele, L. and Walker, R., (1991), "Single Sided Ventilation", *12th AIVC Conf.*, Ottawa, Canada, Sept. 24-27, vol. 1, pp. 73-98.
- Vandaele, L and Wouters, P., (1989), "Air Flows Through Large Openings. An Overview of Existing Approaches", IEA Annex XX, Subtask 2 Report.
- Vellozzi, J. and Cohen, E., (1968), "Gust Response Factors", *J. Struc. Div., ASCE*, 94, No. ST6, Proc. Paper 5980.
- Vickery, B.J., (1970), "On the Reliability of Gust Loading Factors", *Proc. of the Technical Meeting Concerning Wind Loads on buildings and Structures*, NBS, Building Science Series 30, Washington, D.C., pp. 93-104.
- Vrins, E.M.H., (1986), "Ventilation Through an Opened Window as a Result of Turbulent Airflows", TNO Relft #2390.
- Walton, G.N., (1989), "Airflow Network Models for Element-Based Building Airflow Modelling", *ASHRAE Trans.*, vol. 95, pt. 2.
- Walton, G.N., (1983), Thermal Analysis Research Program Reference Manual, NBSIR 83-2655, NBS, U.S.
- Wouters, P., (1987), "The Problematic of Ventilation in Buildings", DPWB, National programma RD energie.
- Ziegler, F. and Schueller, G.I. (Eds) (1987), *Nonlinear Stochastic Dynamic Engineering Systems*, IUTAM Symposium Innsbruck/Igls, Austria, June 21-26, Springer-Verlag, Berlin.

# **APPENDIX A**

## **EXPERIMENTAL SETUP AND PROCEDURE**

### **A.1. LABORATORY EXPERIMENTAL SETUP**

The experimental setup includes the chamber, damper unit, tracer gas unit, sensors, and data acquisition system (Figure A.1).

#### **Chamber and Opening**

The chamber has dimensions of 7.5'×15.5'×7.7' (2.3m×4.7m×2.4m) and a volume of 900 ft<sup>3</sup> (25 m<sup>3</sup>). It is built of two 3/4" plywood boards and filled with vertical wood stud frames and fibre glass insulation. Two laminated doors and two small single-glazing peep-windows are located on the same facade of the chamber. The cracks are sealed with caulking compound from the inside.

A purpose-provided opening is placed through the chamber wall. The opening is filled with straws of 20cm in length and 0.5cm in diameter. This restrains the airflow through the opening to only pulsating airflow by eliminating the possibility of eddy penetrations. Therefore the fundamental relations between the wind-induced fluctuating pressure and the resultant airflow can be examined without interference from the turbulent eddies in the air stream.

Parameters of flow equations for the opening and the chamber porosity are measured by fan pressurization tests. When the opening is sealed, the chamber has approximately 1/20 ach (air changes per hour) in 50 Pascal pressurization tests.

### **Fluctuating Pressure Generation - The Damper Unit**

The damper unit is to provide a fluctuating pressure on and airflow through the opening according to the signal received from the data acquisitions system. As shown in Figure A.2, the damper unit consists of the damper and its control system, suction fans (#1 and #2), the venturi tube for measuring airflow rate, and 3" plumbing tube for connections.

A round damper disk is located inside a cylinder and is motivated by a serve motor with gear head (ratio of 1:69). A feedback (proportional) controller is employed to control the angle of the damper disk according the set point signal that is provided by the data acquisition system. The controller is adjusted so that the rising time (of the step response of the damper disk angle) is less that 0.2 second and, the overshooting is less than 5%. The accuracy of the steady-state positioning of the damper disk angle is about 0.8°. Since the purpose is to provide a temporally varying pressure, the steady-state positioning accuracy is not important.

The mechanism of the whole damper unit is as follows. When a signal (0 to 5 Volts) arrives at the damper angle controller (every 0.2 second), the controller directs the motor to turn the damper to a corresponding angle. The change of the damper angle causes variations of the airflow through the fan #1. In turn, the pressure generated at the

outside of the opening varies. After 0.2 second and before the damper angle reaches the steady-state (which takes 3 times of the rising time), another signal arrives and the above process repeats.

The purpose of the fan #2 is to generate a reverse flow through the opening. The direction of fan #2 is set to be the opposite of that of fan #1. The speed of fan #2 is set to a certain value. When the damper is at a certain angle, the airflow blown by the fan #1 equals to the airflow drawn by the fan #2. Positive pressures are generated when the damper angles are greater and negative for smaller damper angles.

The goal of the damper unit is to generate pressures that have resemblance to the real situation. This is achieved by letting the generated pressures have a power spectrum *similar* to a given one. It does not require the pressures to be exact in either the time or the frequency domains. Whatever pressures generated are the excitation force for the ventilation of the chamber and are taken as the input to the fluctuating airflow model. The only condition is that the spectrum of the generated pressures is similar to a given one. Therefore, requirements for the damper and fans are not very strict. The generating routine used in the numerical simulation program (equations 6-7 and 6-8) is employed. Preliminary tests show satisfactory performance of the damper unit.

### **Data Acquisition System**

The data acquisition system is a SAFE 8000 (Control Microsystems Inc.) with analog input card, analog output card, digital I/O card and thermal couple card. It has a capability of measuring up to 96 thermal couple input channels, 10 range-adjustable

analog input channels with 12 bit accuracy, 16 digital 1 bit input channels, and providing four 0 to 10 volts analog output channels of 12 bit accuracy.

The data acquisition runs programs in the SAFE BASIC language. In addition to the arithmetic, logical, flow control and subroutine capabilities of the conventional BASIC programming language, the SAFE BASIC (*SAFE BASIC Syntax and User Manual*, Control Microsystem Inc., Montreal, Canada, 1984) include commands to set timer and software/hardware interrupt, to perform necessary analog and digital input/output, and to communicate with user.

The interface between the user and the SAFE 8000 is achieved by a personal computer with RS-232 connection. In addition, the PC serves as an input/edit medium of the BASIC program in the SAFE; a control centre during execution of the program; and a data logger to save data sent by the SAFE to disk files. The communication software used on the PC is XTALK version 3.

### **Tracer Gas Measurement Unit**

The tracer gas measurement system has following components: an injection system, a sampling system, a gas chromatograph analyzer, and a calibration setup (Figure A.3).  $\text{SF}_6$  is used as the tracer gas.

The injection system injects controlled quantities of  $\text{SF}_6$  into the chamber. In the decay tests, a syringe is used to inject pure  $\text{SF}_6$  into the chamber. The amount is calculated by the formula:

$$S = C^* \times V \times 10^{-3} \quad (ml) \quad (A-1)$$

where  $C^*$  is the expected  $SF_6$  concentration level in ppb,  $V$  is the volume of the chamber in cubic meter.

The sampling system takes the sample of air to the analyzer. A 12 channel sampler (Analyzer System Ltd., *Instruction Manual: 12 Point Ambient Air Monitor*, 1987) is used. It can be operated either by automatic circuit (switching every 2 minutes) or by manual button pushing. A T-connector and two flow meters are used to maintain the flow rate of the sampling air to the analyzer at 34 cc/min.

The analyzer is a gas chromatograph (GC) analyzer with an electron capture detector (ECD) (Model 3400). The chromatographic column is specially designed for fast  $SF_6$  detection. A digital sequencializer operates the pneumatic backflushing valve. The analysis time is shorten to 20 seconds, 6 seconds for the sample injection to the column and 14 for backflushing. Continuous sampling is possible at three times per minute. The data can either be printed on papers or be transmitted to the PC through a RS-232 communication line.

The calibration of the analyzer is performed. The setup include the zero gas and  $SF_6$  1 ppm calibration gas, two mass flow meters and a Y-connector. One mass flow meters is calibrated for controlling nitrogen ( $N_2$ ) flow rate, the other for 1 ppm  $SF_6$ . The flow rate to the analyzer is maintained at 34 cc/min (same as when samples are analyzed). The calibration curve is shown in Figure A.4.



### Pressure Transducers and Flow Meter

Digital pressure transducers (*Model MP6KP, MP Series 4 Autozero Digital Micromanometers User Manual*, Air-Neotronics Ltd., Oxford, UK) are used for measuring pressures. The transducers have negligible zero drift because the zero checking is automatically performed every 2 minutes inside the transducers). The span drift is less than 0.1% of the range in use (100 Pascal) per °C. For the airflow rate measurement, venturi tube with hot-wire anemometer is used.

## **A.2. EXPERIMENTAL PROCEDURE**

Each experiment is performed in several steps: flow equation estimation, fluctuating airflow, and steady-state airflow. The following is a detailed description of each step.

### Test Step 1: Experiment Preparation and Tracer Gas Injection

Before an experiment starts, all instruments are turned on and are allowed to stabilize for an hour. The fan speed are set by adjusting the variac attached to each fan. An instrument testing routine is executed to verify status of sensors and the data acquisition system. The GC analyzer is checked for repeatability of the calibration at selected points.

Then, a calculated amount (according to equation A-1) of tracer gas  $\text{SF}_6$  is put into

vacuum tubes and subsequently released into the test chamber. A mixing fan is used to let the tracer gas completely mixed within the chamber.

### Test Step 2: Flow Equation Estimation

During the mixing, pressurization tests are performed to provide data for flow equation estimation. The damper angle is increased or decreased step by step from minimum to maximum. There is a time lag of 1 to 2 seconds between every two steps to allow the flow to reach the steady-state condition. The pressures at external end of the opening and inside the chamber, as well as the airflow through the opening are monitored. During this test, the condition of the operations of the two fans are the same for the later parts of the experiment.

### Test Step 3: Fluctuating Airflow Test

The main part of the SAFE BASIC control program is executed. The data acquisition system sends out a temporally fluctuating signal to the damper every 0.2 second. A fluctuating pressure is thus generated at the external end of the opening. Pressure and airflow data are collected at 5 Hz. Air samples from the chamber is also drawn to the GC analyzer, and the tracer gas concentrations are measured every 20 second. This part of experiment is conducted for approximate 45 minutes. No mixing fan is used.

The output (to damper control) signal of the data acquisition system is calculated from a pre-stored data set. This data set is first generated on a VAX computer (using routing in equations 6-7 and 6-8), and then transferred to the PC and put into the data storage area of the SAFE BASIC control program.

The control and data acquisition program is based on the concept of event interrupts. The program enters a idle loop after initialization and interrupt settings. At every 0.2 second, the sampling routine interrupts the idle loop, measures the related pressures and airflow rate, sends out damper angle signals, and then returns the program control to the idle loop. The use interface routine allows interruptions of the program execution and alterations to the program control parameters.

#### Test Step 4: Flow Equation Estimation

The pressurization test procedure of the test step 2 is performed again after the fluctuating airflow test to verify the characteristics of the opening and chamber porosity.

#### Test Step 5: Constant Airflow Test

The damper is set to a constant angle, which produces approximately the equal amount of pressure on the opening as to the (estimated) mean value of the pressures in the test step 3. A steady-state airflow test is conducted for about 30 minutes. Tracer gas decay is measured.

Tests are divided into two groups: one-directional and flow-reversal. In one-directional experiments, the fan #2 was sealed. The airflow through the opening always flows into the chamber. In the two-directional experiments, the fan #2 was in operation. The airflow may be in both directions depending on the angle of the damper.



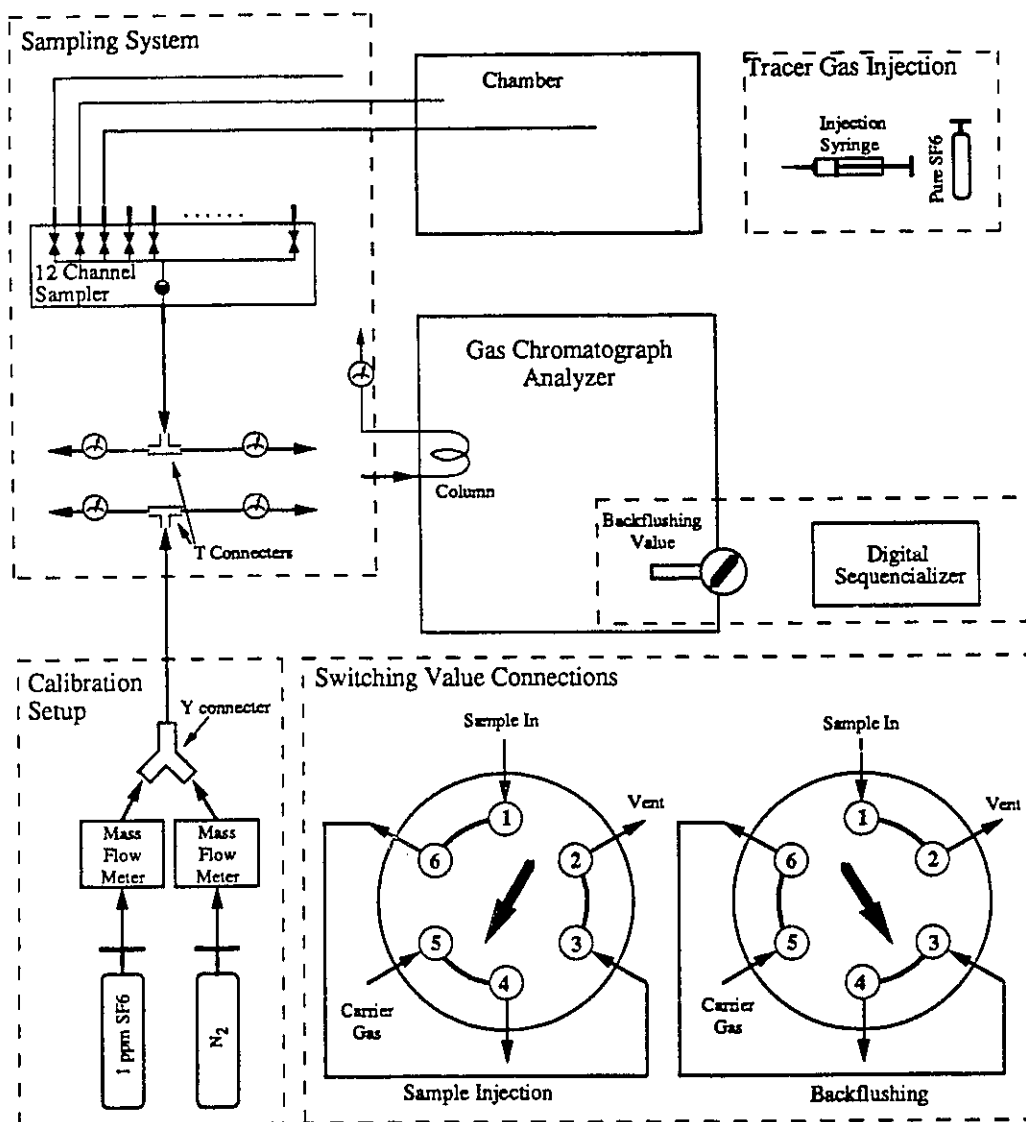


Figure A.3. Tracer Gas Measurement System

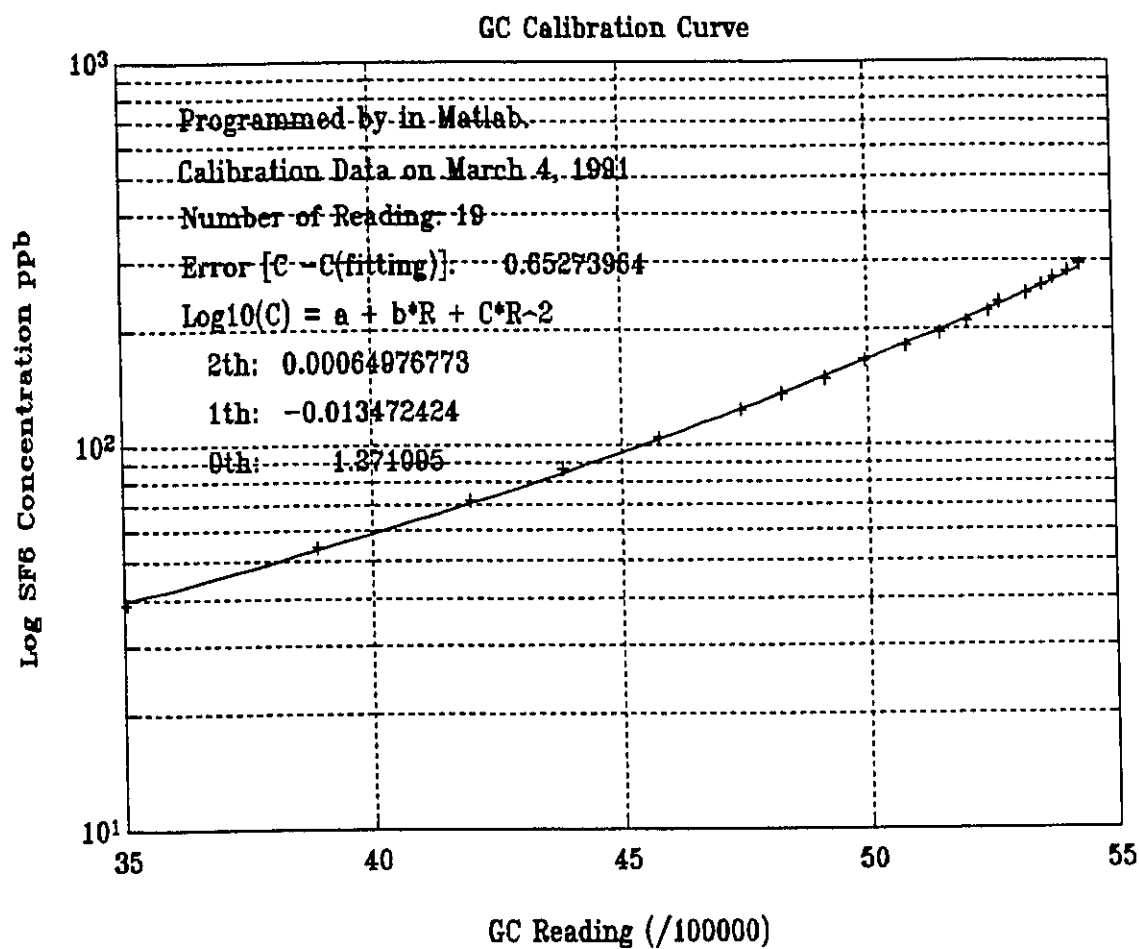


Figure A.4. Calibration Curve of the GC Analyzer